





# **A study of biochemical and physiological properties of normal and functionally impaired skeletal muscles**

Submitted by  
Susan Kate Bortolotto, B. Sc. (Hon.)

A thesis submitted in the total fulfilment of the requirements for the  
degree of  
**Doctor of Philosophy**



Muscle Cell Biochemistry Laboratory, School of Life Science and Technology,  
Footscray Park Campus,  
Victoria University

GPO Box 14428 Melbourne City Mail Centre, Victoria, 8001  
Australia

March 2000

22454621

FTS THESIS  
612.74 BOR  
30001006983169  
Bortolotto, Susan Kate  
A study of biochemical and  
physiological properties of  
normal and functionally

# Table of contents

Summary	ix
Declaration	xvi
Acknowledgments	xvii
List of publications	xix
List of abbreviations	xxi
List of figures	xxiv
List of tables	xxix

## Chapter 1 Introduction

<b>1.1</b>	<b>Structure of a skeletal muscle cell</b>	<b>1</b>
	<i>Cell specific structures.</i>	1
	<i>Other cellular components.</i>	4
<b>1.2</b>	<b>Diversity of skeletal muscles and skeletal muscle fibres</b>	<b>5</b>
	<i>Fibre typing methods using enzyme-based histochemistry.</i>	7
	<i>Fibre typing method using contractile properties of intact muscle fibres (physiological method).</i>	8
	<i>Fibre typing based on a combination of histochemical methods or a combination of histochemical and physiological methods.</i>	9
<b>1.3</b>	<b>Molecular events and structures involved in twitch muscle contraction</b>	<b>9</b>
1.3.1	Excitation	10
	<i>DHP receptors and <math>Ca^{2+}</math> release channels.</i>	10
1.3.1.1	Effectors of $Ca^{2+}$ release from the SR	14
	<i>Endogenous modulators.</i>	15
	<i>Caffeine.</i>	16

1.3.2	Contraction, myofibrillar proteins and methods used to study myofibrillar proteins	19
1.3.2.1	Basic concepts in gel electrophoresis	20
	<i>SDS-PAGE separation of proteins.</i>	22
1.3.2.2	Major proteins in thin filaments	22
	<i>Isoforms of regulatory proteins</i>	24
1.3.2.3	Major proteins in thick filaments	25
1.3.2.3.1	MLC isoforms	26
1.3.2.3.2	MHC isoforms	27
	<i>MHC isoform nomenclature.</i>	28
1.3.2.3.3	Myosin isoforms (isomyosins; myosin isozymes)	29
1.3.2.4	Biochemical analysis of myofibrillar protein isoform composition and fibre typing	30
1.3.2.4.1	Myosin isoform composition	30
1.3.2.4.2	Regulatory protein and MLC isoform composition	30
1.3.2.4.3	MHC isoform composition	31
	<i>Detection of MHC isoforms by SDS-PAGE.</i>	31
	<i>Detection of MHC isoforms by immunohistochemistry.</i>	32
1.3.2.5	Molecular events in skeletal muscle contraction	33
1.3.3	Relaxation	36
<b>1.4</b>	<b>Skinned fibre preparations and their use in studying events of the E-C-R cycle</b>	37
	<i>Physiological methods for fibre typing.</i>	38
<b>1.5</b>	<b>Comparison of fibre typing techniques</b>	39
<b>1.6</b>	<b>Muscle plasticity</b>	42
<b>1.7</b>	<b>The aims of this study</b>	43

## Chapter 2 General methods

<b>2.1</b>	<b>Animals</b>	46
<b>2.2</b>	<b>Preparation of whole muscle homogenates</b>	46
	<i>Muscle dissection and storage.</i>	46
	<i>Muscle homogenisation.</i>	48
	<i>Protein determination.</i>	48
<b>2.3</b>	<b>Preparation of single muscle fibres</b>	49
2.3.1	Dissection of single muscle fibre segments	49
2.3.2	Measurement of single muscle fibre segments	50
2.3.3	Skinning of single muscle fibre segments	52
<b>2.4</b>	<b>Measurement of contractile activation characteristics of single, skinned fibre segments</b>	53
2.4.1	Description of the force measuring system	53
2.4.2	Calibration of the force transducer	55
2.4.3	Attaching single fibre segments to the force measuring system	55
2.4.4	Measurement of the sarcomere length of a single fibre segment	58
2.4.5	Activating solutions	60
2.4.5.1	Preparation of solutions for determining $\text{Ca}^{2+}$ - and $\text{Sr}^{2+}$ - activation characteristics	60
2.4.5.1.1	Titration of solutions for determining $\text{Ca}^{2+}$ - and $\text{Sr}^{2+}$ - activation characteristics	63
	<i>Titration of solution A.</i>	64
	<i>Titration of solution B.</i>	64
	<i>Titration of solution D.</i>	66
	<i>Calculation of pCa.</i>	66
	<i>Calculation of pSr.</i>	67
2.4.5.2	Procedure used to expose fibre segments to series of calcium/strontium buffered solutions	68
2.4.6	Data analysis	68

2.4.6.1	Force measurements	68
2.4.6.2	Contractile activation characteristics for skinned fibres	71
<b>2.5</b>	<b>SDS-PAGE analysis of single muscle fibres or whole muscle</b>	<b>74</b>
2.5.1	Set up of electrophoresis equipment	74
2.5.2	Sample preparation	76
2.5.3	Staining of the SDS-PA gels	78
	<i>Bio-Rad silver staining.</i>	78
	<i>Hoefer silver staining.</i>	79
2.5.4	Densitometry	79
2.5.5	Estimation of MHC isoform and MLC2 isoform composition in whole muscle homogenates	81

### **Chapter 3 An investigation into effects of various electrophoretic parameters on the separation of MHC isoforms in rat skeletal muscle.**

<b>3.1</b>	<b>Introduction</b>	<b>84</b>
<b>3.2</b>	<b>Method</b>	<b>86</b>
	<i>SDS-PAGE.</i>	86
	<i>DATA ANALYSIS.</i>	86
<b>3.3</b>	<b>Results</b>	<b>88</b>
3.3.1	Effects of changing various electrophoretic parameters in two gel systems on the separation of MHC isoforms in rat skeletal muscle	88
3.3.1.1	Alteration of parameters in the 'Laemmli' gel systems	89
3.3.1.1.1	Composition of the separating gel	89
	<i>Acrylamide concentration.</i>	89
	<i>%C value.</i>	91
	<i>Tris concentration.</i>	91

	<i>Glycerol concentration.</i>	93
	<i>Glycine concentration.</i>	96
3.3.1.1.2	Stacking gel	98
3.3.1.1.3	Running conditions	98
	<i>Electric Field.</i>	98
	<i>Running time.</i>	101
	<i>Running temperature.</i>	101
	<i>Separation of slow (I) MHC isoforms.</i>	104
3.3.1.2	Alteration of parameters in the Talmadge and Roy protocol	106
3.3.1.2.1	Composition of the separating and stacking gels	106
	<i>[Glycerol] in the separating gel.</i>	106
	<i>Composition of the stacking gel.</i>	108
3.3.1.2.2	Running conditions	108
	<i>Running buffer.</i>	108
	<i>Electric field.</i>	110
3.3.1.2.3	Mozdziak version of the Talmadge & Roy protocol	113
3.3.1.3	Evaluation of the gel systems used in this study	115
<b>3.4</b>	<b>Discussion</b>	124

**Chapter 4. Myosin Heavy Chain isoform composition and  $\text{Ca}^{2+}/\text{Sr}^{2+}$ -activation characteristics of single fibres from soleus, EDL and diaphragm muscles of adult rat.**

<b>4.1</b>	<b>Introduction</b>	132
<b>4.2</b>	<b>Methods</b>	134
	<i>Animals and muscle dissection.</i>	134

	<i>Preparation of Triton-skinned, single muscle fibre segments.</i>	134
	<i>Determination of <math>Ca^{2+}/Sr^{2+}</math>-activation characteristics of chemically skinned, single muscle fibre segments.</i>	135
	<i>Data analysis.</i>	136
	<i>SDS-PAGE analysis of MHC and MLC isoforms.</i>	137
	<i>Statistics.</i>	138
<b>4.3</b>	<b>Results</b>	139
4.3.1	Fibre types classified according to MHC composition	139
4.3.2	Fibre types classified according to $Ca^{2+}/Sr^{2+}$ -activation characteristics	143
4.3.3	The correlation between the MHC isoform based- and $Ca^{2+}/Sr^{2+}$ -activation properties-based fibre typing methods	146
4.3.4	Fibre diameter, maximum specific force and $Ca^{2+}/Sr^{2+}$ -activation characteristics of fibres types according to MHC composition	148
	<i>Fibre diameter.</i>	148
	<i><math>CaF_{max}/CSA</math> and <math>CaF_{max}/SrF_{max}</math>.</i>	150
	<i><math>Ca^{2+}/Sr^{2+}</math>-activation characteristics.</i>	151
4.3.5	Force oscillations of myofibrillar origin	160
4.3.6	Myosin light chain expression in fibres typed according to MHC isoform composition	165
<b>4.4</b>	<b>Discussion</b>	168
	<i>Fibre type populations in SOL, EDL and DPH muscles of SHR and WKY rats.</i>	169
	<i>Method for fibre size determination.</i>	172
	<i>MHC composition and <math>Ca^{2+}/Sr^{2+}</math>-activation characteristics under 'near-physiological' conditions.</i>	173
	<i>A comparison between the MHC isoform based- and <math>Ca^{2+}/Sr^{2+}</math>-activation properties-based muscle fibre typing methods.</i>	176

## **Chapter 5. Fibre type population and Ca<sup>2+</sup> activation properties of single fibres in soleus muscles from SHR and WKY rats.**

<b>5.1</b>	<b>Introduction</b>	180
<b>5.2</b>	<b>Methods</b>	182
	<i>Animals.</i>	182
	<i>Preparation of single muscle fibre segments.</i>	183
	<i>Determination of Ca<sup>2+</sup>-activation characteristics of chemically skinned, single muscle fibres.</i>	183
	<i>SDS-PAGE analysis of MHC and MLC isoforms.</i>	186
	<i>Statistics.</i>	187
<b>5.3</b>	<b>Results</b>	187
5.3.1	Physical characteristics	187
5.3.2	MHC isoform composition of whole muscles	189
5.3.3	MLC2 isoform composition of whole muscles	192
5.3.4	Fibre type populations yielded by random dissection	192
5.3.5	Correlation between MHC isoform composition, MLC2 composition, and fibre type populations	197
5.3.6	Calcium activation characteristics of single fibres	199
<b>5.4</b>	<b>Discussion</b>	204

## **Chapter 6. Effect of caffeine on single muscle fibres in SHR and WKY rats.**

<b>6.1</b>	<b>Introduction</b>	210
<b>6.2</b>	<b>Materials and Methods</b>	211
	<i>Animals.</i>	211
	<i>Skinned fibre preparation.</i>	212
	<i>Solutions and force measurements.</i>	212

	<i>SDS-PAGE analysis of MHC isoforms in single muscle fibre segments.</i>	213
	<i>Statistical analyses.</i>	214
<b>6.3</b>	<b>Results</b>	214
6.3.1	Types of fibres examined and strategy used for determining caffeine threshold for contraction	214
6.3.2	Low caffeine induced force responses are related to SR Ca <sup>2+</sup> release	218
6.3.3	Strain-related and fibre type-related differences in caffeine threshold for contraction at endogenous SR-Ca <sup>2+</sup> load	221
6.3.4	Strain-related and fibre type-related differences in caffeine threshold for contraction at maximal SR-Ca <sup>2+</sup> load	223
6.3.5	Strain-related and fibre type-related differences in the relative caffeine thresholds for maximal and endogenous SR-Ca <sup>2+</sup> loads	225
<b>6.4</b>	<b>Discussion</b>	228
	 Concluding Remarks	 234
	Bibliography	238
	Appendix 1	264
	Appendix 2	266
	Appendix 3	268
	Appendix 4	269
	Appendix 5.1	270
	Appendix 5.2	273
	Appendix 5.3	275

## SUMMARY

The main aim of this study was to increase our understanding of the diversity and plasticity of skeletal muscle by using (i) normal and functionally impaired rat muscles from normotensive and spontaneously hypertensive rats, (ii) single, skinned fibre preparations, and (iii) a combination of biochemical [SDS-polyacrylamide gel electrophoresis (SDS-PAGE) analyses of Myosin Heavy Chain (MHC) isoform composition in single fibres and whole muscle homogenates] and physiological (single fibre measurements of contractile activation characteristics and caffeine thresholds for contraction) methods. From the beginning of this work it became clear, however, that the number of different protocols used for electrophoretic separation of MHC isoforms was almost as high as the number of studies using this method. Furthermore, all gel systems described so far in the literature proved to have a relatively low reproducibility in this and other laboratories. Finally, there was no published study in which the impact of changing different electrophoretic parameters on MHC isoform separation was examined in a systematic manner. Thus, some efforts had to be also directed towards closing this knowledge gap. The information generated in the present study can be summarised as follows:

1. A survey was carried out on studies published over the last 17 years (1983-1999) that involved electrophoretic separation of MHC isoforms using SDS-PAGE; these studies originated from different laboratories or from the same laboratory at

different times. The purpose of this survey was to assess the extent of variability in the methodological protocols and to identify trends in electrophoretic parameter variation. The data, tabulated according to electrophoretic parameter and to the basic gel system used by the authors, identified [acrylamide] and [glycerol] (in the separating gel and in the stacker), the strength of electric field (E), expressed as voltage (V), current (I) or V/cm, and the running time, as the most frequently altered parameters in method optimisation.

2. The effects of these and other electrophoretic parameters on the separation of three pairs of near-neighbour rat MHC isoforms (I and IIb, IIb and IIc and IIc and IIa) were quantitated for two well known gel systems (Laemmli and Talmadge & Roy), using the densitometrically measured distance between MHC isoform bands ( $\Delta$ ) as an indicator of band separation, and the smallest  $\Delta$  that could be detected by the densitometric software (0.4 mm) as the detection limit. The parameters examined include: [acrylamide]<sub>separating gel</sub>, %C, [Tris]<sub>separating gel</sub>, [glycerol]<sub>separating gel</sub>, [glycine]<sub>separating gel</sub>, [glycerol]<sub>stacker</sub>, electric field, running time and temperature (for the Laemmli gel system), [glycerol]<sub>separating gel</sub>, stacker composition, composition of the running buffer, electric field (for the Talmadge & Roy gel system) and sample size (for both systems). The data showed that both in the Laemmli and Talmadge & Roy systems, the direction and the magnitude of the effect of most parameters on MHC separation was dependent on the pair of MHC isoforms under consideration, and for some parameters, on the range of values, such that optimising a given parameter with respect to the separation of one pair of MHC isoform bands would

have either no impact or a detrimental impact on the separation of the other pairs of MHC isoform bands. This may explain, in part, the low reproducibility of SDS-PAGE protocols aiming to separate effectively all MHC isoforms.

3. A comprehensive investigation of the relationship between MHC expression and isometric activation characteristics (and by implication, of the compatibility between the fibre typing method based on MHC composition and that based on  $\text{Ca}^{2+}/\text{Sr}^{2+}$ -activation characteristics) was carried out using a broad range of fibre types randomly dissected from soleus (SOL), extensor digitorum longus (EDL) and diaphragm (DPH) muscles of male adult rats. The isolated fibres were chemically skinned and their  $\text{Ca}^{2+}$ - and  $\text{Sr}^{2+}$ -activation characteristics (maximum  $\text{Ca}^{2+}/\text{Sr}^{2+}$ -activated force per cross-sectional area,  $\text{Ca}^{2+}/\text{Sr}^{2+}$ -activation threshold, sensitivity to  $\text{Ca}^{2+}/\text{Sr}^{2+}$ , degree of cooperativity in development of  $\text{Ca}^{2+}/\text{Sr}^{2+}$ -activated force and the presence of force oscillations of myofibrillar origin) were compared, under near-physiological conditions with respect to the temperature and chemical composition of the activating solutions. The data obtained do not support a *tight* correlation between MHC composition and contractile activation characteristics as such. For example, significant differences were observed with respect to sensitivity to  $\text{Ca}^{2+}/\text{Sr}^{2+}$  and degree of cooperativity in development of  $\text{Ca}^{2+}/\text{Sr}^{2+}$ -activated force between fibres expressing MHCI isoform only and fibres expressing one or several MHCII isoforms, but not between different subtypes of fibres expressing one or several MHCII isoforms. An unexpected finding of this study was that some fast fibre types from SOL muscle

displayed significantly higher sensitivity to  $\text{Ca}^{2+}$  than fibres of the same type from EDL and DPH muscles. According to  $\text{Ca}^{2+}/\text{Sr}^{2+}$ -activation parameters, the fibres examined in this study belonged to 5 groups: simple fast, simple slow, composite slow-slow, composite slow-fast and composite fast-fast. Each fibre segment was also electrophoretically typed based on the myosin heavy chain (MHC) isoform expression. Based on this parameter, the fibres belonged to 10 distinct groups: I, IIA, IID, IIB, I+IIA, I+IID, IIA+IID, IIB+IID, I+IIA+IID and IIA+IIB+IID. The results demonstrate that while slow-twitch fibres from rat soleus muscles can be appropriately identified using fibre typing methods based on either the MHC isoform composition or the  $\text{Ca}^{2+}/\text{Sr}^{2+}$ -activation characteristics, both methods are needed to fully characterize a fast-twitch fibre. This is because for fast-twitch fibres one can neither distinguish between pure and hybrid fibres based on  $\text{Ca}^{2+}/\text{Sr}^{2+}$ -activation characteristics nor accurately predict the  $\text{Ca}^{2+}/\text{Sr}^{2+}$ -activation characteristics of a given fibre from its pattern of MHC expression. The partial rather than full correlation of the two fibre typing methods further demonstrates that MHC expression and isometric  $\text{Ca}^{2+}/\text{Sr}^{2+}$ -activation characteristics are not causally related.

4. A small subpopulation of the fibres used to examine the correlation between MHC composition and contractile activation characteristics was also employed for investigating the relationship between MHC isoform and MLC isoform expression. The purpose of this limited study was to assess whether rat skeletal muscles follow the rule of myofibrillar protein isoform co-expression previously suggested for

human muscle. Electrophoretic analyses of MHC and MLC isoforms revealed that pure (IIA) and hybrid (IIA+IID; IIA+IIB+IID) fast type fibres from SOL and DPH muscles contained slow as well as fast MLC isoforms; it was, therefore, concluded that MHC and MLC isoform expression are not tightly correlated in these two rat muscles.

5. Electrophoretic analyses of muscle proteins in whole muscle homogenates and single muscle fibre segments were used to examine MHC and myosin light chain 2 (MLC2) isoform composition and fibre type populations in soleus muscles from spontaneously hypertensive rats (SHRs) and their age-matched normotensive controls (WKY), at three stages in the development of high blood pressure (4-wk, 16-wk and 24-wk of age). Chemically skinned single fibre preparations were used to determine contractile parameters and these fibres were then also examined for MHC expression. The results show that at all three ages examined: (i) SHR soleus contained a lower proportion of MHC I and MLC2 slow (MLC2s) and a higher proportion of MHC IIa, MHC II d and MLC2 fast (MLC2f) isoforms than the age-matched controls; (ii) random dissection of single fibres from SHR and WKY soleus produced four populations of fibres: type I, type IIA, hybrid type I+IIA and hybrid type IIA+IID, and (iii) single fibre dissection from SHR soleus yielded a lower proportion of type I fibres, a higher proportion of fast-twitch fibres (type IIA and IIA+IID) and a higher proportion of hybrid fibres (type I+IIA and IIA+IID) than the homologous muscles from the age-matched WKY rats. Since the presence of hybrid fibres is most commonly viewed as a marker of muscle transformation,

these data suggest that SHR soleus undergoes transformation well into adulthood. The data showed also that for a given fibre type, there were no significant differences between SHR and WKY soleus muscles with respect to any of the  $\text{Ca}^{2+}$ -activation properties examined. This finding indicates that the lower specific tensions reported in the literature for SHR soleus muscles are not due to strain- or hypertension-related differences in the function of the contractile apparatus or regulatory system.

6. The possibility that SOL muscles from spontaneously hypertensive rats displayed lower kinetic parameters because of alterations in SR structure/function was explored in a series of experiments in which caffeine thresholds for contraction ( $\text{caff-th}_E$ ;  $\text{caff-th}_M$ ), at two SR- $\text{Ca}^{2+}$  loads (endogenous and maximal), and their ratio ( $R_{\text{caff-th}}$ ; parameter used as indicator of slow-twitch/fast-twitch SR characteristics for a given fibre) were determined using mechanically skinned single fibres dissected from SOL muscles of SHR and age-matched WKY rats. Mindful of the relatively high fast-twitch fibre content of SHR soleus muscles, fast-twitch fibres from WKY-EDL muscles were also included in the study as a reference for caffeine threshold determinations. Advantage was also taken of the presence of several fibre types in the population of single fibres used in order to examine the correlation between MHC isoform expression and SR caffeine threshold related-characteristics. The data showed that the proportion of fibres with fast-twitch SR characteristics was 5.3 times higher in the group of SHR-SOL type I fibres than in the group of WKY-SOL type I fibres. This finding (i) can explain in part the lower

kinetic parameters displayed by SHR-SOL muscles, and also (ii) suggests that there is no tight correlation between MHC isoform composition and SR characteristics.

The latter was confirmed by the large variability in caffeine threshold values (CV range: 18-67%) displayed by fibres in each fibre type group examined.

## Declaration

This thesis contains no material that has been presented or accepted for the award of any other degree or diploma in this or any other university. Except where specifically indicated in the text, the data presented herein is the result of work of the author, and to the best of my knowledge and belief, has not been previously written or published by any other person.

Susan Kate Bortolotto

## Acknowledgements

Firstly, I would like to thank my supervisor, Assoc. Prof. Gabriela Stephenson, it was her initial belief in me that allowed me to undertake a PhD, and her dedication and support and that allowed me to finally finish. I thank her whole-heartedly for all she has taught me in the muscle research area over the last 4 years and the time she has put in to help me finally achieve my goal.

A special thanks to Prof. George Stephenson, who had the patience to teach me all I need to know about single muscle fibres.

Thank you to Dr. Michael Patterson who gave up his time to thoroughly edit the final draft of this thesis.

Thank you to Debbie Ramsey and all the staff at the Baker Medical Research Animal House who taught how to use the equipment to measure the blood pressure of the rats.

To the many people I have worked with in the Muscle Cell Biochemistry Laboratory and the students at Victoria University who have allowed me to have a great working environment, without which it would have been very hard to complete my doctorate.

I would like to the following people in particular: Domenica Trifilio for technical assistance, Maria Cellini for collaborating with me on the study presented in Chapter 4,

Craig Goodman for being a constant source of journal articles and reference books, Brett O'Connell for scanning pictures for my thesis and reviving my computer many times, Peter Florey for dropping in for a chat every now and then, and Long Nguyen for helping me with the Atomic Absorption Spectrophotometer.

To all my family and friends who have supported and encouraged me over the last 4 years, I'm sure you are all as happy as I am that I have finally finished. Special thanks to my Mum and Dad who have always been there for me, and have given me every opportunity to do the best I can.

To my wonderful husband, Damian Smith, for supporting me in many ways over the last 4 years. Words cannot express how indebted I am for his support, patience, encouragement and belief that I would finally finish this. Now maybe we go fishing more often, I promise!!!!

## List of Publications

### Refereed papers

1. **Bortolotto, S.K.**, D.G. Stephenson, and G.M.M. Stephenson. Fiber type populations and  $\text{Ca}^{2+}$ -activation properties of single fibers in soleus muscles from SHR and WKY rats. *American Journal of Physiology*. 276(Cell Physiology 45): C628-C637, 1999.
2. **Bortolotto, S.K.**, D.G. Stephenson, and G.M.M. Stephenson. Partial correlation between  $\text{Ca}^{2+}$ - and  $\text{Sr}^{2+}$ - activation properties of the contractile apparatus and myosin expression in single soleus muscle fibres of the rat' *Journal of Physiology (London)*. 505: 89P-90P, 1997.
3. Cundasamy, K., **S.K. Bortolotto**, and G.M.M. Stephenson. An electrophoretic study of myosin heavy chain expression in skeletal muscles from rats of different gender and strain. *Proceedings of the Australian Physiological and Pharmacological Society*. 27(2): 160P, 1996.

1. **Bortolotto, S.K.**, M. Cellini, D.G. Stephenson, and G.M.M. Stephenson. Myosin heavy chain composition and  $\text{Ca}^{2+}/\text{Sr}^{2+}$ -activation characteristics of single fibers from soleus, EDL and diaphragm muscles of adult rat. *Am. J. Physiol.* (under review, Ms. No. C572-9)
2. **Bortolotto, S.K.**, D.G. Stephenson, and G.M.M. Stephenson. A study on caffeine thresholds for contraction in single, mechanically skinned muscle fibres from SHR and WKY rats. (in preparation)

**Conference Presentations (non-referred)**

1. **Bortolotto, S.K., D.G. Stephenson, and G.M.M. Stephenson.** A single fibre study of fibre type composition and contractile activation characteristics of soleus muscle from spontaneously hypertensive rat. *Proceedings of the Australian Physiological and Pharmacological Society.* 29(2): 40P, 1998.
2. **Bortolotto, S.K., D.G. Stephenson, and G.M.M. Stephenson.** A comparison of myosin expression and contractile characteristics in single soleus muscle fibres of the rat. *Proceedings of the Australian Physiological and Pharmacological Society.* 28(2): 83P, 1997.
3. **Bortolotto, S.K., D.G. Stephenson, and G.M.M. Stephenson.** Fibre type specific effects of low molecular weight myofibrillar protein extraction on Ca<sup>2+</sup>-activated force in rat skeletal muscle. Proceeding of the *Australian Society for Biochemistry and Molecular Biology.* 28: Pos-274-01, 1996.

## List of abbreviations

A	acrylamide
ACh	acetylcholine
ATP	adenosine triphosphate
B	methylenebisacrylamide cross-linker reagent
<i>caff-th</i>	caffeine threshold
<i>caff-th<sub>E</sub></i>	caffeine threshold at endogenous SR-Ca <sup>2+</sup> load
<i>caff-th<sub>M</sub></i>	caffeine threshold at maximal load
Ca <sup>2+</sup>	calcium ion
CaF <sub>max</sub>	maximum Ca <sup>2+</sup> -activated force
COMP <sub>f-f</sub>	composite fast-fast fibres
COMP <sub>s-f</sub>	composite slow-fast fibres
COMP <sub>s-s</sub>	composite slow-slow fibres
CP	creatine phosphate
CSA	cross-sectional area
CV	coefficient of variation
DHP	dihydropyridine
DL	detection limit
DPH	diaphragm
EGTA	Ethyleneglycol-bis-(β-aminoethyl-ether)-N,N <sup>1</sup> - tetra acetic acid
EDL	extensor digitorum longus
FG	fast-twitch glycolytic fibres
FKBP	FK binding protein
FOG	fast-twitch oxidative glycolytic fibres
FT	fast-twitch
HDTA	hexamethalenediamine <i>N,N,N',N'</i> -tetraacetic acid
HEPES	N-[2-Hydroxyethyl]piperazine-M <sup>p</sup> -[2-ethanesulfonic acid]
jSR	junctional SR

$K_{app}$	apparent affinity constant
mATPase	myosin ATPase
MHC	Myosin Heavy Chain
MLC	Myosin Light Chain
MW	molecular weight
pCa	$-\log[Ca^{2+}]$
pSr	$-\log[Sr^{2+}]$
$P_t$	% maximum force
$R_{caff-th}$	ratio of $caff-th_M/caff-th_E$
RyR	ryanodine receptors (or calcium release channels)
RT	room temperature (19-25°C)
SDS	sodium dodecyl sulfate
SDS-PAGE	sodium dodecyl sulfate- polyacrylamide gel electrophoresis
$S_{fast}$	simple fast fibres
SHR	Spontaneously hypertensive rat
SO	slow-twitch oxidative fibres
SOL	soleus
SR	sarcoplasmic reticulum
$Sr^{2+}$	strontium ion
$SrF_{max}$	maximum $Sr^{2+}$ -activated force
$S_{slow}$	simple slow fibres
ST	slow-twitch
TC	terminal cisternae
TEMED	<i>N,N,N',N'</i> -tetramethylethylenediamine
Tm	tropomyosin
TnC	Troponin C
TnI	Troponin I
TnT	Troponin T
T tubules	transverse tubules
wk	week

<b>WKY</b>	<b>Wistar-Kyoto rat</b>
<b>%C</b>	<b>proportion of %T that is the cross-linker</b>
<b>%T</b>	<b>the total concentration of monomer used to produce the gel</b>

## List of figures

<b>Figure no.</b>	<b>Figure title</b>	<b>Page</b>
1.1	Arrangement of fibres in a skeletal muscle tissue.	2
1.2	Arrangement of cellular components in a skeletal muscle fibre.	3
1.3	Light micrograph of part of a single fibre containing a large number of nuclei.	6
1.4A	Cross-sectional view of a triad.	12
1.4B	Diagrammatic representation of the protein complexes believed to be involved in the detection of the signal produced by the T-system depolarisation.	12
1.4C	Diagrammatic representation of the relative position of RyR and DHP receptors at triads of skeletal muscle.	12
1.5	Scheme of the mammalian skeletal muscle ryanodine receptor showing potential calmodulin binding sites, potential nucleotide binding sites and Ca <sup>2+</sup> activation sites.	17
1.6	Basic structure of thin and thick filaments.	23
1.7	Sarcomere pattern of mammalian skeletal muscle.	34
2.1	Location of the EDL and SOL skeletal muscles and the DPH muscle.	47
2.2	Video camera-monitor system used to measure the size of single fibres with a pair of callipers.	51
2.3A	Force apparatus.	54
2.3B	Diagrammatic representation of the electrical circuit.	54
2.4	Calibration curve of force transducer.	56
2.5A	Surgeon's double knot.	57
2.5B	Tying the single fibre segment to the stainless steel pin.	57
2.6	Setup used to measure sarcomere length of single fibre preparations.	59
2.7	Example of titration curves used to calculate [EGTA] <sub>excess</sub> in solutions A and solution D.	65

2.8	Order of solutions (using 1 batch of solutions) used to determine contractile activation parameters of a skinned fibre preparation.	69
2.9	Representative chart recording of force responses produced by a fast-twitch single muscle fibre in a complete experiment.	70
2.10	An example of the chart recording produced from a slow-twitch SOL fibre and the calculations necessary in correcting for fibre deterioration between maximum force responses developed within an activation cycle.	72
2.11	Electrophoresis equipment.	75
2.12	Analysing MHC isoform bands.	80
2.13A	Relationship between $\Delta OD1_{MHCi}$ expressed in arbitrary units and the total protein concentration in the homogenate sample.	82
2.13B	Relationship between $\Delta OD2_{MHCi}$ expressed in arbitrary units and the total protein concentration in the homogenate sample.	82
3.1	The effect of acrylamide concentration ( $[A]$ ) on the separation of MHC isoforms I and IIb, and IIad and IIb.	90
3.2	The effect of %C value on the separation of MHC isoforms IIb and I, and IIad and IIb.	92
3.3	The effect of $[Tris]$ on the separation of MHC isoforms IIb and I, IId and IIb, and IIa and IId.	94
3.4	The effect of $[glycine]$ on the separation of MHC isoforms IIb and I, and IIad and IIb.	97
3.5	The effect of $[glycerol]$ in the stacking gel on the separation of MHC isoforms IIb and I, and IIad and IIb.	99
3.6	The effect of varying the electric field (E) on the separation of MHC isoforms.	100
3.7	The effect of running time of the separation of MHC isoforms IIb and I, and IIad and IIb.	102

3.8	The effect of running temperature on the separation of MHC isoforms IIb and I, IIc and IIb, and IIa and IIc.	103
3.9	A representative electrophoretogram showing the separation of two MHC I isoform bands on a gel ran at 2-4°C.	105
3.10	The effect of varying [glycerol] on the separation of MHC isoforms.	107
3.11	The effect of replacing the T-R with the 'L <sup>G+</sup> ' in the 'T-R' gel system, on the separation of MHC isoforms bands IIb and I, IIc and IIb, and IIa and IIc.	109
3.12	The effect of replacing the T-R running buffer with the D-B running buffer, in the 'T-R' gel system, on the separation of MHC isoforms IIb and I, IIc and IIb, and IIa and IIc.	111
3.13	The effect of the electric field on the separation of MHC isoforms IIb and I, IIc and IIb, and IIa and IIc.	112
3.14	The separation of MHC isoforms IIb and I, IIc and IIb, and IIa and IIc using the 'T-R' Mozdziak gel system.	114
3.15	Factors found to alter consistently the effectiveness of MHC isoform separation.	116
3.16	Factors that do not affect the separation of MHC isoforms on the gel systems considered in this study.	118
3.17	Electrophoretograms of best and worst gels with respect to the separation of all four MHC isoforms in three different gel systems.	119
3.18	Frequency distribution of $\Delta_{IIb-I}$ , $\Delta_{IIc-IIb}$ and $\Delta_{IIa-IIc}$ for the 'Laemmli' gel system.	122
3.19	Frequency distribution of $\Delta_{IIb-I}$ , $\Delta_{IIc-IIb}$ and $\Delta_{IIa-IIc}$ for the 'T-R' gel system.	123
3.20	Relative proportion of studies that modified the specified electrophoretic parameters in the original gel protocols of 'Laemmli' and 'T-R' when trying to separate mammalian MHC isoforms.	131

4.1	Representative electrophoretogram of fibres belonging to the 10 different fibre types found in a population of fibres dissected from the SOL, EDL and DPH muscles of adult SHR and WKY rats.	140
4.2	The proportion of pure and hybrid fibre types in the fibre type populations dissected from SOL, EDL, and DPH muscles of adult SHR and WKY rats.	142
4.3	Representative force-pCa and force-pSr curves for 'simple' fibres.	144
4.4	Representative force-pSr curves for 'composite' fibres.	145
4.5	The proportions of different MHC-based fibre groups comprised in each class of fibres defined by $\text{Sr}^{2+}$ -activation characteristics.	147
4.6	Correlation between the proportion of fast MHC isoforms expressed by single fibres and their relative sensitivity to $\text{Ca}^{2+}/\text{Sr}^{2+}$ expressed as pCa <sub>50</sub> -pSr <sub>50</sub> .	161
4.7	Proportions of SOL, EDL and DPH muscle fibres from each MHC-based fibre type group that produced force oscillations when subjected to submaximally activating $\text{Ca}^{2+}$ solutions.	162
4.8	Estimated frequency of force oscillations developed by different MHC-based fibre types.	164
4.9	Electrophoretograms of myofibrillar proteins from two single fibres.	167
5.1	Apparatus used to measure blood pressure of rats.	184
5.2	Representative electrophoretic profile of MHC isoforms detected in soleus muscles from 24-wk-old WKY rats and SHRs.	190
5.3A	Representative electrophoretogram of low molecular weight muscle proteins from 24-wk-old WKY and SHR soleus muscles.	193
5.3B	Bar chart for the ratio MLC2 <sub>s</sub> /MLC2 <sub>t</sub> in soleus muscles of 4wk-, 16wk-, and 24wk-old SHRs and WKY rats.	193
5.4	Representative electrophoretogram of MHC isoform composition of the fibre types yielded, upon random dissection, by soleus muscles of SHR and WKY rats.	195

5.5A	The relationship between the proportion of MLC2s isoform and MHCI isoform in soleus muscles from SHRs and WKY rats.	198
5.5B	The correlation between the relative content of each MHC isoform detected in the soleus muscle and the proportion of corresponding fibre type derived from the analysis of single fibre segments obtained by random microdissection of the contralateral soleus muscle.	198
6.1	Representative chart recordings of force responses and the data plot used when determining $caff-th_E$ and $caff-th_M$ of a single muscle fibre.	217
6.2	Representative chart recording of force responses produced by a fibre segment incubated in Solution <i>R</i> after having been exposed to Solution <i>Th-caff<sub>x</sub></i> .	219
6.3	Graph showing that gradual decrease in SR-Ca <sup>2+</sup> content after exposure of skinned fibre preparation to solutions containing the caffeine concentrations indicated on x-axis.	220
6.4	The frequency distribution of $R_{caff-th}$ values from WKY type I fibres from the SOL muscle and WKY type II fibres from the EDL muscle.	227
6.5	The percentage of type I soleus fibres from SHR and WKY rats that displayed SR <sup>slow</sup> or SR <sup>fast</sup> properties.	229

## List of tables

Table no.	Table title	Page
1.1	Methods for fibre typing based on enzyme-based histochemistry.	8
1.2	Inter-fibre related differences with respect to the cellular/molecular structure of participants involved in excitation events.	14
2.1	Compositions of solutions A, B, C, D, used to measure $\text{Ca}^{2+}$ - and $\text{Sr}^{2+}$ - activation characteristics.	61
2.2	Volumes required to obtain series of $\text{Ca}^{2+}$ -activating solutions.	62
2.3	Volumes required to obtain series of $\text{Sr}^{2+}$ -activating solutions.	63
3.1	The effect of varying [glycerol] on the separation of MHC isoforms.	96
3.2	Parameters used to evaluate the effectiveness of three gel systems.	120
3.3	Effectiveness of different parameters with respect to the separation of MHC isoform pairs IIb and I, IId and IIb, and IIa and IId in the 'Laemmli' gel systems.	128
3.4	Effectiveness of different parameters with respect to the separation of MHC isoform pairs IIb and I, IId and IIb, and IIa and IId in the 'T-R' gel systems.	129
4.1	pCa and pSr values of activating solutions.	135
4.2	The proportions of fibres displaying $S_{\text{slow}}$ , $S_{\text{fast}}$ and COMP activation characteristics in each class of electrophoretically defined fibre types.	141
4.3	Diameter, $\text{CaF}_{\text{max}}/\text{CSA}$ and ratio $\text{CaF}_{\text{max}}/\text{SrF}_{\text{max}}$ of electrophoretically-typed fibres from SOL, EDL and DPH muscles of adult rat.	149
4.4a	pCa <sub>10</sub> , pSr <sub>10</sub> and pCa <sub>10</sub> -pSr <sub>10</sub> values of electrophoretically-typed fibres from SOL, EDL and DPH muscles of adult rat.	152

4.4b	pCa <sub>50</sub> , pSr <sub>50</sub> and pCa <sub>50</sub> -pSr <sub>50</sub> values of electrophoretically-typed fibres from SOL, EDL and DPH muscles of adult rat that produced simple force-pSr curves.	153
4.4c	nCa and nSr values of electrophoretically-typed fibres from SOL, EDL and DPH muscles of adult rat which developed simple force-pSr curves.	155
4.4d	pCa <sub>50</sub> , pSr <sub>50</sub> and pCa <sub>50</sub> -pSr <sub>50</sub> of electrophoretically-typed fibres from SOL, EDL and DPH muscles of adult rat that produced composite force-pSr curves.	157
4.4e	MHC isoforms composition, sensitivity to Ca <sup>2+</sup> /Sr <sup>2+</sup> -activation and the degree of cooperativity of the regulatory system with respect to Ca <sup>2+</sup> /Sr <sup>2+</sup> -activation in four slow/fast (I+IIA) hybrid fibres obtained from SOL muscles of adult SHR and WKY rats.	159
4.5	The presence of slow and fast MLC isoform bands on SDS-PA gels of myofibrillar proteins from a population of pure and hybrid fibres that produced simple and composite force-pSr curves.	166
5.1	pCa values of activating solutions.	186
5.2	Physical characteristics of SHR and WKY rats.	188
5.3	MHC isoform composition of soleus muscles from SHR and WKY rats.	189
5.4	Fibre type populations in soleus muscles from WKY and SHR.	196
5.5	Fibre diameter and maximum Ca <sup>2+</sup> -activated force/cross sectional area (CaF <sub>max</sub> /CSA; kN/m <sup>2</sup> ) of electrophoretically typed, single soleus muscle fibres from WKY and age-matched SHR.	201
5.6	Sensitivity to calcium of the myofibrillar compartment (pCa <sub>50</sub> ) in chemically skinned, electrophoretically-typed, single soleus muscle fibres from WKY and age-matched SHR.	203

5.7	The degree of cooperativity within the myofibrillar system with respect to calcium regulation of the contractile response ( $n_{Ca}$ ) in chemically skinned, electrophoretically typed, single soleus muscle fibres from WKY and age-matched SHR.	204
6.1	Compositions of solutions used to determine caffeine threshold for contraction.	213
6.2	Fibre types of randomly dissected single fibres in SOL and EDL muscles from SHR and WKY.	215
6.3	Caffeine threshold at endogenous SR- $Ca^{2+}$ load [ $caff-th_E$ (mM)] in SOL and EDL fibres from SHR and WKY rats.	222
6.4	Caffeine threshold at maximal SR- $Ca^{2+}$ load [ $caff-th_M$ (mM)] in SOL and EDL fibres from SHR and WKY rats.	222
6.5	Relative caffeine threshold for maximal and endogenous SR- $Ca^{2+}$ loads ( $R_{caff-th} = caff-th_M/caff-th_E$ ).	226
A1	Composition of separating gels in the Laemmli and in the Talmadge & Roy gel systems.	264
A2	Composition of stacking gels in four gel systems.	264
A3	Composition of running buffers in three gel systems.	265

# Chapter 1

## Introduction

### 1.1 Structure of a skeletal muscle cell

Musculo-skeletal system is a term describing a large family of muscle tissues (eg. in the human body there are over 400 skeletal muscles) that are generally but not exclusively attached to bones, and are distinguishable in light microscopy by their striation pattern (hence their classification as striated muscles). The major role of skeletal muscles is to generate force and movement under voluntary control.

The skeletal muscle tissue is composed of a large number of elongated cells (more commonly referred to as muscle fibres), specialised for contraction, that are arranged in parallel (see Fig. 1.1) and act independently. Skeletal muscle cells contain a number of cell specific internal structures as well as several cellular components that are present also in non-muscle cells.

*Cell specific structures.* Electron micrographs of skeletal muscle fibres reveal that 85-90% of the total muscle fibre volume is occupied by bundles of specialised filaments, called myofibrils (represented diagrammatically in Fig. 1.2), which are regarded as the contractile elements of the cell (Loughlin, 1993). Also unique to a

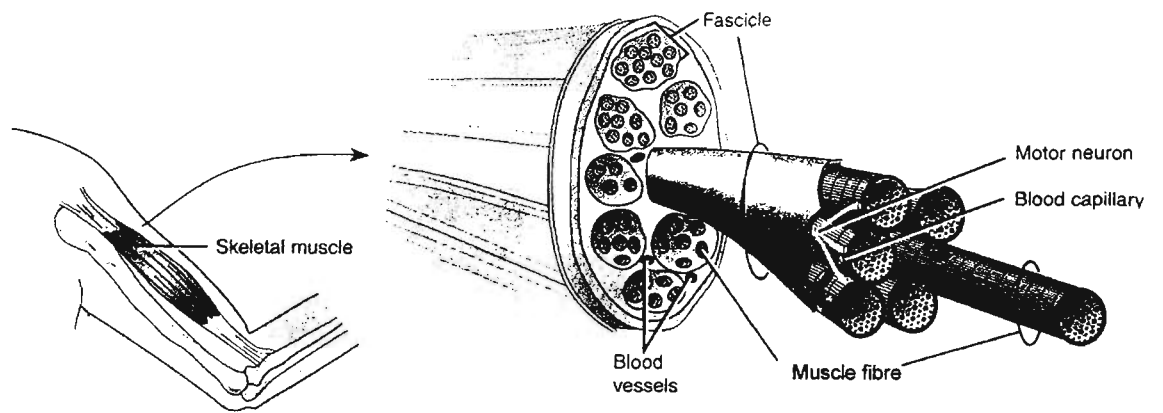


**Figure 1.1** Arrangement of fibres in a skeletal muscle tissue (Reproduced from Tortora & Grabowski, 1996).

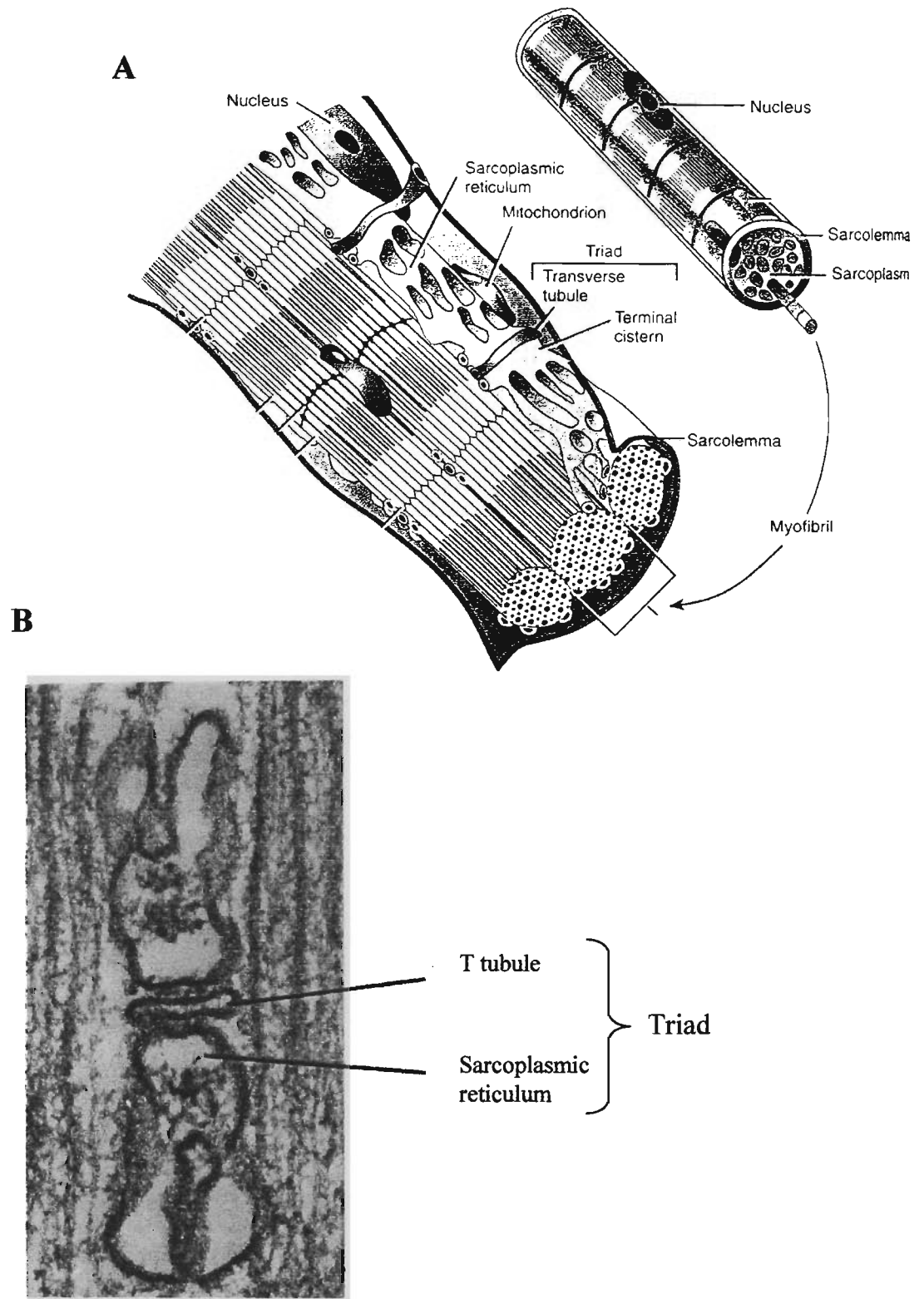


**Figure 1.2 Arrangement of cellular components in a skeletal muscle fibre.** A. Diagrammatic display (modified from Tortora & Grabowski, 1996). B. Electron micrograph of longitudinal section of muscle showing the components of a triad (modified from Aidley, 1998).

muscle cell are two functionally interdependent membrane systems; the transverse (T) tubules (which together form the T-system) and the sarcoplasmic reticulum (SR) (see Fig. 1.2). The T tubules, which are formed by inward extensions of the plasma membrane, extend transversely across the sarcoplasm, at right angles to the long axis of the cell. The SR is a membranous network comprising longitudinal tubules that surround the myofibrils (longitudinal SR) and flattened sacs (terminal cisternae; TC) in which  $\text{Ca}^{2+}$  (the activator ion in muscle contraction) is stored. The SR regions rich in TC are referred to as junctional SR (jSR). Ultrastructural studies have shown that in a skeletal muscle fibre, the T-system and the SR communicate at specialised junctions, known as triads, which are formed when two terminal cisternae are closely opposed to each side of a T tubule (Fig. 1.2). Together, these two membrane systems are involved in the initiation and termination of contraction by controlling  $\text{Ca}^{2+}$  movements within a muscle fibre.

*Other cellular components.* In addition to the aforementioned specialised structures, skeletal muscle fibres have been shown to contain several cellular components (such as plasma membrane, mitochondria, nuclei, lysosomes and peroxisomes) that are found in all eukaryotic cells. It is interesting to note however, that even these structures display characteristics that are specific to skeletal muscle cells. Thus:

- (i) the plasma membrane (sarcolemma) is electrically excitable and contains regions specialised for nerve muscle communications (motor end plate regions). Motor end plate regions are rich in acetylcholine receptors and a number of specific ion channels ( $\text{K}^+$ ,  $\text{Na}^+$ ,  $\text{Cl}^-$ ,  $\text{Ca}^{2+}$ )

- (ii) mitochondria occupy only a small volume of the fibre and have been found to be located both in the intermyofibrillar space and under the sarcolemma (Pearson & Young, 1989),
- (iii) a skeletal muscle fibre contains not one but a large number of nuclei (see Fig. 1.3), all of which shift from a central to a subsarcolemmal position during muscle cell development and vice versa during regeneration (Franzini-Armstrong & Fischman, 1994),
- (iv) in a normal skeletal muscle fibre, the lysosomal system is poorly developed compared with other eukaryotic cells (Alroy & Kolodny, 1994), and
- (v) there are indications that some skeletal muscles contain a peroxisomal system which maybe involved in extra mitochondrial fatty acid oxidation (Ontko, 1994).

Within the context of this thesis, only the specialised internal structures (the T-system, SR, and myofibrillar compartment) will be discussed in more detail in relation to their role in muscle contraction.

## **1.2 Diversity of skeletal muscles and skeletal muscle fibres**

Differences between skeletal muscles have been noted from the beginning of muscle research. As early as 1874, French physician and physiologist Ranvier (1874), first recognised that muscles differed with respect to colour (red or white muscles) and speed of contraction (fast or slow muscles). Later, it was discovered that muscles could also be distinguished by type of twitch response (twitch or tonic muscles). It is

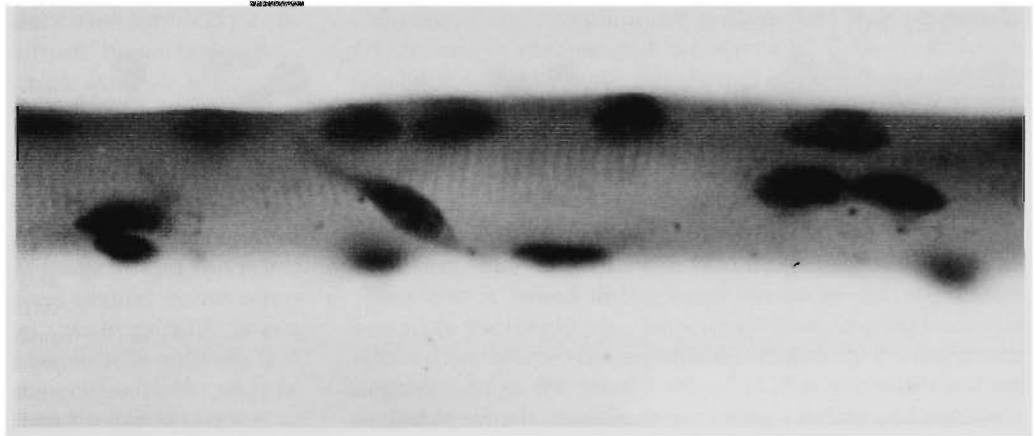


**Figure 1.3** Light micrograph of part of a single fibre containing a large number of nuclei (x 1000) (Reproduced from Bischoff, 1994).

now widely accepted that structural and functional differences exist not only between muscles but also between single muscle fibres and that most skeletal muscles contain a variety of fibre types which can be distinguished on the basis of a number of criteria (for review see Pette & Staron, 1990).

Regarding the diversity of twitch skeletal muscle fibres it is interesting to note that: (i) the number of structural, functional and molecular differences between fibres increases as new physiological and biochemical methods for muscle fibre analyses are developed and refined and (ii) only some of these differences have become criteria for fibre typing.

This section will concentrate on histochemical fibre typing methods based on inter-fibre differences in enzyme activities and on a physiological method based on inter-fibre differences with respect to speed of contraction. Fibre typing methods based on inter-fibre differences in MHC isoform composition and in the sensitivity of the contractile-regulatory system to activator ions will be discussed in sections 1.3.2.4.3 and 1.4, respectively.

*Fibre typing methods using enzyme-based histochemistry.* As comprehensively reviewed by Pette and Staron (1990), two major histochemical approaches are currently used for distinguishing fibre types: one based on differences with respect to the activity or pH stability of myosin ATPase (mATPase), the other based on differences with respect to activities of enzymes of aerobic and anaerobic energy metabolism. The fibre types distinguished using these approaches are shown in Table 1.1.

**Table 1.1 Methods for fibre typing based on enzyme-based histochemistry.**

<b>Criterion for fibre typing</b> (first research team to distinguish and name the fibre types)	<b>Fibre types</b>
<b>mATPase activity</b> (Engel, 1962)	type I; type II
<b>pH stability of mATPase activity</b> (Brooke & Kaiser, 1970)	type I; type IIA; type IIB; type IIC
(Staron & Pette, 1986)	type I; type IC; type IIC; type IIA; type IIAB; type IIB
<b>enzymes of aerobic oxidative metabolism</b> succinate dehydrogenase, malate dehydrogenase, cytochrome oxidase and NADH tetrazolium reductase (Ogata and Mori, 1964)	high mitochondrial content; intermediate mitochondrial content; low mitochondrial content
<b>enzymes of anaerobic metabolism</b> glycerol phosphate oxidase and lactate dehydrogenase (Peter <i>et al.</i> , 1972)	high activity; low activity

*Fibre typing method using contractile properties of intact muscle fibres (physiological method).*

Early measurements of isometric twitch contraction times in isolated motor units of rat muscle (where a motor unit consists of a neuron and all the muscle fibres it innervates) led to the detection of three fibre type groups: fast-twitch, intermediate-twitch and slow-twitch (Close, 1967). Intermediate- and slow-twitch motor units were found in soleus (SOL) muscles, whereas the extensor digitorum longus (EDL) was composed almost entirely of fast-twitch motor units.

*Fibre typing based on a combination of histochemical methods or a combination of histochemical and physiological methods.* After comparing results obtained with oxidative enzymes and phosphorylase activity, Dubowitz and Pearse (1960) stated that muscle fibres could be grouped into two types: type 1 fibres (high oxidative, low glycolytic activity) and type 2 fibres (low oxidative, high glycolytic activity). Later on Barnard *et al.* (1971) combined enzyme-based histochemical methods with measurement of twitch contraction times, a strategy which allowed them to distinguish three major fibre types: slow-twitch oxidative (SO) fibres, fast-twitch oxidative glycolytic (FOG) fibres and fast-twitch glycolytic (FG) fibres.

The advantages and limitations of the aforementioned fibre typing methods will be discussed later in this chapter (see section 1.5) in relation to the fibre typing methods described in sections 1.3.2.4.3 and 1.4.

### **1.3 Molecular events and structures involved in twitch muscle contraction**

A cycle of three major processes, *vis.* excitation, contraction and relaxation (collectively referred to also as the E-C-R cycle), must take place in order for contraction to occur in a twitch skeletal muscle (Stephenson *et al.*, 1998). At a cellular level, the E-C-R cycle involves the following sequence of events: (i) initiation and propagation of an action potential along the sarcolemma and T-system, (ii) detection of the T-system depolarisation signal and signal transmission from the

T tubule to the SR, (iii)  $\text{Ca}^{2+}$  release from the SR, (iv) transient rise of myoplasmic  $[\text{Ca}^{2+}]$ , (v) transient activation of the  $\text{Ca}^{2+}$  regulatory system and of the contractile apparatus, (vi)  $\text{Ca}^{2+}$  reuptake by the SR  $\text{Ca}^{2+}$  pump and  $\text{Ca}^{2+}$  binding to myoplasmic sites (Stephenson *et al.*, 1998). The molecular intricacies of these events and the way they are influenced by the diversity of muscle protein expression is far from being understood (Moss *et al.*, 1995, Stephenson *et al.*, 1995).

### 1.3.1 Excitation

A skeletal muscle fibre will remain at rest until stimulated by a signal received from a motoneuron. This signal is carried by acetylcholine (ACh), a neurotransmitter which is released from internal compartments in the nerve terminals and binds to specific receptors in the motor endplate region. The binding of ACh to its receptors in the sarcolemma initiates a wave of depolarisation which spreads without decrement along the sarcolemma and into the T-system; this type of membrane depolarisation is known as an action potential. It is now well established that the upstroke of an action potential is maintained by the regenerative activation of the  $\text{Na}^+$  channels while membrane repolarisation results from the inactivation of  $\text{Na}^+$  channels and activation of delayed rectifier  $\text{K}^+$  channels.

*DHP receptors and  $\text{Ca}^{2+}$  release channels.* The depolarisation of T tubules activates a series of voltage-sensitive, multisubunit protein complexes [known as dihydropyridine receptor (DHPR) complexes] that are located in the T-system membrane at the level

of the triads, and are arranged regularly in groups of four, called tetrads. Electron microscope studies have shown that each tetrad is in close proximity to specialised structures (referred to as foot regions or feet; see Fig. 1.4A) which span the gap between the jSR and the DHP receptors. The foot regions have been found to represent the cytoplasmic domains of a group of SR-protein complexes involved in muscle contraction, the  $\text{Ca}^{2+}$  release channels or ryanodine receptors (RyR), so named due to their function in  $\text{Ca}^{2+}$  movements across the SR membrane and to their ability to bind ryanodine.

Three separate RyR isoforms, encoded for by three different genes, have been identified in mammalian tissues: RyR1 (found predominantly in skeletal muscle), RyR2 (found predominantly in cardiac muscle) and RyR3 (found predominantly in brain and smooth muscle) (for review see Meissner, 1994). During post-natal development, all mammalian skeletal muscles co-express RyR3 and RyR1, but RyR3 is no longer expressed in adult muscles with the exception of SOL and diaphragm (DPH) muscles which express a small amount.

Each SR  $\text{Ca}^{2+}$  release channel is composed of four identical isomers; in turn, each of the four isomers is tightly associated with a small protein, the FK binding protein (FKBP), which dissociates from the RyR upon binding the immunosuppressant drug FK506 (Sorrentino & Reggiani, 1999). FKBP is believed to coordinate the activation of the four isomers to act as a single RyR release channel (Herrmann-Frank *et al.*, 1999). Other proteins associated with the SR and believed to play a role in the regulation of the SR- $\text{Ca}^{2+}$  release are calsequestrin (a luminal protein acting as the main  $\text{Ca}^{2+}$  binding protein in the SR) and triadin (believed to connect the

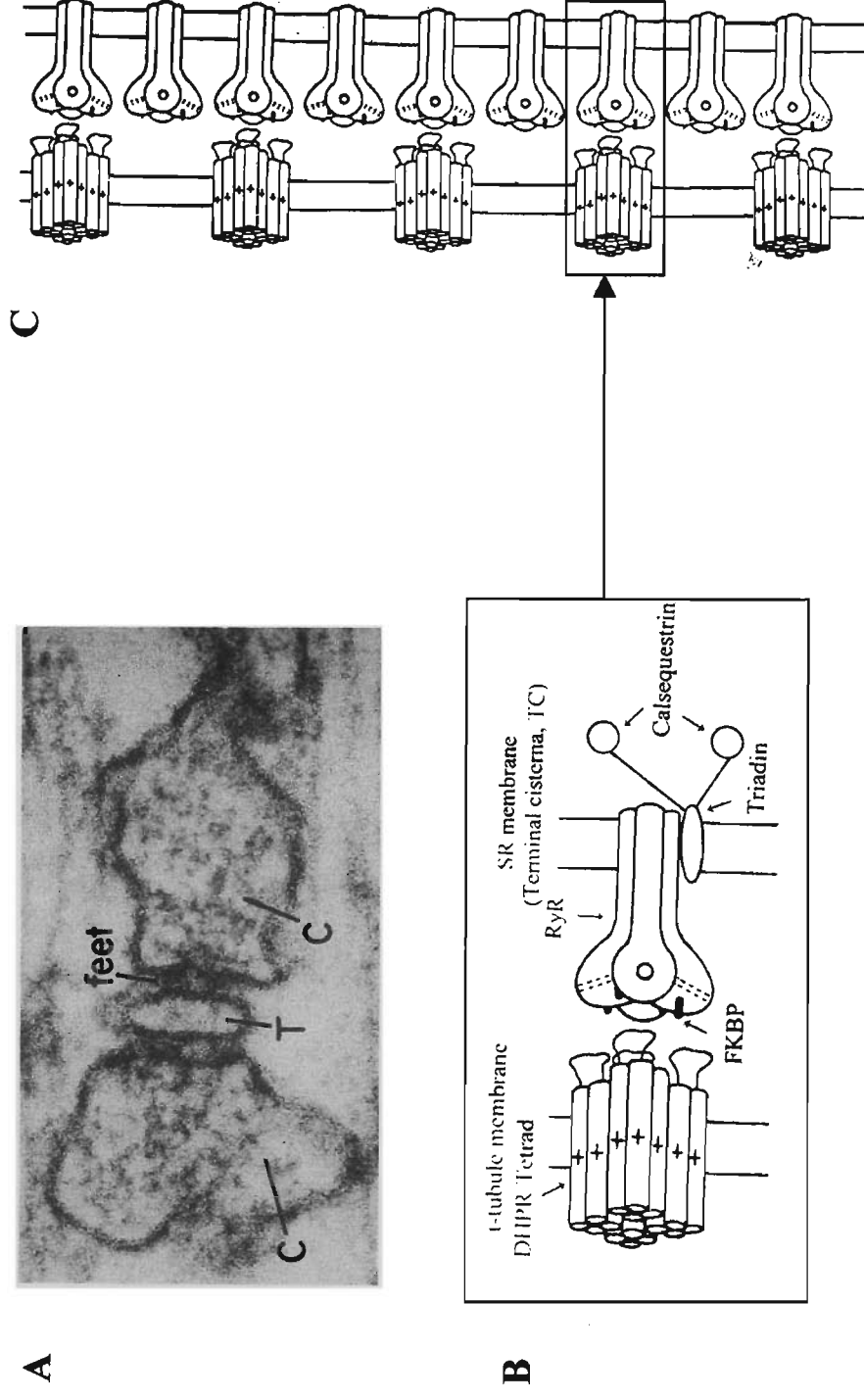


**Figure 1.4** A. Cross-sectional view of a triad (x 300,000). The T tubule (T) in the center is flanked by the two TC of the SR (C) (reproduced from Martonosi, 1994). B. Diagrammatic representation of the protein complexes believed to be involved in the detection of the signal produced by the T-system depolarisation (modified from Herrmann-Frank *et al.*, 1999). C. Diagrammatic representation of the relative position of RyR and DHP receptors at triads of skeletal muscle (modified from Herrmann-Frank *et al.*, 1999).

RyR with calsequestrin) (Lamb, 1999). Details of the SR proteins believed to be involved in the detection of the signal produced by T-system depolarisation are shown in the diagram in Fig. 1.4B.

The actual mechanism(s) involved in transmission of the excitatory signal from the DHP receptors to the RyRs is (are) not fully understood although many have been hypothesised (Melzer *et al.*, 1995; Herrmann-Frank *et al.*, 1999). For example, it is known that under resting physiological conditions,  $Mg^{2+}$  (1 mM) exerts an inhibitory action on  $Ca^{2+}$  release, by binding to a low-affinity inhibitory site on the RyRs and keeping them closed despite a strong stimulatory effect of ATP on channel opening (Stephenson *et al.*, 1995). A mechanism proposed for transmission of the impulse is that the depolarisation signal is sensed by the tetrad and is transmitted via the four cytoplasmic loops to the RyR to cause a 10-20 fold decrease in the affinity of the RyR inhibitory site for  $Mg^{2+}$  (Stephenson *et al.*, 1998). This would result in the dissociation of  $Mg^{2+}$  from the inhibitory site on the RyR causing the channels to open under the stimulatory action of ATP, thus allowing  $Ca^{2+}$  release from the SR and further increasing the open time of the channel (see section 1.2.1.2).

It is interesting to note that, regardless of the mechanism involved in signal transmission between DHP receptors and RyRs, each tetrad faces one RyR, but only half the RyRs face a tetrad (Fig. 1.4C), implying that half of the RyRs are not under direct voltage sensor control. It has been suggested that the RyRs not coupled to DHP receptors either inactivate rapidly or are non-functional (Stephenson *et al.*, 1995).

In Table 1.2 are listed some of the currently known differences between slow-twitch and fast-twitch muscle fibres with respect to the cellular/molecular structure of

participants involved in excitation events (for details of these differences and of their physiological implication see reviews by Rüegg, 1992; Stephenson *et al.*, 1998). Note that none of these differences has become a criterion for fibre typing.

**Table 1.2 Inter-fibre related differences with respect to the cellular/molecular structure of participants involved in excitation events.**

ST, slow-twitch; FT, fast-twitch.

Structure	Differences	Reference
motor endplate	larger in ST than in FT	Fahim <i>et al.</i> , 1984
Na <sup>+</sup> channels	lower density in ST than in FT	Milton & Behforouz, 1995
T-system (% fibre volume)	lower in ST (0.14) than in FT (0.27)	for review see Rüegg, 1992
DHP receptors	fewer (3-5 times) in ST than in FT	Delbono & Meissner, 1996
jSR (% fibre volume)	lower in ST (0.96) than in FT (1.62)	for review see Rüegg, 1992
SR total (% fibre volume)	lower in ST (3.15) than in FT (4.99)	for review see Rüegg, 1992
RyR closed time	longer in ST than in FT	Lee <i>et al.</i> , 1991
SR luminal [Ca <sup>2+</sup> ]	higher in ST than in FT	Fryer & Stephenson, 1996
number of calsequestrin isoforms	2 in ST versus 1 in FT	Damiani & Margreth, 1994

#### 1.3.1.1 Effectors of Ca<sup>2+</sup> release from the SR

The rate of Ca<sup>2+</sup> release from the SR depends on the number, conductance, average opening time and opening frequency of the SR Ca<sup>2+</sup> release channels, and on the electrochemical gradient for Ca<sup>2+</sup> across the SR membrane (Stephenson *et al.*, 1998). Since most research efforts in this area have been focused on modulators of channel opening time, only effectors of Ca<sup>2+</sup> release from the SR will be discussed in this section.

The identity and mechanism of action of endogenous modulators of electrochemical  $\text{Ca}^{2+}$  gradient across the SR membrane are less well known because the  $\text{Ca}^{2+}$  concentration within the jSR depends on a number of parameters which include: the activity of the SR  $\text{Ca}^{2+}$  pump (see section 1.3.3), the rate of  $\text{Ca}^{2+}$  efflux from the SR and the concentration and binding properties of sarcotubular  $\text{Ca}^{2+}$ -binding proteins such as calsequestrin.

*Endogenous modulators.* The average open time of the SR  $\text{Ca}^{2+}$  release channel appears to be modified by a number of endogenous factors such as  $\text{Mg}^{2+}$ ,  $\text{Ca}^{2+}$ , ATP, pH, phosphorylation, inorganic phosphate, calmodulin and lipid metabolites (Stephenson *et al.*, 1995), but the mechanism of action and physiological relevance of most of these factors are not well known. This section will draw attention to the modulators whose effect on the SR  $\text{Ca}^{2+}$  release is more fully understood, namely  $\text{Ca}^{2+}$ ,  $\text{Mg}^{2+}$ , ATP and calmodulin.

Calcium ions have been shown to affect SR  $\text{Ca}^{2+}$  release in a biphasic manner, being activatory at low concentrations (up to 100  $\mu\text{M}$ ) and inhibitory at higher concentrations (for review see Herrmann-Frank *et al.*, 1999). Based on these data it has been postulated that SR  $\text{Ca}^{2+}$  release channels contain two types of binding sites for  $\text{Ca}^{2+}$ : high affinity binding sites (activatory) and low affinity binding sites (inhibitory), where the low affinity binding sites also bind  $\text{Mg}^{2+}$ . In contrast to  $\text{Ca}^{2+}$ , magnesium ions and ATP do not affect the  $\text{Ca}^{2+}$  release channel in a dose-dependent manner. It has been reported that  $\text{Mg}^{2+}$  inhibits SR  $\text{Ca}^{2+}$  release and this inhibition appears to be due to either  $\text{Mg}^{2+}$  induced reduction in the affinity of  $\text{Ca}^{2+}$  for the

activatory sites or to the binding of  $Mg^{2+}$  to the inhibitory sites. The mechanism of action of ATP on the  $Ca^{2+}$  release channel is not well known; however it has been shown that ATP and  $Ca^{2+}$  are both required to fully activate the channel and a number of potential nucleotide binding sites have been postulated (Fig. 1.5 and see Herrmann-Frank *et al.*, 1999).

The effect of calmodulin on the SR  $Ca^{2+}$  release channel is not dependent on its concentration but on its molecular form. Thus,  $Ca^{2+}$  free calmodulin activates the  $Ca^{2+}$  release channels, thereby promoting  $Ca^{2+}$  release, whereas the  $Ca^{2+}$  calmodulin complex inhibits the process. These effects involve the binding of either of the two forms to several (up to nine) sites tentatively located in the C-terminal half of the protein (see Fig. 1.5 and for review see Herrmann-Frank *et al.*, 1999).

*Caffeine.* Caffeine (1,3,7 trimethylxathine; FW: 194.2;  $pK_a$  0.8) is one of the best pharmacological modulators of SR  $Ca^{2+}$  release. Due to its neutrality at physiological pH and its low molecular weight, caffeine can easily penetrate biological membranes and therefore can be used on a variety of muscle preparations: (i) whole muscle, (ii) intact muscle fibres, (iii) preparations in which the SR compartment is accessible to external regulators (skinned muscle fibre preparation, isolated SR vesicles) and (iv) purified channels incorporated into lipid bilayers. Experiments carried out with these types of preparations have shown that:

- (i) in intact muscle preparations (whole tissue or single fibres), caffeine induces potentiation of twitch responses at low concentrations (0.1-2 mM) and contracture at high concentrations (eg.  $\geq 3.6$  mM) (Horowicz, 1994),

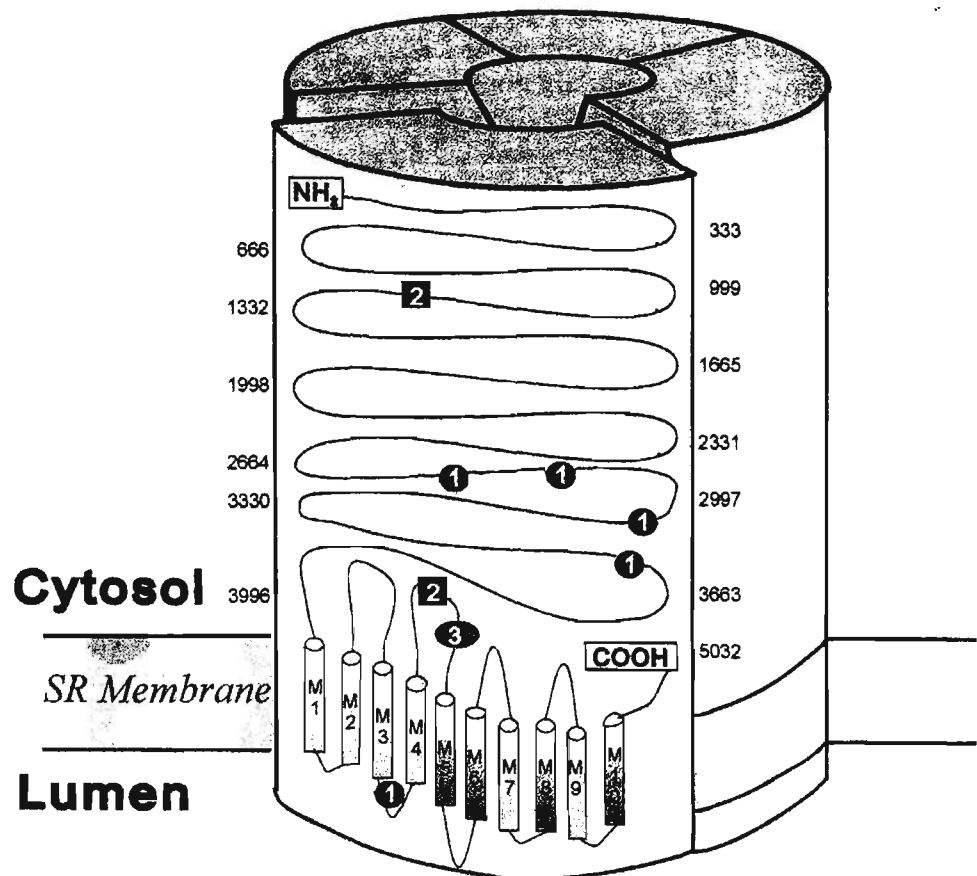


**Figure 1.5** Scheme of the mammalian skeletal muscle ryanodine receptor showing potential calmodulin binding sites (1), potential nucleotide binding sites (2) and Ca<sup>2+</sup> activation sites (3) (as it can be deduced from the sequence of the human receptor and from electron microscopy data) (modified from Herrmann-Frank *et al.*, 1999). For details regarding position of naturally occurring mutations and phosphorylation sites see Herrmann-Frank *et al.*, 1999.

- (ii) caffeine acts directly on the jSR in SR vesicles and its effect is positively correlated with the  $\text{Ca}^{2+}$  content of the SR and with the ambient temperature (Isaacson *et al.*, 1970),
- (iii) caffeine acts directly on the  $\text{Ca}^{2+}$  release channels as shown by Rousseau *et al.* (1988) using purified channels incorporated into planar lipid bilayers.

An important concept used in muscle research involving caffeine is 'the caffeine threshold for contractile activation', which refers to the lowest concentration of caffeine producing a defined force response. Caffeine thresholds have been determined in a variety of muscle preparations which include whole muscles, bundles of fibres, single intact and skinned fibres (for review see Herrmann-Frank *et al.*, 1999). The force response most commonly used in caffeine threshold determinations is 10% of the maximum  $\text{Ca}^{2+}$ -activated force (Salviati *et al.*, 1989; Mitsumoto *et al.*, 1990; Adnet *et al.*, 1993) although other values (e.g. 5%; Shah *et al.*, 1988; Danieli-Betto *et al.*, 1995) have also been used by some laboratories.

The activatory action of caffeine on the SR- $\text{Ca}^{2+}$  release is the result of an increase in the open time, decrease in the closed time and an increase in opening frequency of  $\text{Ca}^{2+}$  release channels but does not involve a change in their unit conductance. It is interesting to note that despite the advances made in understanding the mechanism of action of caffeine on  $\text{Ca}^{2+}$  release channels, the identity and location of the caffeine binding sites are not yet known.

As has been discussed by Herrmann-Frank *et al.* (1999), recent evidence shows that at high concentrations (>5 mM) caffeine is capable of activating RyR1 in

the absence of endogenous modulators such as  $\text{Ca}^{2+}$ , while at low concentration of caffeine there is an interplay between the effects produced by caffeine,  $\text{Ca}^{2+}$ ,  $\text{Mg}^{2+}$  and ATP on the  $\text{Ca}^{2+}$  release channel. Thus, Sarközi *et al.*, (1998) showed that the response of the RyR1 to caffeine is potentiated by ATP and is inhibited by  $\text{Mg}^{2+}$ , and Murayama *et al.* (1998) showed that low concentrations (<5 mM) of caffeine increase the affinity of the  $\text{Ca}^{2+}$  activation and decrease the affinity of the  $\text{Ca}^{2+}$  inactivation sites for  $\text{Ca}^{2+}$ .

An increased understanding of the cellular mechanism of action of caffeine has enabled researchers to use this drug for probing SR properties in normal muscles and for diagnosing SR abnormalities in diseases such as malignant hyperthermia. In the present study, caffeine thresholds at two different SR- $\text{Ca}^{2+}$  loads (endogenous and maximal) have been used to compare SR properties in spontaneously hypertensive rats (SHR) and their age-matched normotensive controls (see Chapter 6).

### 1.3.2 Contraction, myofibrillar proteins and methods used to study myofibrillar proteins

As introduced in section 1.1, myofibrils are the contractile elements of the muscle cell. Each myofibril has been found to comprise two major types of filaments, thick and thin. The thick filaments are composed largely of contractile protein, myosin, while the thin filaments are composed of actin and the regulatory proteins, tropomyosin (Tm) and the troponin (Tn) complex. As will be described in section 1.3.2.5, the mechanical performance of a muscle cell is the result of the complex cyclical interaction between myosin, ATP and actin, regulated by  $\text{Ca}^{2+}$  via the

regulatory proteins.

It is now well established that all myofibrillar proteins that play a role in muscle contraction exist in different molecular forms (isoforms), which can be examined using SDS-polyacrylamide gel electrophoresis. The source of myofibrillar protein polymorphism varies. Some isoforms are products of different genes (eg. one of the subunits that make up the Tn complex), while others are generated from the same gene by different splicing patterns (eg. another subunit in the Tn complex). Before discussing in detail the protein components of the thin and thick filaments, and results of electrophoretic studies on muscle protein isoforms, a brief introduction into the basic concepts in gel electrophoresis will be given.

#### 1.3.2.1 Basic concepts in gel electrophoresis

Electrophoresis is a powerful biochemical method used to separate proteins and other macromolecules such as RNA and DNA. When placed in an electric field these charged molecules will move in solution towards the electrode of opposite charge, with a speed (referred to as electrophoretic mobility) which depends on their charge, shape and size. The majority of current electrophoretic techniques are carried out in acrylamide or agarose gels; this allows not only the separation of species of interest but also their detection as bands on the gel matrix.

Polyacrylamide is the most common matrix used for the separation of proteins as it is chemically inert. A polyacrylamide gel is formed by the polymerisation of the acrylamide (A) monomer with the methylenebisacrylamide cross-linker reagent (B)

into long chains that are covalently cross-linked. Polymerisation is initiated with ammonium persulfate and the catalyst, N,N',N',N'-tetramethylethylenediamine (TEMED). The pore size of any given polyacrylamide gel is determined by two parameters which can be controlled experimentally. These parameters are: (i) the total concentration of monomer used to produce the gel (%T; A + B expressed as %, w/v), and (ii) the proportion of %T represented by the cross-linker (%C; ratio of B/T expressed as %). For any given %C, increasing/decreasing %T will result in gel with smaller/larger pores. In contrast, varying %C for any given %T, will affect the gel pore size in a biphasic manner. Thus an increase in %C up to 5% will decrease the pore size, while a further increase in %C over 5% will produce an increase in the pore size as well as a disorganisation of the gel matrix (Allen *et al.*, 1984).

The most commonly used gel system in protein electrophoresis is a discontinuous system which comprises two separate gels (stacking and separating gel) of different pH (stacking gel-pH 6.8, separating gel-pH 8.8), different pore size (stacking gel %T =3-4%, separating gel %T  $\geq$ 6), and three buffers (stacking gel buffer, separating gel buffer and running buffer) which differ with respect to pH and ionic composition. In such a system the proteins first stack, in the stacking gel, into a very thin zone between the leading ion (usually Cl<sup>-</sup>) from the stacking gel buffer and the trailing ion (usually glycine) from the running buffer. As the leading ion, proteins and trailing ion enter the separating gel, their relative mobility changes such that Cl<sup>-</sup> and glycine migrate ahead of the proteins; this allows individual proteins in a protein mixture to separate according to size, shape and charge (Allen *et al.*, 1984).

*SDS-PAGE separation of proteins.* Sodium DodecylSulfate-PolyAcrylamide Gel Electrophoresis (SDS-PAGE), as developed by Laemmli (1970) (for technical details see Appendix 1), is probably the most popular electrophoretic techniques common for separating proteins. SDS (an anionic detergent) not only denatures proteins, but also masks the intrinsic charges of the proteins under study. As a result, the shape and charge of the proteins are the same and separation occurs only according to differences in molecular weight.

### 1.3.2.2 Major proteins in the thin filament

Quantitative studies have shown that actin makes up to 20% of the myofibrillar protein while Tm and the Tn complex, represent about 8% (Pearson & Young, 1989). In skeletal muscle, globular actin monomers (MW~ 42 kDa) aggregate to form long, double-helical filamentous polymers with a defined polarity. Two elongated Tm dimers (each with a MW~ 35 kDa) form a helical filament that lays in the major groove of the actin filament and spans seven actin monomers as shown in Fig. 1.6A. In a non-contracting (relaxed) muscle Tm covers the myosin binding sites on actin, thereby inhibiting the interaction between the active site of actin in the thin filament and the myosin head of the thick filament.

One molecule of the Tn complex occurs for every seven actin monomers, and consists of three different subunits: troponin T (Tn T; MW~30 kDa), troponin I (Tn I; MW~21 kDa) and troponin C (Tn C; MW~18 kDa), with each subunit believed to have a different physiological role (Fig. 1.6A) (Craig, 1994). Tn T is the Tm-binding

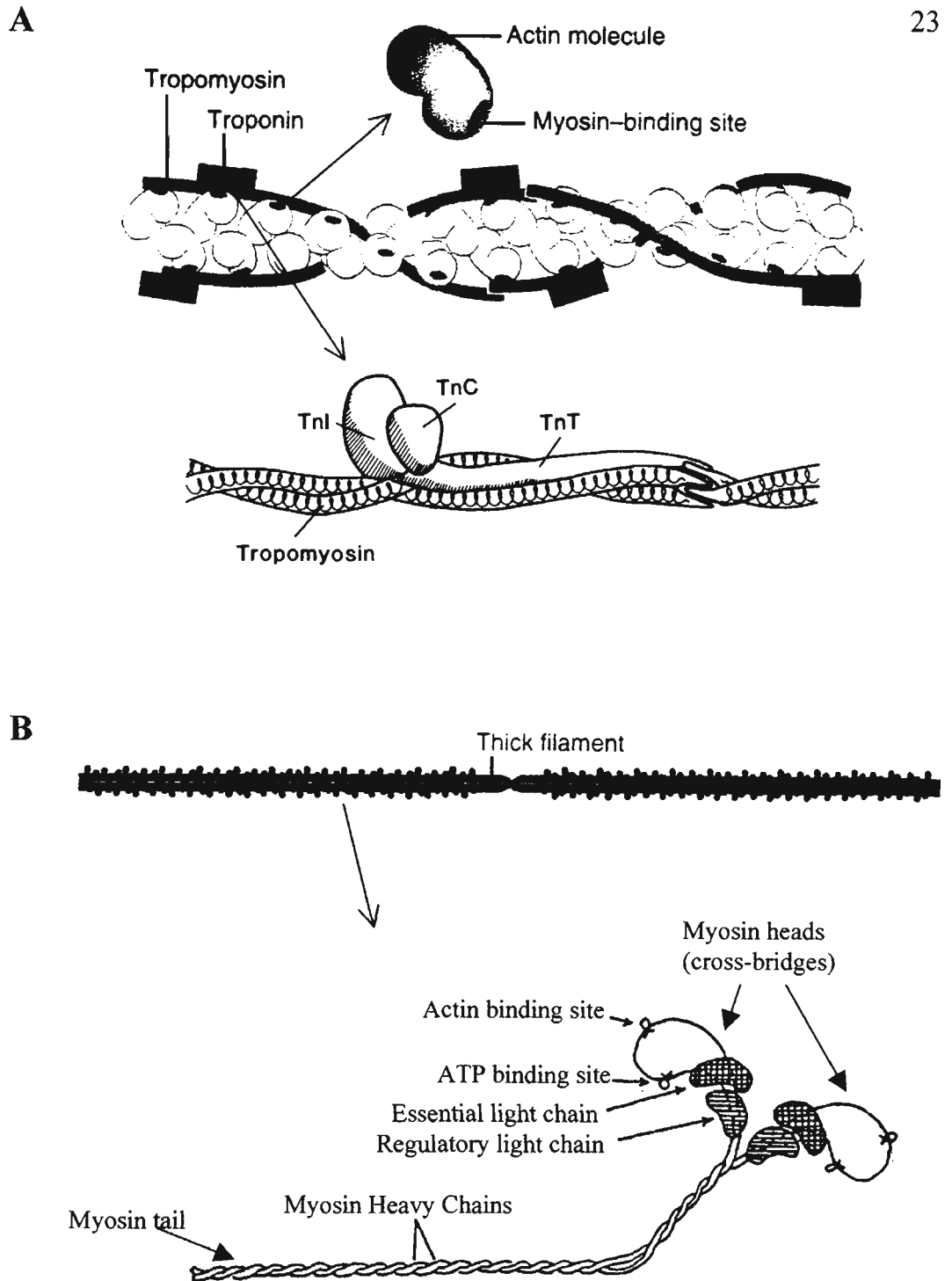


**Figure 1.6 Basic structure of thin and thick filaments.** A. Diagrams showing the major components of the thin filament (actin, Tm and Tn complex) (modified from Tortora & Grabowski, 1996) and the proposed interaction between Tm and Tn subunits (Craig, 1994). B. Thick filaments contain myosin molecules shaped like two intertwined golf clubs with their long shafts coiled together to form a thick tail and with their heads sticking out (modified from Tortora & Grabowski, 1996; Eddinger, 1998). Note the location of the essential and regulatory light chains.

subunit, which also binds to Tn C, but its precise role in muscle contraction is unclear. Tn I, the inhibitory subunit, can bind actin and inhibit the actin-myosin interaction in the absence of any of the other troponin subunits. This inhibition is enhanced in the presence of Tm and becomes reversible and  $\text{Ca}^{2+}$ -sensitive when the intact Tn complex is present. Tn C, which is the  $\text{Ca}^{2+}$ -binding subunit, can also bind to Tn I and Tn T and possibly to actin. In the presence of  $\text{Ca}^{2+}$  ions Tn C can remove the inhibition of actin-myosin interaction that Tn I imposes on the thin filament (Schiaffino & Reggiani, 1996). As will be discussed in the following section, all regulatory proteins (tropomyosin, Tn T, Tn I and Tn C) have been found to occur in various molecular forms which differ with respect to molecular weight ('molecular weight variants') or charge ('charge variants'). Although much work has been performed to date on these regulatory proteins their precise physiological role in muscle contraction is still not fully understood.

*Isoforms of regulatory proteins.* Tropomyosin had been shown to exist as two molecular weight variants,  $\alpha$  and  $\beta$ , which can assemble as  $\alpha\alpha$ ,  $\beta\beta$ -homodimers or  $\alpha\beta$ -heterodimers. Furthermore, fast and slow isoforms of the  $\alpha$  subunit have also been detected (Tm- $\alpha$ fast and Tm- $\alpha$ slow). The complexity of the tropomyosin system may even be greater, as it is believed that Tm- $\beta$  may also exist as fast and slow isoforms (Pette and Staron, 1990).

The same complexity has been found with respect to Tn T isoform expression. To date 10 isoforms of Tn T have been identified by SDS-PAGE, two slow (Tn T-s), four fast (Tn T-f) and four cardiac (Tn T-c) (Schiaffino & Reggiani, 1996).

In contrast to Tm and Tn T, Tn I appears to be less complex, thus, there are only three known isoforms of Tn I, fast (Tn I-f), slow (Tn I-s) and cardiac (Tn I-c). In skeletal mammalian fibres, Tn C exists in two isoforms, one slow (Tn C-s) and one fast (Tn C-f) that have major differences in the  $\text{Ca}^{2+}$  binding regions. As a result, Tn C-f contains four divalent cation binding sites (two high affinity  $\text{Mg}^{2+}/\text{Ca}^{2+}$  binding sites and two low affinity  $\text{Ca}^{2+}$  binding sites), while Tn C-s contains only three of these sites (lacks one of the low affinity  $\text{Ca}^{2+}$  binding site) (for review see Moss *et al.*, 1985). Tn C-s and Tn C-f isoforms differ also with respect to their relative affinity for  $\text{Ca}^{2+}$  and  $\text{Sr}^{2+}$  (Ebashi & Endo, 1968), which translates into different sensitivity of the contractile apparatus to  $\text{Sr}^{2+}$  and  $\text{Ca}^{2+}$  in fibres containing predominately or exclusively one of the Tn C isoforms. This difference has been creatively used as a rapid physiological method for fibre typing by Takagi & Endo (1977) and Fink *et al.* (1986) (for details see section 1.4). It is important to note that in this study Tn C isoforms could not be separated and visualized using general SDS-PAGE protocols. This has also been reported by other laboratories (Babu *et al.*, 1986; Metzger, 1996).

### 1.3.2.3 Major proteins in the thick filament

The thick filament is composed mostly of myosin, which makes up to 54% of myofibrillar protein (Craig, 1994). Myosins exist as a large superfamily of proteins which can be grouped into 15 distinct groups based on phylogenetic analyses. The myosins that form filaments in muscles cells, which will be discussed throughout this study, are classed as conventional class II myosins. The other superfamilies are all

composed of other non-conventional myosins (Sellers, 2000). Each myosin II molecule consists of two heavy chains (each of MW ~ 200 kDa) and four light chains (each of MW from 16-30 kDa) (Syrový, 1987) and is shaped like two intertwined golf clubs with their long shafts coiled together to form a thick tail with two protruding heads (see Fig. 1.6B). The myosin heavy chain head contains the ATP- and actin binding sites and is connected to the long tail by a thin neck to which two myosin light chains (MLCs) are bound. The four myosin light chains which are associated with the two myosin heads, consist of two essential (alkali) light chains, LC1 and/or LC3, and two regulatory (phosphorylatable) light chains, LC2. Each myosin head comprises an essential and a regulatory MLC (see Fig. 1.6B). Like the protein components of the troponin-tropomyosin regulatory system, MHCs, essential MLCs and regulatory MLCs are coded for by multigene families and have been found to exist as electrophoretically distinguishable isoforms (see below).

#### 1.3.2.3.1 MLC isoforms

As listed by Schiaffino & Reggiani (1996), mammalian skeletal muscle contains two regulatory MLC isoforms, MLC2fast (MLC2f) and MLC2slow (MLC2s), and five major essential MLC isoforms, two of which exist in fast skeletal muscle fibres (MLC1f and MLC3f), two in slow skeletal muscle fibres (MLC1slow-b and MLC1slow-a) and one in developing skeletal muscle and in cardiac muscle (MLC1embryonic/atrial).

### 1.3.2.3.2 MHC isoforms

To date ten MHC molecular weight variants have been identified in mammalian muscle fibres based on protein and mRNA analyses (d'Albis & Butler-Browne, 1993; Pette & Staron, 1990). These include:

- two 'developmental' MHCs,  $MHC_{emb}$  and  $MHC_{neo}$  - found in the developing and regenerating muscle fibres, particularly embryonic and neonatal muscles respectively.
- one slow-tonic isoform:  $MHCI_{ton}$ , found in the slow-tonic fibres of rat extraocular and jaw-closing muscles.
- one slow-twitch isoform:  $MHCI$  (also referred to  $MHCI\beta$ ).

Note: Recently Fauteck & Kandarian (1995) reported that the commonly observed MHC I band can be separated into two bands:  $MHC I\beta$  (so named as it co-migrates with cardiac  $\beta$ -MHC) and  $MHC Ia$ , which has a higher mobility than  $MHCI\beta$ . This finding was later confirmed by Hämäläinen & Pette (1996) who also noticed a faint band that migrated slightly faster than MHC I on SDS-PAGE. Hämäläinen & Pette dismissed the possibility that this faint band was the  $\alpha$ -cardiac MHC isoform, as preliminary immunohistochemical studies with an antibody raised against  $\alpha$ -cardiac MHC produced negative results.

Galler *et al.* (1997a) reported that the  $MHC Ia$  isoform possesses slower kinetic properties than  $MHC I\beta$ , a result recently confirmed by Thompson & Brown (1999). The exact number of  $MHCI$  isoforms expressed in adult twitch skeletal muscle is still unclear given the results of Yu *et al.* (1998), who

showed that soleus fibres from young hyperthyroid female rats contain an  $\alpha$  cardiac-like myosin isoform with a lower electrophoretic mobility than the MHC I isoform.

- one 'cardiac-type' slow isoform: MHC $I\alpha$  - found in the extraocular, diaphragm and masseter muscles.
- three fast-twitch isoforms: MHCIIa, MHCII $d$ , MHCIIb - of increasing electrophoretic mobility
- two 'super-fast' isoforms: MHC<sub>com</sub> and MHCII $m$  - found in superfast-contracting fibres of extraocular and laryngeal muscles and in masticatory muscles, respectively.

The four MHCs: MHCIIa, MHCII $d$ , MHCIIb and MHC $I$ , which are regarded as the predominant isoforms in adult mammalian skeletal muscles, will be discussed in this study.

*MHC isoform nomenclature.* It is important to note that, for unknown reasons, different research groups tend to develop their own nomenclature rather than adopting the set of names generated when the MHC isoforms were first identified. For example when MHCII $d$  was first identified by Bär & Pette (1988) it was labelled as MHCII $d$ . Later on, Schiaffino *et al.* (1989) labelled this isoform as type 2X. Since then MHCII $d$  has been referred to under different names such as IId (Sugiura *et al.*, 1993; Hämäläinen & Pette, 1995), IIX (Talmadge & Roy, 1993; Sullivan *et al.*, 1995), IId(x) (Pette *et al.* 1999), IIX (Haddad *et al.*, 1997), 2X (Schiaffino *et al.*, 1989; Prezant *et al.*, 1997) and 2X/D (Snoj-Cvetko *et al.*, 1996). This inconsistency in nomenclature becomes

very confusing when comparing papers concerned with MHC expression. The confusion is further amplified by the inconsistent use of nomenclature for fibre types. For example, a single fibre containing both MHC isoforms IId and IIb has been referred to as type IIXB (Sant'Ana Pereira *et al.*, 1997) or type IIx/IIb (Caiozzo *et al.*, 1997).

The nomenclature used in this study for MHC isoforms and fibre types is that used by Hämaläinen & Pette (1988) i.e. MHC isoforms IIa, IId, IIb and I, and fibre types IIA, IID, IIB and I. Fibre types expressing more than one isoforms (eg. IIa and IId) are referred to as type IIA+IID.

#### 1.3.2.3.3 Myosin isoforms (isomyosins; myosin isozymes)

Given the large number of possible MHC and MLC isoforms, it is not surprising that myosin (the hexamer comprising 2 MHCs and 4 MLCs) exists also as different isoforms. For example, in an early study of Hoh (1975) it was shown that fast and slow rat skeletal muscles contain two molecular forms of myosin (isomyosins) that can be distinguished by non-denaturing gel electrophoresis (see below). It is important to note that isomyosins are also referred to as myosin isoenzymes (d'Albis *et al.*, 1982) or myosin isozymes (Gillespie *et al.*, 1996), because as will be explained in section 1.3.2.5, myosin has an intrinsic ATPase activity.

According to Pette & Staron (1990), about 19 isomyosins have been identified in mammalian skeletal muscles by non-denaturing gel electrophoresis. These include nine fast isomyosins (FM1a, FM1d, FM1b, FM2a, FM2d, FM2b, FM3a, FM3d,

FM3b), three slow isomyosins (SM1, SM2, SM3), three developmental isomyosins (eM1, eM2, eM3), three neonatal isomyosins (nM1, nM2, nM3), a family of muscle specific isomyosins (IM) and a group of special fast and slow isomyosin reported for specialised muscles of the cat and rat.

#### 1.3.2.4 Biochemical analysis of myofibrillar protein isoform composition and fibre typing

##### 1.3.2.4.1 Myosin isoform composition

As already mentioned, isomyosins can be separated electrophoretically under non-denaturing conditions using the sodium pyrophosphate gel method developed by Hoh (1975). The method involves the use of a continuous gel system (one gel, one buffer) in which  $T\%=3.36$ ,  $\%C=4.8$ , the buffer contains in addition to Tris and glycine, ATP and glycerol, samples are solubilised in 50% glycerol, and the gels are run at  $\sim 8^{\circ}\text{C}$ . It is not easy to determine the number of fibre types that could be identified by this method; however according to Pette & Staron (1990), the occurrence of at least 60 combinations of MHCs and MLCs would be possible if one considered only MHCI, MHCIIa, MHCIIb, MLC1s, MLC2s, MLC1f, MLC2f and MLC3f.

##### 1.3.2.4.2 Regulatory protein and MLC isoform composition

The separation of regulatory proteins and MLC isoforms by SDS-PAGE can be achieved easily, particularly if gradient gels are being used. It is interesting to

note, however, that inter-fibre differences with respect to regulatory and/or MLC isoform composition have not been used as criteria for fibre typing.

#### 1.3.2.4.3 MHC isoform composition

MHC isoform composition of whole muscle or single fibre preparations can be detected using immunohistochemistry or SDS-PAGE and has become a widely preferred method for fibre typing.

*Detection of MHC isoforms by SDS-PAGE.* Detection of MHC isoform composition by SDS-PAGE can be carried out with whole muscle homogenates, crude myosin extracts, purified myosin and segments of single muscle fibres. The separated isoforms can be identified based on relative migration, by co-migration with purified proteins or by positive immuno-staining of protein bands on Western blots. It is important to note that single muscle fibres can express one MHC isoform only (pure fibres) or a combination of two or more MHC isoforms (hybrid fibres).

The first electrophoretic analysis of MHC isoforms by SDS-PAGE was reported by Carraro & Catani (1983), who detected two MHC isoforms (fast and slow) in purified myosin from rat skeletal muscle. In this study Carraro & Catani used a slightly modified version of the Laemmli protocol (1970) in which 25% glycerol was included in the separating gel. Further improvement of the Laemmli method by Danieli Betto *et al.* (1986) (for details of these modifications see Appendix 5.1), who used both purified myosin and single fibre segments, allowed separation of three

MHC isoforms, I, IIa and IIb and identification of three pure muscle fibre types, I, IIa and IIb, and two hybrid fibre types, I+IIa and IIa+IIb. In 1988, Bär and Pette, using the Laemmli gel system (1970) and gradient gels discovered a third fast MHC isoform (MHCIIId), which was detected in ten different rat muscles. This discovery and widespread awareness that MHCIIId isoforms could comigrate with either MHCIIa or MHCIIb prompted: (i) reconsideration of muscles and fibres previously classified based on their MHCIIa and MHCIIb content (for review see Pette & Staron, 1990) and (ii) the pursuit of gel systems which allowed for effective and reproducible separation of all four MHC isoforms. The issue of effectiveness and reproducibility of MHC isoform separation by SDS-PA gel systems has been addressed in the study presented in Chapter 3.

*Detection of MHC isoforms by immunohistochemistry.* MHC isoform analyses by immunohistochemistry have been carried out in whole muscle cryosections (Schiaffino *et al.*, 1989), in single fibre segments and along the length of an individual muscle fibre (Edman *et al.*, 1988). An important aspect of this method involves the production of monoclonal antibodies specific for individual MHC isoforms which display minimum cross reactivity. Whole muscle cryosections (~10µm thick) or single fibre segments are then incubated with a battery of antibodies and checked for positive reactivity. When the antibody for a given MHC isoform is not available (as has been the case for MHCIIId) and when this isoform does not react with any of the available antibodies, its presence in a cryosection or single fibre segment is deduced from the negative reaction produced by the cryosection/fibre with the non-reacting

antibodies. This type of 'negative' staining technique was first used on cryosections of rat skeletal muscle by Schiaffino *et al.* (1989).

Using immunohistochemistry, the MHC isoform antibodies available in 1991, and a population of 74 single fibres from adult rat muscles, Bottinelli *et al.* (1991) identified all four pure fibre types (I, IIA, IIB and IID). Although no hybrid fibres were detected in this study, the authors stated that MHC-based immunohistochemistry should be able to identify some hybrid fibres (such as I+IIA, IIA+IIB and I+IIB), but not others (such as IIA+IID and IID+IIB) as an antibody specific for MHC IId is not yet available.

#### 1.3.2.5 Molecular events in skeletal muscle contraction

As already stated, the mechanical performance of a muscle cell is the result of a complex series of  $\text{Ca}^{2+}$ -regulated cyclical interactions between myosin heads (acting as cross-bridges between the thick and thin filaments), actin and ATP. The alignment of the filaments in the myofibrillar region gives rise to the unique pattern detected in muscle fibres by low-magnification electron microscopy (see Fig. 1.7). This pattern consists of alternating dark and light regions intersected by a number of lines. The dark regions known as A bands, are regions occupied by overlapping thick and thin filaments; within the A band is the H zone, which appears less dense than the rest of the A band and contains only thick filaments. Dividing the H zone is a region of higher density called the M line that consists of myosin heads linking adjacent thick filaments together.

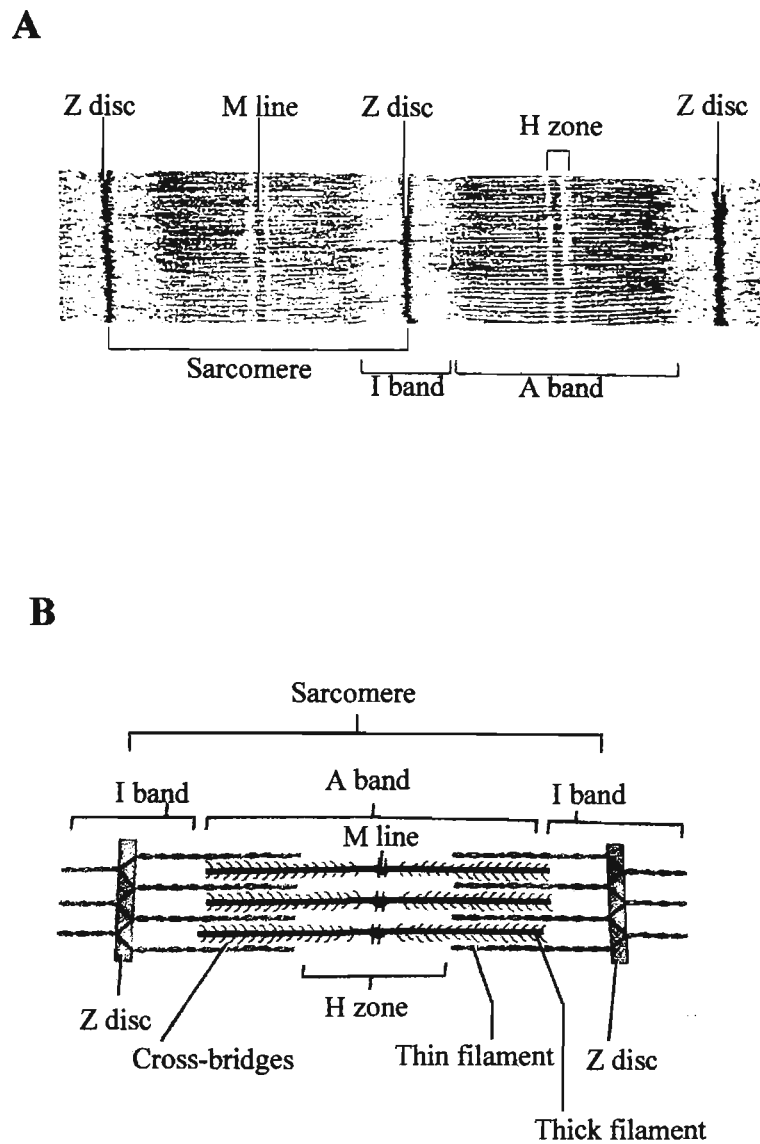


**Figure 1.7 Sarcomere pattern of mammalian skeletal muscle.** A. Electron micrograph of two sarcomeres consisting of light and dark regions (reproduced from Tortora & Grabowski, 1996). B. Diagrammatic presentation of the regions detectable in the structure of the sarcomere (modified from Tortora & Grabowski, 1996).

The light regions known as I bands consist of thin filaments only, where the I band is divided by a dark line referred to as the Z disc/line. The region between two adjacent Z lines is referred to as a sarcomere; the sarcomere which comprises a central A band flanked by two half I bands represents the contractile unit of a muscle fibre. In a relaxed mammalian muscle fibre the sarcomere length is about  $2.6\mu\text{m}$  (Bagshaw, 1982).

The amazing speed at which muscles contract depends upon the thick and thin filaments being held in correct alignment and at an optimal distance from each other. This is made possible by several structural proteins which include  $\alpha$ -actinin (the actin cross-linking protein that anchors the actin filaments to the Z discs), nebulin, (a large protein that regulates the assembly and length of thin filament) and titin (a spring like protein extending from the thick filaments to the Z disc, that keeps thick filaments centred in the sarcomere and gives sarcomeres their elastic quality).

It is now well established that the sequence of molecular events that lead to contraction is the same in all skeletal muscle fibres regardless of the fibre type. These events include: (i) ATP hydrolysis by myosin ATPase activity, (ii) ATP hydrolysis-induced conformational changes in the myosin molecule, particularly in the head-neck region (activation of cross-bridges), (iii)  $\text{Ca}^{2+}$  binding to Tn C and associated conformational change in the Tn-Tm complex (which releases the inhibition of myosin-actin interaction) and (iv) force producing interaction between actin and myosin (power stroke). During the “power stroke” the myosin heads release the products of the myosin ATPase reaction i.e. ADP and  $\text{P}_i$  (Tortora & Grabowski, 1996). Once the power stroke is complete, ATP combines with the ATP-binding sites

on the myosin heads and in doing so it allows for the detachment of the myosin head from actin. This cycle is then repeated for as long as ATP is available and the  $\text{Ca}^{2+}$  level is high around the thin filament. If the sarcomere length of a contracting muscle fibre is not fixed, the thick and thin filaments slide and the muscle fibre shortens. However if the sarcomere length of a contracting muscle fibre is fixed (i.e. during isometric contraction), the power stroke does not result in fibre shortening.

### 1.3.3 Relaxation

The final step in the E-C-R cycle, referred to as relaxation, involves the dissociation of  $\text{Ca}^{2+}$  from Tn C and the endergonic re-uptake of  $\text{Ca}^{2+}$  by the SR. It has been proposed by Gerday & Gillis (1976) that skeletal muscle relaxation involves also parvalbumin, a single  $\text{Ca}^{2+}$  and  $\text{Mg}^{2+}$  binding protein (MW ~12 kDa) located in the cytoplasm, which would act as a 'calcium shuttle' transporting  $\text{Ca}^{2+}$  from TnC to the calcium pump. As has been stated by Rüegg (1992), however, the parvalbumin hypothesis of muscle relaxation is quite controversial and therefore will not be considered further here.

The  $\text{Ca}^{2+}$  pump [also referred to as the SERCA pump (where SERCA stands for sarco/endoplasmic reticulum  $\text{Ca}^{2+}$  ATPase)] is located throughout the SR membrane, except for the jSR regions facing the T tubules. Two  $\text{Ca}^{2+}$  ions are pumped into the SR for every molecule of ATP hydrolysed. The action of the pump is aided by the  $\text{Ca}^{2+}$ -binding protein calsequestrin, which binds  $\text{Ca}^{2+}$ , such that more  $\text{Ca}^{2+}$  is removed from the sarcoplasm (Stephenson *et al.*, 1998). The SERCA pump

occurs as different isoforms; thus, SERCA1a is the major isoform in fast-twitch skeletal muscle and SERCA2a is the major isoform in slow-twitch skeletal muscle (Loukianov *et al.*, 1998). The density and total number of pumps are also muscle fibre related, being smaller in slow-twitch fibres than in fast-twitch fibres. As expected, this results in slow-twitch fibres displaying a much lower rate of  $\text{Ca}^{2+}$  uptake by the SR (for review see Stephenson *et al.*, 1998). It is interesting to note that, like other fibre type related differences in the SR, differences related to  $\text{Ca}^{2+}$  pumps have not been used as a basis for fibre typing.

## **1.4 Skinned fibre preparations and their use in studying events of the E-C-R cycle**

Intact muscle fibre preparations do not allow access to internal compartments involved in E-C-R. To overcome this limitation, single fibres are skinned (demembrated), mechanically or chemically.

The method of mechanically skinning muscle fibres was first used by Natori (1954) who removed the sarcolemma of frog fibres. As described in detail in section 2.3.3, single fibres are mechanically skinned by peeling back the sarcolemma from the main body of the fibre, a process that is accompanied by the spontaneous sealing of the T-system. Mechanically skinned muscle fibres have been successfully used to probe the function of contractile apparatus (eg. Fink *et al.*, 1986), SR (Fryer & Stephenson, 1996), signal transmission between the T-system and the SR (Lamb & Stephenson, 1991) and for fibre typing by using  $\text{Ca}^{2+}/\text{Sr}^{2+}$ -activation parameters (see

next section).

Several methods for chemically skinning a single fibre have been developed, including the treatment/incubation of fibres with glycerol (50%; Brenner, 1998), EDTA (3mM; Winegrad, 1971), EGTA (5-10 mM; Wood *et al.* 1975), saponin (50 µg/mL; Rüegg, 1992) or detergent (eg. 0.5-2% Triton X-100; Brenner, 1998; Williams *et al.*, 1993). It is important to point out that the usefulness of chemically skinned preparations is related to the effect of the skinning agent on molecular participants in the E-C-R cycle. For example, Triton X-100 skinned preparations can be used for determining activation characteristics of the contractile apparatus (for details of these parameters see section 2.4.6.2) but not for probing functions of the T-system or SR because Triton destroys the intracellular membrane systems as well as the sarcolemma. Another limitation of the chemically skinned fibre preparation is that during skinning and storage of the fibre, soluble proteins and metabolites may leach out into the incubation medium (Bagshaw, 1982). All chemically skinned muscle fibre preparations, regardless of the skinning agents used, can be employed for fibre typing by physiological methods.

*Physiological methods for fibre typing.* An early study by Takagi & Endo (1977), performed on guinea pig SOL and EDL muscle fibres, distinguished two groups of fibres, which differed with respect to the sensitivity of the contractile apparatus to  $\text{Sr}^{2+}$ . Based on these findings the authors proposed that inter-fibre differences in sensitivity to  $\text{Sr}^{2+}$ -activation could be used as a criterion for fibre typing. A later study by Fink *et al.* (1986) revealed that mammalian muscle fibres displayed

differences not only with respect to  $\text{Sr}^{2+}$ -sensitivity but also with respect to other contractile activation characteristics such as the Hill coefficients of the force-pCa and force-pSr curves. For definition of these and other contractile activation parameters see sections 2.4.6.2 and 4.2.

## 1.5 Comparison of fibre typing techniques

The techniques for muscle fibre typing described in sections 1.2 (enzyme-based histochemistry and contractile speed) and 1.3.2.4 (MHC composition-based immunohistochemistry), are based on different criteria and have distinct advantages and disadvantages. For example, both enzyme-based histochemistry and immunohistochemistry can be performed on muscle cross-sections, thereby allowing determination of the relative proportion of different fibre types, fibre type localisation within the body of the muscle and fibre size. However, there are some hybrid fibre types that neither of these techniques is able to detect, nor are these techniques able to quantitate MHC expression in the hybrid fibre types they can detect. Further disadvantages of these two methods are related to antibody specificity and to species differences with respect to pH stability of mATPase activity (Pette *et al.*, 1999). Thus, a set of MHC antibodies raised against MHC isoforms of one species may not be useful when used for another species. Alternatively, a set of antibodies raised against one MHC isoform may cross react with other MHC isoforms. Similarly, the pH conditions optimised for one species may not be valid for another species.

As illustrated by the present study, SDS-PAGE can be applied to whole muscle homogenates and single muscle fibres dissected randomly or (if required) selectively from a given muscle. This method allows for: (i) rapid determination of changes in the MHC isoform expression, (ii) detection of pure and hybrid fibres regardless of the number or identity of MHC isoform expressed, (iii) quantitation of the relative proportion of MHC isoforms co-expressed by a single fibre and (iv) estimation of the relative proportion of fibre types in a muscle if the population of dissected single fibres is relatively large. The SDS-PAGE strategy for fibre typing has also a number of disadvantages. Thus, this technique is not able to provide accurate information on the relative proportion of different fibre types within the whole muscle nor on fibre type localisation. Furthermore, as it will be shown in this study (Chapter 3) there are intrinsic problems related to the ability of any of the available gel systems to separate effectively and reproducibly all MHC isoforms. Finally, misclassification of hybrid fibres as pure fibres by SDS-PAGE can occur if one of MHC isoforms is expressed in amounts lower than the detection limit of the staining method employed.

How compatible are different fibre typing methods? A limited survey of studies using different fibre typing methods shows that the degree of compatibility varies according to the methods compared. For example, two methods that have been claimed to be fully compatible are the kinetics of stretch activation and MHC composition determined by SDS-PAGE (Galler *et al.*, 1997b). The implication of this compatibility is that in a later study, Galler (1999) could use results obtained from kinetics of stretch activation experiments to predict the MHC isoform composition of

single fibres.

Fibre typing techniques have also been shown to be incompatible and as result produce conflicting data when used to examine experimentally-induced changes in the fibre type composition of a given muscle. For example, in two similar studies on the effect of corticosteroid treatment on rat diaphragm, van Balkom *et al.* (1997) showed a change in the fibre type proportions and the size of all fibre types using immunohistochemistry, while Sieck *et al.* (1999) showed no change in the fibre type proportions and only a change in the size of type II fibres using histochemistry (mATPase activity).

It is interesting to note that even fibre typing methods reported earlier to show a high degree of compatibility such as mATPase-based histochemistry and SDS-PAGE determination of MHC isoform composition (Staron & Pette, 1986) have been found to be incompatible under certain conditions. Thus, the relationship between the two methods does not appear to hold for a single hybrid fibre containing three MHC isoforms (Sant'ana Pereira *et al.*, 1995).

To date, no comprehensive studies have been performed on the correlation between MHC-based fibre typing (where MHC isoform composition is determined by SDS-PAGE) and the physiological fibre typing method based on differences in contractile activation characteristics. This issue has been the focus of the study described in Chapter 4.

## 1.6 Muscle plasticity

The fibre type composition of a given skeletal muscle can change significantly under the influence of physiological and pathological factors. This property is referred to as muscle plasticity. It is believed that a muscle's plasticity as well as its diversity (as defined in section 1.2), allow the muscle tissue to respond appropriately to a wide spectrum of mechanical demands. This is interesting considering the highly ordered structure and abundance of protein isoforms involved. The assemblage of the various muscle protein isoforms appears to differ markedly between species, strains and muscles and even between individual fibres of a given muscle.

It is now widely accepted that a change in the MHC isoform composition of a given muscle is a useful indicator of muscle plasticity. For example, it has been shown that the MHC isoform composition varies significantly during the course of animal development (Sugiura *et al.*, 1992; Larsson *et al.*, 1993; Pette & Staron, 1997). Other factors that determine and/or regulate the MHC isoform expression of a skeletal muscle include: mechanical demand (e.g. intense exercise), neural activity (as animals learn more complex skills of locomotion), hormonal output, and pathological conditions such as hypertension (Carlsen & Gray, 1987; Gray *et al.*, 1994a & 1994b; Lewis *et al.*, 1994), insulin resistance (Bassett, 1994), diabetes (Rutshmann *et al.*, 1984) and muscular dystrophy (Heene, 1975). In the study described in Chapter 5, MHC isoform and fibre type composition of SOL muscle from spontaneously hypertensive rats (SHR) and normotensive controls (WKY) were examined at three stages of development of hypertension.

The appearance of hybrid fibres is markedly increased during muscle transformation and hybrid fibres are assumed to bridge the gap between pure fibre types. The combinations of MHC isoforms most commonly found in a hybrid fibre (such as I and IIa, IIa and IIc, IIc and IIb) follow the 'nearest neighbour' rule of MHC isoform co-expression that has been proposed to reflect the direction of fibre type transformation I→IIA→IID→IIB (Pette *et al.*, 1999). However, recent studies on slow-to-fast muscle transformation induced by hindlimb suspension and hyperthyroidism (Caiozzo *et al.*, 1998) have discovered hybrid fibres containing 'atypical non-nearest neighbour' MHC isoform combinations (eg. IIB and I).

## 1.7 The aims of this study

The overall aim of this study was to increase our understanding of the diversity and plasticity of skeletal muscles by using (i) normal and functionally impaired muscles of normotensive and spontaneously hypertensive rats, (ii) single, skinned fibre preparations, and (iii) a combination of biochemical (SDS-PAGE analyses of MHC isoform composition in single fibres and whole muscle homogenates) and physiological (single fibre measurements of contractile activation characteristics and caffeine thresholds for contraction) methods. More specifically, this study has addressed the following related research questions (rq):

(rq-1) do hybrid fibres occur in non-transforming muscles of functionally normal adult rats?

- (rq-2) do hybrid fibres containing an 'atypical' combination of MHC isoforms occur in functionally normal, non-transforming rat muscles?
- (rq-3) is there a correlation between fibre type (based on MHC composition) and contractile activation characteristics?
- (rq-4) can either the MHC-based or the  $\text{Ca}^{2+}/\text{Sr}^{2+}$ -activation-based fibre typing method give full information on the structural and functional characteristics of a single fibre, when used by itself?
- (rq-5) how tight is the correlation between MHC and MLC expression in rat skeletal muscle?
- (rq-6) is there a correlation between fibre type (based on MHC composition) and caffeine threshold for contraction?
- (rq-7) do SHR soleus muscles contain a higher proportion of MHCII isoforms than soleus muscles of age-matched normotensive controls?
- (rq-8) does a population of single fibres dissected from SHR soleus muscles contain a larger proportion of type II fibres than a fibre population dissected from soleus muscles of age-matched normotensive controls?
- (rq-9) are functional differences previously reported for soleus muscle in SHR and WKY rats accompanied by differences in functional characteristics of the SR or contractile apparatus?

From the beginning of this study it became clear that several issues regarding the separation of MHC isoforms by SDS-PAGE had to be addressed. As a result,

efforts were directed towards answering the following methodological questions (mq):

- (mq-1) how different with respect to technical details and/or effectiveness of band separation are the SDS-PAGE protocols that have been used in different laboratories, over the last 16 years, to study MHC isoforms?
- (mq-2) how effective are various electrophoretic parameters (such as [acrylamide], [bisacrylamide], %C value, etc.) in altering the separation of MHC isoforms by SDS-PAGE?
- (mq-3) how reproducible are the SDS-PAGE protocols most commonly used for the separation of MHC isoforms?

## Chapter 2

### General Methods

#### 2.1 Animals

The animals used in this study were male rats aged 4-24 weeks. The rats were housed in a temperature controlled environment (22°C) with a 12:12hr light-dark cycle and had access to food and water *ad libitum*. On the day of the experiment, rats were killed by deep halothane inhalation according to the guidelines of Victoria University Animal Experimentation Ethics Committee.

#### 2.2 Preparation of whole muscle homogenates

*Muscle dissection and storage.* Immediately after animals death, the required muscle, extensor digitorum longus (EDL), soleus (SOL) or diaphragm (DPH) (for location of these muscles see Fig. 2.1) was carefully dissected while avoiding cutting or stretching the muscle whenever technically possible, and blotted dry on filter paper (Whatman 1) to remove any excess blood.

For electrophoretic analyses of myofibrillar proteins, the whole muscle was homogenised either immediately post-dissection or after being stored at -20°C for up

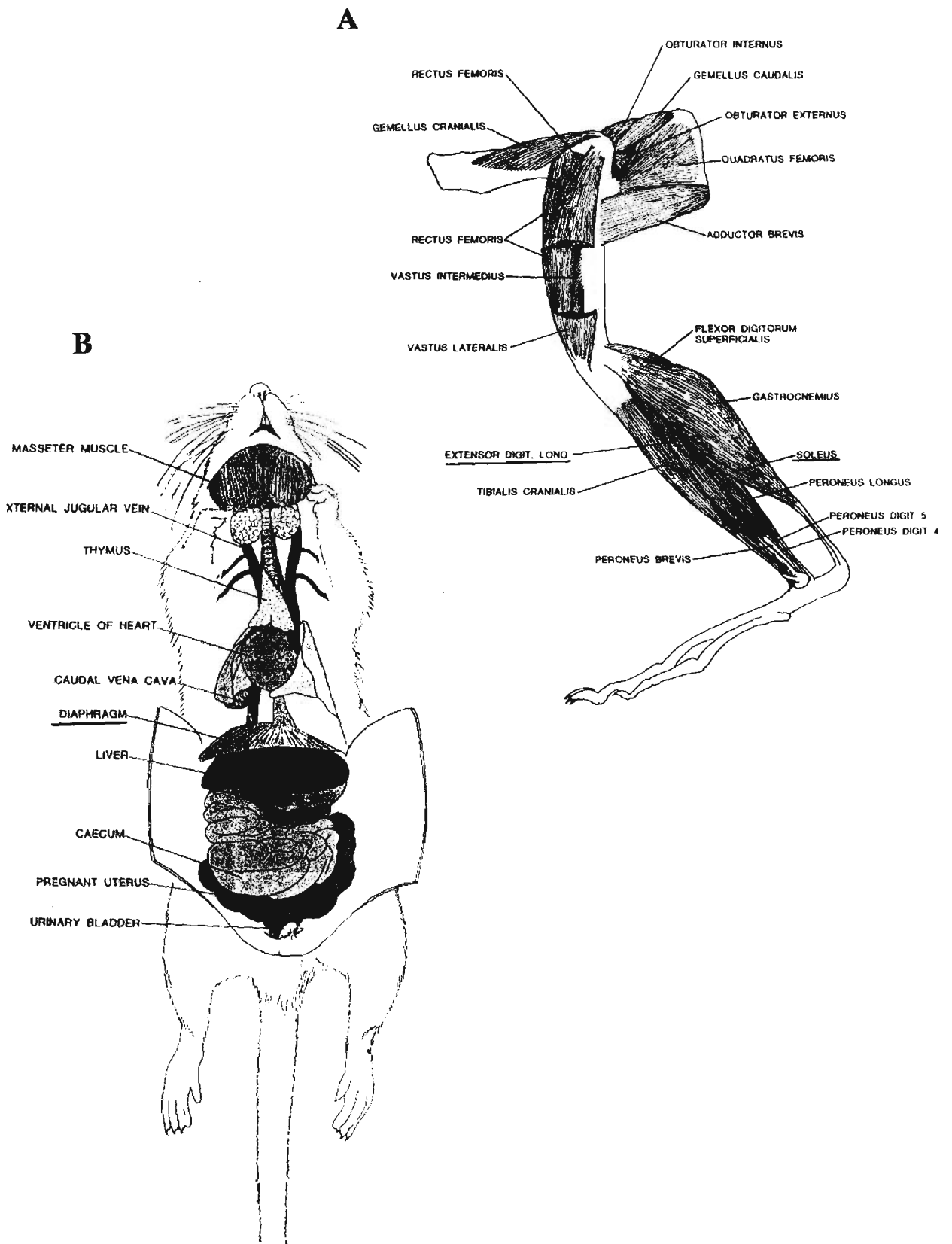


**Figure 2.1** Location of the EDL and SOL skeletal muscles (A) and the DPH muscle (B) (reproduced from Chiasson, 1988).

to two months (for details of the homogenisation protocol see the next section). It should be noted that no qualitative differences were detected in the electrophoretic pattern of myofibrillar proteins between homogenates of fresh and stored muscles. For single fibre analysis, the freshly dissected muscle was placed directly into a Petri dish layered with a bed of Sylgard 184 transparent resin (Dow Corning, USA) and covered with liquid paraffin oil (AJAX Chemicals). While not being used at room temperature (RT; 19-25°C) for fibre dissection and fibre mounting onto the force measuring system (operations that took 15-20 min on average), the muscle preparation was stored at 4-8°C for up to 30 hours. The number of fibres used from one muscle preparation for measuring contractile activation parameters ranged between 5-10.

***Muscle homogenisation.*** The muscle was placed in 6 volumes (where 1 volume  $\cong$  mass of the muscle) of relaxing solution (for details of the composition and preparation of the relaxing solution see section 2.4.5.1) and homogenised with either a manual glass/glass homogeniser or a handheld OMNI TH (Tissue) Homogenizer with a 7mm diameter flat bottom generator probe.

***Protein determination.*** The protein concentration of whole muscle homogenates was determined using the Bradford protein assay (Bradford, 1976) and bovine serum albumin (BSA) as standard.

## 2.3 Preparation of single muscle fibres

### 2.3.1 Dissection of single muscle fibre segments

Freshly dissected muscles were fixed firmly to the Sylgard resin bed with entomological pins inserted into the tendons, for SOL and EDL, and into the outer area of the DPH. Single fibres were isolated under paraffin oil, with the aid of a dissecting microscope (Motic, magnification range 6.4-40, China), fibre optic light source (Euromex, Holland), fine jewellers forceps (No. 5 Dumont, Switzerland) and iris scissors (Vannas, Germany). The strategy for single fibre dissection differed slightly between hindlimb muscles (SOL and EDL), which have a spindle-like shape and retain both tendons post-dissection, and DPH, a sheet-like, almost circular muscle. Briefly, for SOL and EDL the fibre isolation procedure involved the following steps: (i) the Petri dish containing the muscle to be dissected was placed in such a way that the tendon from which dissection would start was closest to the experimenter; this tendon was unpinned/freed, (ii) a small incision was made into the epimysium (the dense, fibrous connective tissue surrounding the entire muscle) to allow free access to bundles of fibres; the incision was made in parallel with the fibres, starting from the free end of the muscle, (iii) a bundle of 5-10 fibres (about 1 cm in length) was partially dissected (one end still being attached to the muscle), and (iv) single fibres were carefully teased away from the body of the bundle, while the free end of the bundle was held down with a pair of forceps. Note that at this point the other end of the single fibre segment was still attached to the muscle. For the

DPH, the procedure for isolation of single fibres was essentially the same as for SOL and EDL, except that the initial incision into the epimysium was made anywhere around the circumference. After isolation, the fibre segment was ready to be skinned (see section 2.3.3) or used unskinned for myofibrillar protein analysis (see section 2.5).

When isolating single fibre segments, the paraffin oil plays three important roles:

- 1) it facilitates the visualisation of the single fibre by having a different refractive index,
- 2) it precludes fibre/swelling-water loss when fibre segments are prepared, and
- 3) it confers the fibre a quasicircular cross-sectional area through the surface tension exerted on the fibre at the fibre/oil interface.

### 2.3.2 Measurement of single muscle fibre segments

A video camera-monitor system (Olympus) and a pair of callipers (Mitutoyo, Japan) (see Fig. 2.2) were used to measure the length ( $l$ ) and width of the fibre segment (in at least three places along its length), on the monitor screen while still under paraffin oil. Distances on the screen were calibrated using a graticule. The volume of a fibre segment was calculated assuming it to be cylindrical with a diameter ( $d$ ) equal to the mean value of the fibre width.

$$volume = \frac{\pi d^2}{4} \times l \quad (\text{Eq 1})$$



**Figure 2.2** Video camera-monitor system used to measure the size of single fibres with a pair of callipers.

### 2.3.3 Skinning of single muscle fibre segments

For determination of contractile activation parameters, the surface membrane of single fibre segments was removed (fibre segments were skinned) by chemical (Chapters 4 and 5) or mechanical (Chapter 6) means. As previously shown (Stephenson *et al.*, 1994), the skinned muscle fibre preparation allows direct activation of the myofibrillar compartment in solutions of carefully controlled free calcium/strontium concentrations.

For chemical skinning a single fibre preparation was first mounted on the force measuring system (see section 2.4.3) and then was incubated for 10 min in a relaxing solution (see section 2.4.5.1) containing 2% Triton. This strategy is known to disrupt cellular membranes without affecting the contractile system (Stephenson *et al.*, 1989).

For mechanical skinning, the outer most layer (assumed to contain endomysium and sarcolemma) was carefully removed, using forceps, starting from the free end of the single fibre, which was held to the bottom of the resin bed with a another pair of forceps. This was achieved by pinching a small region of the outermost layer, and peeling it away until a cuff like structure was produced. Note that at this point the skinned muscle fibre preparation was still attached to the body of the muscle.

## 2.4 Measurement of contractile activation characteristics of single, skinned fibre segments

### 2.4.1 Description of the force measuring system

The apparatus consisted of a micromanipulator (Prior, UK), a microscope (Olympus, magnification range 6.7-40), a chart recorder (Linear, 1 mV-5 V) and a laboratory jack (see Fig. 2.3A). Attached to the micromanipulator were a piezzo-resistive force transducer (Sensoror, Horten, Norway) consisting of two resistors ( $R_1$ ,  $R_2$ ) that formed part of a circuit bridge (for details of the electrical circuit see Fig. 2.3B) and a pair of fine forceps. The other part of the circuit bridge ( $R_3$ ,  $R_4$ ) together with the power supply (PS) and preamplifier (PreA) were built into a separate electronic box (EB). A stainless steel pin was attached with shellac to the force transducer.

All solutions used throughout the experiments were contained in 2.5ml Perspex wells, aligned in a tray that was positioned under a Perspex cover to minimise evaporation of the solutions. The tray cover was attached to a laboratory jack, which enabled the Perspex tray to be elevated or lowered. To ensure that no damage to the fibre would occur while the fibre was being moved through the air-solution interface, the transfer of the skinned preparation from one solution to another, did not exceed 5 seconds (Moisescu & Thieleczek, 1978).

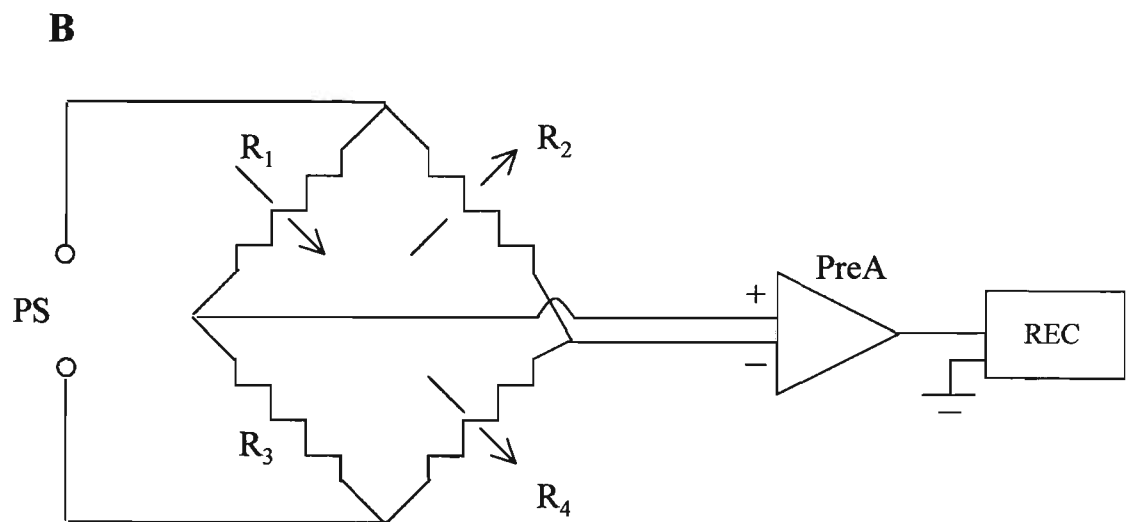
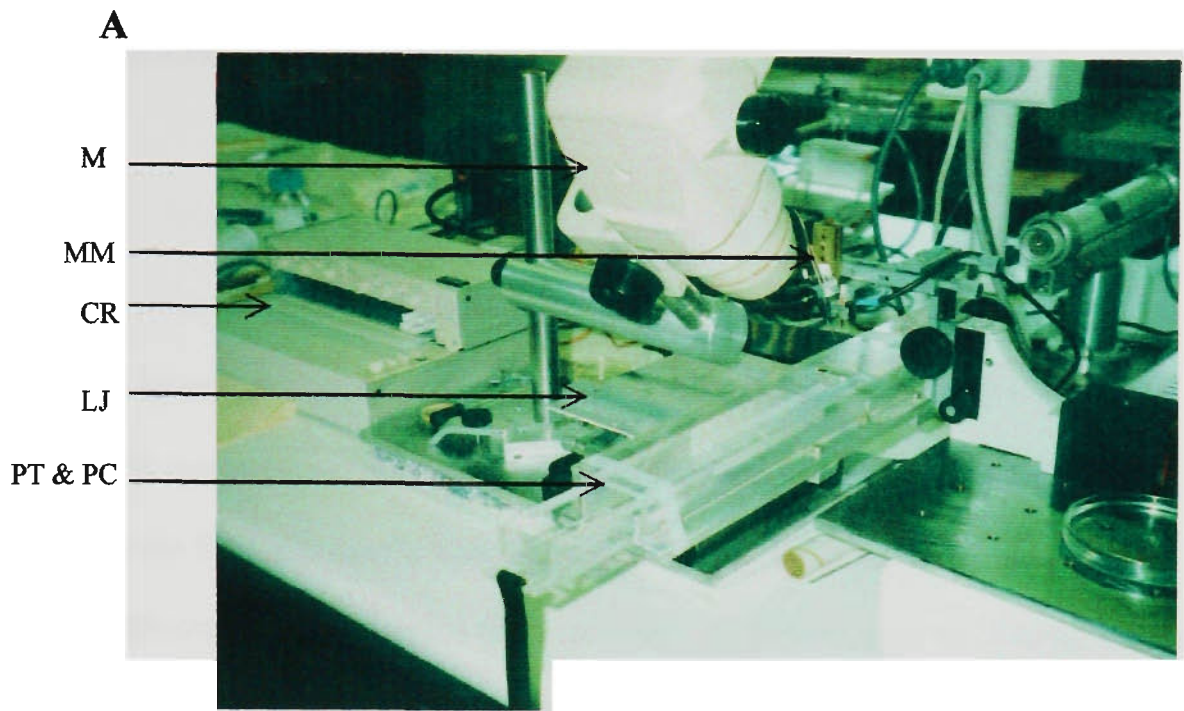


**Figure 2.3 A. Force apparatus.** Consisted of microscope (M), micromanipulator (MM), chart recorder (CR), laboratory jack (LJ), Perspex tray and Perspex cover (PT & PC). (Force transducer, forceps and electronic box not shown). **B. Diagrammatic representation of the electrical circuit.** R<sub>1</sub>, R<sub>2</sub>, strain-sensistive resistors (1 kohm) associated with the transducer; R<sub>3</sub>, fixed resistor (1 k ohm); R<sub>4</sub>, adjustable resistor for balancing the bridge; PS-power supply, 10V DC; PreA-preamplifier; REC-recorder.

## 2.4.2 Calibration of the force transducer

To calculate the force produced by a skinned fibre segment, the force transducer was calibrated with small weights ranging from 66 to  $932 \times 10^{-3}$  N (where  $9.8 \text{ N} = 1 \text{ kg weight}$ ). For this purpose, the micromanipulator was laid on its side, so that the pin was in a horizontal position and each of the weights were placed on the pin where the fibre was usually tied. The signals produced by the force transducer for each weight were recorded on the chart recorder. A calibration curve of signal versus force was constructed (see Fig. 2.4) and the force per chart deflection was calculated to be  $6.28 \times 10^{-6} \text{ N/mm @ } 10 \text{ mV}$ .

## 2.4.3 Attaching single fibre segments to the force measuring system

For measuring contractile activation parameters, the Petri dish containing the skinned fibre segment, still attached at one end to the body of the whole muscle, was placed under the forceps/force transducer setup. The free end of the fibre segment was attached with finely braided surgical silk (Deknatel No.10-0) to the stainless steel pin; the other end was clamped between the tips of the fine forceps and the segment was cut from the muscle immediately under the cuff. To attach the fibre to the pin, a surgeon's knot (double knot; Fig 2.5A) was constructed; the inner knot was then tied to the free end of the skinned single fibre segment, the outer knot was carefully tied to the bottom of the stainless steel pin and the remains of the silk were cut close to the pin (Fig. 2.5B). All these procedures were carried out under the microscope. The tip

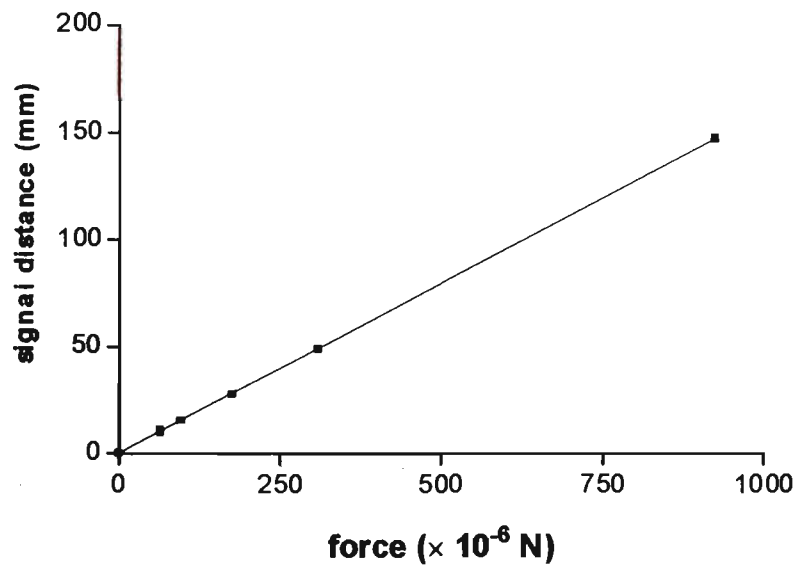


**Figure 2.4 Calibration curve of force transducer.** The signals recorded for each known force were recorded on the chart recorder. Chart speed was 2cm/min;  $r^2=1.000$ .

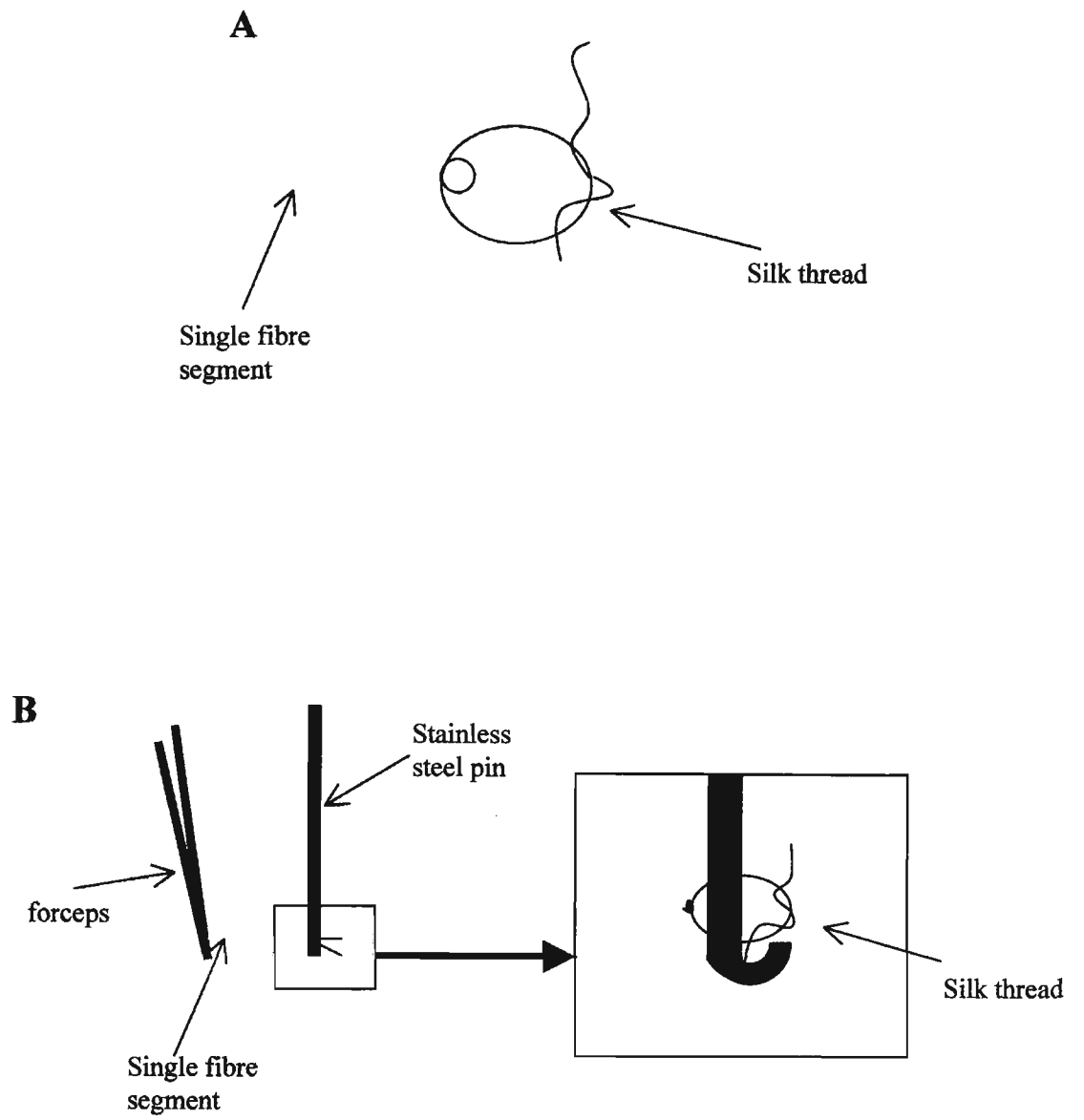


**Figure 2.5 A. Surgeon's double knot. B. Tying the single fibre segment to the stainless steel pin.**

of the forceps and the tip of the pin could be adjusted in three-dimensions to ensure that the fibre was properly aligned with respect to the force transducer. The slack length of the fibre segment was obtained by releasing the slightly stretched fibre until no measurable force could be detected ( $<2.5 \mu\text{N}$ ) and the preparation appeared to be 'taut'.

#### 2.4.4 Measurement of the sarcomere length of a single fibre segment

Average length of sarcomeres in single fibre segments was measured from the diffraction pattern produced by the sarcomeres on an opaque screen when a HeNe laser beam (wavelength =  $0.633\mu\text{m}$ ) illuminated the mounted preparation. The mounted 'taut' fibre was placed into a  $1\text{cm}^3$  spectrophotometric vial containing relaxing solution (see composition in section 2.4.5.1), and the laser beam was positioned to pass through the fibre as shown diagrammatically in Fig. 2.6. The sarcomere length in  $\mu\text{m}$  (SL) was calculated from the following equation:

$$\text{SL} = 0.633 \times \sqrt{\left(\frac{D}{a}\right)^2 + 1} \quad (\text{Eq 2})$$

where  $D$  = distance between fibre preparation and screen and  $a$  = distance between the primary diffraction and the first order diffraction maxima (see also Fig. 2.6).

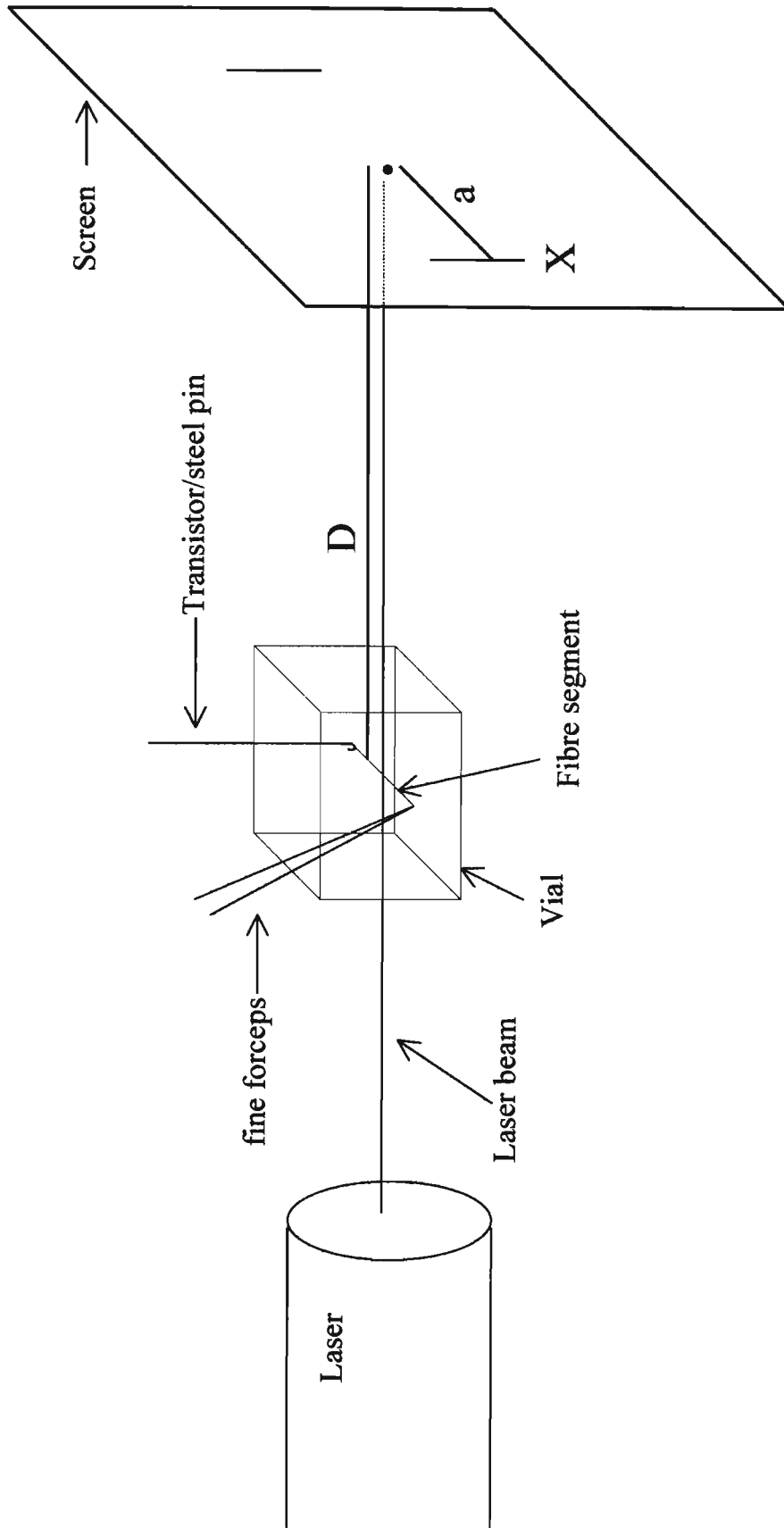


**Figure 2.6** Setup used to measure sarcomere length of single fibre preparations (not drawn to scale).

$D$  = distance between fibre preparation and screen

$a$  = distance between the primary diffraction and the first order diffraction maxima ( $X$ )

## 2.4.5 Activating solutions

### 2.4.5.1 Preparation of solutions for determining $\text{Ca}^{2+}$ - and $\text{Sr}^{2+}$ - activation characteristics

The composition of the bathing solutions used in the skinned fibre experiments (shown in Table 2.1), mimic that of the natural physiological (*in vivo*) environment within the fibre (i.e. the myoplasm) (Stephenson & Williams, 1981).

The strategy used to prepare solutions A (relaxing solution), B (maximally  $\text{Ca}^{2+}$  activating solution), C (preactivating solution) and D (maximally  $\text{Sr}^{2+}$  activating solution) involved the following: (i) HEPES, MgO, EGTA, HDTA,  $\text{CaCO}_3$  and  $\text{SrCO}_3$  were weighed as appropriate and added to the respective beakers, filled with half of the volume of distilled water required (Note: the presence of HEPES, EGTA and HDTA provided the acidic environment necessary for dissolving MgO,  $\text{CaCO}_3$  and  $\text{SrCO}_3$  in solution), (ii) the aforementioned reagents were continuously stirred on low heat (50-60°C) for approximately 30 min and then the solutions were cooled to RT (19-25°C) (Note: after this procedure all carbonate in solution B and D should have been removed), (iii) the required volume of a KOH/ $\text{NaN}_3$  mixture was added to each of the cooled solutions, the pH was adjusted to approximately 6.90 with 4M KOH, and ATP and CP were added as powder, (iv) the volume of each solution was then raised to ~10mL less than the required volume and the pH was adjusted to  $7.10 \pm 0.01$  using 4M KOH, making sure that the final pH value was not overshoot. Finally, the solutions were made up to the required volume and the pH was re-checked. Addition of ATP and CP at a later stage was essential to

ensure that they did not denature at the temperature and pH required to solubilise the other reagents. The final concentration of KOH added to solutions A, C (no carbonate) and B, D (carbonate) were similar indicating that all carbonate had been removed by the heating process. The content of Mg in MgO was checked by Atomic Absorption Spectrophotometry to ensure the appropriate amount of Mg was added to the solutions.

**Table 2.1 Compositions of solutions A, B, C,D, used to measure  $\text{Ca}^{2+}$ - and  $\text{Sr}^{2+}$ - activation characteristics.**

Component	Final concentration of components (mM)			
	A	B	C	D
HEPES	90	90	90	90
$\text{K}^+$	126	126	126	126
$\text{Na}^+$	36	36	36	36
$\text{Mg}_{\text{total}}$	10.3	8.1	8.5	8.5
$\text{EGTA}_{\text{total}}$	50	50	-	50
$\text{HDTA}_{\text{total}}$	-	-	50	-
$\text{Ca}^{2+}_{\text{total}}$	-	48.5	-	-
$\text{Sr}^{2+}_{\text{total}}$	-	-	-	40
$\text{ATP}_{\text{total}}$	8	8	8	8
CP	10	10	10	10
$\text{NaN}_3$	1	1	1	1

Solutions containing different ionised  $[\text{Ca}^{2+}]$  were obtained by mixing the relaxing solution (Solution A; for composition see Table 2.1) with a maximally  $\text{Ca}^{2+}$ -activating solution (Solution B; for composition see Table 2.1) in various proportions

(see Table 2.2; Ashley & Moiescu, 1977). Similarly, solutions containing different  $[\text{Sr}^{2+}]$  were obtained by mixing solution A with maximally  $\text{Sr}^{2+}$ -activating solution (solution D, for composition see Table 2.1) in various proportions (see Table 2.3; Moiescu & Thieleczek, 1978). A preactivating solution (solution 2) prepared by mixing 2mL solution C with 10  $\mu\text{L}$  solution A was also used to facilitate the rapid activation of the skinned fibre preparation (Moiescu & Thieleczek, 1978) and thus minimise deterioration in the fibre induced by prolonged activation (Rees & Stephenson, 1986). For consistency of results, the solutions used for determining contractile activation characteristics as described in section 2.4.6.2 were prepared in bulk at the beginning of each study (Chapters 4, 5, and 6) and stored as individual aliquots at  $-80^{\circ}\text{C}$ .

**Table 2.2 Volumes required to obtain series of  $\text{Ca}^{2+}$ -activating solutions.**

Solution number	vol. solution A ( $V_A$ ) (mL)	vol. solution B ( $V_B$ ) (mL)	vol. solution C (mL)
1	2.00	-	-
2	0.01	-	1.99
3	1.00	1.00	-
4	0.80	1.20	-
5	0.50	1.50	-
6	0.35	1.65	-
7	0.23	1.77	-
8	0.13	1.87	-
9	0.08	1.92	-
10	0.05	1.95	-
11	0.03	1.97	-
12	-	2.00	-

**Table 2.3 Volumes required to obtain series of Sr<sup>2+</sup>-activating solutions.**

Solution number	vol. Solution A (V <sub>A</sub> ) (mL)	vol. solution C (mL)	vol. solution D (V <sub>D</sub> ) (mL)
1	2.00	-	-
2	0.01	1.99	-
3	1.985	-	0.015
4	1.975	-	0.025
5	1.950	-	0.050
6	1.880	-	0.120
7	1.780	-	0.220
8	1.600	-	0.400
9	1.420	-	0.580
10	1.050	-	0.950
11	0.350	-	1.650
12	-	-	2.000

#### 2.4.5.1.1 Titration of solutions for determining Ca<sup>2+</sup>- and Sr<sup>2+</sup>- activation characteristics

The pH and osmolality of all solutions were  $7.10 \pm 0.01$  at 22°C and  $295 \pm 2$  mosmol/kg, respectively. The ionic strength ( $I = \frac{1}{2} \sum c_i Z_i^2$ ) for these solutions was  $234 \pm 2$  mM. The pCa ( $-\log [Ca^{2+}]$ ) or pSr ( $-\log [Sr^{2+}]$ ) of each solution were determined by titrating solutions A, B and D and calculating the [EGTA] in excess of Ca<sup>2+</sup> or Sr<sup>2+</sup> ([EGTA]<sub>excess</sub>). The [Ca<sup>2+</sup>] and [Sr<sup>2+</sup>] were then calculated with Eqs 5 and 8 described below. Manual titration of solutions was used rather than computer programs as this allowed for accurate determination of [Ca<sup>2+</sup>] when using chemicals and water of unknown calcium content.

*Titration of solution A.* The strategy used to titrate solution A involved the following:

(i) 0.05mL of solution A was mixed with 3.95mL of 150mM KCl/60 mM HEPES solution (KCl was necessary to prevent large changes in ionic strength so that all changes in pH would be produced only by the binding of  $\text{Ca}^{2+}$  to excess EGTA), (ii) 40 $\mu\text{L}$  of 1M  $\text{MgCl}_2$  was added to the solution in order to saturate the ATP with  $\text{Mg}^{2+}$  and thus, prevent the liberation of protons from ATP when  $\text{Ca}^{2+}$  is added, before the endpoint of the titration is reached, (iii) the pH of the solution was adjusted to 7.2 with 0.4M KOH, (iv) the solution was titrated with 1 $\mu\text{L}$  aliquots of 0.25M  $\text{CaCl}_2$  (see Fig 2.7A) until only a change of 0.001 pH units was detected, then the titration was completed by adding 4 $\times$ 5 $\mu\text{L}$  aliquots of 0.25M  $\text{CaCl}_2$ . The endpoint of the titration was determined by graphing the results as seen in Fig. 2.7A. To calculate the  $[\text{EGTA}]_{\text{excess}}$ , the amount of  $\text{CaCl}_2$  required to reach the end point ( $\mu\text{moles}$ ) was divided by the initial volume of solution A (mL) (Moiescu & Thieleczek, 1979).

eg. from Fig 2.7A.  $[\text{EGTA}]_{\text{excess of sol. A}} = 2.50\mu\text{moles} / 0.05\text{mL} = 50\text{mM}$ .

*Titration of solution B.* The major difference between solutions A and B, relevant to the titration process, was that solution B contained a markedly lower  $[\text{EGTA}]_{\text{excess}}$ .

To accommodate for this difference, the titration strategy described in the previous section was altered for solution B as follows: (i) 2.0mL of solution B was mixed with 2.0mL 150 mM KCl/60 mM HEPES and 40 $\mu\text{L}$  of 1 M  $\text{MgCl}_2$ . All other steps were identical with those described for solution A and  $[\text{EGTA}]_{\text{excess}}$  was calculated as explained for solution A.

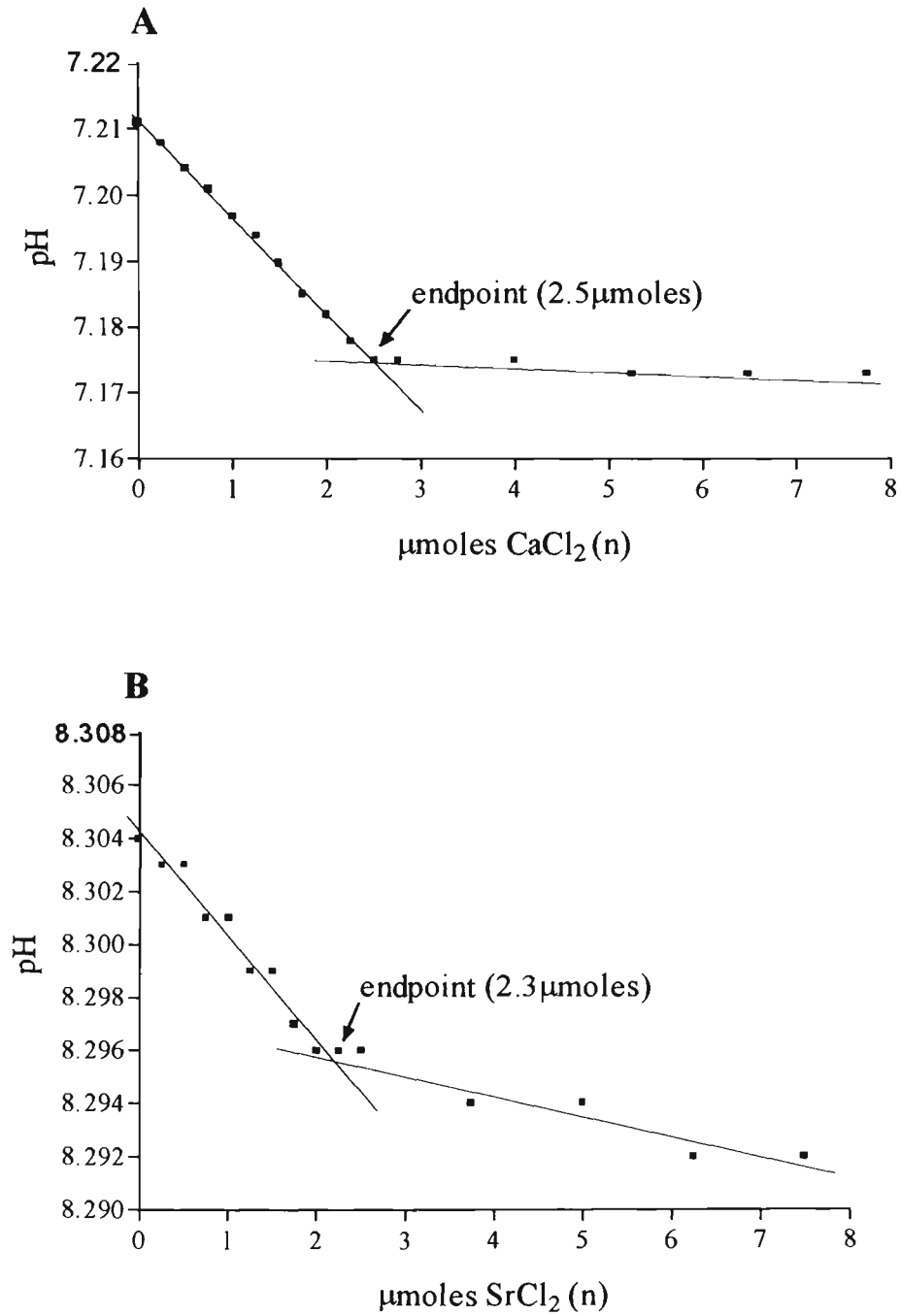


**Figure 2.7** Example of titration curves used to calculate  $[\text{EGTA}]_{\text{excess}}$  in solutions A (panel A), and solution D (panel B).  $[\text{EGTA}]_{\text{excess}}$  is required to determine the pCa and pSr (see Eq 3-8, section 2.4.5.1.1) of the solutions used for contractile activation of single muscle fibres.

*Titration of solution D.* Solution D was titrated as follows: (i) 0.25mL of solution D was mixed with 3.75mL of 150 mM KCl/60 mM HEPES and 40 $\mu$ L of 1 M MgCl<sub>2</sub>, (ii) the pH of the solution was adjusted to 8.3 with 0.4M KOH to ensure that the endpoint was reached above pH 8.1 where the affinity of Sr<sup>2+</sup> for EGTA was sufficiently high, (iv) the solution was titrated with 10 $\times$ 1 $\mu$ L aliquots of 0.25 M SrCl<sub>2</sub> (see Fig. 2.7B), then the titration was completed with 4 $\times$ 5 $\mu$ L aliquots of 0.25 M SrCl<sub>2</sub>. The end point of the titration was determined by graphing the results as seen in Fig. 2.7B. To calculate the [EGTA]<sub>excess</sub>, the amount of SrCl<sub>2</sub> required to reach the end point ( $\mu$ moles) was divided by the initial volume of solution D (mL)

eg. from Fig 2.7B, [EGTA]<sub>excess in sol. D</sub> = 2.30 $\mu$ moles /0.25mL = 9.2 mM.

*Calculation of pCa.* The apparent affinity constant ( $K_{app}$ ) of Ca<sup>2+</sup> to EGTA was assumed to be  $4.78 \times 10^6 \text{ M}^{-1}$ , a value measured earlier by West & Stephenson (1993) for conditions identical to those used in this study.

The pCa values of solutions 3-12, were calculated using the volumes of solutions A and B (as listed in Table 2.2.), the values for [EGTA]<sub>excess</sub> calculated as described in the previous sections and Eq 3, 4 and 5 ( $V_A$ , volume of solution A;  $V_B$ , volume of solution B; Sol. A, solution A; Sol. B, solution B).

$$[\text{EGTA}]_{\text{free}} = \frac{(V_B \times [\text{EGTA}]_{\text{excess of Sol. B}}) + (V_A \times [\text{EGTA}]_{\text{excess of Sol. A}})}{V_{A+B}} \quad (\text{Eq 3})$$

$$[\text{CaEGTA}] = [\text{EGTA}]_{\text{excess of Sol. A}} - [\text{EGTA}]_{\text{free}} \quad (\text{Eq 4})$$

$$[\text{Ca}^{2+}] = \frac{[\text{CaEGTA}]}{[\text{EGTA}]_{\text{free}} \times K_{\text{app}}} \quad (\text{Eq 5})$$

*Calculation of pSr.* The apparent affinity constant ( $K_{\text{app}}$ ) of  $\text{Sr}^{2+}$  to EGTA was assumed to be  $1.53 \times 10^4 \text{ M}^{-1}$ , a value also measured earlier by West & Stephenson (1993) for conditions identical to those used in this study.

It is important to note that in the stock strontium solution (solution D), only 80% of the total EGTA was bound to  $\text{Sr}^{2+}$ , while the other 20% was free ( $\text{EGTA}_{\text{free}}$ ). The pSr values of solutions 3-12, were calculated using the volumes of solutions A and D (as listed in Table 2.3), the values for  $[\text{EGTA}]_{\text{excess}}$  calculated as described in the previous sections and Eq 6, 7 and 8 ( $V_A$ , volume of solution A;  $V_D$ , volume of solution D; Sol. A, solution A; Sol. D, solution D)

$$[\text{EGTA}]_{\text{free}} = \frac{(V_D \times [\text{EGTA}]_{\text{excess of Sol. D}}) + (V_A \times [\text{EGTA}]_{\text{excess of Sol. A}})}{V_{A+D}} \quad (\text{Eq 6})$$

$$[\text{SrEGTA}] = [\text{EGTA}]_{\text{excess of Sol. A}} - [\text{EGTA}]_{\text{free}} \quad (\text{Eq 7})$$

$$[\text{Sr}^{2+}] = \frac{[\text{SrEGTA}]}{[\text{EGTA}]_{\text{free}} \times K_{\text{app}}} \quad (\text{Eq 8})$$

### 2.4.5.2 Procedure used to expose fibre segments to series of calcium/strontium buffered solutions

When measuring contractile activation parameters, the fibre was exposed first to a complete set (12) of  $\text{Ca}^{2+}$  solutions, then to a complete set (12) of  $\text{Sr}^{2+}$  -solutions, and once again to the complete set of  $\text{Ca}^{2+}$  solutions (for preparation of solutions see section 2.4.5). Within each set, the order of solutions and exposure time were as described in the flow chart shown in Fig. 2.8. An example of force responses produced by a fast-twitch single muscle fibre in a complete experiment is shown in Fig. 2.9.

## 2.4.6 Data analysis

### 2.4.6.1 Force measurements

The height of each force response was measured from the baseline generated when the fibre was incubated in the relaxing solution. In order to define the parameters describing the relationship between force and  $\text{Ca}^{2+}$  or  $\text{Sr}^{2+}$  concentrations listed in section 2.4.6.2, the fraction of the maximum  $\text{Ca}^{2+}$ -activated force ( $\text{CaF}_{\text{max}}$ ) or  $\text{Sr}^{2+}$ -activated force ( $\text{SrF}_{\text{max}}$ ) developed by a fibre segment in various activating solutions (% max. force;  $P_i$ ) had to be calculated. This was done by dividing the steady-state isometric force attained in a solution of a particular pCa or pSr by the interpolated value of the maximum  $\text{Ca}^{2+}$ - or  $\text{Sr}^{2+}$ - activated force response as

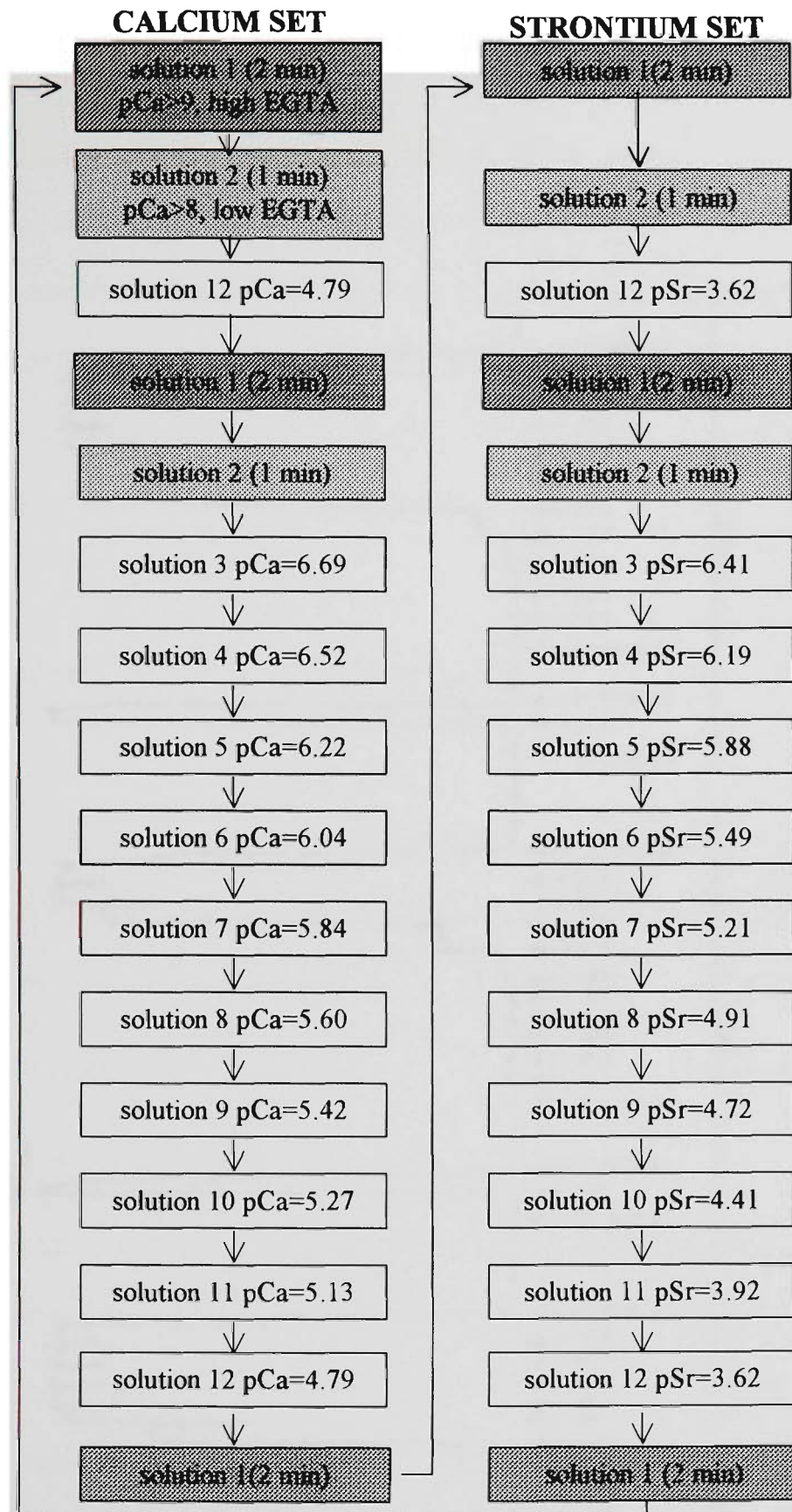


**Figure 2.8 Order of solutions (using 1 batch of solutions) used to determine contractile activation parameters of a skinned fibre preparation.** For proportions of solutions A, B, C and D used to prepare solutions 1-12 in each set refer to Tables 2.2 and 2.3. The fibre segment was exposed to each of the activating solutions (clear boxes) until the maximum response was achieved (<5secs.). Note that solutions 1 and 2 from the calcium set (shaded boxes) were also used for the strontium activation cycle.

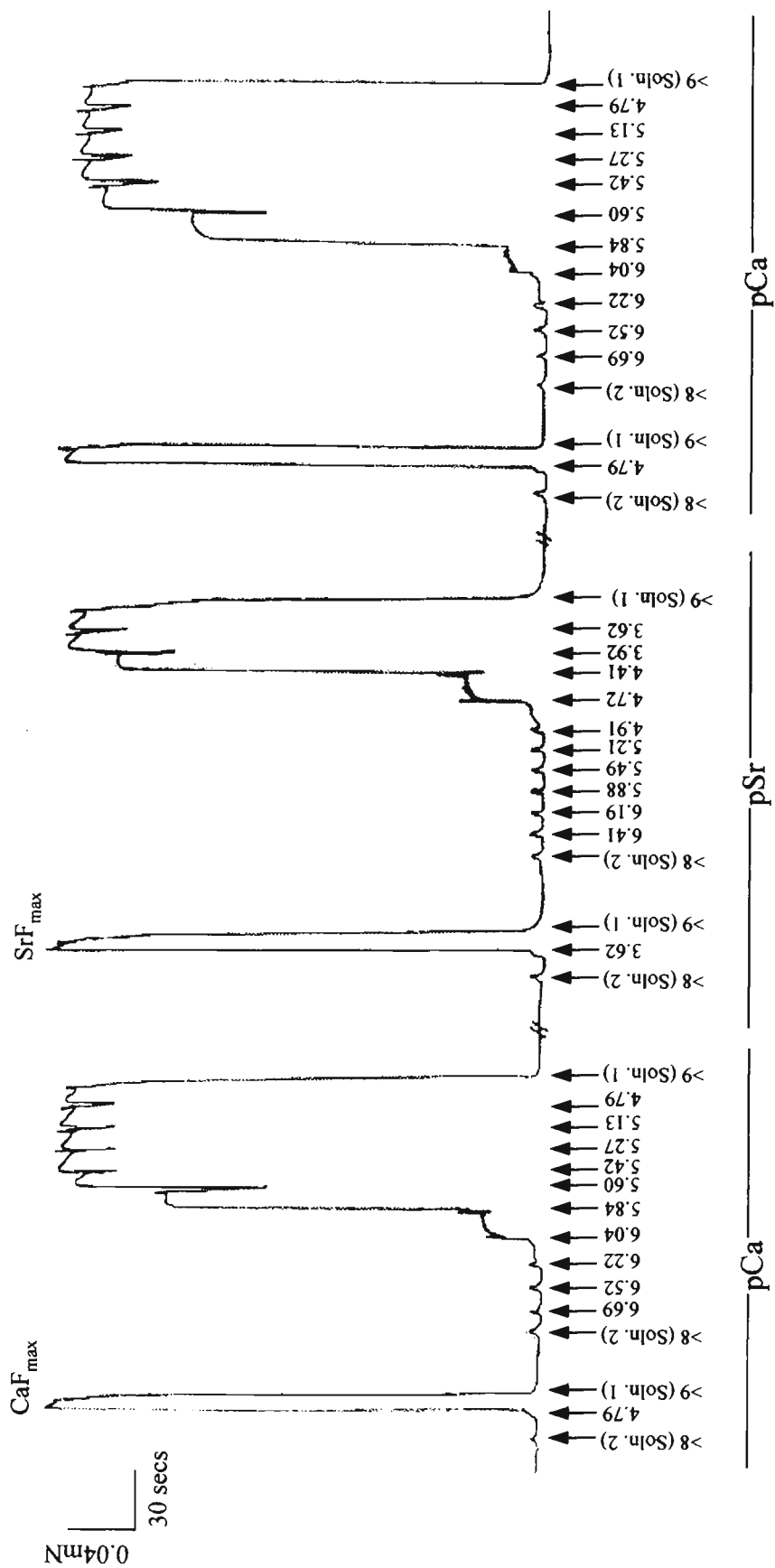


**Figure 2.9** Representative chart recording of force responses produced by a fast-twitch single muscle fibre in a complete experiment. For details of the solutions see section 2.4.5 (Values of pCa and pSr taken from Chapter 4).

described in detail elsewhere (Rees & Stephenson, 1987). This strategy, explained in detail in Fig. 2.10, corrects for the small degree of deterioration in force production associated with the repeated activation of the skinned fibre preparation. For  $\text{Ca}^{2+}$ -activation experiments where two  $\text{Ca}^{2+}$ -activation cycles were performed for each fibre, the average of the two  $P_t$  values obtained for each pCa were used to calculate the contractile activation parameters.

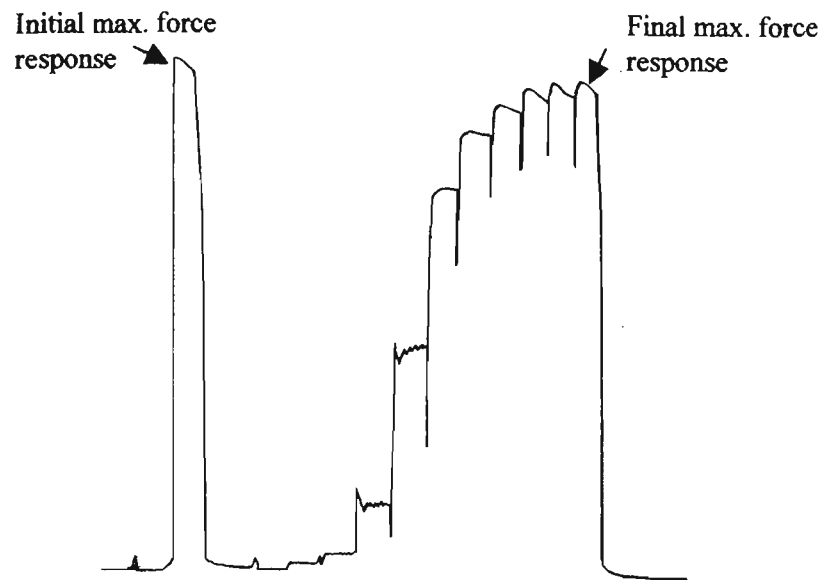
#### 2.4.6.2 Contractile activation characteristics for skinned fibres

Using PRISM software (GraphPad Software Inc.),  $P_t$  was then plotted against the pCa/pSr values in those solutions and theoretical Hill curves of type described by the equation

$$P_t = 1 / [1 + 10^{n_i (x - x_{50})}] \quad (\text{Eq 9})$$

were fitted through the data points using a nonlinear regression analysis protocol (GraphPad Prism software). In Eq 9,  $n_i$  is the associated Hill coefficient,  $x$  is pCa or pSr and  $x_{50}$  is the pCa or pSr value where 50% of the maximum isometric force (pCa<sub>50</sub>, pSr<sub>50</sub>) is reached. In the present study, the curves described by Eq 9 are called 'simple' Hill curves.

As the best computer-fitted simple Hill curves did not pass through all the data points, a criterion had to be defined for deciding what was a 'well-fitted' curve.



Example of calculation

Initial max. force response = 123.7 mm (on the chart recorder)

Final max. force response = 119.4 mm (on the chart recorder)

$\Delta$  (initial max. response - final max. response) = 4.3 mm

Number of activations (N) between initial and final max. responses = 11

Correction factor (CF) for each activation =  $4.3/11=0.39$

Correction factor for the Nth activation ( $CF_{Nth}$ ) =  $0.39\text{mm} \times Nth$

Activation number (Nth)	Force response for the Nth activation (mm)	$CF_{Nth}$	Corrected max. force response (Initial max. response - $CF_{Nth}$ ) (mm)	$P_t$ (% maximum force)	
				Corrected max. force	Non-corrected max. force
2	2.1	0.78	122.92	1.7	1.7
3	4.6	1.17	122.53	3.8	3.7
4	16.3	1.56	122.14	13.3	13.2
5	57.9	1.95	121.75	47.6	46.8
6	93.7	2.35	121.35	77.2	75.7
7	107.1	2.74	120.96	88.5	86.6
8	113.4	3.13	120.57	94.1	91.7
9	117.1	3.52	120.18	97.4	94.7
10	118.6	3.91	119.79	99.0	95.9
11	119.4	4.30	119.40	100.0	96.5

**Figure 2.10** An example of the chart recording produced from a slow-twitch SOL fibre and the calculations necessary in correcting for fibre deterioration between maximum force responses developed within an activation cycle. The same strategy was used for both calcium and strontium activation (Note: trace of slow-twitch fibre is not drawn to scale).

Taking into consideration experimental errors involved in estimating the position of the data points in the force-pCa/pSr plots, it was decided that a well-fitted curve to the data points must pass no further than  $0.05 \text{ CaF}_{\text{max}}$  (or  $\text{SrF}_{\text{max}}$ ) from individual data points in the force-pCa (pSr) plots. Therefore, if the force-pCa and force-pSr plots for a particular fibre were deemed to be well-fitted by the best curve derived from the simple Hill equation (Eq 9), that fibre was classified as a 'simple' fibre. For all fibres investigated in this study, the range of force-pCa data points for the two complete sets of data, lied no further than  $0.05 \text{ CaF}_{\text{max}}$  from simple Hill curves, i.e. all fibres examined were simple fibres with respect to  $\text{Ca}^{2+}$  activation.

It is important to note that in Chapter 4, fibres were examined for both  $\text{Ca}^{2+}$  and  $\text{Sr}^{2+}$ -activation characteristics and that some of these fibres did not fit the 'simple' fibre category with respect to  $\text{Sr}^{2+}$ -activation. Details of the strategy used to analyse the data for such fibres are given in Chapter 4.

The following activation parameters were determined for each individual fibre segment:

- (i) maximum  $\text{Ca}^{2+}$ -activated force per cross sectional area ( $\text{CaF}_{\text{max}}/\text{CSA}$ ;  $\text{kN}/\text{m}^2$ ), determined from the amplitude of the first force response of a mechanically skinned fibre in the maximally  $\text{Ca}^{2+}$ -activating solution and from its estimated cross-sectional area measured in paraffin oil before exposure to aqueous solution,
- (ii)  $\text{pCa}_{10}$  (activation threshold for  $\text{Ca}^{2+}$ ), the pCa where 10% of  $\text{CaF}_{\text{max}}$  was produced,
- (iii)  $\text{pSr}_{10}$  (activation threshold for  $\text{Sr}^{2+}$ ), the pSr where 10%  $\text{SrF}_{\text{max}}$  was produced,

- (iv)  $pCa_{50}$  (sensitivity to  $Ca^{2+}$ ), the  $pCa$  where 50% of  $CaF_{max}$  was produced,
- (v)  $pSr_{50}$  (sensitivity to  $Sr^{2+}$ ), the  $pCa$  where 50% of  $SrF_{max}$  was produced,
- (vi)  $n_{Ca}$  (minimum number of cooperating  $Ca^{2+}$ -binding sites) (Stephenson & Williams, 1981),
- (vii)  $n_{Sr}$  (minimum number of cooperating  $Sr^{2+}$ -binding sites),
- (viii)  $pCa_{10} - pSr_{10} = \log([Sr^{2+}]/[Ca^{2+}])$  ( $\Delta_{10}$ , relative threshold for  $Ca^{2+}$  and  $Sr^{2+}$ ) and
- (ix)  $pCa_{50} - pSr_{50} = \log([Sr^{2+}]/[Ca^{2+}])$  ( $\Delta_{50}$ ; relative sensitivity to  $Ca^{2+}$  and  $Sr^{2+}$ ).

## 2.5 SDS-PAGE analysis of single muscle fibres or whole muscle

### 2.5.1 Set up of electrophoresis equipment

All SDS-PAGE analyses were performed on the Hoefer 260 Mighty Small unit (Fig. 2.11B). Only a brief description will be given of the electrophoresis setup, because all details regarding the preparation of gels and set up of the unit are provided in the Hoefer 260 product manual. The gels were prepared manually at RT using  $10 \times 10.5$  cm glass plates, 0.75mm spacers and the SE 235 multiple gel caster (see Fig. 2.11A). The heights of the 2 gels were 8.8 cm (separating gel) and 2.0 cm (stacking gel). All ingredients were mixed in a conical flask and the polymerising agents, ammonium persulfate (AP) and N,N,N',N'-tetramethylethylenediamine (TEMED), were added last. If the gel was used on the same day, the separating gel was overlaid with distilled water and the stacking gel was poured after 2 hours. If the gel was used the following day, the layer of water was replaced with 0.2% SDS

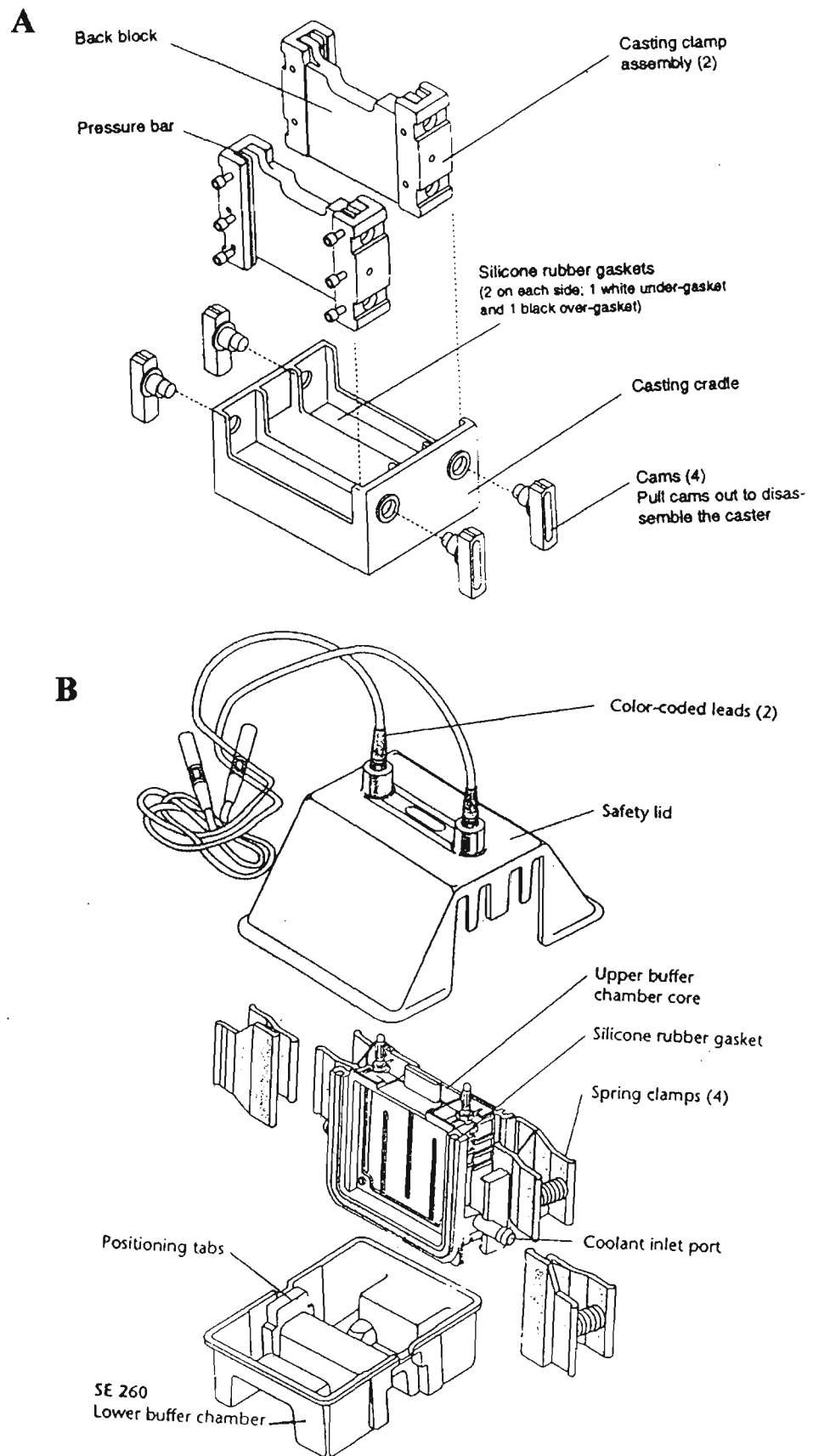


**Figure 2.11 Electrophoresis equipment.** A. The gels were prepared manually using the SE 235 multiple gel caster. B. Gels were run in the SE 260 electrophoresis setup (reproduced from Hoefer Gel Electrophoresis Unit Instructions).

and the gel was left covered overnight. The stacking gel was formed using a 15-well comb and allowed to set for 45-60 minutes. After the stacking gel was set, the comb was carefully removed to avoid damaging the wells and the remaining unpolymerised polyacrylamide solution was removed from the electrophoretic wells using strips of filter paper cut to fit the shape of the wells. Once clean, the wells were filled with the appropriate running buffer (running buffer for upper chamber).

Following the loading of samples, the appropriate running buffer was placed into the lower chamber, the lid was placed in position and the unit was connected to the power supply.

At the end of the electrophoresis run, the power supply was turned off, the setup was dismantled, the gel plates were carefully separated, the stacking gel was removed and the separating gel was further treated as described in section 2.5.3.

## 2.5.2 Sample preparation

The single fibres to be analysed by SDS-PAGE were placed in 12 $\mu$ L SDS-PAGE solubilizing buffer (62.5 mM Tris, 2.3% SDS, 5%  $\beta$ -mercaptoethanol, 12.5% glycerol, 13.6% sucrose, 0.01% bromophenol blue, 0.1 mM phenyl methylsulfonyl fluoride, 2  $\mu$ M leupeptin, and 1  $\mu$ M pepstatin) either immediately after dissection under paraffin oil or after first being examined for contractile characteristics as described above. In both cases, the single muscle fibre segments were incubated in the solubilising buffer for 24 hrs at room temperature and then boiled for 5 min. The MHC-composition of single muscle fibres was examined by loading in each

electrophoretic well a 6  $\mu\text{L}$  sample aliquot containing the equivalent of 0.025-0.05 nL fibre/ $\mu\text{L}$ . For MLC composition analyses, a 10  $\mu\text{L}$  sample aliquot containing the equivalent of 0.3-0.4 nL fibre/ $\mu\text{L}$  was loaded per electrophoretic well.

To analyse MHC or MLC expression in whole muscle homogenates (prepared as described in section 2.2), each homogenate was diluted with SDS-PAGE solubilising buffer and boiled for 5 min. The MHC composition of a whole muscle homogenate was examined by loading in each electrophoretic well a 6  $\mu\text{L}$  sample aliquot containing 0.05 mg protein/mL. For MLC composition analyses a 10  $\mu\text{L}$  sample aliquot containing 0.15 mg protein/mL was loaded per electrophoretic well.

To aid in identification of the MHC composition of muscle homogenates and single fibres, a laboratory MHC marker containing all 4 MHC isoforms was prepared by mixing 0.05 mg protein/mL of each of the solubilised homogenates of SOL and EDL. The MHC isoforms in the laboratory marker were identified based on data reported in the literature and on SDS-PAGE analysis of MHC isoforms in rat muscles containing one dominant isoform: SOL (MHCI), DPH (MHCIID) and levator ani (MHCIIB) (Hämäläinen & Pette, 1995). The MLC isoform bands were identified on the basis of data reported in the literature, of the electrophoretic mobility of purified rat MLC isoforms (personal communication; Brett O'Connell), and of SDS-PAGE analysis of low-molecular-weight myofibrillar proteins in segments of single fibres containing only one fast or one slow MHC isoform.

### 2.5.3 Staining of the SDS-PA gels

Two different silver-staining methods were used in this study, the acidic method (Hofer protocol) for detecting MHC isoform bands and the alkaline method (Bio-Rad protocol) (Srový & Hodný, 1991) for detecting MLC isoform bands. The Hofer protocol was used for detection of MLC bands because of its ability to produce minimum background staining and sharp bands. The Hofer protocol produced also minimum background staining when applied to MHC gels; however, in this case they failed to produce bands as sharp as the Bio-Rad protocol. A number of measures were taken to ensure even staining of the protein bands and minimum background staining. These included (i) thorough cleaning of the glass staining dishes, (ii) clean dishes used for each staining step, (iii) constant shaking of gels throughout the staining procedure.

After staining, the gels were scanned wet or were first dried between two pieces of cellophane, then scanned and finally stored dry. Details regarding scanning are given in section 2.5.4. No significant differences ( $P < 0.05$ ,  $n=3$ ) were observed between the intensities of bands MHCIIa ( $27.2 \pm 0.4\%$  vs  $29.1 \pm 0.1\%$ ), MHCII d ( $47.9 \pm 0.3\%$  vs  $46.1 \pm 0.2\%$ ), MHCII b ( $7.8 \pm 0.5\%$  vs  $7.5 \pm 0.5\%$ ) and MHC I ( $17.1 \pm 0.4\%$  vs  $17.3 \pm 0.2\%$ ) when results obtained with gels that were scanned wet or dry were compared.

*Bio-Rad silver staining.* The gels were fixed (50% methanol/10% acetic acid/5% glycerol) for a minimum of 30 min and rinsed twice for 10 min in distilled water. The gels were then stained in a solution containing 0.24 M  $\text{NaCO}_3$ , 0.1%

AgNO<sub>3</sub>, 0.1% NH<sub>4</sub>NO<sub>3</sub>, 0.5% tungstosilicic acid and 0.14% formaldehyde, until the desired staining was reached. The staining reaction was stopped in 5% acetic acid.

*Hoefler silver staining.* The gels were fixed (40% ethanol/10% acetic acid) for a minimum of 30 min and then placed in a sensitising solution (30% ethanol, 0.125% glutardialdehyde, 0.2% sodium thiosulfate and 0.83 mM sodium acetate) for another 30 min. The gels were then washed in distilled water three time for 5 min and then placed in silver reaction solution (0.25% silver nitrate and 0.015% formaldehyde) for 20 min followed by another wash step (2 × 1 min). The protein bands were developed in 0.24 mM sodium carbonate and 0.0074% formaldehyde and the staining was stopped in 0.04 mM EDTA-Na<sub>2</sub> for a minimum of 10 min.

#### 2.5.4 Densitometry

A Molecular Dynamics Personal Densitometer was used for scanning the gels with the aid of the ImageQuaNT software version 4.1 (Molecular Dynamics). The protein bands were analysed either with respect to band separation (by measuring the distance between bands) or relative proportion of protein band (by volume quantitation).

After optimising the contrast with the grey/color adjust window, the distance between bands was measured by creating first a line graph that showed the peaks corresponding to the individual protein bands (see Fig. 2.12A), and then measuring the distance between the peaks, corresponding to the bands. Volume quantitation was

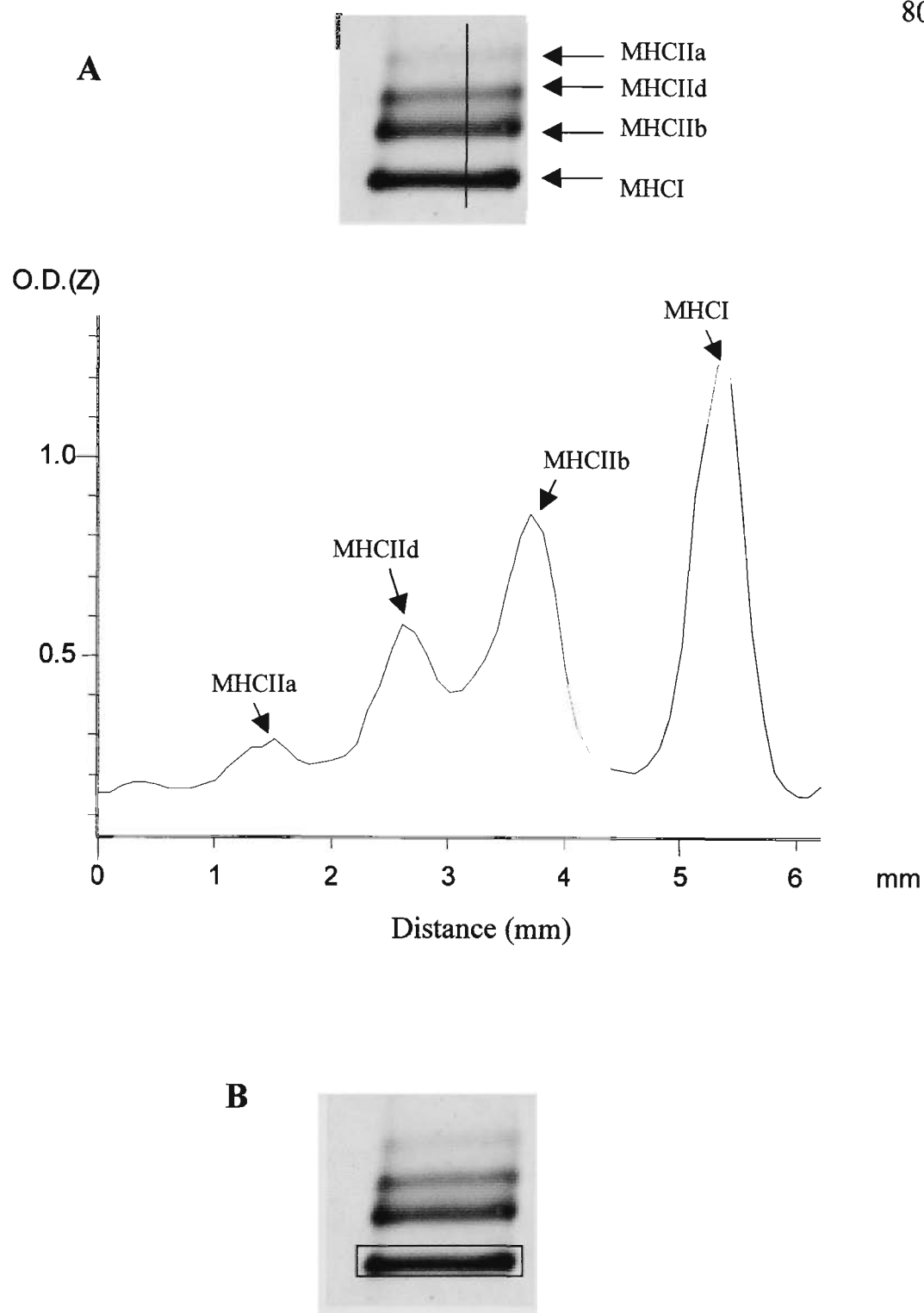


**Figure 2.12 Analysing MHC isoform bands.** A. The strategy used for measuring the distance between the peaks (a line is drawn through the bands and their pixel intensity and distance along the line is represented in the graph; O.D, optical density). B. The strategy used for volume quantitation (a box is drawn around the protein band and the pixel intensity within the box is analysed).

performed by drawing a box around the protein band and then analysing pixel intensities within the box (see Fig. 2.12B).

### 2.5.5 Estimation of MHC isoform and MLC2 isoform composition in whole muscle homogenates

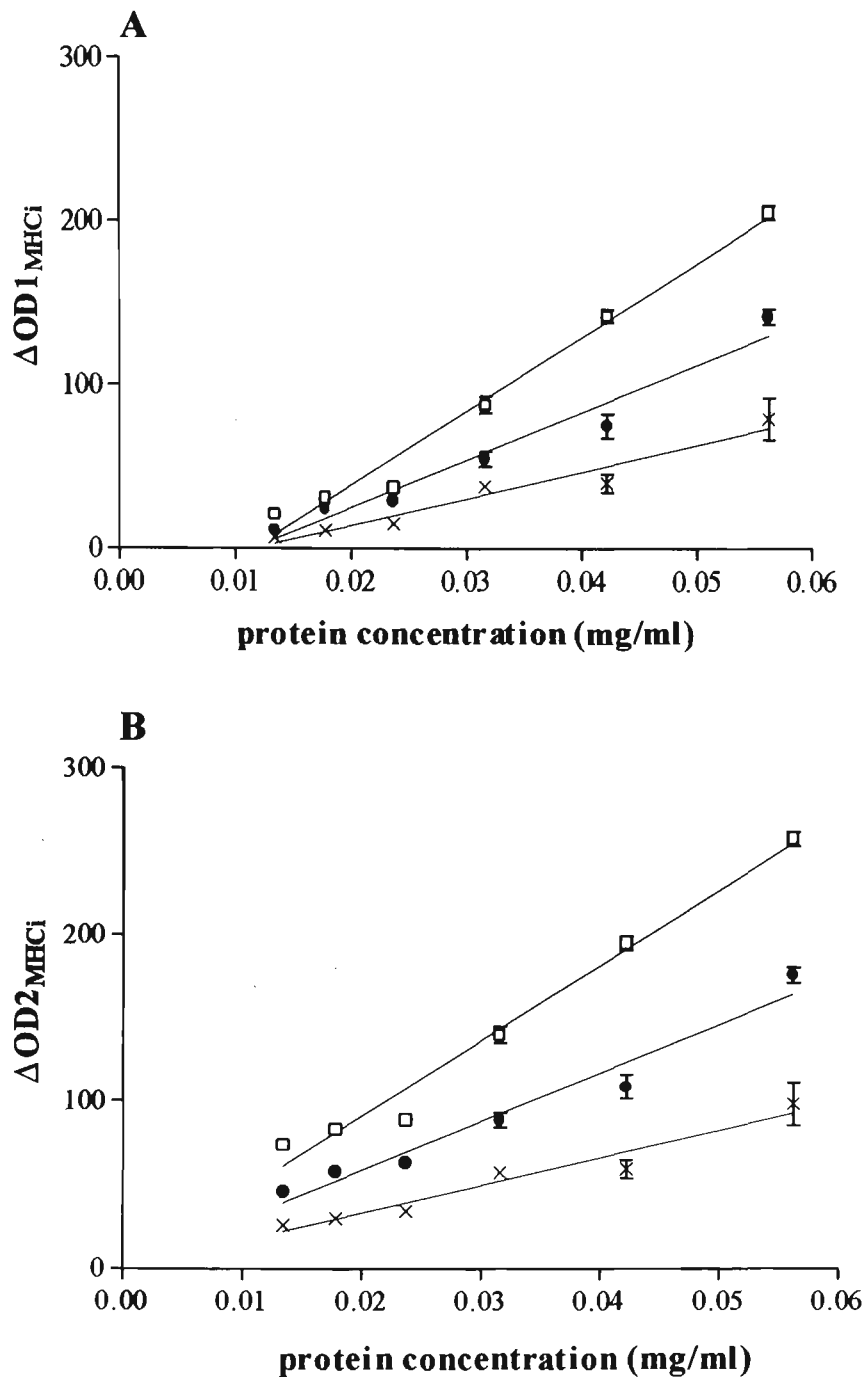
The gels for both high and low molecular weight proteins were analysed using a Molecular Dynamics Personal Densitometer and the volumetric quantitation method with background correction provided by the ImageQuaNT software version 4.1 (Molecular Dynamics).

Fig. 2.13A illustrates the relationship between  $\Delta OD1_{MHC_i}$  (the computed difference between the optical density of the protein band corresponding to  $MHC_i$  and that of the background) and the total protein concentration in the homogenate sample (over the range 0.01 to 0.06 mg/ml). As seen in Fig. 2.13A,  $\Delta OD1_{MHC_i}$  was linearly related to the total protein concentration for each MHC isoform detected ( $r^2_{MHC_I} = 0.98$ ;  $r^2_{MHC_{IIa}} = 0.96$ ;  $r^2_{MHC_{IIb}} = 0.95$ ).

The linear functions represented in Fig. 2.13A are described by the equation

$$\Delta OD1_{MHC_i} = a_i C + b_i \quad (\text{Eq 10})$$

where  $C$  is the total protein concentration in the homogenate sample,  $a_i$  is the slope of the line for  $MHC_i$  and  $b_i$  is the intercept of the line for  $MHC_i$  with the y-axis. Direct proportionality between total protein concentration in the homogenate sample



**Figure 2.13** A. relationship between  $\Delta OD1_{MHCi}$  (computed difference between optical density of the protein band corresponding to  $MHC_i$  isoform and that of the background) expressed in arbitrary units and the total protein concentration in the homogenate sample. B relationship between  $\Delta OD2_{MHCi}$  (an optical parameter derived from  $\Delta OD1_{MHCi}$  as explained in section 2.5.5) expressed in arbitrary units and the total protein concentration in the homogenate sample.  $\square$ ,  $MHC_i$ ;  $\bullet$ ,  $MHC_{IIa}$ ;  $\times$ ,  $MHC_{IIb}$ .

and a second optical parameter ( $\Delta OD2_{MHC_i}$ ), derived from  $\Delta OD1_{MHC_i}$ , can be obtained by transferring  $b_i$  from the right to the left side of Eq 10, i.e.

$$\Delta OD2_{MHC_i} = \Delta OD1_{MHC_i} - b_i = a_i C \quad (\text{Eq 11})$$

The result of this mathematical manipulation is shown in Fig. 2.13B. The concentration of each MHC isoform in the muscle homogenate sample ( $[MHC_i]$ ) is proportional to the total protein concentration,  $C$ , i.e

$$[MHC_i] = \alpha_i C \quad (\text{Eq 12})$$

where  $\alpha_i$  is the fraction of total protein representing the  $MHC_i$  component.

Substituting  $C$  in Eq 11 with  $[MHC_i]/\alpha_i$  from Eq 12 results in a direct proportionality between  $\Delta OD2_{MHC_i}$  and  $[MHC_i]$ :

$$\Delta OD2_{MHC_i} = [MHC_i] a_i / \alpha_i \quad (\text{Eq 13})$$

If the silver stain reacts in a similar manner with all myosin heavy chain isoforms, then the ratio  $a_i / \alpha_i$  should have a constant value, which is independent of the MHC isoform. This simple mathematical manipulation then allows the direct estimation of the relative proportion of each MHC isoform in a given homogenate sample, from the data generated by the densitometer software, using the expression:

$$[MHC_i] / \Sigma [MHC_i] (\%) = 100 \Delta OD2_{MHC_i} / \Sigma \Delta OD2_{MHC_i} \quad (\text{Eq 14})$$

## Chapter 3

# An Investigation into Effects of Various SDS-PAGE Related Parameters on the Separation of MHC Isoforms in Rat Skeletal Muscle

### 3.1 Introduction

The SDS-discontinuous gel system described originally by Laemmli (1970) is the most widely used polyacrylamide gel system in studies concerned with the separation of protein mixtures under dissociating conditions. The major characteristics of the Laemmli system include the use of (i) two gels (separating gel and stacking gel) of different length, pH and porosity, (ii) bis-acrylamide concentration equivalent to a %C value of 2.6%, (iii) chloride and glycine as the leading and trailing anions, (iv) Tris as the major cation and (v) a single running buffer system (for definition of basic concepts in gel electrophoresis see section 1.3.2.1). Details regarding the composition of the separating gel, stacking gel and running buffer are shown in Tables A1-A3, Appendix 1.

Many studies involving separation of MHC isoforms in mammalian muscle preparations used 'Laemmli' gel systems, i.e. slightly modified versions of the

original Laemmli gel system. Some of the minor modifications made in these studies include, addition of glycerol to the separating gel (Carraro & Catani, 1983), the use of a non-uniform (gradient) separating gel (Bar & Pette, 1988) and the use of higher concentrations of Tris and Glycine in the running buffer (Danieli-Betto *et al.*, 1986).

In 1993, Talmadge & Roy described an electrophoretic system [referred to henceforth as the Talmadge & Roy (T-R) gel system; for details of the composition of different components see Tables A1-A3, Appendix 1], deemed to produce a complete electrophoretic resolution of MHC isoforms. The T-R gel system displays several notable differences to the Laemmli gel system. These include: a reduced %C value (2.0%), the addition of glycine (100 mM) to the separating gel and of EDTA (4 mM) to the stacking gel, a decrease in [Tris] (200 mM) in the separating gel, an increase in [SDS] (0.4%) and the use of two running buffers. Like the Laemmli gel system, the T-R gel system has been subjected to minor modifications by researchers, who in the process of seeking further improvement in the separation of MHC isoforms, generated a family of 'T-R' gel systems.

A brief survey of 72 studies (listed in Appendix 5) concerned with the separation of MHC isoforms showed that a small proportion (8 out of 72; listed in Appendix 5.3) did not include a reference for the gel system used. The gel systems used for further modification in 64 of these studies were either Laemmli (see list in Appendix 5.1) or T-R systems (see list in Appendix 5.2). Over the past five years, the Laemmli and T-R gel systems appear to have been equally used (with further minor modifications) for the separation of MHC isoforms.

The main aim of this present study was to examine the effect of various parameters on the ability of SDS-PA gels to separate the MHC isoforms (I, IIb, IIc and IIa) expressed in adult rat skeletal muscle. This was achieved by using gel systems derived from the Laemmli and from the T-R protocols and the laboratory MHC marker (i.e. a muscle sample containing all four MHC isoforms).

### 3.2 Methods

*SDS-PAGE.* Details related to the set up of the gel apparatus and to basic electrophoretic procedures, such as gel preparation, sample preparation, gel staining and densitometry, can be found in the appropriate sections within Chapter 2.

Throughout this chapter, a defined set of values for electrophoretic parameters will be referred to collectively as the gel system.

The MHC laboratory marker, a mixture of SOL and EDL muscle homogenates containing all 4 MHC isoforms, was prepared as described in section 2.5.2.

*DATA ANALYSIS.* The parameter used to evaluate the ability of a gel to separate the MHC isoforms present in the MHC sample was the distance between two near-neighbour isoform bands detected in a single gel lane. This distance was determined densitometrically as described in section 2.5.4. The following symbols were used throughout this chapter when referring to the separation of MHC isoforms on a gel:

$\Delta$  : distance between any two MHC isoforms

$\Delta_{\Pi a-\Pi d}$  : distance between MHC isoforms  $\Pi a$  and  $\Pi d$

$\Pi ad$  : composite band produced by the co-migration of MHC isoforms  $\Pi a$  and  $\Pi d$

$\Pi ad-\Pi b$  : distance between the composite band  $\Pi ad$  and MHC isoform band  $\Pi d$

The smallest inter-band distance that could be detected with the software used in this study, i.e. the detection limit (DL), was 0.4mm.

The effect of various parameters on the electrophoretic separation of MHC isoforms was evaluated by measuring the distance between the following pairs of near-neighbour MHC isoform bands:  $\Pi b$  and  $I$  ( $\Delta_{\Pi b-I}$ ),  $\Pi d$  and  $\Pi b$  ( $\Delta_{\Pi d-\Pi b}$ ) or  $\Pi ad$  and  $\Pi b$  ( $\Delta_{\Pi ad-\Pi b}$ ) for gel systems that did not separate MHC isoform bands, and  $\Pi a$  and  $\Pi d$  ( $\Delta_{\Pi a-\Pi d}$ ). The time-consuming aspect of MHC isoform analysis by SDS-PAGE (the minimum time taken to produce one set of results was approximately 28 hrs) did not allow replication of experiments in which effects of various parameters were examined and thus precluded subsequent statistical analysis of significance. This methodological limitation was circumvented when comparing sets of data, by using a strategy that involved the following: the MHC sample was electrophoresed many times ( $n=18$ ), under identical conditions, distances between the protein bands of interest ( $\Delta_{\Pi b-I}$ ,  $\Delta_{\Pi d-\Pi b}$ ,  $\Delta_{\Pi a-\Pi d}$ ) were measured, and the mean and coefficient of variation ( $CV=1SD$  expressed as percent of the mean) were calculated for each pair of MHC isoforms. The appropriate CV value was used as a lower limit when deciding whether a parameter had a 'convincing effect' on the separation of near-neighbour MHC isoform bands. The CV values calculated using this strategy and subsequently used in data analyses are as follows: 10% (for  $\Delta_{\Pi b-I}$ ), 30% (for  $\Delta_{\Pi d-\Pi b}$ ) and 16% (for  $\Delta_{\Pi a-\Pi d}$ ). In other words, to be convincing, the effect of a given parameter on the

separation of MHC isoforms would have to be 10% (for  $\Delta_{\text{IIb-I}}$ ), 30% (for  $\Delta_{\text{IIId-IIb}}$ ) and 16% (for  $\Delta_{\text{IIa-IIId}}$ ) higher/lower than the reference.

### 3.3 Results

#### 3.3.1 Effects of changing various electrophoretic parameters in two gel systems on the separation of MHC isoforms in rat skeletal muscle

The SDS-PAGE related parameters examined in the present study belong to one of two groups, the composition of the separating and stacking gels and the running conditions (which include the composition of the running buffer). Initial attempts to separate MHC isoforms using the original protocols of Laemmli (1970) and Talmadge & Roy (1993) failed to produce satisfactory results. Minor modifications to these protocols produced two families of laboratory gel systems referred to as 'Laemmli' gel systems and 'T-R' gel systems, which were subsequently used to examine the effects of the parameters under consideration. Results presented in some sections were collected from several gel systems; details of these gel systems are provided in Appendices 2-4. To assist with finding these details, gels were coded according to the place where the results were mentioned (F-figure; T-table; txt-text). For example, details of the gel system used for generating the data shown in Figs 3.1A and Fig 3.1B will be found in the appropriate appendix under the name gel F3.1A,B.

### 3.3.1.1 Alteration of parameters in the 'Laemmli' gel systems

Most of the data presented in this chapter are concerned with the separation of MHC isoforms IIb and I, IId and IIb, or IIad and IIb (for gel systems in which MHC isoforms IIa and IId co-migrated) and IIa and IId. A limited number of data, presented in section 3.3.1.1.3 are concerned with the separation of two MHC I bands.

#### 3.3.1.1.1 Composition of the separating gel

**Acrylamide concentration.** In Fig. 3.1 is represented the effect of increasing acrylamide concentration ( $[A]$ ) in the separating gel on the distance between the MHC isoform bands indicated on the y-axis. Note that MHC isoforms IIa and IId co-migrated on all the gels analysed for Fig. 3.1. The gels used to generate the data shown in Fig. 3.1A and 3.1B contained the same concentration of the cross-linker bis-acrylamide ( $[B] = 0.153\%$ , w/v), but different %C values (1.5-2.5%). As seen in Fig. 3.1A, an increase of  $[A]$  from 6-10%, led to a gradual decrease in the distance between MHC isoforms IIb and I, so that at 10%  $[A]$ ,  $\Delta_{IIb-I}$  was 46% lower than at 6%  $[A]$ . It is interesting to note that in this gel system  $\Delta_{IIb-I}$  (1.4mm) was more than three times higher than the densitometer detection limit (DL, 0.4mm), even in the least effective separating gel ( $[A]=10\%$ ). An increase in  $[A]$  over the same range had no convincing effect ( $< 30\%$ ) on  $\Delta_{IIad-IIb}$ , which remained just above the detection limit (Fig. 3.1B). Similar effects of  $[A]$  on  $\Delta_{IIb-I}$  and  $\Delta_{IIad-IIb}$  were obtained for gels in which %C was kept constant and  $[B]$  was varied (see Fig. 3.1C and 3.1D). Taken together these data

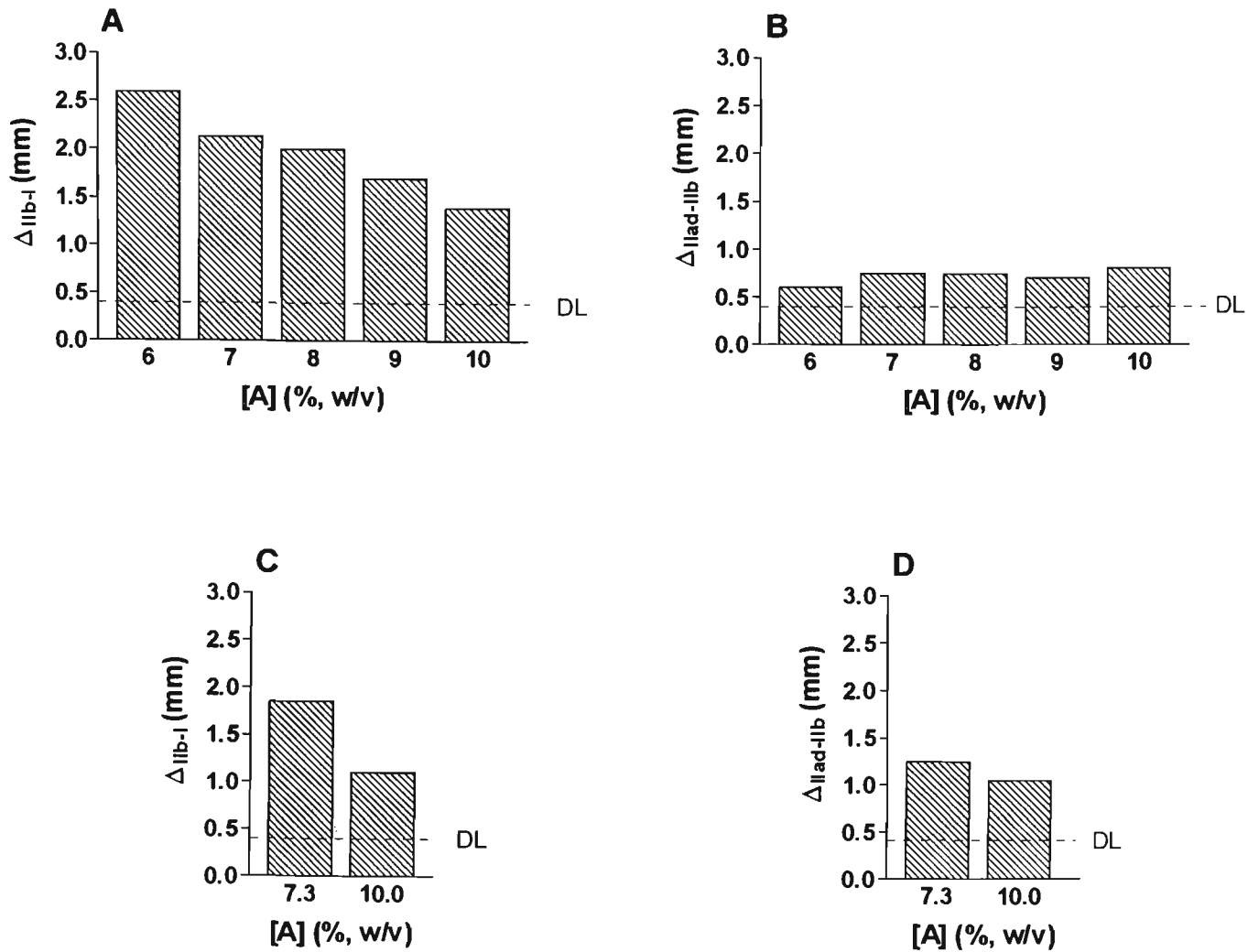


**Figure 3.1** The effect of acrylamide concentration ([A]) on the separation of MHC isoforms I and IIb (panels A and C) and IIad and IIb (panels B and D). Gels used to produce the data presented in panels A and B contained constant [B] and gel used for panels C and D contained constant %C. For details of gel F3.1A,B (i.e. for the gel system that generated the data presented in panels A and B) and gel F3.1C,D see Appendix 2.

suggests that (i) varying [A], while maintaining [B] or %C constant, altered the separation of near-neighbour fast and slow MHC bands, but not near-neighbour fast/fast MHC bands regardless of the gel system, and (ii) for a given gel system, the [A] that produced the best separation for MHC isoforms IIb and I, produced only minor separation of MHC isoforms IIc and IIb and failed to separate MHC isoforms IIa and IIc.

*%C value.* It is well established that, for a given gel system, an increase in %C over the range 0-5% decreases the pore size of the gel matrix (Allen *et al.*, 1984). As shown in Fig. 3.2A, an increase in %C when [A] was kept constant ([A]=7.3%) had no convincing effect on  $\Delta_{IIb-I}$  over the range 1.5-1.8%, but was accompanied by a 26% decrease in  $\Delta_{IIb-I}$  when %C was increased from 1.8 to 2.5%. The effect of varying %C over the range 1.5-2.5% on  $\Delta_{IIad-IIb}$  was highly inconsistent (Fig. 3.2B). Thus,  $\Delta_{IIad-IIb}$  decreased when %C increased from 1.5 to 1.6% (-42%) and from 1.7 to 1.8% (-22%), but increased by 29% and 50% when %C was increased from 1.6 to 1.7% and 1.8 to 2.5%, respectively. In the gel system used for this series of experiments, manipulation of %C failed to separate MHC isoforms IIa and IIc, which co-migrated as one band IIad. Similar effects of %C on  $\Delta_{IIb-I}$  and  $\Delta_{IIad-IIb}$  were seen in two other gel systems (data not shown).

*Tris concentration.* The effect of [Tris] on MHC isoform separation was examined at values above that used by Laemmli (1970) in his original protocol (375 mM). The gel

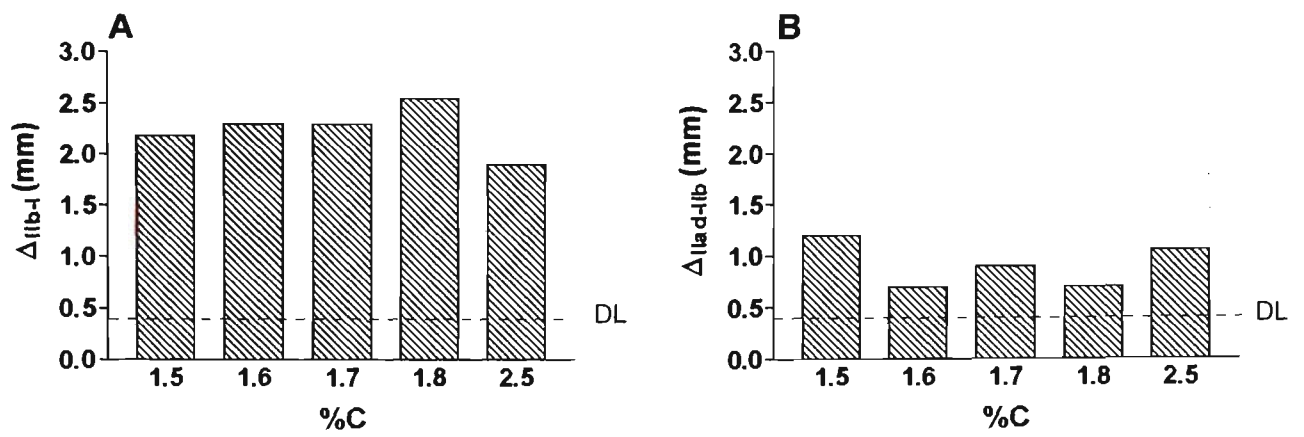


**Figure 3.2** The effect of %C value on the separation of MHC isoforms IIb and I (panel A) and IIad and IIb (panel B). For details of gel F3.2 see Appendix 2.

system used in this series of experiments separated all MHC isoforms and the results are shown in Fig. 3.3. As seen in Fig. 3.3A, an increase in [Tris] from 375 mM to 500 mM was accompanied by a 20% decrease in  $\Delta_{\text{Ib-I}}$ ; a more marked decrease in  $\Delta_{\text{Ib-I}}$  (-54%) was observed when [Tris] in the separating gel was increased to 700 mM (Fig. 3.3A), such that at this concentration the separation between MHC isoforms Ib and I was only 1.4 times DL.

When [Tris] was increased from 375 mM to 500 mM or to 700 mM (Fig. 3.3B),  $\Delta_{\text{IId-Ib}}$  increased by 62% and 77%, respectively, but in this gel system the separation of MHC isoform bands IId and Ib was lower than  $2 \times \text{DL}$  even at 700 mM Tris. Varying [Tris] over the range 375-700 mM produced an inconsistent effect on  $\Delta_{\text{IIa-IId}}$ . Thus, an increase in [Tris] from 375-500 mM was accompanied by a slight increase in  $\Delta_{\text{IIa-IId}}$  (+ 21%); however, when [Tris] was increased to 700 mM  $\Delta_{\text{IIa-IId}}$  decreased by 35% (Fig. 3.3C).

It is noteworthy that in the gel system used to generate the data for this section, 500 mM Tris in the resolving gel allowed satisfactory separation of all MHC isoforms (Fig. 3.3).

*Glycerol concentration.* In an earlier study, Danieli-Betto *et al.* (1986) reported an improvement in the separation of MHC isoforms in rat skeletal muscle by SDS-PAGE when 40% (v/v) glycerol was included in the separating gel of a 'Laemmli' gel system. To examine the effectiveness of glycerol in the concentration range used by Danieli-Betto and others (Schiaffino *et al.*, 1989; Daugaard *et al.*, 1998) on rat MHC isoform separation, gels containing two different [glycerol] within the range 35-42.5%

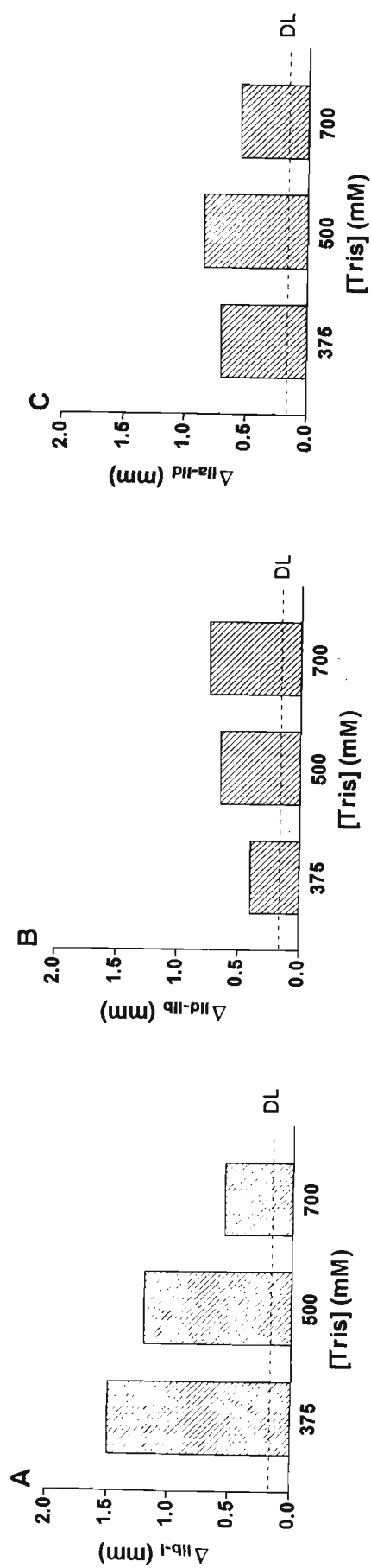


**Figure 3.3** The effect of [Tris] on the separation of MHC isoforms IIb and I (panel A), IId and IIb (panel B), and IIa and IId (panel C). For details of gel F3.3 see Appendix 2. Note that in the original Laemmli (1970) protocol, the separating gel contained 375mM Tris.

(35% vs 37%; 37% vs 40% and 40% vs 42.5%) were compared with respect to their ability to resolve MHC bands IIb and I and IIc and IIb in the lab marker. The data presented were collected from 8 gel systems, none of which separated MHC bands IIa and IIc.

As seen in Table 3.1,  $\Delta_{IIb-I}$  was larger than the detection limit in all 16 gels used for this study. An increase in [glycerol] from 37 to 40% (in gel systems 3-6) was accompanied by a consistent increase in  $\Delta_{IIb-I}$  in all 4 gel systems, particularly in gel system 3 (+120%), gel system 4 (+92%), and gel system 6 (+280%). A further increase in [glycerol] from 40% to 42.5% produced no effect on  $\Delta_{IIb-I}$  in gel system 7 and only a slight effect (+13%) in gel system 8. No convincing effect on the separation of MHC's IIb and I bands was observed when [glycerol] in the resolving gel was decreased from 37% to 35% (see gel systems 1 and 2). These data indicate that, for glycerol, the concentration range 37 to 40% is optimum with respect to the separation of MHC IIb and I bands, regardless of other components in the gel system.

The effect of [glycerol] on the separation of MHC bands IIad and IIb showed a different pattern to that described for MHC isoform bands IIb and I. For example, as seen in Table 3.1,  $\Delta_{IIad-IIb}$  was altered inconsistently by an increase in [glycerol] from 37 to 40% (gel system 3: +43%, gel system 4: -12%, gel system 5: -100%, gel system 6: -38%). Moreover, an increase in [glycerol] from 35 to 37% (gel systems 1 and 2) did not affect  $\Delta_{IIad-IIb}$  and, in gels containing 40% and 42.5% glycerol, all MHC II isoforms co-migrated regardless of the gel systems used (gel systems 7 and 8). Clearly, for the gel systems examined here, an increase in [glycerol] from 35 to 37% did not improve the separation of MHC isoform bands IIb and IIad.

**Table 3.1 The effect of varying [glycerol] on the separation of MHC isoforms.**

For details of each gel system refer to Appendix 3.

Gel system	$\Delta_{\text{Ib-I}}$ (mm)				$\Delta_{\text{Iad-Ib}}$ (mm)			
	[glycerol] (v/v)				[glycerol] (v/v)			
	35%	37%	40%	42.5%	35%	37%	40%	42.5%
1	0.85mm	0.80mm			1.25mm	1.15mm		
2	2.10mm	2.20mm			1.60mm	1.70mm		
3		1.00mm	2.20mm			1.75mm	2.50mm	
4		1.20mm	2.30mm			1.70mm	1.50mm	
5		2.40mm	2.60mm			0.95mm	0	
6		0.60mm	2.30mm			0.65mm	0.40mm	
7			3.50mm	3.60mm			0	0
8			1.80mm	2.05mm			0	0

*Glycine concentration.* To improve the resolution of myofibrillar proteins, Porzio and Pearson (1977) developed a SDS-PAGE gel system in which the separating gel contained glycine, the trailing ion in the original Laemmli (1970) protocol. The results of this study show (Fig. 3.4) that in the absence of [glycine], the separation of MHC bands Iib and I was 9 x DL, while fast MHC bands co-migrated. An increase in [glycine] from 0 mM to 50 mM was accompanied by a 41% decrease in  $\Delta_{\text{Ib-I}}$  (Fig 3.4A) and 100% increase (to a value equal with 2 x DL) in  $\Delta_{\text{Iad-Ib}}$ . (Fig. 3.4B).

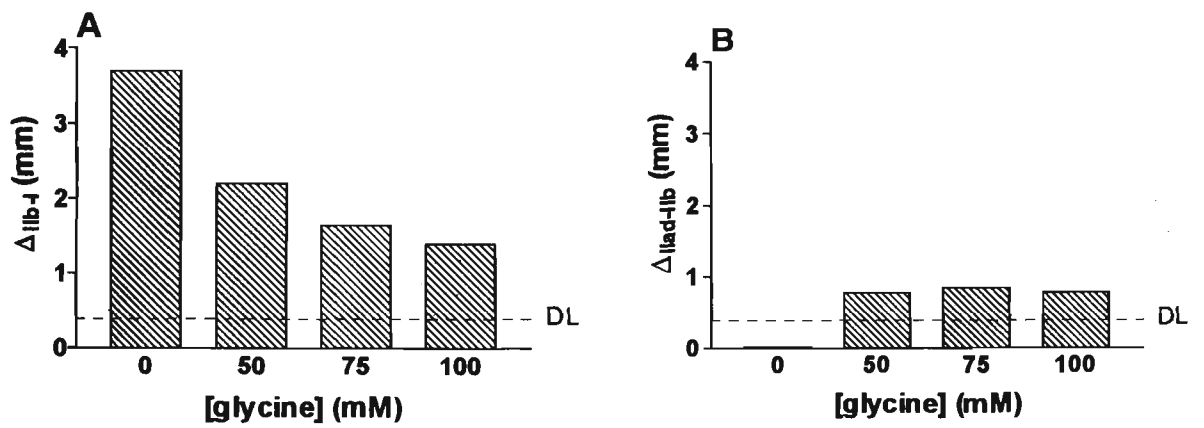


**Figure 3.4** The effect of [glycine] on the separation of MHC isoforms IIb and I (panel A), and IIad and IIb (panel B). For details of gel F3.4 see Appendix 2.

Increasing [glycine] from 50 mM to 100 mM produced a further decrease in  $\Delta_{\text{Ib-I}}$  (at an apparently lower rate) (Fig 3.4A), but no further change in  $\Delta_{\text{Iad-Ib}}$  (Fig. 3.4B).

### 3.3.1.1.2 Stacking gel

As discussed previously (section 3.3.1.1.1), Danieli-Betto *et al.* (1986) used 40% glycerol both in the separating and stacking gel to enhance the separation of MHC isoforms by SDS-PAGE. The results of this study show (Fig. 3.5) that adding 40% glycerol to the modified stacker had no convincing effect on  $\Delta_{\text{Ib-I}}$  (Fig. 3.5A) or on  $\Delta_{\text{Iad-Ib}}$  (Fig. 3.5B). Note that this gel system was also unable to separate MHC isoform bands IIa and IIc.

### 3.3.1.1.3 Running conditions

*Electric field.* The data (collected with two 'Laemmli' gel systems) on the effect of the electric field ( $E$ ) on MHC isoform separation are presented in Fig 3.6. The electric field is expressed as volts/cm (V/cm), where the length of the gel (8.8 cm) was measured from the bottom of the electrophoretic well to the bottom of the glass plates. As seen in Fig. 3.6A, 3.6C and 3.6E, an increase in  $E$  from 11.4 V/cm to 13.6V/cm produced a slight increase (+15%) in  $\Delta_{\text{Ib-I}}$  (Fig. 3.6A), no convincing effect on  $\Delta_{\text{Iad-Ib}}$  (+13%) (Fig. 3.6C) and an increase in  $\Delta_{\text{IIa-IIc}}$  (+29%) (Fig. 3.6E). When  $E$  was increased, in another gel system, from 11.4 V/cm to 17.0 V/cm a similar increase was observed for both  $\Delta_{\text{Ib-I}}$  (+56%) (Fig. 3.6B) and  $\Delta_{\text{Iad-Ib}}$  (+57%) (Fig 3.6D).

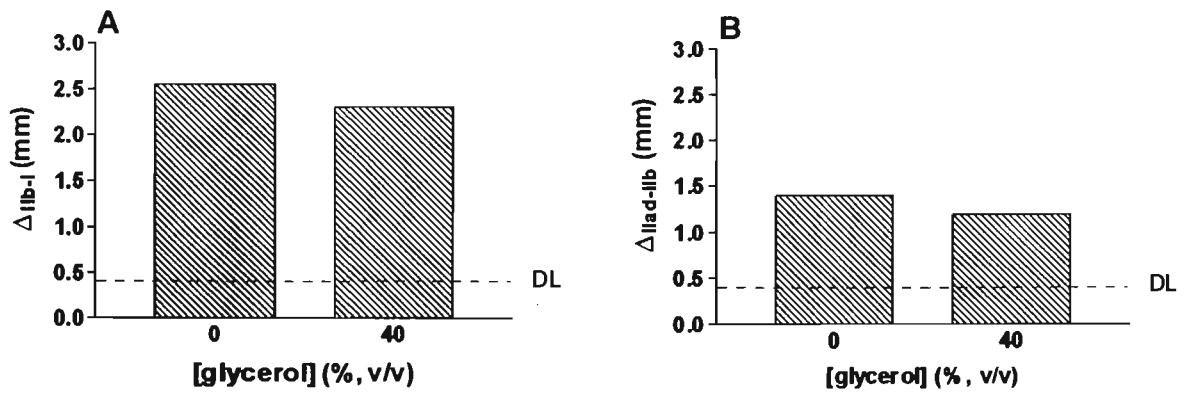


**Figure 3.5** The effect of [glycerol] in the stacking gel on the separation of MHC isoforms IIb and I (panel A), and IIad and IIb (panel B). For details of gel F3.5 see Appendix 2.

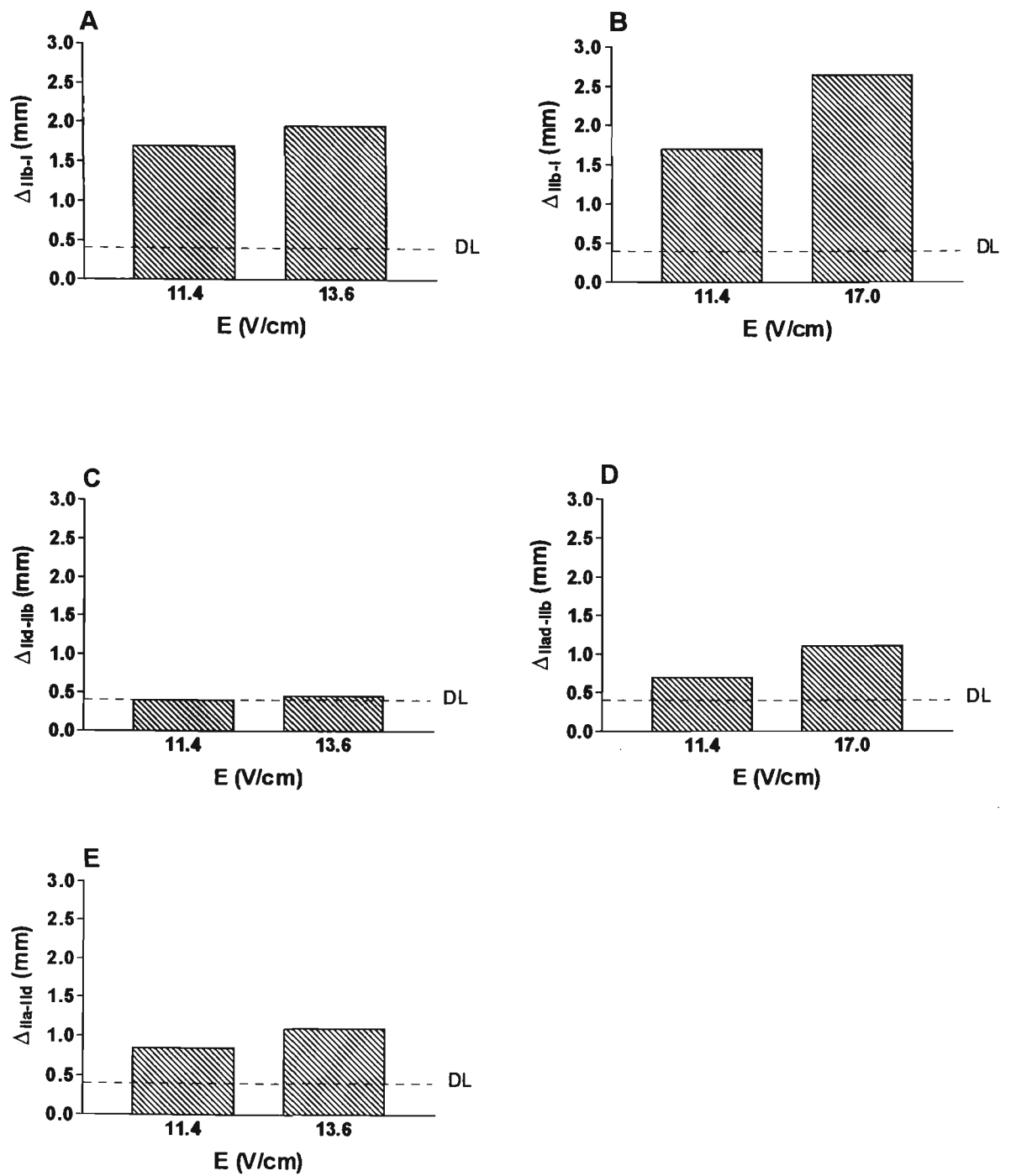


**Figure 3.6** The effect of varying the electric field (E) on the separation of MHC isoforms. For details of gel F3.6A,C,E and gel F3.6B,D see Appendix 2.

No separation of MHC isoform bands IIa and IIc was achieved on the second gel system. Taken together, these data suggest that increasing E over the range 11.4 to 17.0V/cm had a positive effect on the separation of all pairs of MHC isoforms examined. It is important to note that the gels run at 17.0 V/cm, were kept at 2-4°C to minimise Joule heating that increases diffusion and decreases band sharpness (Allen *et al.* 1984).

**Running time.** An increase in the running time from 24 to 34 hrs (Fig. 3.7), produced a 175% increase in  $\Delta_{IIb-I}$  (Fig. 3.7A) but only a 48% increase in  $\Delta_{IIad-IIb}$  (Fig. 3.7B). In this gel system, MHC isoform bands IIa and IIc co-migrated at both time points. These data suggests that in a given 'Laemmli' gel system, an increase in the running time affects the separation of different MHC isoform bands in a similar manner, but the magnitude of the effect may be dependent on the pair of MHC isoform bands under consideration.

**Running temperature.** The effect of the running temperature of a gel system on MHC isoform separation was examined over three temperature ranges [2-4°C (refrigerator), 12-14°C (ice box) and 16-21°C (water-cooling)]. As seen in Fig. 3.8A, an increase in the running temperature from 2-4°C to 12-14°C was found to increase  $\Delta_{IIb-I}$  by 68% (from 3.1×DL to 5.3×DL). A further increase in the temperature range to 16-21°C produced an increase in  $\Delta_{IIb-I}$  by 110% (from 5.3×DL to 11×DL). The separation of MHC isoform bands IIc and IIb (Fig. 3.8B) was the same at running temperatures 2-4°C and 12-14°C (2.1×DL), but a further increase in the temperature to 16-21°C,

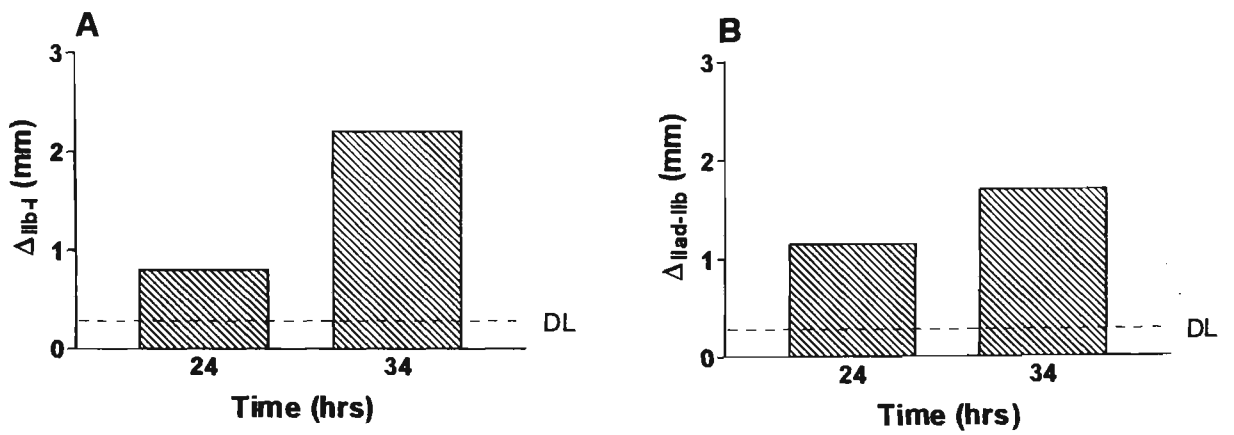


**Figure 3.7** The effect of running time on the separation of MHC isoforms IIb and I (panel A), and IIad and IIb (panel B). For details of gel F3.7 see Appendix 2.

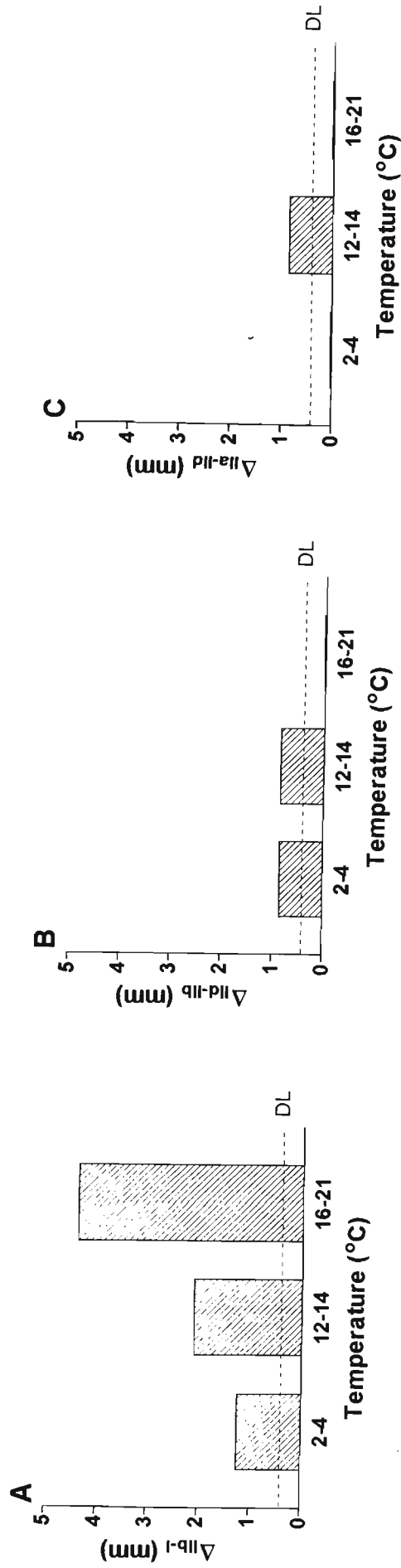


**Figure 3.8** The effect of running temperature on the separation of MHC isoforms I Ib and I (panel A), I Id and I Ib (panel B), and I Ia and I Id (panel C). For details of gel F3.8 see Appendix 2.

4

1

caused MHC isoform bands IId and IIb to co-migrate. In this gel system, MHC isoform bands IIa and IId were found to separate at 12-14°C (2.1×DL) (Fig 3.8C), but not at lower temperatures in the ranges 2-4°C or 16-21°C. Clearly, in this gel system a running temperature of 12-14° C would have to be chosen when attempting to separate all four MHC isoform bands expressed in the adult rat muscle.

*Separation of slow (I) MHC isoforms.* Thirteen of the gels used to assess the effect of low running temperature ( $\leq 14^{\circ}\text{C}$ ) on the separation of MHC isoform bands showed two protein bands of different intensity in the gel region of MHC I isoform (Fig. 3.9). The gels were produced using 10 different gel systems which are listed in Appendix 4 (gel txt-2 to gel txt-11).

The appearance of a second protein band in the MHC I region was an interesting discovery as this extra band only seemed to appear under certain gel conditions (as detailed in Appendix 2, gel F3.9). This extra band was ruled out as being artifactual as it appeared in 13 similar gels and displayed a lower intensity than MHC I. As this fainter band migrated faster than MHC I, it was assumed to be MHC Ia, previously described by Fauteck & Kandarín (1995) and Galler *et al.* (1997a) (see section 1.3.2.3.2).

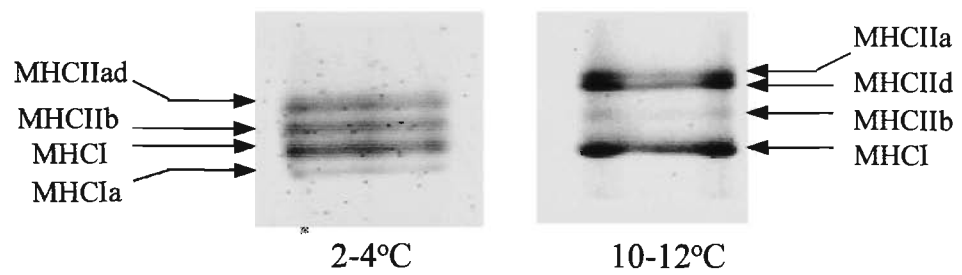


**Figure 3.9** A representative electrophoretogram showing the separation of two MHC I isoform bands on a gel run at 2-4°C. Note that no such separation occurred in the same gel system run at 10-12°C. For details of gel F3.9 see Appendix 2.

### 3.3.1.2 Alteration of parameters in the Talmadge and Roy protocol

#### 3.3.1.2.1 Composition of the separating and stacking gels

*[Glycerol] in the separating gel.* The original gel system of Talmadge & Roy (1993) contained 30% glycerol in the separating gel. In the present study, the separation of MHC isoform bands at varying [glycerol] within the range 30-45%, was examined using three different 'T-R' gel systems (Fig. 3.10). As seen in Fig. 3.10A, an increase in [glycerol] from 30 to 40%, did not have a convincing effect on  $\Delta_{\text{Ib-I}}$ . When [glycerol] was increased to 42.5% (Fig. 3.10B) or to 45% (Fig. 3.10C),  $\Delta_{\text{Ib-I}}$  was increased by 25% and 117%, respectively.

No separation of MHC isoform bands IId and IIb was obtained when the separating gel contained 30% glycerol, but when [glycerol] was increased to 40%,  $\Delta_{\text{IId-IIb}}$  increased by 100% to a value equal with  $1.3 \times \text{DL}$  (Fig. 3.10D). A more pronounced increase in  $\Delta_{\text{IId-IIb}}$  was observed in gels containing 42.5% glycerol (+39%; Fig. 3.10E) and 45% glycerol (+50%; Fig. 3.10F).

All three gel systems used in this study separated MHC isoform bands IIa and IId. The two bands co-migrated at 30% glycerol, but an increase in [glycerol] from 30% to 40% increased the separation of MHC bands IIa and IId by 100% to  $1.5 \times \text{DL}$  (Fig. 3.10G). Increasing [glycerol] from 40 to 42.5% had no convincing effect on  $\Delta_{\text{IIa-IId}}$  (Fig. 3.10H), while increasing it from 40% to 45% decreased  $\Delta_{\text{IIa-IId}}$  by 44% (Fig. 3.10I).

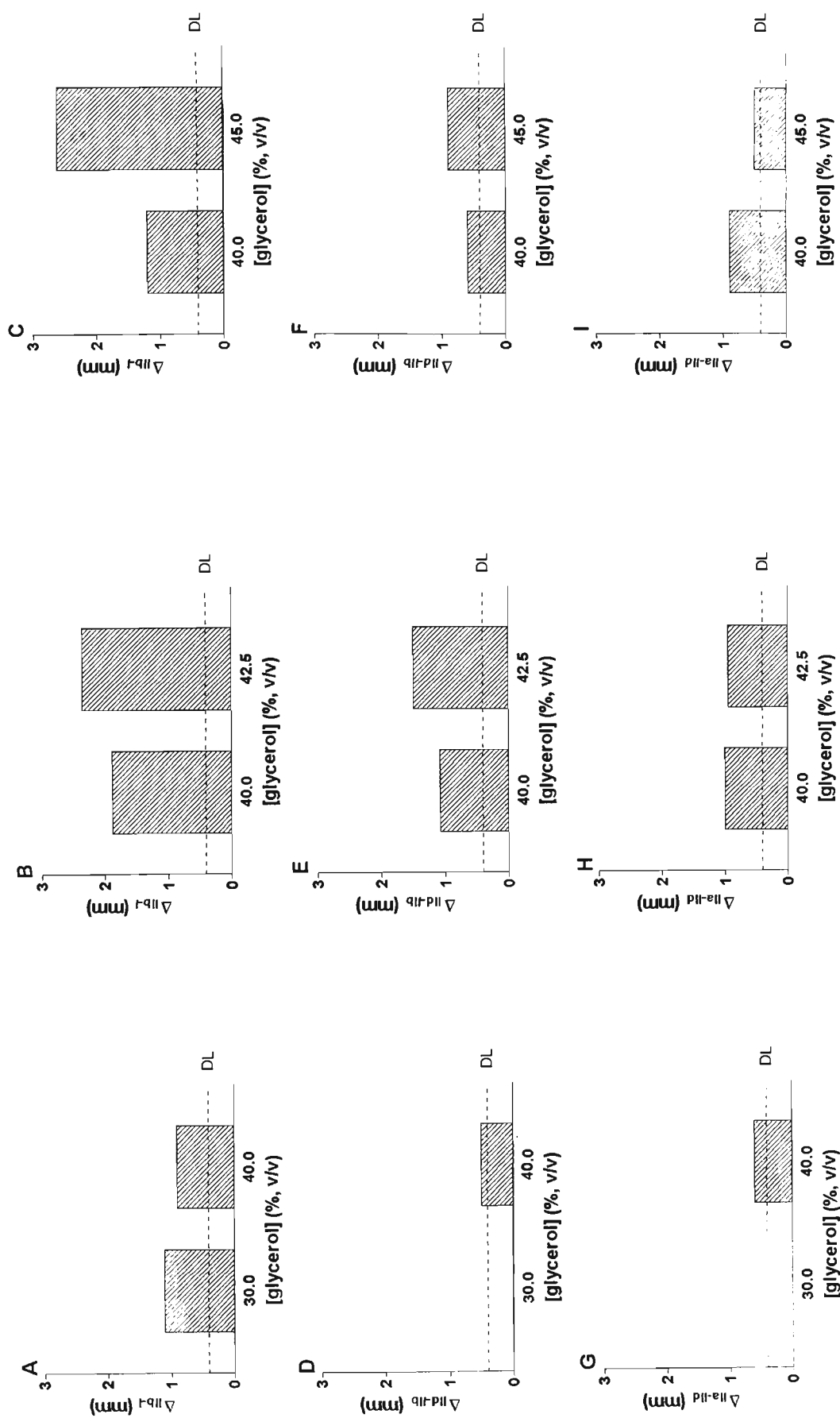


**Figure 3.10 The effect of varying [glycerol] on the separation of MHC isoforms.** It should be noted that, for each pair of MHC isoforms examined, the band separation in gels containing 40% glycerol, differed between gel systems (see for example panels A, B and C). These differences are probably due to differences between the electric fields used with the three gel systems that generated the data shown. For details of

A visual survey of the data presented in Fig. 3.10 suggests that the gel system containing 42.5% glycerol in the resolving gel was the most effective for separating all four MHC isoforms in the MHC marker.

*Composition of the stacking gel.* A notable difference between the Laemmli (1970) and Talmadge & Roy (1993) gel systems relates to the composition of the stackers used (Table A2, Appendix 1). The effectiveness of two Talmadge and Roy gels, which used either the Talmadge & Roy (T-R) stacker or a 'Laemmli' stacker (Laemmli's modified stacker containing 40% glycerol; 'L<sup>G+</sup>'), in separating MHC isoforms were compared and results are shown in Fig 3.11. As seen in Fig 3.11A and Fig. 3.11B, the use of the two different stackers showed no convincing effect on either  $\Delta_{\text{IIb-I}}$  or on  $\Delta_{\text{IIa-IIb}}$ . However, as seen in Fig 3.11C, the value of  $\Delta_{\text{IIa-IId}}$  obtained in the T-R gel system using the 'L<sup>G+</sup>' stacker was 50% lower than that using the T-R stacker and only 1.4 times higher than the detection limit. These data indicate that the 'T-R' gel system used in this series of experiments was most effective in separating all four MHC isoforms when employed in conjunction with the T-R stacker.

#### 3.3.1.2.2 Running conditions

*Running buffer.* The use of two different buffers in the cathode and anode compartments is a major feature of the Talmadge & Roy (1993) SDS-PAGE protocol. In contrast, only one running buffer is used in the Laemmli (1970) and in modified Laemmli gel systems, such as that of Danieli-Betto *et al.* (1986). In this study, the

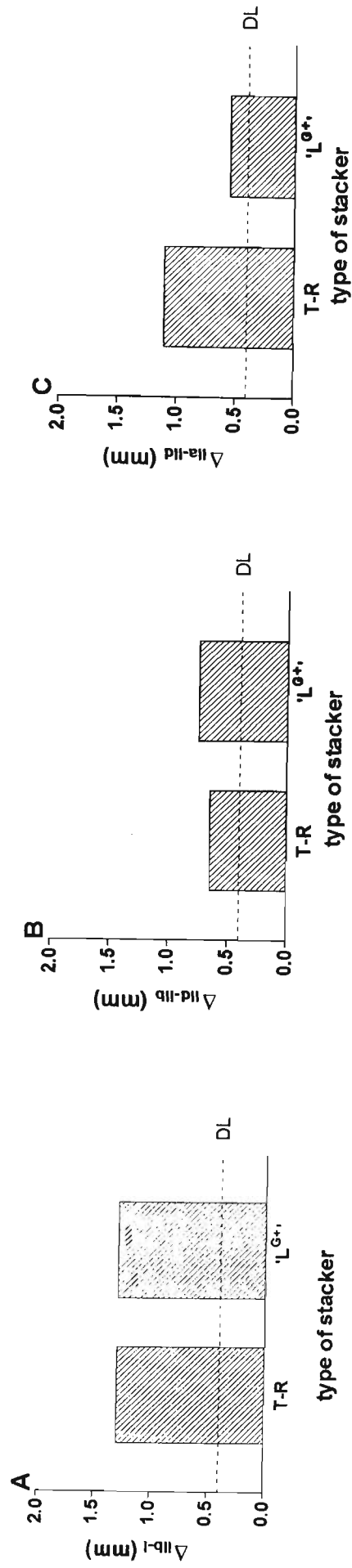


**Figure 3.11** The effect of replacing the T-R stacker (Talmadge and Roy, 1993) with the 'L'G+' (Laemmli, 1970 + 40% glycerol), in the 'T-R' gel system, on the separation of MHC isoform bands IId and I (panel A), IId and IIb (panel B), and IId and IIc (panel C). For details of stackers see Table A2, Appendix 1 and for details of gel F3.11 see Appendix 2.

Talmadge and Roy buffer (T-R) and the single running buffer of Danieli-Betto *et al.* (1986) (D-B) were compared on a Talmadge & Roy gel system with respect to the separation of MHC isoforms. The composition of these buffers is shown in Table A3, Appendix 1. As shown in Fig. 3.12A, the Talmadge & Roy system used with the D-B running buffer produced a 4.2 times greater separation of MHC isoform IIb and I than when used with the T-R running buffer. In contrast, the use of the Talmadge & Roy gel system in conjunction with the D-B running buffer caused the fast MHC isoform bands to co-migrate (Fig. 3.12B and 3.12C).

It is interesting to note when a 'Laemmli' gel system was run with the T-R running buffer, all MHC isoform bands co-migrated (data not shown).

*Electric field.* The effect of varying E on the separation of MHC isoform bands using the Talmadge & Roy gel system was examined and results are shown in Fig. 3.13. Increasing E from 9.7 to 14.8V/cm was accompanied by a gradual increase in  $\Delta_{IIb-I}$  so that at 14.8V/cm,  $\Delta_{IIb-I}$  was 50% higher than at 9.7V/cm (Fig. 3.13A). A further increase of E from 14.8 to 17.0V/cm produced no convincing effect on  $\Delta_{IIb-I}$  (Fig. 3.13A). The separation of MHC isoform bands IId and IIb were not convincingly affected by an increase in E from 9.7 to 17.0V/cm (Fig. 3.13B). The greatest effect on MHC isoform separation in this gel system was observed with MHC isoforms IIa and IId. Thus, an increase in E from 9.7 to 14.8V/cm was accompanied by a 94% increase in  $\Delta_{IIa-IId}$ , from 1.5×DL to 3.3×DL; however, a further increase of E from 14.8 to 17.0V/cm, reduced  $\Delta_{IIa-IId}$  to 1.4×DL (Fig. 3.13C). Clearly, in this gel

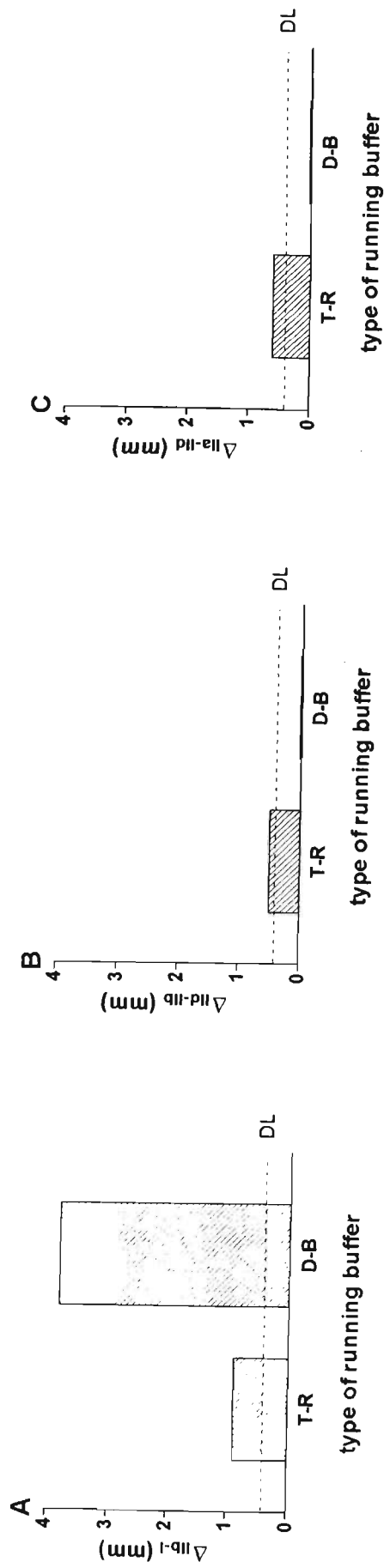
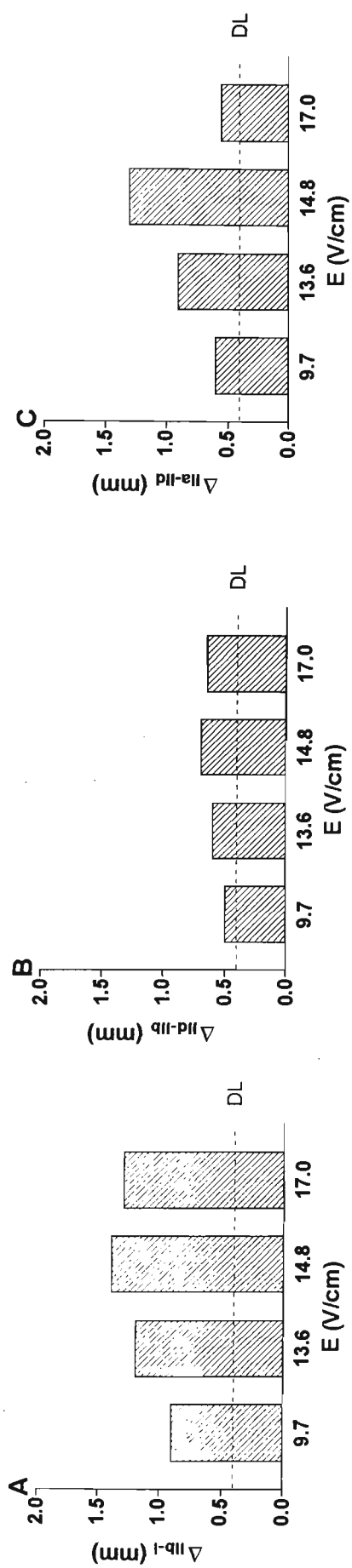


Figure 3.12 The effect of replacing the T-R running buffer (Talmadge & Roy, 1993) with the D-B running buffer (Danieli-Betto *et al.* 1986), in the 'T-R' gel system, on the separation of MHC isoforms IId and I (panel A), IId and IIb (panel B), and IId and IIa and IIc (panel C). For details of running buffers see Table A3, Appendix 1 and for details of gel F3.12 see Appendix 2.

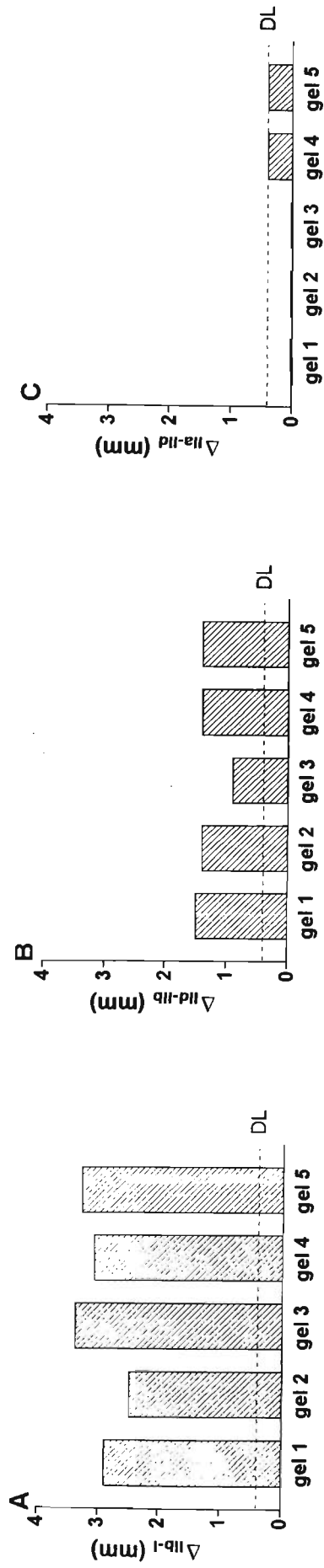


**Figure 3.13** The effect of the electric field (E) on the separation of MHC isoforms IIb and I (panel A), IId and IIb (panel B), and IIa and IId (panel C). For details of gel F3.13 see Appendix 2.

system an E value of 14.8 V/cm produced the best separation of all MHC isoform bands.

### 3.3.1.2.3 Mozdziak version of the Talmadge & Roy protocol

Recently Mozdziak *et al.* (1999) separated the MHC isoforms IIa, IId and I in rat soleus muscle using a modified version of the Talmadge & Roy (1993) SDS-PAGE protocol. The most notable feature of the Mozdziak protocol was the replacement of the original T-R stacker with a stacker used by Fritz *et al.* (1989) in which N,N' diallyltartardiamide rather than bis-acrylamide was used as a cross-linker and the %C value was increased from the original 2% to 15% (for composition of stackers see Table A1, Appendix 1). In the present study, the effectiveness of the Mozdziak protocol, in which a high concentration of bis-acrylamide (rather than N,N' diallyltartardiamide) was used as the cross-linker in both separating and stacking gels, was examined with respect to the separation of the four MHC isoforms in the MHC sample; the data obtained with five different gels are presented in Fig. 3.14. As seen in Fig 3.14A and Fig. 3.14B, the MHC isoform bands IIb and I, and IId and IIb were well separated on all five 'Mozdziak' gels;  $\Delta_{IIb-I}$  ranged from 6.3 to 8.5×DL and  $\Delta_{IId-IIb}$  ranged from 2.3 to 3.8×DL. In contrast,  $\Delta_{IIa-IId}$  (Fig. 3.14C) was equal with the detection limit in two gels and lower than DL in the three remaining gels.

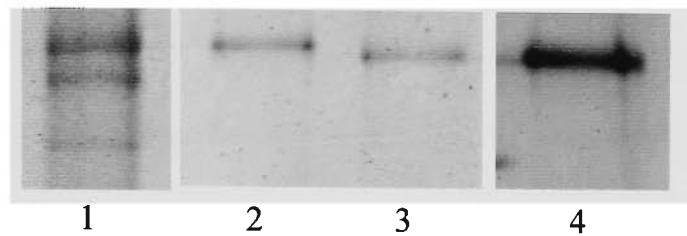
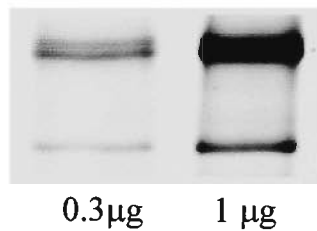
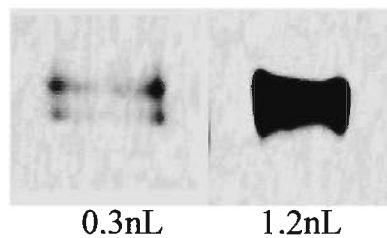


**Figure 3.14** The separation of MHC isoforms IIb and I (panel A), IIb and IIb (panel B), and IIa and IIa (panel C) using 'T-R' Mozdziak gel system. For details of gel F3.14 see Appendix 2.

### 3.3.1.3 Evaluation of the gel systems used in this study

The usefulness of a gel system for separating protein bands in a complex sample is usually judged based on its ability to resolve the bands of interest above what is deemed to be the detection limit (*separation effectiveness* or *effectiveness*) and on the *reproducibility* of results. In this study it was decided to regard a gel as being effective with respect to the separation of any given pair of MHC isoform bands, if the distance between the two MHC isoform bands was  $\geq 2 \times \text{DL}$  (i.e. 0.8mm). This decision was taken to allow for errors in estimating the amount of protein applied per electrophoretic well. The reproducibility of a gel system was defined as the percentage of effective gels it generated.

In the previous section, it was shown that changes in several parameters altered the degree of MHC isoform separation in the gel systems under consideration. Two other factors that were found to alter consistently the effectiveness of separation, regardless of the gel system used, were the MHC isoform composition in the muscle sample and the amount of protein applied per electrophoretic well. In Fig 3.15A is shown the electrophoretogram of a gel used to analyse a muscle homogenate sample known to contain all four MHC isoforms (lane 1) and three single fibres, two of which contained only one MHC isoform (lanes 2 and 3), and one which contained 2 MHC isoforms, IIa and IId (lane 4). The gel failed to separate MHC isoform bands IIa and IId in the whole muscle homogenate sample and in the single fibre co-expressing MHC isoform bands IIa and IId. This gel however, could still be used to distinguish between a single fibre containing MHC isoform IIa (lane 2) from a single fibre

**A MHC isoform composition****B Amount of protein homogenate applied****C Amount of fibre volume applied**

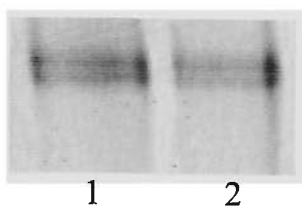
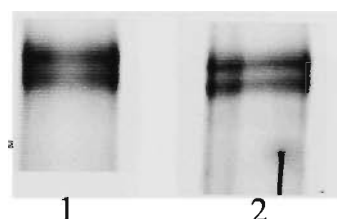
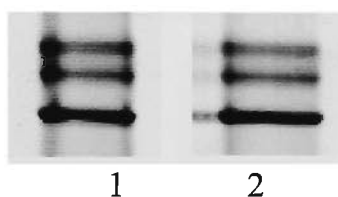
**Figure 3.15 Factors found to alter consistently the effectiveness of MHC isoform separation.** A. MHC isoform composition (Lane 1, muscle homogenate containing all 4 MHC isoforms; lane 2, single fibre containing MHC IIa isoform; lane 3, single fibre containing MHC IIc; lane 4, single fibre containing MHC isoforms IIa and IIc). B. Amount of homogenate sample applied per electrophoretic well. C. Amount of fibre volume applied per electrophoretic well. For details of gel F3.15A, gel F3.15B,C see Appendix 2.

containing MHC isoform IId (lane 3), when the two fibres were run side by side.

The effectiveness of a gel to separate MHC isoforms was also decreased when the amount of sample protein applied per electrophoretic well was higher than a certain value, which in this study was found to be 0.3  $\mu\text{g}$  protein for whole muscle homogenates and 0.3 nL fibre volume for single fibre segments. As seen in Fig. 3.15B and 3.15C, larger amounts of sample applied per electrophoretic well precluded the separation of two neighbouring MHC isoforms.

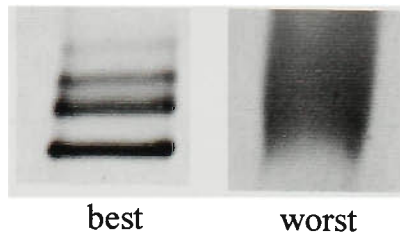
As shown in Fig. 3.16, changing some parameters had no impact on the profile of MHC isoforms on SDS-PA gels. For example, the effectiveness of 'Laemmli' gel systems to separate MHC isoforms IIa, IId, IIb and I in rat skeletal muscle, did not depend on the reducing agent used in the solubilising buffer (Fig. 3.16A) or the polymerisation time of the separating gel (Fig 3.16B). Also, samples solubilised with Laemmli or Mozdziak solubilising buffers produced the same MHC isoform profile on 'Mozdziak' gels (Fig 3.16C).

The majority of the data presented in this thesis were obtained with 25 gels belonging to a 'Laemmli' gel system (Chapter 4&5), 21 gels belonging to a 'Talmadge & Roy' gel system (Chapter 4) and 5 gels belonging to a 'Mozdziak' gel system (Chapter 6). The effectiveness of these three gel systems were compared and the data are presented in Table 3.2. Examples of 'best' and 'worst' gels for each of the three gel systems are shown in Fig. 3.17.

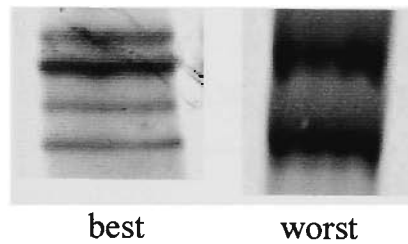
**A Reducing agent****B Polymerisation time****C Type of solubilising buffer**

**Figure 3.16 Factors that do not affect the separation of MHC isoforms on the gel systems considered in this study.** A. Reducing agent in the solubilising buffer (Lane 1,  $\beta$ -mercaptoethanol; lane 2, DTT). B. Polymerisation times of the separating gel (Lane 1, 2 hours; lane 2, overnight) C. Different solubilising buffers [Lane 1, Laemmli (1970); lane 2, Mozdziak *et al.* (1999)]. For details of gelF 3.16A, gelF 3.16B and gelF 3.16C see Appendix 2.

**A 'Laemmli' gel system.**



**B 'T-R' gel system.**



**C 'T-R' Mozdziak gel system.**

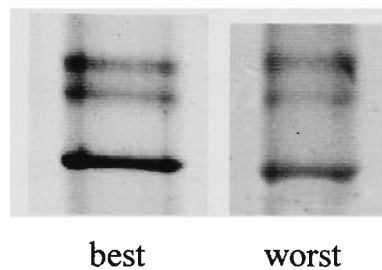


**Figure 3.17** Electrophoretograms of best and worst gels with respect to the separation of all four MHC isoforms in three different gel systems. A. 'Laemmli' gel system . B. 'T-R' gel system. C. 'T-R' Mozdziak gel system. For details of gel F3.17A, gel F3.17B and gel F3.17C see Appendix 2.

**Table 3.2 Parameters used to evaluate the effectiveness of three gel systems.**

Note that the detection limit for densitometric analyses is 0.4mm. For details regarding the gels see Appendix 3.

gel system (code for gel identification in Appendix 3)	# of gels	$\Delta_{\text{Ib-I}}$ (mm)		$\Delta_{\text{IId-Ib}}$ (mm)		$\Delta_{\text{IIa-IId}}$ (mm)	
		mean $\pm$ SD	range	mean $\pm$ SD	range	mean $\pm$ SD	range
'Laemmli' gel T3.2-1	25	1.33 $\pm$ 0.86	0-4.50	0.56 $\pm$ 0.41	0-1.20	0.80 $\pm$ 0.49	0-1.45
'T-R' gel T3.2-2	21	3.51 $\pm$ 0.81	1.90-5.00	1.08 $\pm$ 0.53	0-1.75	0.64 $\pm$ 0.37	0-1.10
'T-R' Mozdziak gel T3.2-3	5	3.04 $\pm$ 0.36	2.50-3.40	1.32 $\pm$ 0.24	0.90-1.50	0.16 $\pm$ 0.22	0-0.40

As indicated by the  $\Delta$  values in Table 3.2, all 'T-R' gels (including the 'T-R' Mozdziak gels) were able to separate MHC isoforms Iib and I, whereas on some of the 'Laemmli' gels all MHC isoforms co-migrated in a broad band as seen in Fig. 3.17A (worst). The average values for  $\Delta_{\text{Ib-I}}$  in the 'T-R' protocols were at least twice as high as the average  $\Delta_{\text{Ib-I}}$  achieved with the 'Laemmli' gel system.

Separation of the two fast MHC isoform IId and Iib was always achieved with the 'T-R' Mozdziak gel system, but not on some of the 'Laemmli' and 'T-R' gels. Interestingly, the average values for  $\Delta_{\text{IId-Ib}}$  produced by 'T-R' and 'T-R' Mozdziak gels were once again twice as high as those obtained with the 'Laemmli' gel system.

A few gels of each gel system failed to separate MHC isoform bands IIa and IId. The average  $\Delta_{\text{IIa-IId}}$  values for 'Laemmli' gel system was higher than 'T-R' gel system, which in turn was higher than the 'T-R' Mozdziak gel system.

The data shown in Table 3.2 allow a comparison of  $\Delta_{\text{Ib-I}}$ ,  $\Delta_{\text{IId-Ib}}$  and  $\Delta_{\text{IIa-IId}}$  for each gel system. It is clear from these data that all three gel systems were more

effective in separating the fast and slow MHC isoforms  $\Pi b$  and  $I$  than fast and fast MHC isoforms  $\Pi d$  and  $\Pi b$ , and  $\Pi a$  and  $\Pi d$ . In both 'T-R' gel systems,  $\Delta_{\Pi b-I}$  was higher than  $\Delta_{\Pi d-\Pi b}$ , which in turn was higher than  $\Delta_{\Pi a-\Pi d}$ , while in the 'Laemmli' gel system  $\Delta_{\Pi b-I}$  was higher than  $\Delta_{\Pi a-\Pi d}$ , which was higher than  $\Delta_{\Pi d-\Pi b}$ .

In order to obtain further information about the effectiveness and reproducibility of the Laemmli and T-R gel systems, the values of  $\Delta_{\Pi b-I}$ ,  $\Delta_{\Pi d-\Pi b}$  and  $\Delta_{\Pi a-\Pi d}$  were represented using frequency distribution plots for each gel system. The data presented were obtained from 230 'Laemmli' gels and 91 'T-R' gels. As shown in Fig. 3.18A, 87% of 'Laemmli' gels were effective in separating MHC isoforms  $\Pi b$  and  $I$ . In contrast only 52.6% of the gels were effective with respect to the separation of MHC isoforms  $\Pi d$  and  $\Pi b$  (Fig. 3.18B) and only 22.6% of the gels were effective in separating MHC isoforms  $\Pi a$  and  $\Pi d$  (Fig. 3.18C). A similar result was found for the reproducibility of 'T-R' gels, shown in Fig. 3.19. Thus, the proportions of effective gels in the 'T-R' gel system were 83.5% for  $\Delta_{\Pi b-I}$  (Fig. 3.19A), 41.8% for  $\Delta_{\Pi d-\Pi b}$  (Fig. 3.19B) and only 29.6% for  $\Delta_{\Pi a-\Pi d}$  (Fig. 3.19C).

As seen in Fig 3.18A, in one 'Laemmli' type gel,  $\Delta_{\Pi b-I}$  reached a value as high as 5.6 mm ( $14 \times DL$ ); a similar value ( $12 \times DL$ ) for  $\Delta_{\Pi b-I}$  was observed with some 'T-R' gels (Fig. 3.19A). By comparison, the maximum values of  $\Delta$  for the fast MHC isoforms achieved with the 'Laemmli' gels were  $7 \times DL$  ( $\Delta_{\Pi d-\Pi b}$ , Fig 3.18B) and  $4 \times DL$  ( $\Delta_{\Pi a-\Pi d}$ , Fig 3.18C) and with the 'T-R' gels were  $5 \times DL$  ( $\Delta_{\Pi d-\Pi b}$ , Fig 3.19B) and  $4 \times DL$  ( $\Delta_{\Pi a-\Pi d}$ , Fig 3.19C). These data demonstrate that the MHC isoforms most difficult to separate are the fast isoforms.

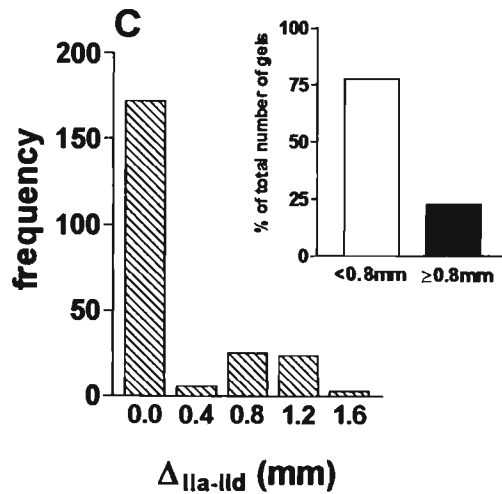
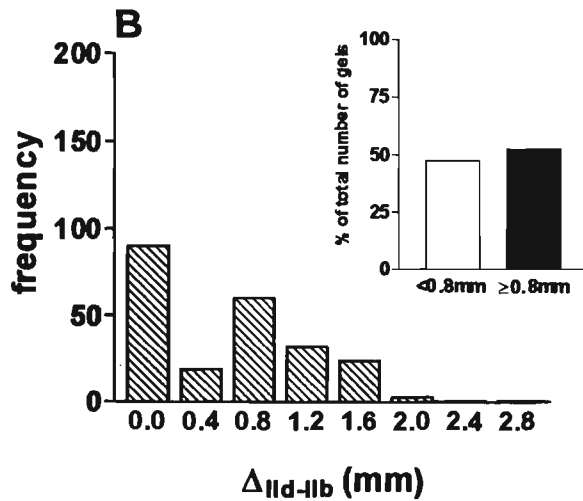
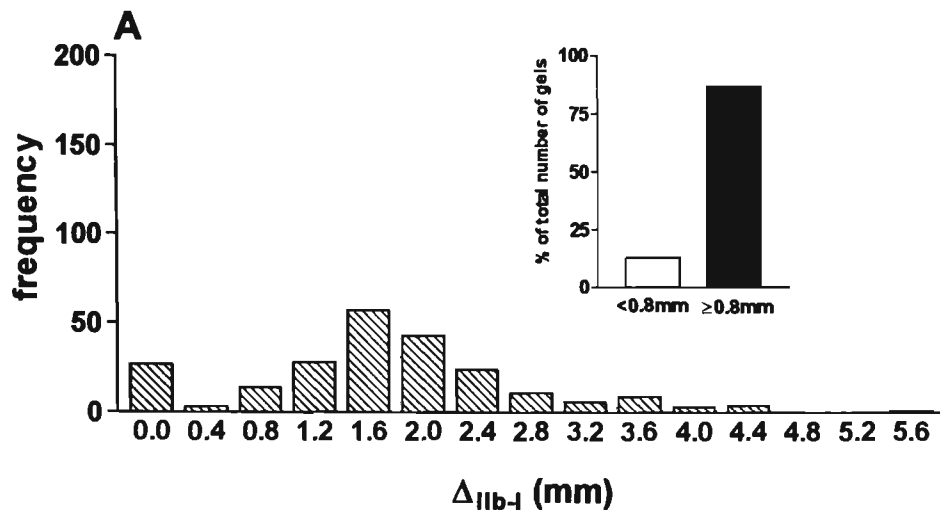


**Figure 3.18** Frequency distribution of  $\Delta_{IIb-I}$  (panel A),  $\Delta_{IIc-IIb}$  (panel B) and  $\Delta_{IIa-IIc}$  (panel C) for the 'Laemmli' gel system. The data originated from 230 gels. The relative proportion of effective gels, estimated by adding all gels on which  $\Delta \geq 0.8$  mm is shown in inserts.

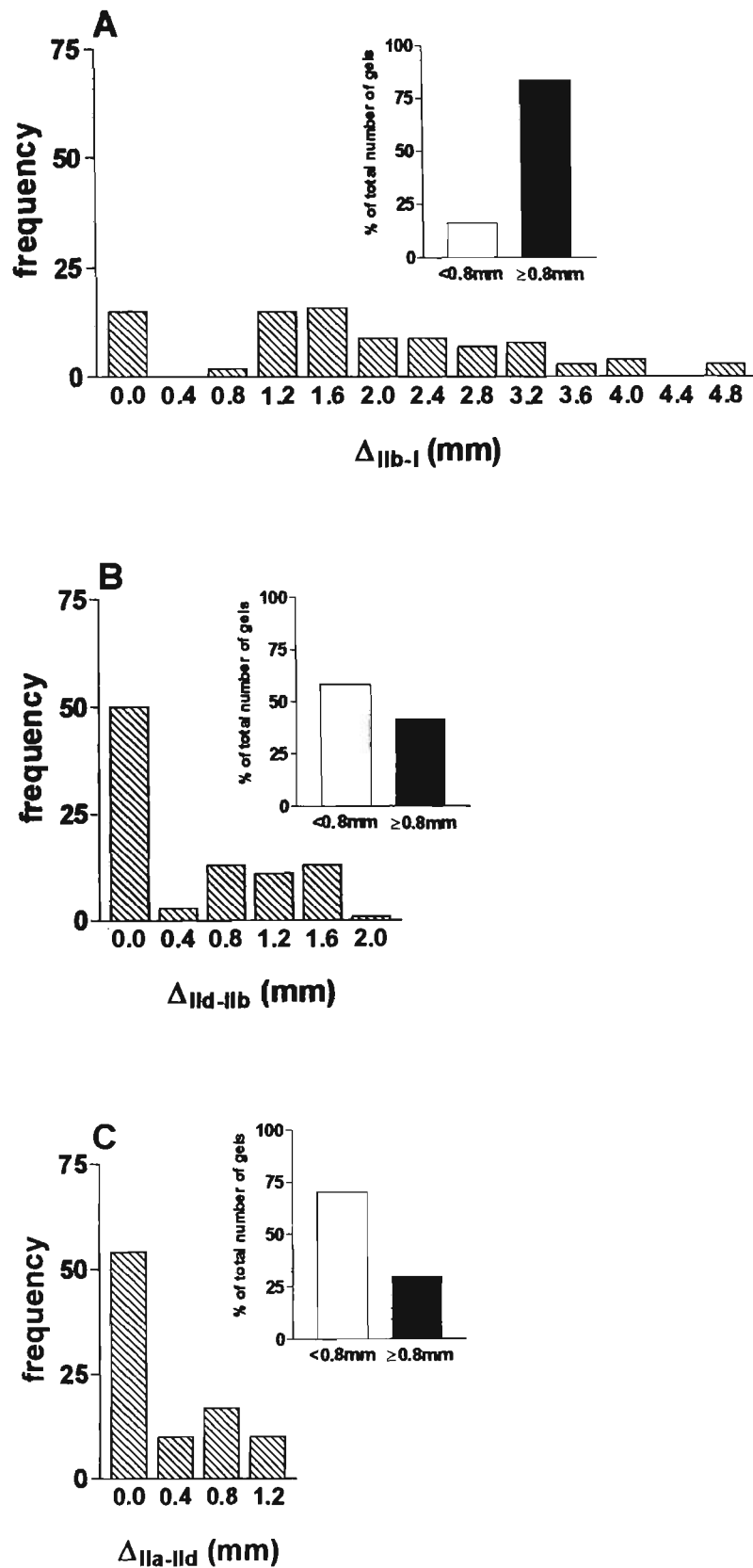


**Figure 3.19** Frequency distribution of  $\Delta_{IIb-I}$  (panel A),  $\Delta_{IIc-IIb}$  (panel B) and  $\Delta_{IIa-IIc}$  (panel C) for the 'T-R' gel system. The data originated from 91 gels. The relative proportion of effective gels, estimated by adding all gels on which  $\Delta \geq 0.8$  mm is shown in inserts.

### 3.4 Discussion

Currently, the most widely used method for electrophoretic analysis of MHC isoform composition is SDS-PAGE, which allows separation and visualisation of MHC isoforms, identification of MHC isoforms (when used in conjunction with immunoblotting), and quantification of the relative proportion of individual MHC isoforms in a complex mixture. SDS-PAGE analysis of MHC isoform expression is a low-cost and convenient method that has the unique ability to identify hybrid fibres (Bottinelli *et al.*, 1991; Härmäläinen & Pette, 1995; Pette *et al.*, 1999). Furthermore, this method can be performed on whole muscle homogenates, MHC extracts, and single fibre segments as small as 0.3nL fibre volume. The popularity of SDS-PAGE in muscle research is reflected by the large number of studies published in recent years (>171 in 12 months) that used this method to investigate the heterogeneity and plasticity of mammalian skeletal muscle.

A survey of 72 studies [spanning the period between the time when Carraro & Catani first used SDS-PAGE to separate mammalian MHC isoforms (Carraro & Catani, 1983) and the end of 1999], reveals major technical differences between SDS-PAGE protocols used by the same laboratory at different times or by different laboratories (see Appendices 5.1 and 5.2), and major differences in the effectiveness of MHC separation achieved with these protocols. For example, in 1996 one laboratory (Blough *et al.*) described a new method which was claimed to enhance

electrophoretic separation and resolution of MHC in mammalian skeletal muscle; two years later the same laboratory published a study in which MHC isoforms were analysed using a protocol which differed markedly from the earlier one with respect to the composition of the separating gel, stacking gel, running buffer and the running conditions (Reiser & Kline, 1998). The electrophoretograms of MHC isoform samples shown in the respective papers are also very different. Thus, in the electrophoretograms presented in the earlier paper (Blough *et al.*, 1996) one can clearly see MHC I and the slowest migrating fast MHC isoform bands, but it is difficult to distinguish between the other two fast MHC isoform bands. In the later paper (Reiser & Kline, 1998), all 4 MHC isoform bands are clearly distinguishable in a tibialis anterior muscle sample.

The lack of a unique SDS-PAGE protocol for the separation of the four main MHC isoforms in rat muscles, noted as a result of this survey, can be regarded as an indication of the inability of any one gel system to effectively and reproducibly separate these protein species. The effectiveness and reproducibility of the separation of MHC isoform pairs Iib and I, Iid and Iib and Iia and Iid, were extensively examined in the present study using 230 'Laemmli' type gels and 91 'T-R' type gels. The results showed, that in both systems, the effectiveness and reproducibility of MHC isoform separation were related to one other and both depended on the pair of MHC isoforms under consideration. Thus, in both systems, the proportion of successful gels with respect to the separation of MHC isoforms Iib and I was higher than 80%, and on some gels  $\Delta_{Iib-I}$  was as high as  $12-14 \times DL$ . The reproducibility of gels with respect to the separation of MHC isoforms Iid and Iib, in both gel systems,

was markedly lower (52.6% for 'Laemmli' and 41.8% for 'T-R') than  $\Delta_{\text{Ib-I}}$  and the maximum value for  $\Delta_{\text{IId-Ib}}$  was no higher than  $7 \times \text{DL}$ . In both gel systems, the lowest reproducibility (<30%) and effectiveness (< $4 \times \text{DL}$ ) of separation was noted for the fast MHC isoforms IIa and IId.

The existence of MHC isoform IId was first recognised in 1988 (Bär & Pette). Since then a large number of studies have used SDS-PAGE analysis of MHC composition in whole muscle homogenates, MHC extracts or single muscle fibres. A survey of 63 papers reporting data for muscles expected to contain MHC IIa and IId isoforms, showed that in 13 studies the authors failed to separate these isoforms. It is interesting to note that only 6 of these 13 studies commented on the co-migration of MHC isoform bands IIa and IId, and only 1 group made a quantitative statement regarding the reproducibility of the gel system used to separate MHC isoforms IIa and IId. Thus, LaFramboise *et al.* (1990) stated that only 20% of their SDS-PA gels were able to separate MHC isoforms IIa and IId, a value similar to that reported in the present study.

It is surprising that so far, there has been no systematic study on the effectiveness of different electrophoretic parameters on the separation of MHC isoforms by SDS-PAGE, given the low reproducibility of the gels systems used (particularly for the fast MHC isoforms IIa, IId and IIb). The need for such a study has been emphasised also by Schiaffino & Salviati (1998) and by Reiser & Kline (1998).

In the present study, a number of parameters related to the composition of the separating and stacking gels and the running conditions were tested for effectiveness with respect to the separation of MHC isoforms in both 'Laemmli' and 'T-R' gel systems. A summary of the data organised by the pair of MHC isoforms under consideration and by parameter effectiveness (ineffective or enhancing) is presented in Table 3.3 for 'Laemmli' gel systems and Table 3.4 for 'T-R' gel systems.

A notable result found in both systems was that the effect of most parameters, within the range examined, was MHC isoform dependent. For example, in the 'Laemmli' gel system, decreasing  $[A]_{sep}$  from 10 to 6% increased  $\Delta_{IIb-I}$ , but had no effect on  $\Delta_{IIc-IIb}$  and  $\Delta_{IIa-IIc}$ . Also increasing  $E$  over the range 11.4 to 17.0 V/cm and the running time from 24 to 34 hrs, produced larger values for  $\Delta_{IIb-I}$  and  $\Delta_{IIc-IIb}$  but had no effect on  $\Delta_{IIa-IIc}$ . Varying some parameters produced opposite effects on the separation of different MHC isoforms pairs. Thus, increasing  $[Tris]_{sep}$  from 375 to 500 mM, reduced  $\Delta_{IIb-I}$ , but enhanced  $\Delta_{IIc-IIb}$  and  $\Delta_{IIa-IIc}$ . It is important to note that even if altering a parameter changed  $\Delta$  for two different pairs of MHC isoforms in the same direction (increase or decrease), the magnitude of this change was also MHC isoform dependent. For example, varying the running time from 24 to 34 hrs, increased  $\Delta_{IIb-I}$  by 175%, but  $\Delta_{IIc-IIb}$  only by 48% (see Fig. 3.7).

**Table 3.3 Effectiveness of different parameters with respect to the separation of MHC isoform pairs  $\Pi$ b-I,  $\Pi$ d- $\Pi$ b, and  $\Pi$ a- $\Pi$ d in the 'Laemmli' gel systems.**

$\Delta_{\Pi b-I}$		$\Delta_{\Pi d-\Pi b}$		$\Delta_{\Pi a-\Pi d}$	
ineffective parameter (range)	enhancing parameter (range)	ineffective parameter (range)	enhancing parameter (range)	ineffective parameter (range)	enhancing parameter (range)
$\%C_{sep}$ (1.5 $\Rightarrow$ 1.8%)	$[A]_{sep}$ (10 $\Rightarrow$ 6%)	$[A]_{sep}$ (6 $\Rightarrow$ 10%)	$[Tris]_{sep}$ (375 $\Rightarrow$ 500mM)	$[A]_{sep}$ (6 $\Rightarrow$ 10%)	$[Tris]_{sep}$ (375 $\Rightarrow$ 500mM 700 $\Rightarrow$ 500mM)
$[glycerol]_{sep}$ (35 $\Rightarrow$ 37% & 40 $\Rightarrow$ 42.5%)	$\%C_{sep}$ (2.5 $\Rightarrow$ 1.8%)	$[Tris]_{sep}$ (500 $\Rightarrow$ 700mM)	$[glycerol]_{sep}$ (42.5 $\Rightarrow$ 40%)	$\%C_{sep}$ (1.5 $\Rightarrow$ 2.5%)	<b>E</b> (11.4 $\Rightarrow$ 13.6V/cm)
<b>40% glycerol in the stacker</b>	$[Tris]_{sep}$ (700 $\Rightarrow$ 500mM 500 $\Rightarrow$ 375mM)	$[glycerol]_{sep}$ (35 $\Rightarrow$ 40%)	$[glycine]_{sep}$ (0 $\Rightarrow$ 50mM)	$[glycerol]_{sep}$ (35 $\Rightarrow$ 42.5%)	<b>rT</b> (12 $\Rightarrow$ 14°C)
	$[glycerol]_{sep}$ (37 $\Rightarrow$ 40%)	$[glycine]_{sep}$ (50 $\Rightarrow$ 100mM)	<b>E</b> (11.4 $\Rightarrow$ 17.0V/cm)	$[glycine]_{sep}$ (0 $\Rightarrow$ 100mM)	
	$[glycine]_{sep}$ 100 $\Rightarrow$ 0mM	<b>40% glycerol in the stacker</b>	<b>Rt</b> (24 $\Rightarrow$ 34hrs)	<b>40% glycerol in the stacker</b>	
	<b>E</b> (11.4 $\Rightarrow$ 17.0V/cm)	<b>E</b> (11.4 $\Rightarrow$ 13.6V/cm)	<b>rT</b> (16-21 $\Rightarrow$ 12-14°C)	<b>E</b> (11.4 $\Rightarrow$ 17.0V/cm)	
	<b>Rt</b> (24 $\Rightarrow$ 34hrs)	<b>rT</b> (2-4 $\Rightarrow$ 12-14°C)		<b>Rt</b> (24 $\Rightarrow$ 34hrs)	
	<b>rT</b> (2-4 $\Rightarrow$ 16-21°C)			<b>rT</b> (2-4 $\Rightarrow$ 16-21°C)	

rT, running temperature; Rt, running time

**Table 3.4 Effectiveness of different parameters with respect to the separation of MHC isoform pairs  $\Pi\text{b-I}$ ,  $\Pi\text{d-}\Pi\text{b}$ , and  $\Pi\text{a-}\Pi\text{d}$  in the 'T-R' gel systems.**

$\Delta_{\Pi\text{b-I}}$		$\Delta_{\Pi\text{d-}\Pi\text{b}}$		$\Delta_{\Pi\text{a-}\Pi\text{d}}$	
ineffective parameter (range)	enhancing parameter (range)	ineffective parameter (range)	enhancing parameter (range)	ineffective parameter (range)	enhancing parameter (range)
[glycerol] <sub>sep</sub> (30 $\Rightarrow$ 40%)	[glycerol] <sub>sep</sub> (40 $\Rightarrow$ 45%)	stacker type (T-R or 'L <sup>G+</sup> ')	[glycerol] <sub>sep</sub> (30 $\Rightarrow$ 45%)	[glycerol] <sub>sep</sub> (40 $\Rightarrow$ 42.5%)	[glycerol] <sub>sep</sub> (30 $\Rightarrow$ 40% 45 $\Rightarrow$ 40%)
stacker type (T-R or 'L <sup>G+</sup> ')	running buffer type (D-B > T-R)	E (9.7 $\Rightarrow$ 17.0V/cm)	running buffer type (T-R > D-B)		stacker type (T-R or 'L <sup>G+</sup> ')
E (14.8 $\Rightarrow$ 17.0V/cm)	E (9.7 $\Rightarrow$ 14.8V/cm)				running buffer type (T-R > D-B)
					E (9.7 $\Rightarrow$ 14.8V/cm 17.0 $\Rightarrow$ 14.8V/cm)

For some parameters the effectiveness with respect to the separation of a given MHC isoform pair was dependent on the range examined. For example, in the 'Laemli' gel system  $\Delta_{\Pi\text{d-}\Pi\text{b}}$  was enhanced by an increase of [Tris] from 375 to 500 mM, but was unchanged by a further increase of [Tris] to 700 mM.

The dependence of parameter effectiveness on the identity of MHC isoforms explains in part the difficulty encountered by researchers seeking to optimise a gel system for separation of all MHC isoforms; clearly it would be much easier to optimise a gel system with respect to the separation of a given pair (MHC isoforms

IIb and I or IId and IIb or IIa and IId). Thus, if the aim of a study was to achieve good separation of MHC isoforms IIa and IId, the optimisation strategy would have to include modification of the enhancing parameters listed in Table 3.3 for the 'Laemmli' gel system or Table 3.4 for the 'T-R' gel system, within the range indicated, but not of the parameters listed as ineffective.

In this context it was interesting to assess which parameters were modified by other groups concerned with the separation of mammalian MHC isoforms, and how frequently a given parameter was modified either from the original protocol of Laemmli or the original protocol of Talmadge & Roy. The group of papers considered for this purpose comprised 46 studies using 'Laemmli' gel systems (listed in Appendix 5.1) and 17 studies using 'T-R' gel systems (listed in Appendix 5.2). The results of this analysis are presented in Fig. 3.20. A careful examination of frequency plots for the two gel systems, reveals that some parameters of the separating gel, stacker and the running conditions have been subjected to modifications more frequently in the 'Laemmli' gel systems (Fig. 3.20A) than the 'T-R' gel systems (Fig. 3.20B). For example, modifications to [A] and [glycerol] in the separating gel were made in all 46 studies using the 'Laemmli' gel system, but only in four and three studies, respectively, using the 'T-R' gel system. Also it is interesting to note that one of the parameters ( $[\text{glycine}]_{\text{sep}}$ ) that was found in the present study to enhance the separation of MHC isoforms IId and IIb in the 'Laemmli' gel system, was not used in any of the studies using the 'Laemmli' system covered in this survey.

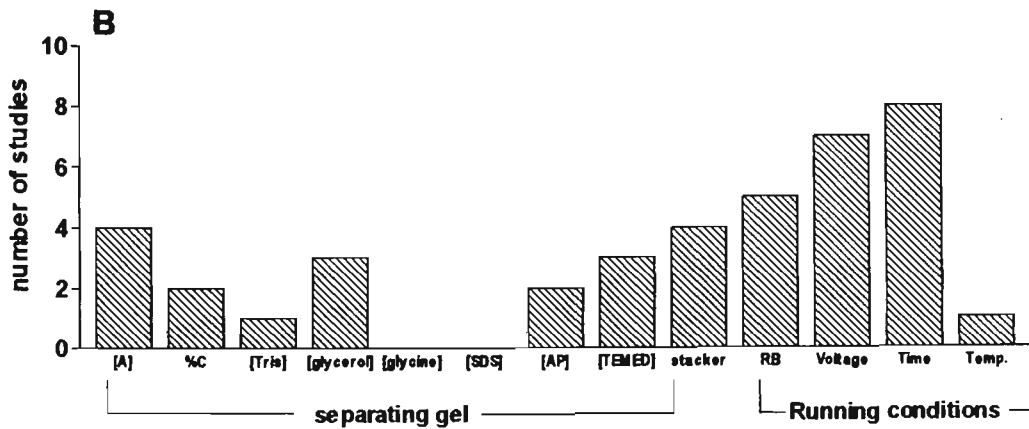
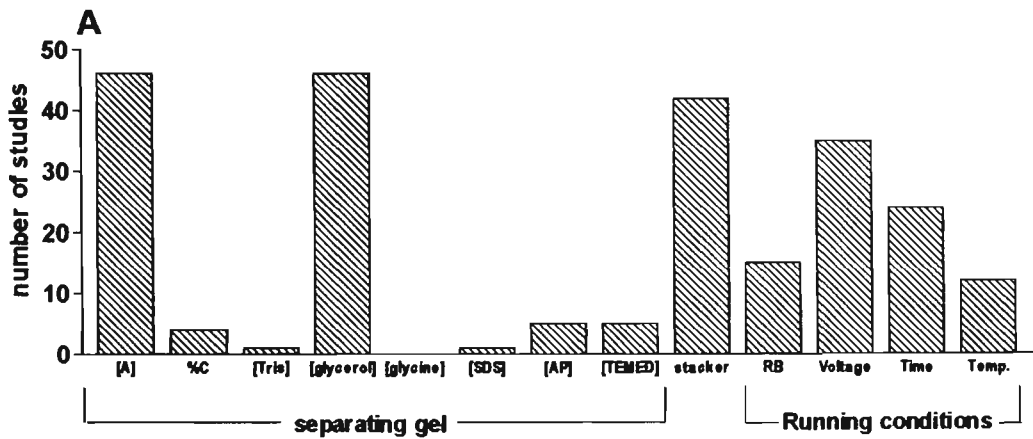


**Figure 3.20** Relative proportion of studies that modified the specified electrophoretic parameters in the original gel protocols of 'Laemmli' (panel A) and 'T-R' (panel B) when trying to separate mammalian MHC isoforms. Symbols on x-axis are: [A], [acrylamide]; %C, %C value; [AP], [ammonium persulfate]; RB, running buffer; Temp., temperature.

## Chapter 4

# Myosin Heavy Chain Isoform Composition and $\text{Ca}^{2+}/\text{Sr}^{2+}$ - Activation Characteristics of Single Fibres from Soleus, EDL and Diaphragm Muscles of Adult Rat

### 4.1 Introduction

Mammalian skeletal muscle fibres contain a multitude of MHC isoforms that confer specific characteristics to the contractile apparatus with respect to myofibrillar ATPase activity and velocity of shortening (Moss *et al.*, 1995; Schiaffino & Reggiani, 1996). The contractile phenotype of a muscle fibre is described, however, not only by its myofibrillar ATPase activity and maximum velocity of shortening, but also by characteristics associated with the process of isometric activation by  $\text{Ca}^{2+}$  such as  $\text{Ca}^{2+}$  threshold for activation, sensitivity to  $\text{Ca}^{2+}$ , maximum  $\text{Ca}^{2+}$ -activated force per cross-sectional area and degree of cooperativity in development of  $\text{Ca}^{2+}$ -activated force. Moreover, skeletal muscle fibres display quite striking differences with respect to some contractile activation characteristics when  $\text{Sr}^{2+}$  instead of  $\text{Ca}^{2+}$  is used as the

activating ion (Fink *et al.*, 1986). To date, the correlation between MHC isoform expression and contractile activation characteristics of skeletal muscle fibres has not been examined in sufficient depth to provide a solid basis for understanding the extent of MHC isoform involvement in molecular events underlying the process of contractile activation.

It is important to note also that MHC isoform composition (Pette & Staron, 1990) and  $\text{Ca}^{2+}/\text{Sr}^{2+}$ -activation characteristics (Fink *et al.*, 1986, Wilson & Stephenson, 1990) have often been used separately as criteria for fibre typing in biochemical and physiological studies of muscle contractility (see also section 1.4). If MHC isoform composition and  $\text{Ca}^{2+}/\text{Sr}^{2+}$ -activation characteristics were tightly correlated, then the two methods should be comparable, i.e. each method used alone should enable the experimenter to learn about both the physiological and biochemical profile of a given fibre. Alternatively, if MHC isoform composition and  $\text{Ca}^{2+}/\text{Sr}^{2+}$ -activation properties were not tightly correlated, the two methods should be used in tandem when seeking to characterise a muscle fibre in molecular and functional terms. Thus, furthering the understanding of the correlation between MHC isoform expression and isometric activation characteristics has both theoretical and methodological implications. The aim of this study was to explore this issue by employing a broad range of fibre types obtained by random dissection from SOL (predominantly slow-twitch), EDL (predominantly fast-twitch) and DPH (mixed-twitch) muscles of adult rats to determine a number of  $\text{Ca}^{2+}$ - and  $\text{Sr}^{2+}$ -activation characteristics of single muscle fibres under near-physiological conditions. The fibre population examined contained pure fibres (expressing one MHC isoform only) of all four types known to occur in trunk and limb

muscles of rodents (type I, IIA, IID and IIB) and several types of hybrid fibres expressing combinations of two or three MHC isoforms. The MLC isoform expression in a subpopulation of fibres was also investigated in order to assess whether the rule of myofibrillar protein isoform co-expression recently suggested by Bottinelli *et al.* (1999) for human muscle holds also for rat skeletal muscles.

## 4.2 Methods

*Note: Experiments with DPH fibres were carried out in collaboration with Maria Cellini.*

**Animals and muscle dissection.** The animals used in this study were forty-three male adult rats (Wistar-Kyoto, WKY and spontaneously hypertensive rats, SHR) aged 15- to 24-wk. The SHRs were used because in the work described in Chapter 5 it was found that SHR soleus muscles are enriched in IIA, I+IIA and IIA+IID fibres and that there are no differences with respect to  $Ca^{2+}$ -activation characteristics between fibres of the same type from age-matched SHR and WKY animals. The rats were supplied by the Baker Medical Research Institute (Melbourne, Australia), housed at La Trobe University Animal House, and stored and killed as described in section 2.1. The SOL, EDL and DPH muscles were dissected and stored as described in section 2.2.

**Preparation of Triton-skinned, single muscle fibre segments.** All EDL and DPH muscles and 51% of the SOL muscles used in this study were obtained from WKY rats.

In order to increase the proportion of fast and hybrid fibres in the population of SOL fibres, SOL muscles dissected from SHR animals were also used. Single fibres were isolated, measured and chemically skinned as described in section 2.3. Following contractile experiments, single fibre segments were analysed for myofibrillar protein isoforms as described in the following sections.

*Determination of Ca<sup>2+</sup>/Sr<sup>2+</sup>-activation characteristics of chemically skinned, single muscle fibre segments.* Ca<sup>2+</sup>/Sr<sup>2+</sup>-activation characteristics were determined at an average sarcomere length of  $2.65 \pm 0.02 \mu\text{m}$  (n=45), which was measured as described in section 2.4.4. The Ca<sup>2+</sup>/Sr<sup>2+</sup>-activation solutions were prepared as described in section 2.4.5 and the pCa and pSr values are shown in Table 4.1. Only fibre segments for which a complete set of Ca<sup>2+</sup>/Sr<sup>2+</sup>-activation characteristics and MHC profile was obtained have been used in this study.

**Table 4.1 pCa and pSr values of activating solutions.**

Solution number	SOL fibres		EDL and DPH fibres	
	pCa	pSr	pCa	pSr
1	>9	>9	>9	>9
2	>8	>8	>8	>8
3	6.68	6.40	6.69	6.41
4	6.51	6.17	6.52	6.19
5	6.21	5.87	6.22	5.88
6	6.02	5.48	6.04	5.49
7	5.81	5.19	5.84	5.21
8	5.55	4.90	5.60	4.91
9	5.34	4.70	5.42	4.72
10	5.15	4.39	5.27	4.41
11	4.96	3.88	5.13	3.92
12	4.27	3.55	4.79	3.62

**Data analysis.** Force responses were measured and  $P_t$  values (where  $P_t$  is expressed as % maximum force) were calculated as described in section 2.4.6.1.  $P_t$  was then plotted against the pCa/pSr values and theoretical Hill curves were fitted through the data points using a nonlinear regression analysis protocol (GraphPad Prism software). All 241 fibres investigated in this study fitted the ‘simple’ fibre category (as defined in section 2.4.6.2) with respect to  $Ca^{2+}$ -activation and 233 fibres with respect to  $Sr^{2+}$ -activation. Data for these fibres were analysed as described in section 2.4.6.2. For eight fibres, the best-fitted simple  $Sr^{2+}$ -Hill curve passed outside the individual experimental data points by more than 5% of the maximum activated force. In this case, a combination of two Hill curves (‘composite’ curve) was used to fit the experimental data points (Wilson & Stephenson, 1990) with the GraphPad Prism software:

$$P_t = w_1 / [1 + 10^{n_{Sr1} (pSr - pSr_{50/1})}] + w_2 / [1 + 10^{n_{Sr2} (pSr - pSr_{50/2})}] \quad (\text{Eq 1})$$

where  $w_1$  and  $w_2$  are normalised weighting factors ( $w_1 + w_2 = 1$ ),  $n_{Sr1}$ ,  $n_{Sr2}$  are the corresponding Hill coefficients and  $pSr_{50/1}$ ,  $pSr_{50/2}$  are the corresponding  $pSr_{50}$  values for the two Hill curves. Fibres that were characterised by simple Hill curves for both  $Ca^{2+}$  and  $Sr^{2+}$  are referred to as ‘simple’ fibres, whereas fibres that displayed simple Hill curves for  $Ca^{2+}$  but composite curves for  $Sr^{2+}$  are referred to as ‘composite’ fibres.

Since the force-pSr data points for all 8 fibres could be well fitted by composite Hill curves derived from Eq 1, these fibres were classified as ‘composite’ fibres. ‘Simple’ fibres were further subdivided into two groups based on their relative sensitivity to  $\text{Ca}^{2+}$  and  $\text{Sr}^{2+}$  expressed as  $\text{pCa}_{50}$ - $\text{pSr}_{50}$  ( $\Delta_{50}$ ): ‘simple slow’ fibres ( $S_{\text{slow}}$ ; 119 fibres) ( $\Delta_{50} \leq 0.5$ ) and ‘simple fast’ fibres ( $S_{\text{fast}}$ ; 114 fibres) ( $\Delta_{50} \geq 1.0$ ). The ‘composite’ fibres were also further subdivided into three groups based on their relative sensitivity to  $\text{Ca}^{2+}$  and  $\text{Sr}^{2+}$ : ‘composite slow-slow’ fibres ( $\text{COMP}_{\text{s-s}}$ ; 2 fibres) ( $\text{pCa}_{50} - \text{pSr}_{50/1}$ ,  $\text{pCa}_{50} - \text{pSr}_{50/2} \leq 0.5$ ), ‘composite slow-fast’ fibres ( $\text{COMP}_{\text{s-f}}$ ; 4 fibres) ( $\text{pCa}_{50} - \text{pSr}_{50/1} \leq 0.5$  and  $\text{pCa}_{50} - \text{pSr}_{50/2} \geq 1$ ) and ‘composite fast-fast’ fibres ( $\text{COMP}_{\text{f-f}}$ ; 2 fibres) ( $\text{pCa}_{50} - \text{pSr}_{50/1}$ ,  $\text{pCa}_{50} - \text{pSr}_{50/2} \geq 1$ ).

$\text{Ca}^{2+}$ - and  $\text{Sr}^{2+}$ -activation parameters [ $\text{CaF}_{\text{max}}$ ,  $\text{pCa}_{10}$ ,  $\text{pSr}_{10}$ ,  $\text{pCa}_{50}$ ,  $\text{pSr}_{50}$  ( $\text{pSr}_{50/1}$  and  $\text{pSr}_{50/2}$  for ‘composite’ fibres),  $n_{\text{Ca}}$ ,  $n_{\text{Sr}}$  ( $n_{\text{Sr}1}$  and  $n_{\text{Sr}2}$  for ‘composite’ fibres),  $\text{pCa}_{10} - \text{pSr}_{10}$ ,  $\text{pCa}_{50}$ - $\text{pSr}_{50}$ ] were determined as described in section 2.4.6.2. The presence of oscillations at submaximal  $\text{Ca}^{2+}$ -activation ( $< 50\% \text{CaF}_{\text{max}}$ ) was also recorded for a subpopulation of fibres.

*SDS-PAGE analysis of MHC and MLC isoforms.* Details related to the set up of the gel apparatus and to basic electrophoretic procedures, such as gel preparation, sample preparation, gel staining and densitometry, can be found in the appropriate sections within Chapter 2. The gel systems used for MHC isoform analysis are described in Appendix 2 (gelf 3.16BC, gelf 3.17A and gelf 3.17B). An internal standard was

included in each gel (Fig. 4.1, lane 1) to ensure that the gel resolved all four MHC isoforms and enabled for correct identification of MHC bands in single muscle fibres.

MLC isoforms were separated on SDS-PA gels using a separating gel containing [A] = 18% w/v, %C=5.0%, [Tris] = 750 mM pH 9.3, [glycerol] = 10% v/v, [SDS] = 0.1% w/v, and gels were polymerised with 0.025% AP and 0.03% TEMED. The stacking gel contained [A]=3% w/v, %C=4.8%, [Tris] = 125 mM pH 6.8, [glycerol] = 10% v/v, [SDS] = 0.1%, and gels were polymerised with 0.1% AP and 0.05% TEMED. The running buffer contained 50 mM Tris, 380 mM glycine and 0.1% SDS. Gels were run at a constant current (10mA/gel) at RT until the lowest molecular weight marker reached the bottom of the gel (4-5 hrs), and then were stained as described in section 2.5.3. The MLC bands were identified as described in section 2.5.2.

*Statistics.* All data are expressed as means  $\pm$  SE. Unless stated otherwise, statistical comparisons were performed between groups comprising at least three sets of data using a one-way analysis of variance (ANOVA) followed by the Bonferroni test.

Statistical significance was accepted at  $P < 0.05$ .

## 4.3 Results

### 4.3.1 Fibre types classified according to MHC composition

Based on their MHC composition, the 241 single fibre segments examined in the present work (146 SOL fibres, 52 EDL fibres and 43 DPH fibres) belonged to three major groups: (i) pure fibres, expressing only one MHC isoform [fibre types I, IIA, IID/X (referred to in this study as IID), and IIB, Fig 4.1, lanes 2-5], (ii) slow/fast hybrid fibres, co-expressing one slow and one fast (fibre types I+IIA and I+IID, Fig. 4.1, lanes 6 and 7) or one slow and two fast MHC isoforms (fibre type I+IIA+IID, Fig. 4.1, lane 10) and (iii) fast hybrid fibres co-expressing two or three fast MHC isoforms (fibre types IIA+IID, IID+IIB and IIA+IID+IIB, Fig. 4.1, lanes 8, 9 and 11). No hybrid fibres co-expressing 4 MHC isoforms or the combinations of MHC isoforms I + Iib, Iia + Iib, I + Iia + Iib, or I + Iib + Iid were found in this study. As shown in Table 4.2, 73.4% of all fibres contained only one MHC isoform, 23.7% contained two MHC isoforms (2 MHC-hybrids) and 2.9% contained three MHC isoforms (3 MHC-hybrids).

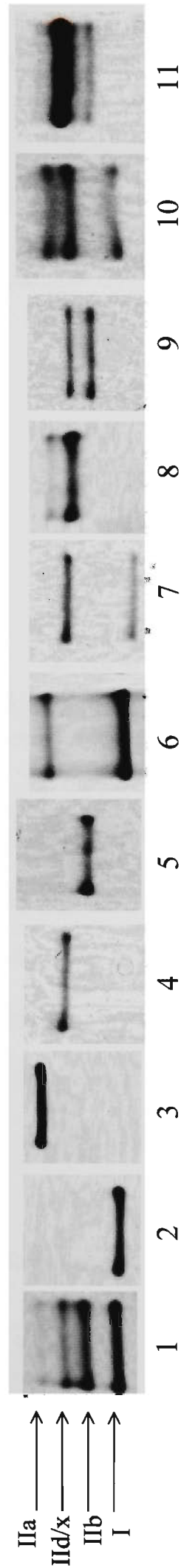


**Figure 4.1** Representative electrophoretogram of fibres belonging to the 10 different fibre types found in a population of fibres dissected from the SOL, EDL, and DPH muscles of adult SHR and WKY rats.

Lane 1, Laboratory marker; lane 2, fibre type I; lane 3, fibre type IIa; lane 4, fibre type IID; lane 5, fibre type IIB; lane 6, fibre type I+IIa; lane 7, fibre type I+IID; lane 8, fibre type IIa+IID; lane 9, fibre type IID+IIB; lane 10, fibre type I+IIa+IID; lane 11, fibre type IA+IID+IIB.

**Table 4.2 The proportions of fibres displaying  $S_{slow}$ ,  $S_{fast}$  and COMP activation characteristics in each class of electrophoretically defined fibre types.**

MHC isoform composition-based fibre type	Number of fibres (% total)	Number of fibres (% total)				
		$S_{slow}$	$S_{fast}$	COMP <sub>s-s</sub>	COMP <sub>s-</sub>	COMP <sub>f-f</sub>
I	120 (49.8)	117 (97.5)	0	2 (1.7)	1 (0.8)	0
I+IIA	5 (2.1)	2 (40)	2 (40)	0	1 (20)	0
I+IID	2 (0.8)	0	0	0	2 (100)	0
I+IIA+IID	5 (2.1)	0	5 (100)	0	0	0
IIA	16 (6.6)	0	16 (100)	0	0	0
IID	35 (14.5)	0	35 (100)	0	0	0
IIB	6 (2.5)	0	6 (100)	0	0	0
IIA+IID	25 (10.4)	0	25 (100)	0	0	0
IID+IIB	25 (10.4)	0	23 (92)	0	0	2 (8)
IIA+IID +IIB	2 (0.8)	0	2 (100)	0	0	0

A summary of the proportion of different fibre types detected in the fibre populations obtained from SOL, EDL and DPH muscles of 43 adult WKY and SHR rats is given in Fig. 4.2. The fibre populations dissected from SOL and DPH contained 89% and 69.7% pure fibres, respectively, while only 32.7% of the EDL fibres displayed a single MHC isoform. The largest proportion of fibres dissected from EDL (65.4%) co-expressed two MHC isoforms [IIa+IId (17.3%) and IId+IIb (48.1%)]. The fibre population obtained from DPH muscles comprised the largest proportion (13.9%) of hybrid fibres co-expressing three MHC isoforms.

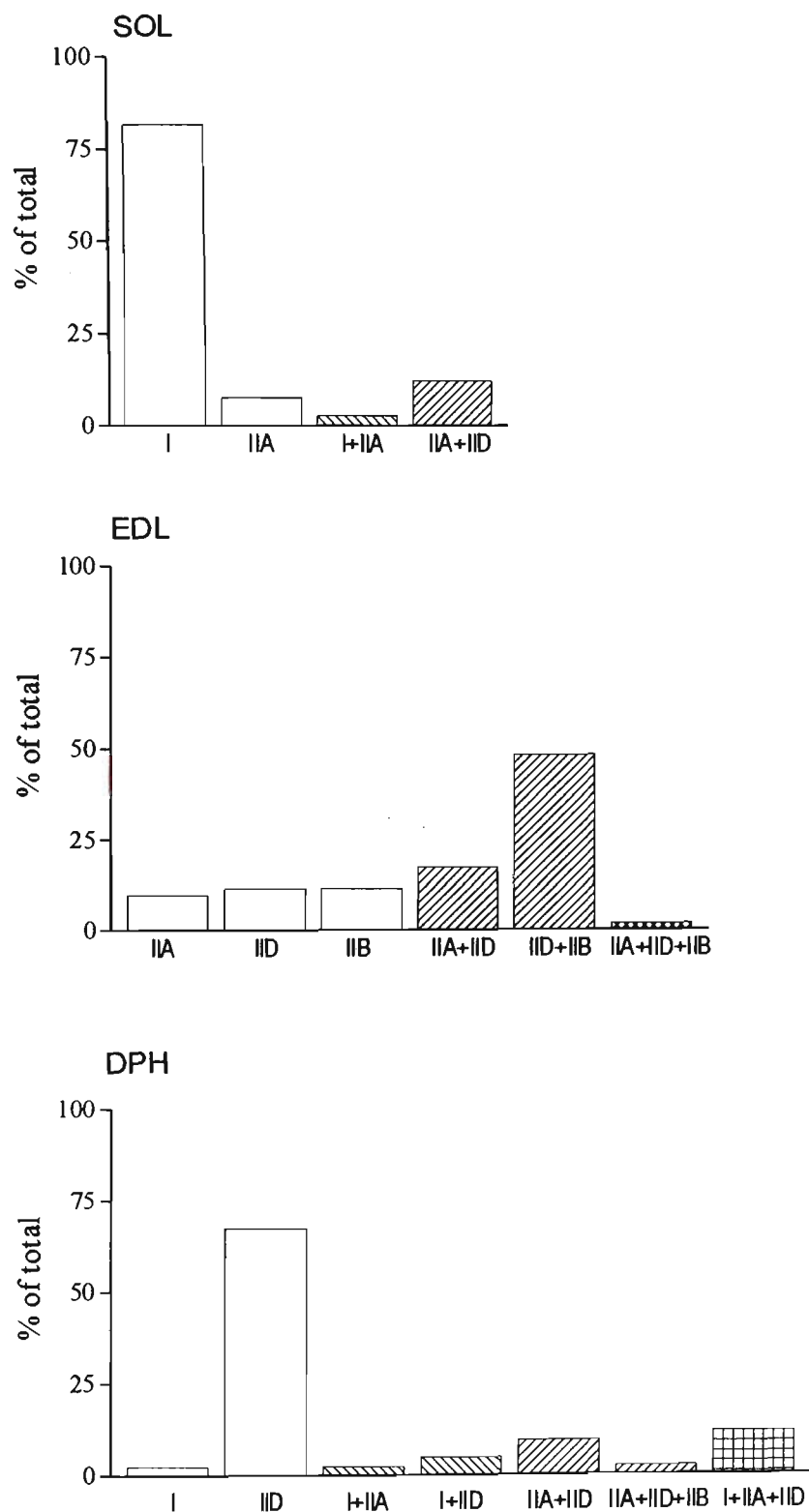


**Figure 4.2** The proportion of pure and hybrid fibre types in the fibre type populations dissected from SOL, EDL and DPH muscles of adult SHR and WKY rats. Individual fibres were typed according to their MHC isoform composition as described in section 4.2.

### 4.3.2 Fibre types classified according to $\text{Ca}^{2+}/\text{Sr}^{2+}$ - activation characteristics

As discussed in sections 1.4 and 2.4.6.2, muscle cell physiologists from several laboratories have classified mammalian fibres according to a number of criteria related to the isometric activation of myofibrillar proteins by  $\text{Ca}^{2+}/\text{Sr}^{2+}$  (Cordonnier *et al.*, 1995; Fink *et al.*, 1986; Mizusawa *et al.*, 1982; Williams *et al.*, 1993; Wilson & Stephenson, 1990). According to two of these criteria, *viz.* the type of Hill curve that fitted best the  $\text{Sr}^{2+}$ -activated force data points (simple or composite) and the relative sensitivity of the contractile-regulatory system to  $\text{Ca}^{2+}$  and  $\text{Sr}^{2+}$  (for details of the criteria see section 4.2), the fibres examined in this study belonged to five groups:  $S_{\text{slow}}$ ,  $S_{\text{fast}}$ ,  $\text{COMP}_{\text{s-s}}$ ,  $\text{COMP}_{\text{s-f}}$  and  $\text{COMP}_{\text{f-f}}$ .

In Fig. 4.3 are shown representative force-pCa and force-pSr curves produced by  $S_{\text{slow}}$  and  $S_{\text{fast}}$  fibres and in Fig. 4.4 are shown the force-pSr curves for  $\text{COMP}_{\text{s-s}}$ ,  $\text{COMP}_{\text{s-f}}$  and  $\text{COMP}_{\text{f-f}}$  fibres. It is worth noting that, based on the condition that the computer-fitted curve should lie no further than 5% of the maximum activated force from the data points (see section 4.2), the rising phase of the force-pSr curve that fitted the data for the  $\text{COMP}_{\text{s-s}}$  and  $\text{COMP}_{\text{f-f}}$  fibres passed through only 3 and 4 experimental points, respectively, while that for the  $\text{COMP}_{\text{s-f}}$  fibre passed through 7 data points (Fig. 4.4). Thus, the probability that a fibre classified as a COMP fibre was a misclassified 'simple' fibre would be lower for  $\text{COMP}_{\text{s-f}}$  and higher for  $\text{COMP}_{\text{f-f}}$  and  $\text{COMP}_{\text{s-s}}$  fibres.

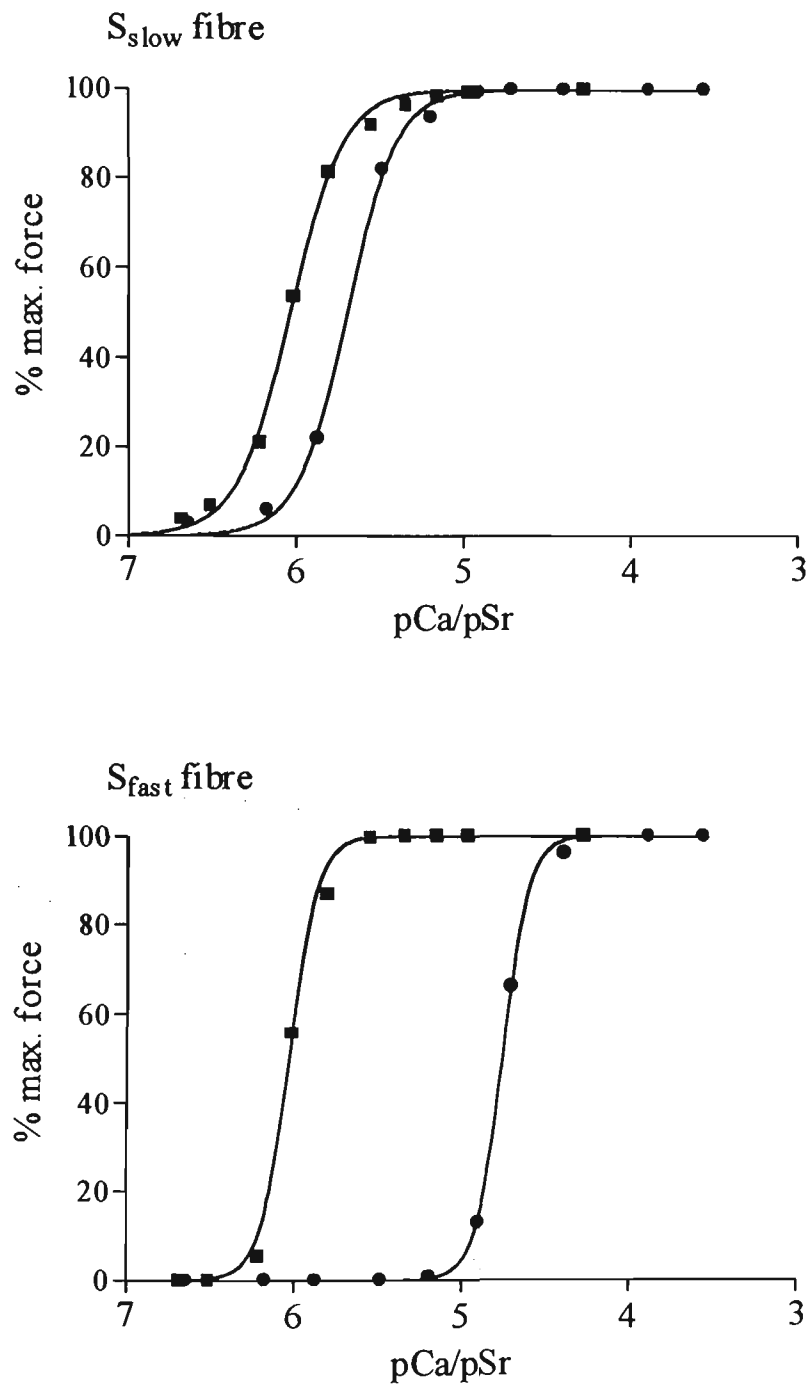


**Figure 4.3** Representative force-pCa (■) and force-pSr (●) curves for 'simple' fibres.

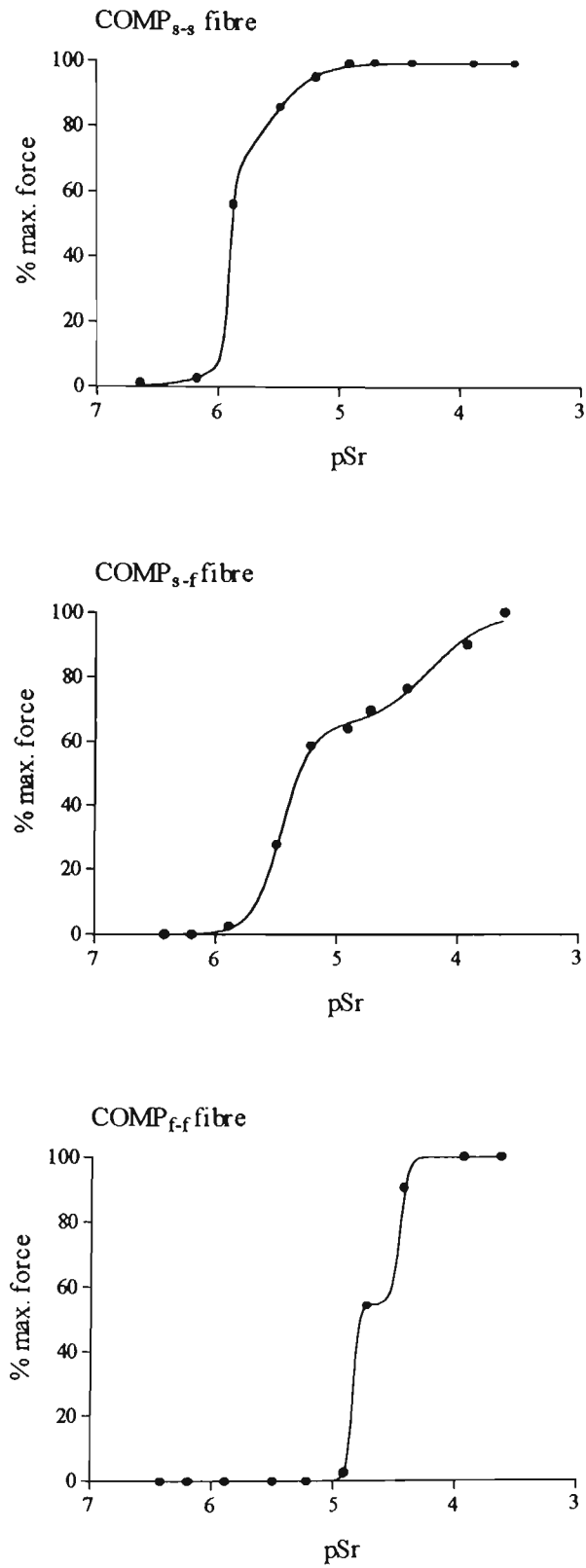
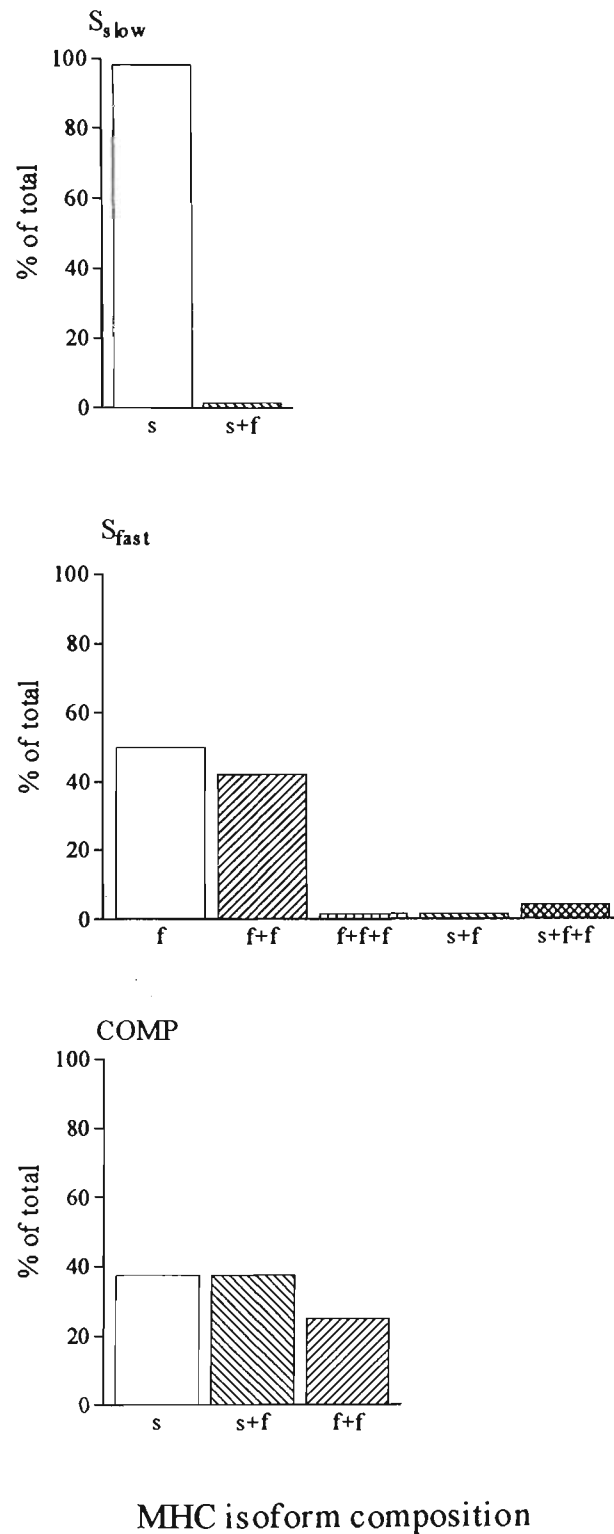


Figure 4.4 Representative force-pSr (●) curves for ‘composite’ fibres.

### 4.3.3 The correlation between the MHC isoform based- and $\text{Ca}^{2+}/\text{Sr}^{2+}$ -activation properties-based fibre typing methods

The proportions of fibres displaying  $S_{\text{slow}}$ ,  $S_{\text{fast}}$  and COMP contractile characteristics in each class of electrophoretically-defined fibre types are provided in Table 4.2. The majority (97.5%) of the pure MHC type I fibres and 40% of hybrid type I+IIA fibres, produced  $S_{\text{slow}}$  force-pSr curves. All pure fast IIA, IID and IIB fibres, all IIA+IID fibres, all IIA+IID+IIB fibres, all I+IIA+IID fibres, 92% of the IID+IIB fibres and 40% of the slow-fast hybrid I+IIA fibres generated force-pSr curves of the  $S_{\text{fast}}$  type. Finally, all hybrid slow/fast I+IID fibres, 20% hybrid slow/fast I+IIA fibres, 8% of the hybrid fast/fast (IID+IIB) fibres and 2.5% type I fibres generated composite force-pSr curves. To allow a full perspective of the correlation between the contractile activation-based and MHC isoform based-fibre typing methods, the data in Table 4.2 are presented in a complementary way, as proportions of different MHC-based fibre groups comprised in each class of fibres defined by  $\text{Sr}^{2+}$ -activation characteristics (Fig. 4.5). Once again, one can see clearly that 98.3% of the 119 fibres that were classified as  $S_{\text{slow}}$  fibres contained only the slow MHC isoform and a small proportion (1.7%) co-expressed a slow and fast MHC isoform. Details of the relative proportion of the two MHC chain isoforms and contractile activation parameters in these and two other hybrid I+IIA fibres are given in Table 4.4e. In contrast, only 50% of the 114  $S_{\text{fast}}$  fibres examined contained one fast MHC isoform, while the other 50% co-expressed two fast MHC, three fast MHC, one slow and one fast MHC and one



**Figure 4.5** The proportion of different MHC-based fibre groups comprised in each class of fibres defined by  $Sr^{2+}$ -activation characteristics.

s, slow MHC isoform I; f, one of the three fast MHC isoforms IIa, IIc and IIb.

slow and two fast MHC isoforms. The population of fibres displaying heterogeneous  $\text{Sr}^{2+}$ -activation characteristics (COMP fibres) was relatively small (8 fibres) and comprised 62.5% fibres that co-expressed 2 MHC isoforms and 37.5% fibres that contained only the slow MHC I isoform.

#### 4.3.4 Fibre diameter, maximum specific force and $\text{Ca}^{2+}/\text{Sr}^{2+}$ -activation characteristics of fibres typed according to MHC composition

Fibre diameter, maximum  $\text{Ca}^{2+}$ -activated force per cross-sectional area ( $\text{CaF}_{\text{max}}/\text{CSA}$ ), ratio  $\text{CaF}_{\text{max}}/\text{SrF}_{\text{max}}$ , sensitivity to  $\text{Ca}^{2+}/\text{Sr}^{2+}$  of the contractile/regulatory system ( $\text{pCa}_{10}$ ,  $\text{pSr}_{10}$ ,  $\text{pCa}_{50}$ ,  $\text{pSr}_{50}$ ), relative sensitivity of the contractile/regulatory system to  $\text{Ca}^{2+}$  and  $\text{Sr}^{2+}$  (indicated by  $\Delta_{10}$  and  $\Delta_{50}$ ) and Hill coefficient ( $n_{\text{Ca}}$  and  $n_{\text{Sr}}$ ) were determined for all 241 fibres examined. For a subpopulation of fibres the presence and frequency of force oscillations when submaximally activated was also determined. Results, grouped according to MHC-based fibre type and muscle type (SOL, EDL, DPH) are presented in Tables 4.3-4.5.

*Fibre diameter.* As seen in Table 4.3, no fibre-type-related differences were found between fibres dissected from SOL or DPH muscles of adult rats. In EDL muscles, however, fibres containing the MHC isoform Iib (IIB and IIB+IID fibres) were larger than IA, IID and IIA+IID fibres.

**Table 4.3. Diameter, CaF<sub>max</sub>/CSA and ratio CaF<sub>max</sub>/SrF<sub>max</sub> of electrophoretically-typed fibres from SOL, EDL and DPH muscles of adult rat. Fibres belonging to IIA, IID, IIB, I+IIA+IID, IIA+IID and IIA+IID+IIB were S<sub>fast</sub> fibres. The number of fibres in each group is indicated in brackets.**

Fibre type	DIAMETER (µm)				CaF <sub>max</sub> /CSA (kN/m <sup>2</sup> )				CaF <sub>max</sub> /SrF <sub>max</sub>			
	SOL	EDL	DPH		SOL	EDL	DPH		SOL	EDL	DPH	
I S <sub>slow</sub> COMP	63.1±1.2 (116) 68.2±4.4 (3)	-	41.0		152.8±7.9 (116) 157.6±26.7 (3)	-	97.3		0.96±0.01 (116) 0.95±0.02 (3)	-	0.87	
IIA	59.9±4.1 (11)	35.0±1.3 (5)§§	-		151.2±21.1 (11)	186.1±35.6 (5)	-		1.04±0.02 (11)♥	0.99±0.07 (5)	-	
IID	-	38.8±2.6 (6)§	59.6±2.9 (29)		-	141.5±39.5 (6)	121.1±21.2 (29)		-	1.01±0.04 (6)	1.11±0.03 (29)	
IIB	-	41.7±1.1 (6)*	-		-	264.6±26.6 (6)*	-		-	1.03±0.01 (6)	-	
I + IIA S <sub>slow</sub> S <sub>fast</sub> COMP	39.3; 69.3 62.4; 45.2	-		65.0	362.0; 115.6 107.8; 333.0	-		63.6	0.93; 0.98 1.06; 0.98	-		1.01
I + IID COMP	-	-	52.0; 75.0		-	-	36.3; 82.8		-	-	1.06; 1.21	
I+IIA+IID	-	-	70.2±6.5 (5)		-	-	141.6±36.3 (5)		-	-	0.99±0.01 (5)	
IIA + IID	69.4±1.8 (12)	34.7±0.8 (9)§§	58.0±6.4 (4)§*		104.6±12.2(12)	105.8±16.4 (9)	110.1±37.7 (4)		1.01±0.01 (12)♥	1.12±0.06 (9)	1.02±0.01 (4)	
IIB + IID S <sub>fast</sub> COMP	-	41.3±0.9 (23) 43.7; 43.5			-	219.1±16.2 (23)* 343.4; 346.8			-	1.03±0.01 (23) 1.03; 0.95		
IIA+IID+IIB	-	38.0	62.0		-	259.5	33.4		-	1.04	0.81	

Values are means ± SE. ♥ Significantly different ( $P < 0.05$ ) from I (S<sub>slow</sub> group). ♦ Significantly different ( $P < 0.05$ ) from IIA+IID. § Significantly different ( $P < 0.05$ ) from IIB+IID. § Significantly different ( $P < 0.05$ ) from SOL. \* Significantly different ( $P < 0.05$ ) from EDL. & Significantly different ( $P < 0.05$ ) from DPH.

Significant differences were found also between fibres of the same type, originating from different muscles. For example, in EDL muscles, type IIA and IID fibres were significantly smaller than type IIA fibres from SOL and type IID fibres from DPH, respectively. Also, the nine hybrid fibres of type IIA+IID dissected from EDL were smaller than SOL and DPH fibres expressing the same combination of MHC isoforms.

$CaF_{max}/CSA$  and  $CaF_{max}/SrF_{max}$ . For each of the fibre type groups that could be subjected to statistical analysis (IIA, IID and IIA+IID), there were no significant differences between the maximum  $Ca^{2+}$ -activated specific forces developed by fibre populations from SOL, EDL and DPH muscles (Table 4.3). In EDL muscles, pure or hybrid fibres containing the fast MHC isoform IIB (IIB and IIB+IID fibres) developed consistently the highest specific forces recorded in this study. These forces were significantly higher than those developed by IIA+IID fibres from EDL. The lowest value for  $CaF_{max}/CSA$  was encountered for the DPH fibre expressing MHC IIA+IID+IIB, suggesting that, in this fibre, not all expressed myosin may have been functional.

The ratio  $CaF_{max}/SrF_{max}$  was close to 1 for all fibre types investigated, which suggests that under the conditions used in this study and for all fibre types examined in this study,  $Ca^{2+}$  and  $Sr^{2+}$  were equally effective in activating the contractile-regulatory system.

*Ca<sup>2+</sup>/Sr<sup>2+</sup>-activation characteristics.* The values of  $pCa_{10}$ ,  $pSr_{10}$ ,  $pCa_{50}$ ,  $pSr_{50}$ ,  $\Delta_{10}$ ,  $\Delta_{50}$ ,  $n_{Ca}$  and  $n_{Sr}$  for the ten MHC-based fibre types examined in this study are presented in Table 4.4a-e. As seen in the Table 4.4a and 4.4b, for each of the three muscles examined, there were no significant differences with respect to  $pCa_{10}$ ,  $pSr_{10}$ ,  $pCa_{50}$ ,  $pSr_{50}$  between fibres expressing only fast MHC isoforms. In EDL only, type IIA+IID fibres displayed a value for  $\Delta_{10}$  which was significantly higher (by 0.04 log units) than that for IID, IIB and IIB+IID fibres.

More marked inter-fibre type differences related to  $Ca^{2+}/Sr^{2+}$ -activation characteristics were found between fibres dissected from SOL muscles. Thus, significant differences with respect to  $pCa_{10}$  and  $\Delta_{10}$  were found between the two SOL type I fibre subgroups  $S_{slow}$  and COMP. Furthermore, both type I- $S_{slow}$  and type I-COMP fibres showed a higher sensitivity to  $Ca^{2+}/Sr^{2+}$ -activation than all SOL fast-twitch fibre types. For the two groups of fast-twitch fibres for which a statistical analysis could be performed (IIA and IIA+IID), this difference was highly statistically significant. The only type I fibre obtained from DPH also displayed higher  $pCa_{10}$ ,  $pSr_{10}$ ,  $pCa_{50}$  and  $pSr_{50}$  values than the DPH fibres containing only fast MHC isoforms.

It is worth noting that type IIA fibres from SOL and EDL muscles differed significantly with respect to  $pCa_{10}$  and  $pCa_{50}$ ; as seen in Table 4.4a and 4.4b, SOL fibres appeared to be more sensitive to  $Ca^{2+}$ -activation by about 0.14 (for  $pCa_{10}$ ) and 0.16 (for  $pCa_{50}$ ) log units than their EDL counterparts. Since there were no muscle-specific differences with respect to sensitivity to  $Sr^{2+}$ -activation between fibres of the

**Table 4.4a. pCa<sub>10</sub>, pSr<sub>10</sub> and pCa<sub>10</sub>-pSr<sub>10</sub> values of electrophoretically-typed fibres from SOL, EDL and DPH muscles of adult rat. Fibres belonging to IIA, IID, IIB, I+IIA+IID, IIA+IID+IIB were S<sub>fast</sub> fibres. The number of fibres in each group is indicated in brackets.**

Fibre type	pCa <sub>10</sub>			pSr <sub>10</sub>			pCa <sub>10</sub> -pSr <sub>10</sub>		
	SOL	EDL	DPH	SOL	EDL	DPH	SOL	EDL	DPH
I									
S <sub>slow</sub> COMP	6.41±0.01 (116) <sup>#</sup> 6.56±0.05 (3) <sup>▼</sup>	-	6.22	6.03±0.01 (116) 6.06±0.06 (3)	-	6.02	0.39±0.01 (116) <sup>#</sup> 0.50±0.03 (3) <sup>▼</sup>	-	0.20
IIA	6.18±0.01 (11) <sup>▼#</sup>	6.04±0.04 (5) <sup>§</sup>	-	4.92±0.01 (11) <sup>▼#</sup>	4.91±0.03 (5)	-	1.26±0.01 (11) <sup>▼#</sup>	1.13±0.01 (5) <sup>§</sup>	-
IID	-	6.04±0.05 (6) <sup>&amp;</sup>	5.94±0.02 (29)	-	4.91±0.05 (6)	4.85±0.02 (29)	-	1.13±0.01 (6) <sup>♦</sup>	1.09±0.02 (29)
IIB	-	6.10±0.04 (6)	-	-	4.97±0.05 (6)	-	-	1.13±0.02 (6) <sup>♦</sup>	-
I + IIA S <sub>slow</sub> S <sub>fast</sub> COMP	6.25; 6.41 6.08; 6.22	-	5.96	5.90; 6.05 5.03; 4.90	-	5.66	0.35; 0.36 1.05; 1.32	-	0.30
I + IID COMP	-	-	5.93; 6.28	-	-	5.58; 5.94	-	-	0.34; 0.35
I+IIA+IID	-	-	5.92±0.04 (5)	-	-	4.77±0.05 (5)	-	-	1.15±0.04 (5)
IIA + IID	6.13±0.03 (12) <sup>▼#</sup>	6.10±0.02 (9)	5.89±0.07 (4) <sup>§*</sup>	4.87±0.02 (12) <sup>▼#</sup>	4.93±0.02 (9) <sup>&amp;</sup>	4.79±0.06 (4)	1.26±0.01 (12) <sup>▼#</sup>	1.17±0.01 (9) <sup>§</sup>	1.11±0.05 (4) <sup>§</sup>
IIB + IID S <sub>fast</sub> COMP	-	6.08±0.02 (23) 5.94; 6.01	-	-	4.94±0.02 (23) 4.82; 4.86	-	-	1.13±0.01 (23) <sup>♦</sup> 1.12; 1.14	-
IIA+IID+IIB	-	6.22	5.80	-	5.10	4.51	-	1.12	1.29

Values are means ± SE. ▼ Significantly different ( $P < 0.05$ ) from I (S<sub>slow</sub>). # Significantly different ( $P < 0.05$ ) from I (COMP). ♦ Significantly different ( $P < 0.05$ ) from IIA+IID. § Significantly different ( $P < 0.05$ ) from SOL. \* Significantly different ( $P < 0.05$ ) from EDL. & Significantly different ( $P < 0.05$ ) from DPH.

**Table 4.4b** pCa<sub>50</sub>, pSr<sub>50</sub> and pCa<sub>50</sub>-pSr<sub>50</sub> values of electrophoretically-typed fibres from SOL, EDL and DPH muscles of adult rat that produced simple force-pSr curves. The values of these parameters for hybrid fibre type group I + IIA are shown in Table 4.3e. The number of fibres in each group is indicated in brackets.

MHC-based fibre type	pCa <sub>50</sub>			pSr <sub>50</sub>			pCa <sub>50</sub> -pSr <sub>50</sub>		
	SOL	EDL	DPH	SOL	EDL	DPH	SOL	EDL	DPH
I	6.08±0.01 (116)	-	5.87	5.70±0.01 (116)	-	5.59	0.38±0.01 (116)	-	0.28
IIA	5.97±0.02 (11)*	5.81±0.03 (5) <sup>§</sup>	-	4.72±0.02 (11)*	4.66±0.03 (5)	-	1.25±0.01 (11)*	1.15±0.02 (5) <sup>§</sup>	-
IID	-	5.71±0.04 (6)	5.62±0.02 (29)	-	4.56±0.04 (6)	4.50±0.02 (29)	-	1.12±0.01 (6)	1.12±0.01 (29)
IIB	-	5.78±0.02 (6)	-	-	4.66±0.02 (6)	-	-	1.12±0.02 (6)	-
I+IIA+IID	-	-	5.64±0.03 (5)	-	-	4.43±0.02 (5)	-	-	1.21±0.02 (5)†
IIA+IID	5.94±0.02 (12)*	5.75±0.02 (9) <sup>§</sup>	5.56±0.08 (4) <sup>§*</sup>	4.65±0.02 (12)*	4.58±0.02 (9)	4.41±0.08 (4) <sup>§*</sup>	1.28±0.01 (12)*	1.17±0.01 (9) <sup>§</sup>	1.16±0.02 (4) <sup>§</sup>
IID+IIB	-	5.77±0.01 (23)	-	-	4.63±0.01 (23)	-	-	1.14±0.01 (23)	-
IIA+IID+IIB	-	5.86	5.64	-	4.72	4.42	-	1.14	1.22

Values are means ± SE. • Significantly different ( $P < 0.05$ ) from I. † Significantly different from ( $P < 0.01$ ) IID. § Significantly different ( $P < 0.001$ ) from SOL. \* Significantly different ( $P < 0.01$ ) from EDL.

same type, the significant differences with respect to  $pCa_{10}$  and  $pCa_{50}$  between homologous SOL and EDL fibres were also translated into significant differences in the values of  $\Delta_{10}$  and  $\Delta_{50}$ , respectively.

The  $n_{Ca}$  and  $n_{Sr}$  values for all fibres examined in this study are presented in Table 4.4c, 4.4d and 4.4e. As seen in Table 4.4c, both groups of fast-twitch fibres dissected from SOL (IIA and IIA+IID) displayed significantly higher  $n_{Ca}$  and  $n_{Sr}$  values than pure type I fibres. In SOL and DPH muscles, no significant differences with respect to  $n_{Ca}$  and  $n_{Sr}$  were found between fast-twitch fibre types, but in EDL, the contractile activation curves for IIA+IID fibres displayed significantly lower slopes (i.e. smaller  $n$  values) than the curves for pure IIA fibres (significantly so for  $n_{Ca}$ ). The IIA+IID fibres dissected from EDL and DPH muscles also displayed significantly lower values for  $n_{Ca}$  and  $n_{Sr}$  than their counterparts in the SOL muscles. It is important to note that the average values for  $n_{Ca}$  and  $n_{Sr}$  recorded for all fibre groups in Table 4.4c which contained more than one fibre, were very similar [index of similarity:  $(n_{Ca} - n_{Sr}) / (n_{Ca} + n_{Sr}) < 0.1$ ; see ref. Wilson & Stephenson, 1990], which suggests that molecular events that follow the binding of the activating ion  $Ca^{2+}$  or  $Sr^{2+}$  to the regulatory system are very similar. Interestingly, the DPH fibre expressing three MHC isoforms (IIa, IIb and II d) had an index of similarity  $> 0.3$ , developed very little force when maximally activated by  $Ca^{2+}$  and also produced even lower force when maximally activated by  $Sr^{2+}$ . However, the level of myosin and actin expression in this fibre appeared normal as judged from the densitometric analysis of the corresponding bands

**Table 4.4c nCa and nSr values of electrophoretically-typed fibres from SOL, EDL and DPH muscles of adult rat which developed simple force-pSr curves.** The values of these parameters for hybrid fibre type group I + IIA are shown in Table 4.3e. The number of fibres in each group is indicated in brackets.

MHC-based fibre type	nCa			nSr		
	SOL	EDL	DPH	SOL	EDL	DPH
I	3.09±0.08 (116)	-	2.78	3.12±0.07 (116)	-	2.23
IIA	4.76±0.28 (11)*	4.33±0.51 (5)	-	4.94±0.33 (11)*	3.96±0.40 (5)	-
IID	-	3.22±0.56 (6)	3.19±0.14 (29)	-	2.94±0.42 (6)	2.94±0.14 (29)
IIB	-	3.21±0.34 (6)	-	-	3.25±0.37 (6)	-
I+IIA+IID	-	-	3.67±0.50 (5)	-	-	3.15±0.50 (5)
IIA+IID	5.20±0.31 (12)*	2.75±0.12 (9)†‡§	2.91±0.15 (4)§	4.71±0.35 (12)*	2.78±0.12 (9)§	2.67±0.37 (4)§
IID+IIB	-	3.26±0.14 (23)	-	-	3.18±0.18 (23)	-
IIA+IID+IIB	-	2.66	5.80	-	2.56	11.02

Values are means ± SE. • Significantly different ( $P < 0.05$ ) from I. † Significantly different ( $P < 0.05$ ) from IIA. § Significantly different ( $P < 0.01$ ) from SOL.

on gels. Taken together, these results indicate that the  $\text{Ca}^{2+}$  regulatory system was impaired in this fibre. The fibre population examined comprised also (i) a group of eight hybrid and pure fibres with respect to MHC composition that produced composite force-pSr curves and (ii) a group of four hybrid fibres that displayed a combination of fast and slow MHC isoforms, but behaved as 'simple' fibres in terms of  $\text{Sr}^{2+}$ -activation. In Table 4.4d and 4.4e are presented the  $\text{Ca}^{2+}/\text{Sr}^{2+}$ -activation characteristics and MHC isoform composition of each individual fibre from these two groups.

As shown in Table 4.4d, the two slow/fast MHC hybrids, which co-expressed MHC isoforms I and IId, behaved as  $\text{COMP}_{s,f}$  fibres. However, there appeared to be no tight quantitative correlation between the proportion of MHC isoforms (estimated densitometrically) and the proportion of the two contractile activation components (see section 4.2). For example, DPH (I+IID) fibre 1 contained 1.6-fold more fast MHC isoform, yet the proportion of the fast component seen in the force-pSr curve was only about half that of the slow component. This numerical discrepancy could be attributed either to a genuine lack of correlation between MHC isoform composition and the contractile activation parameters under consideration, or to difficulties in calculating the correct proportion of the two components from the force-pSr curves, if the two components were not operating in parallel (Lynch *et al.*, 1995b). The rather large values for  $n_{\text{Sr}}$  in several instances in Table 4.4d could be the result of relatively too few data points over the pSr range relevant to the individual components.

**Table 4.4d**  $pCa_{50}$ ,  $pSr_{50}$  and  $pCa_{50}$ - $pSr_{50}$  values of electrophoretically-typed fibres from SOL, EDL and DPH muscles of adult rat that produced composite force-pSr curves.

MHC-based fibre type (muscle of origin)	$pCa_{50}$	$pSr_{50/1}$	$pSr_{50/2}$	$pCa_{50}$ - $pSr_{50/1}$	$pCa_{50}$ - $pSr_{50/2}$	$n_{Ca}$	$n_{Sr1}$	$n_{Sr2}$	Force-pSr		MHC isoform composition
									Component 1 (% total)	Component 2 (% total)	
I+IID (DPH)											
Fibre 1	5.87	5.86	4.83	0.01	1.04	2.30	4.13	5.33	31.9	68.1	17.5% MHCI; 82.5% MHCIIId
Fibre 2	5.55	5.36	4.43	0.19	1.12	2.48	2.29	4.07	42.1	57.9	36.3% MHCI; 63.7% MHCIIId
I+IIA (DPH)											
Fibre 1	5.57	5.46	4.24	0.11	1.33	2.50	3.68	1.88	64.6	35.4	38.3% MHCI; 61.7% MHCIIa
I (SOL)											
Fibre1	6.29	6.01	5.20	0.28	1.09	2.71	5.25	4.19	87.7	12.3	100% MHCI
Fibre2	6.13	5.91	5.64	0.22	0.49	2.75	14.25	2.17	56.6	43.4	100% MHCI
Fibre3	6.17	5.91	5.67	0.26	0.50	2.48	19.12	2.04	53.0	47.0	100% MHCI
IID+IIB (EDL)											
Fibre 1	5.76	4.78	4.48	0.98	1.28	5.32	14.68	8.53	51.2	48.8	70.7% MHCIIId; 29.3% MHCIIb
Fibre 2	5.85	4.84	4.46	1.01	1.39	5.73	18.38	12.92	54.4	45.6	54.5% MHCIIId; 45.5% MHCIIb

Each individual fibre from the second group of COMP in Table 4.4d, *viz.* the type I fibres dissected from SOL muscles, appeared to contain only one MHC isoform (MHCI), yet displayed either slow-fast characteristics (fibre 1:  $pCa_{50}-pSr_{50/1} = 0.28$ ;  $pCa_{50}-pSr_{50/2} = 1.09$ ), or slow-slow characteristics (fibres 2 and 3:  $pCa_{50}-pSr_{50/1} < 0.3$ ;  $pCa_{50}-pSr_{50/2} \leq 0.5$ ). The discrepancy between MHC expression and contractile activation characteristics for fibre 1 could be due to the inability of the densitometric method to detect the presence of a minor fast MHC isoform rather than to its genuine absence, while the discrepancies for fibres 2 and 3 may be due to the data fitting constraints used in this study (i.e. that no force-pSr data points should lie further than  $0.05 SrF_{max}$  from the computer fitted Hill curve; see section 2.4.6.2). The two fibres from the last group in Table 4.4d displayed  $COMP_{f-f}$  characteristics and were also found to express a combination of MHC II<sub>d</sub> and II<sub>b</sub> isoforms.

In Table 4.4e are shown results obtained with four fibres that co-expressed MHC isoforms I and II<sub>a</sub>, but displayed simple force-pSr characteristics. In fibres 1 and 4, the fast MHCII<sub>a</sub> isoform content was higher than 90% and their  $\Delta_{50}$  values were greater than 1, which is a characteristic of fast fibres. Fibres 2 and 3, on the other hand, contained 80-90% MHCI and less than 20% MHC II<sub>a</sub> and their  $\Delta_{50}$  values were less than 0.5, which is characteristic of slow fibres.

**Table 4.4e. MHC isoforms composition, sensitivity to  $\text{Ca}^{2+}/\text{Sr}^{2+}$ -activation and the degree of cooperativity of the regulatory system with respect to  $\text{Ca}^{2+}/\text{Sr}^{2+}$ -activation in four slow/fast (I+IIA) hybrid fibres obtained from SOL muscles of adult SHR and WKY rats.**

	Type of $\text{Sr}^{2+}$ - activation curve	MHC isoform composition	$\text{pCa}_{50}$	$\text{pSr}_{50}$	$\text{pCa}_{50}$ - $\text{pSr}_{50}$	$n_{\text{Ca}}$	$n_{\text{Sr}}$
Fibre 1	$S_{\text{fast}}$	<10% MHCI; >90% MHCIIa	5.98	4.74	1.24	3.98	5.84
Fibre 2	$S_{\text{slow}}$	87.9 % MHCI; 12.1% MHCIIa	6.07	5.58	0.49	5.48	2.93
Fibre 3	$S_{\text{slow}}$	81.6% MHCI; 18.4% MHCIIa	6.09	5.73	0.36	2.96	2.91
Fibre 4	$S_{\text{fast}}$	8.8% MHCI; 91.2% MHCIIa	5.91	4.80	1.11	5.54	4.17

In summary, the data presented in Table 4.4d and 4.4e do not support a tight correlation between MHC composition and contractile activation characteristics as such. Nevertheless, lack of correlation between MHC composition and fast or slow contractile activation characteristics was encountered only in rare instances and this is illustrated in Fig. 4.6 where the relative sensitivity for  $\text{Ca}^{2+}$  and  $\text{Sr}^{2+}$  ( $\text{pCa}_{50}$ - $\text{pSr}_{50}$ ) plotted for all 241 fibres studied as a function of the fast MHC fraction expressed. The data points for fibres expressing either only fast MHC isoforms (ratio  $\text{MHCII}/\text{MHC}_{\text{total}} = 1.0$ ) or only MHCI isoform (ratio  $\text{MHCII}/\text{MHC}_{\text{total}} = 0.0$ ) are clustered in relatively narrow bands that do not overlap and the data points for the 12 fibres that expressed both fast and slow MHCs lie somewhere in between.

#### 4.3.5 Force oscillations of myofibrillar origin

The presence or absence of oscillations in submaximal force responses was assessed in all fibres. Such oscillations can be seen in Fig. 2.8 (Chapter 2) when the fibre was activated in a solution of  $\text{pCa}$  6.02. In Fig. 4.7 are represented the proportions of SOL, EDL and DPH muscle fibres from each MHC-based fibre type group that developed force oscillations when submaximally activated. The resolution for detection of the minimum amplitude of the force oscillations in this study was  $6.5\mu\text{N}$  and this corresponds on average to  $<1\%$  of the maximum force response. It should be pointed out that the inability to detect force oscillations does not necessarily

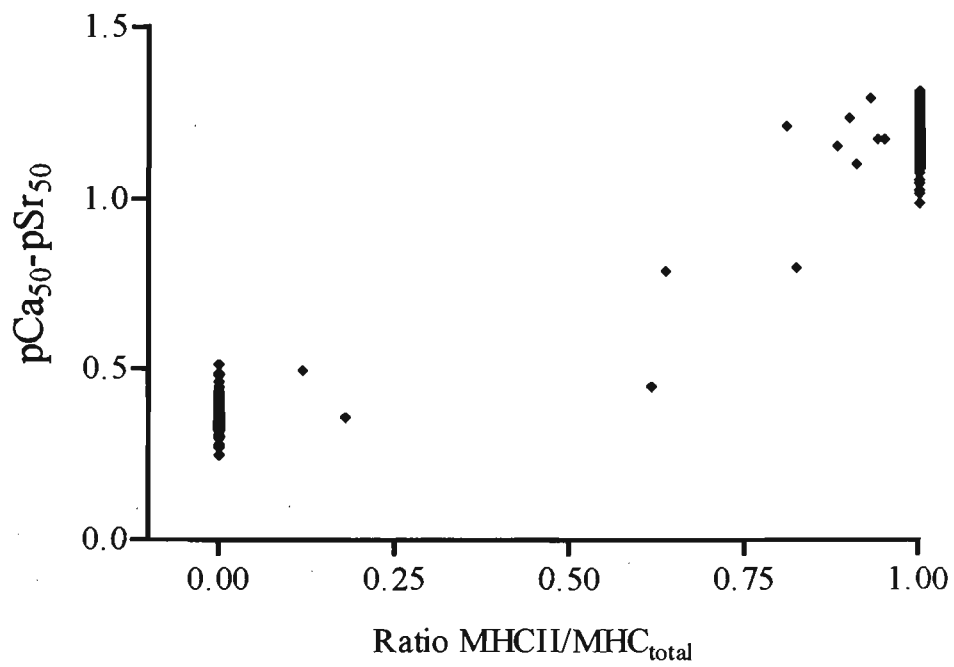


**Figure 4.6** Correlation between the proportion of fast MHC isoforms expressed by single fibres and their relative sensitivity to  $\text{Ca}^{2+}/\text{Sr}^{2+}$  expressed as  $\text{pCa}_{50}\text{-pSr}_{50}$ . Data shown were obtained with 241 fibres.

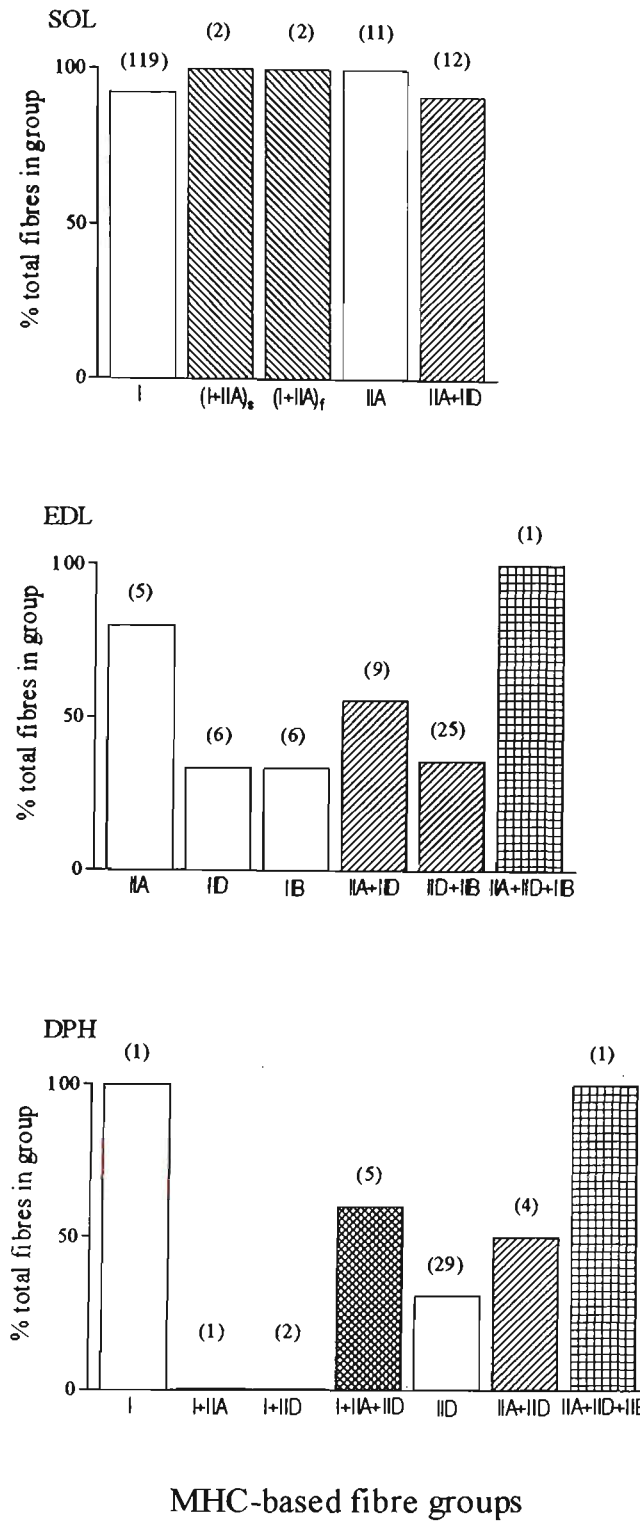


**Figure 4.7 Proportions of SOL, EDL and DPH muscle fibres from each MHC-based fibre type group that produced force oscillations when subjected to submaximally activating Ca<sup>2+</sup> solutions. Numbers in brackets represent total number of fibres in each group.**

indicate absence of such oscillations in the fibre. Since all fibres investigated had the sarcoplasmic reticulum rendered non-functional by the Triton treatment, the oscillations observed were of myofibrillar origin (Fink *et al.*, 1986). Over 90% of SOL fibres developed oscillations, regardless of their MHC composition. EDL and DPH fibres also developed force oscillations, but the proportion of oscillation-producing fibres dissected from these muscles was much lower and varied markedly between groups.

The frequency of force oscillations of myofibrillar origin was estimated for a subpopulation of 62 'simple' fibres (with respect to their force-pCa/pSr characteristics) which displayed oscillations and the results are grouped by MHC-based fibre type in Fig. 4.8. It is worth noting that in SHR and WKY animals, pure fibres of different types, activated submaximally in  $\text{Ca}^{2+}$ -buffered solutions, developed oscillations of increased frequency, in the order  $\text{I} < \text{IIA} < \text{IID} = \text{IIB}$ . Surprisingly, hybrid fibres containing combinations of two or three fast MHC isoforms did not always develop oscillations with frequencies that were intermediate between the frequencies of oscillations developed by the appropriate pure fibre types (compare for example the groups IID + IIB, IID and IIB).

Force oscillations could also be recorded in 5 of the 8 COMP fibres examined in this study when submaximally activated. Thus, force oscillations were recorded in all three type I COMP soleus fibres and in the two IID+IIB COMP fibres from EDL muscle. No force oscillations were observed in the composite fibres from the diaphragm (I + IIA and I + IID).

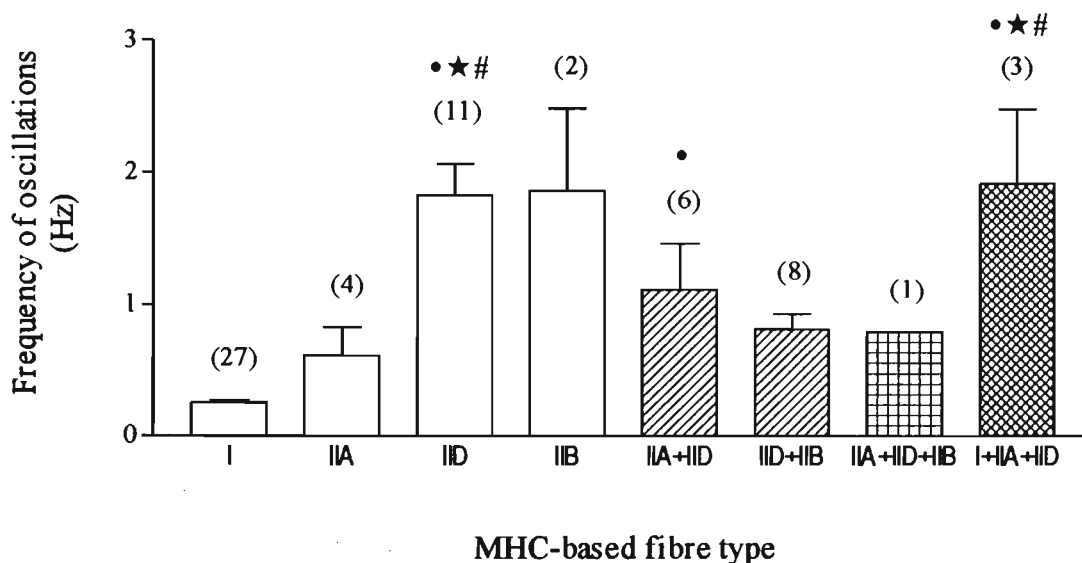


**Figure 4.8** Estimated frequency of force oscillations developed by different MHC-based fibre types. The number of fibres from each group for which the frequency of oscillations could be estimated is indicated in brackets. ● Significantly different from type I fibres ( $P < 0.01$ ). ★ Significantly different from type IIA fibres ( $P < 0.05$ ). # Significantly different from type IID+IIB fibres ( $P < 0.05$ ).

#### 4.3.6 Myosin light chain expression in fibres typed according to MHC isoform composition

The correlation between MLC and MHC isoform expression was examined in a subpopulation of 155 'simple' fibres and 5 'composite' fibres dissected from SOL and DPH muscles. As shown in Table 4.5, there was full agreement between MLC1 and MLC2 isoform expression and MHC isoform composition in most of the fibres with 'simple' force-pSr curves [83% (105/131) of SOL fibres; 91.7% (22/24) of DPH fibres] and in all 'composite' fibres. Isoforms of MLC3 were not included in this analysis due to uncertainty regarding their identity on SDS-PA gels. All type I fibres displayed full correlation between MHC and MLC expression. The pool of fibres which showed disagreement between MHC and MLC isoform composition included pure IIA fast fibres and various types of hybrid fibres (I+IIA, IIA+IID, IIA+IIB+IID). Interestingly, all SOL fibres expressed the slow MLC1 isoform even when only fast MHC isoforms were expressed (Table 4.5). Also, the DPH fibre that expressed a combination of all three fast MHC isoforms (fibre IIA+IID+IIB) expressed the slow isoforms of both types of MLCs, MLC1<sub>s</sub> and MLC2<sub>s</sub>. The electrophoretograms of 2 fibres, one showing full correlation (MHCI + MLC1<sub>s</sub> + MLC2<sub>s</sub>; lane 1), the other only partial correlation (MHCIIa + MHCIIId + MLC1<sub>s</sub> + MLC1<sub>f</sub> + MLC2<sub>f</sub>; lane 2) between the isoform expression of myosin subunits, are presented in Fig. 4.9.

**Table 4.5 The presence of slow and fast MLC isoform bands on SDS-PA gels of myofibrillar proteins from a population of pure and hybrid fibres that produced simple and composite force-pSr curves.**

MHC-based fibre type and muscle source	Number of fibres	MLC1s	MLC1f	MLC2s	MLC2f	force-pCa/pSr based characteristics
<u>SIMPLE FIBRES</u>						
I (SOL)	105	+	-	+	-	S-slow
I+IIA (SOL)	1	+	+	+	+	S-slow
	1	+	-	+	-	S-slow
	2	+	+	+	+	S-fast
I+IIA+IID (DPH)	2	+	+	+	+	S-fast
IIA (SOL)	10	+	+	-	+	S-fast
IID (DPH)	20	-	+	-	+	S-fast
IIA+IID (SOL)	11	+	+	-	+	S-fast
	1	+	+	+	+	S-fast
IIA+IID (DPH)	1	-	+	-	+	S-fast
IIA+IID+IIB (DPH)	1	+	+	+	+	S-fast
<u>COMPOSITE FIBRES</u>						
I (SOL)	3	+	-	+	-	COMP
I+IIA (DPH)	1	+	+	+	+	COMP
I+IID (DPH)	1	+	+	+	+	COMP

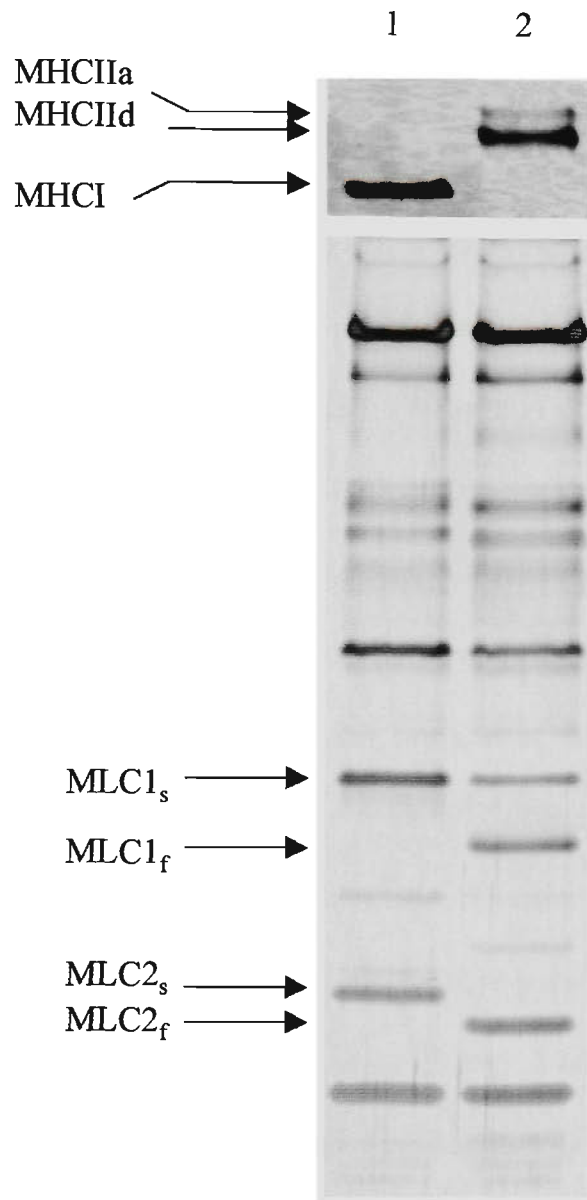


**Figure 4.9 Electrophoretograms of myofibrillar proteins from two single fibres.** Upper panel: MHC isoforms; lower panel: MLC isoform.

Lane 1, fibre type I; lane 2, fibre type IIA+IID.

## 4.4 Discussion

So far, studies concerned with the  $\text{Ca}^{2+}/\text{Sr}^{2+}$ -activation characteristics of single muscle fibres, classified according to MHC isoform composition, have been small in number and involved only a limited range of animals, fibre type groups and/or contractile parameters. For example, Danieli-Betto *et al.* (1990) determined several parameters related to  $\text{Ca}^{2+}$ -activation (but not  $\text{Sr}^{2+}$ -activation) in type I, IIA and IIB fibres from rat SOL, EDL and DPH muscles, but deliberately discarded all hybrid fibres from their analyses. As this study was undertaken prior to the discovery of the MHCIIId/x isoform (Termin *et al.*, 1989a), one cannot therefore be certain about the true identity of the type II fibres. More recently, Cordonnier *et al.* (1995) determined several  $\text{Ca}^{2+}/\text{Sr}^{2+}$ -activation parameters of electrophoretically-typed pure and hybrid fibres of rhesus monkey SOL muscles, but the fibre population examined by these authors contained only type I, IIA and I+IIA fibres. A broader range of human MHC-based fibre types, which included slow-fast, fast-fast hybrid fibres as well as pure fibres (I, IIA, IIB, I+IIA and IIA+IIB), was investigated with respect to contractile activation characteristics by Bottinelli *et al.* (1999), but this study was conducted at 12°C and the authors considered only parameters associated with  $\text{Ca}^{2+}$ -activation of the contractile/regulatory system.

The present work fills in this knowledge gap by considering fibres from ten MHC-based fibre type groups (I, IIA, IID, IIB, I+IIA, I+IID, IIA+IID, IID+IIB, I+IIA+IID and IIA+IID+IIB) and contractile parameters related to both  $\text{Ca}^{2+}$ - and

$\text{Sr}^{2+}$ -activation, under more physiological conditions with respect to the ionic composition and temperature of activating solutions. The fibres, obtained by random dissection from fresh SOL, EDL and DPH muscles of adult rats, were examined systematically with respect to size, maximum  $\text{Ca}^{2+}/\text{Sr}^{2+}$ -activated tension/CSA, threshold to  $\text{Ca}^{2+}/\text{Sr}^{2+}$ -activation ( $p\text{Ca}_{10}$ ,  $p\text{Sr}_{10}$ ), sensitivity of the contractile/regulatory system to  $\text{Ca}^{2+}/\text{Sr}^{2+}$  ( $p\text{Ca}_{50}$ ,  $p\text{Sr}_{50}$ ), relative sensitivity of the contractile/regulatory system to  $\text{Ca}^{2+}$  and  $\text{Sr}^{2+}$  ( $\Delta_{10}$  and  $\Delta_{50}$ ), degree of cooperativity ( $n$ ) between  $\text{Ca}^{2+}/\text{Sr}^{2+}$  binding sites and the presence and frequency of force oscillations of myofibrillar origin.

*Fibre type populations in SOL, EDL and DPH muscles of SHR and WKY rats.* As expected from published data on the fibre type composition of adult rat SOL muscle (85-93% MHC I and 7-15% MHC IIa; Caiozzo *et al.*, 1997; Falempin & In-Albon, 1999; Grossman *et al.*, 1998), the majority of fibres isolated from SOL muscles of WKY and SHR contained only the slow MHCI isoform. A small proportion of SOL fibres contained MHCIIa or a combination of MHC I and IIa isoforms, but most of these fibres were obtained from SOL muscles of spontaneously hypertensive rats. The DPH muscles of WKY rats produced a very large proportion (more than 70%) of fibres expressing only the MHCIIId isoform, a sizeable proportion of fibre expressing MHCIIId in combination with one or two other fast MHC isoforms, and a negligible number of fibres (1/43) expressing only the MHCI isoform. However, 21% of the total number of DPH fibres contained the MHCI isoform, which agrees with other published data (15-26% MHCI; Powers *et al.*, 1997; Prezant *et al.*, 1997). Taken together, these

data provide strong evidence that SOL and DPH muscles of adult rats, regardless of the strain, are rich sources of pure type I and type IID fibres, respectively.

Random dissection of single fibres from EDL muscles of WKY rats produced neither type I fibres nor a large proportion of one particular type of fast fibres. In fact, most EDL fibres examined in this study co-expressed two (particularly IIB+IID) or three fast MHC isoforms, indicating that EDL is a remarkably heterogeneous tissue with respect to fibre-type composition. A relatively large number of IID+IIB fibres (37%) was also detected by Li and Larsson (1996) in a population of EDL fibres (43) randomly dissected from young adult Wistar rats, which suggests that the relatively high proportion of fast-fast hybrid fibres obtained from EDL muscles in the present study is related to the type of muscle from which the fibres were dissected rather than to the rat strain.

So far, hybrid muscles fibres have been largely regarded as fibres in transition, because their proportion was found to increase in muscles undergoing transformation (Pette & Staron, 1997). The possibility that hybrid fibres may also represent stable 'phenotypes' has been recently discussed to some length by Rivero *et al.* (1999) and Talmadge *et al.* (1999) who found that skeletal muscles of clinically healthy, freely moving, untrained horses contain a large proportion of hybrid fibres (>80%) (Rivero *et al.*, 1999) and that hybrid fibres, whose number increased dramatically after spinal cord transection, persisted in high proportion (>80%) a long time (one year) after surgery (Talmadge *et al.*, 1999). As already mentioned, a large proportion (67%) of the EDL fibres and 25.6% of the DPH fibres examined in the present study contained two or three MHC isoforms. If one assumes that these muscles were not undergoing a

process of transformation, because they were obtained from functionally normal, adult animals that had not been subjected to intense or reduced mechanical activity, one can conclude that the hybrid fibre types described here are also stable rather than transitory cellular species.

Two of the 43 DPH fibres examined in this study expressed a combination of MHC isoforms (I + IId), which according to Pette *et al.* (1999) is not compatible with the sequential fibre type transition  $I \leftrightarrow IIA \leftrightarrow IID \leftrightarrow IIB$ . To date no study has reported the presence of fibres displaying 'atypical non-nearest neighbour combination' [(phrase introduced by Pette *et al.* (1999))] of MHC isoforms in normal, non-transforming muscles. Hybrid fibres of type I + IID have been detected, however, by others in non-weight bearing SOL muscles from hyperthyroid rats (Caiozzo *et al.*, 1998) and from rats subjected either to a space flight program or hind-limb suspension (Talmadge *et al.*, 1996).

One possible explanation for this finding is that rat diaphragm fibres undergo a continuous level of transformation even in adult animals that are not subjected to muscle transformation inducing conditions. Alternatively, the two I+IID fibres detected by us in the DPH of WKY rats may be stable rather than transitory entities and as such do not have to obey the rule of 'nearest neighbour' MHC isoform combination predicted by Pette *et al.* (1999) for transforming fibres. Finally, the two fibres could be I+IIA+IID fibres, misclassified as I+IID fibres, because they expressed only a non-detectable amount of MHCIIa isoform. Based on the high intensities of MHC isoform bands I and IId that could be detected on the stained

electrophoretograms (indicating that the sample was overloaded rather than underloaded), this latter possibility appears to be very unlikely.

*Method for fibre size determination.* In the present study, the diameter of a single fibre segment, isolated under oil from a freshly dissected muscle, was assumed to be equal to the mean value of the fibre width, which was measured with a video camera system while the fibre was still under oil (see section 2.3.2). It is important to note that, for a given muscle and a given fibre type (e.g. EDL fibre type IIA), the mean value of the cross-sectional area determined in this manner ( $962 \mu\text{m}^2$ ), agrees very well with that ( $1000 \mu\text{m}^2$ ) reported 10 years earlier by Smith *et al.* (1989), who used a computer program specially designed to estimate the size of single fibres dissected from frozen muscles. The agreement between the values found in this study and those generated from histochemical studies suggests that both methods are equally valid for measuring fibre size. This is further supported by the fact that all observations made in this study regarding inter-fibre type differences (for fibres dissected from muscles of the same type) and inter-muscle differences (for fibres belonging to the same fibre type) with respect to fibre size, are in agreement with previously published data. For example, in agreement with Hernández *et al.* (1996) it was found that type IIA fibres from EDL were significantly smaller than type IIA from SOL. Also, in agreement with Hernández *et al.* (1996) and Smith *et al.* (1989) who studied EDL muscles and Rivero *et al.* (1998) who studied red medial gastrocnemius muscle, it was found that in the EDL muscle, pure and hybrid fibres containing the MHCIIB isoform were significantly larger than other pure or hybrid fast-twitch fibres.

*MHC composition and Ca<sup>2+</sup>/Sr<sup>2+</sup>-activation characteristics under 'near-physiological' conditions.*

When the temperature and ionic composition of the activating solutions were close to physiological conditions, significant inter-fibre type differences were observed with respect to the sensitivity of the myofibrillar compartment to Ca<sup>2+</sup>/Sr<sup>2+</sup>-activation, degree of cooperativity in development of Ca<sup>2+</sup>/Sr<sup>2+</sup>-activated force and relative sensitivity to Ca<sup>2+</sup>/Sr<sup>2+</sup> ( $\Delta_{10}$ ;  $\Delta_{50}$ ) between fibres expressing the slow MHC I isoform and fibres expressing one or several MHC II isoforms. For example, in SOL muscles, type I fibres displayed a higher sensitivity to Ca<sup>2+</sup>/Sr<sup>2+</sup> and lower  $n$  values than type IIA and type IIA+IID fibres. A higher sensitivity to Ca<sup>2+</sup>/Sr<sup>2+</sup> and lower  $n$  values were also observed when COMP type I fibres from SOL were compared with the two COMP type IID+IIB fibres from EDL. These results are in agreement with previous data reported by us (Fink *et al.*, 1986) and others [for review see Schiaffino & Reggiani (1996)] regarding the higher sensitivity to Ca<sup>2+</sup>- and Sr<sup>2+</sup>-activation in slow-twitch compared to fast-twitch fibres.

No significant differences with respect to threshold for Ca<sup>2+</sup>/Sr<sup>2+</sup>-activation and sensitivity of the contractile/regulatory system to Ca<sup>2+</sup> and Sr<sup>2+</sup> were observed between fibres belonging to the 5 fibre type groups from EDL muscles that expressed only fast MHC isoforms (IIA, IID, IIB, IIA+IID and IIB+IID). Furthermore, with the exception of IIA+IID fibres that had a significantly lower  $n_{Ca}$  than IIA fibres, no difference between EDL fibre groups expressing only fast MHC isoforms were found with respect to the minimum number of cooperating Ca<sup>2+</sup>/Sr<sup>2+</sup>- binding sites

( $n_{Ca}$  and  $n_{Sr}$ ). Similar observations were made when comparing the three fibre type groups expressing fast MHC isoforms in DPH muscles (IID, IIA+IID and I+IIA+IID).

These results disagree with previous reports that IIB fibres are more sensitive to  $Ca^{2+}$  than IIA fibres (Danieli-Betto *et al.*, 1990; Eddinger & Moss, 1987) and that the cooperativity between  $Ca^{2+}$ -binding sites in IIB fibres is higher than that in IIA fibres (Danieli-Betto *et al.*, 1990; Eddinger & Moss, 1987). This discrepancy cannot be attributed to muscle-related differences, because data reported by Eddinger & Moss (1987) and Danieli-Betto *et al.* (1990) were obtained with rat diaphragm and rat EDL, respectively. However, marked differences in the composition and temperature of activating solutions were noted between this study and those of Eddinger & Moss (1987), Danieli-Betto *et al.* (1990) and Bottinelli *et al.* (1999), which could be responsible for observed differences between these studies. For example, measurements of  $Ca^{2+}/Sr^{2+}$ -activation characteristics were carried out at 21-23°C in this study, but at 12-15°C in previous studies (Bottinelli *et al.*, 1999; Eddinger & Moss, 1987) and it is possible that the temperature dependence of the various parameters is different between fibre types.

An unexpected finding of this study was that IIA+IID and IIA fibres from SOL displayed significantly higher sensitivity to  $Ca^{2+}$  than IIA+IID fibres from EDL and DPH and IIA fibres from EDL, respectively. This is the first report of inter-muscle differences with respect to  $Ca^{2+}$  sensitivity of isometric tension between fibres of the same fast type. Interestingly, most IIA SOL fibres (10/11) and IIA+IID SOL fibres (11/12) co-expressed  $MLC1_s$  and  $MLC1_f$  isoforms, and the remaining 8% of the (IIA+IID) SOL fibres expressed the slow and fast isoforms of both  $MLC1$  and  $MLC2$ .

In contrast, the type IIA+IID fibre from DPH was found to contain only the fast isoforms of MLC1 and MLC2. These results suggest that the presence of slow MLC isoforms in SOL fibres of types IIA and IIA+IID may contribute to the higher  $\text{Ca}^{2+}$ -sensitivity of isometric force displayed by these fibres when compared with fibres of the same type from DPH muscles.

The presence of slow MLC isoforms in SOL fibres of types IIA and IIA+IID as well as in the fast/fast/fast MHC isoform hybrid (IIA+IID+IIB) dissected from DPH indicates that MHC and MLC isoform expression are not tightly correlated in rat SOL and DPH muscles. This conclusion is in agreement with previous reports from other laboratories [for review see Pette *et al.* (1999)].

It has been reported earlier that in rat SOL muscles, slow-twitch and fast-twitch fibres, submaximally activated by  $\text{Ca}^{2+}$  and  $\text{Sr}^{2+}$ , display myofibrillar oscillations of around 0.3 and 1.0 Hz, respectively (Lynch *et al.*, 1995b). In the present study, it was found that such oscillations were developed not only by fibres from SOL muscles but also by a proportion of pure and hybrid fast fibres from EDL and DPH. It is possible that force oscillations were developed by all EDL and DPH fibres examined, but that the amplitude and frequency of oscillations were such that they could not be detected with the recording system.

The frequency of force oscillations increased markedly in the direction type I < IIA < IID, but appeared to be the same in IID and IIB fibres. Moreover, the frequency of oscillations varied in a non-consistent pattern between hybrid fibres, such that in some hybrids the oscillation frequency was intermediate between those of the

corresponding pure fibres, while in others it was lower. The cause of this inconsistency is not known.

*A comparison between the MHC isoform based- and  $Ca^{2+}/Sr^{2+}$ -activation properties-based muscle fibre typing methods.* Regarding the identification of the slow-twitch fibres, there was almost complete overlap between the MHC isoform-based and the  $Ca^{2+}/Sr^{2+}$ -activation properties-based methods. Thus, 97.5% of the pure MHCI fibres have been identified as  $S_{slow}$  fibre type and 98.3% of the  $S_{slow}$  fibres have been identified as pure MHCI fibres (Table 4.2 and Fig. 4.5). Of the pure type I fibres, 1.7% and 0.8% displayed  $COMP_{s-s}$  and  $COMP_{s-f}$  characteristics, respectively. If one regards the  $COMP_{s-s}$  fibre type as a subtype of slow-twitch fibres, then 99.2% of MHCI fibres displayed slow-twitch  $Ca^{2+}/Sr^{2+}$ -activation characteristics. Conversely, only 1.7% of the type  $S_{slow}$  fibres were hybrid fibres, expressing both MHC isoforms I and IIa. As mentioned in the Results section, the small discrepancy between the two methods with respect to the classification of slow-twitch fibres could be reduced even further if experimental errors in the classification of fibres by two methods are taken into account. Therefore, one could reliably use either of the two methods to identify slow-twitch fibres in the rat muscle.

All fibres which expressed only fast MHC isoforms (MHCIa, MHCIb, MHCIId and combinations thereof) displayed fast  $Ca^{2+}/Sr^{2+}$ -activation characteristics, 98.2% being classified as  $S_{fast}$  and 1.8% as  $COMP_{f-f}$  (Table 4.2). Fast  $Ca^{2+}/Sr^{2+}$ -activation characteristics were also displayed by a small but significant fraction (6.1%) of fibres that contained slow and fast MHC isoforms (4.4% expressing

MHCI+MHCIIa+MHCIIId and 1.7% expressing MHCI+MHCIIa), but all these fibres expressed predominantly fast MHC isoforms. These data indicate that one could broadly predict the  $\text{Ca}^{2+}/\text{Sr}^{2+}$ -activation characteristics of a fibre found to contain one, several or a majority of fast MHC isoforms, but one could not predict the MHC composition of a simple fibre displaying fast  $\text{Ca}^{2+}/\text{Sr}^{2+}$ -activation characteristics.

Further rigorous subclassification of type  $S_{\text{fast}}$  fibres into groups that could be closely related to the expression of specific fast MHC isoforms was not possible, although there was a clear tendency for fibres expressing MHCIIb either alone or in combination with other fast MHC isoforms to produce larger forces per cross-sectional area ( $\text{CaF}_{\text{max}}/\text{CSA}$ ) when maximally activated (Table 4.3). Also, a large proportion (93.8%) of the pure fibres containing the MHCIIa isoform responded with force oscillations when submaximally activated, while a much smaller proportion of IIB (33%) and IID (31%) fibres displayed such oscillations. The frequency of force oscillations in fibres expressing pure fast MHC isoforms was also considerably lower in IIA fibres than in IID or IIB fibres (Fig. 4.8). These differences were, however, not marked or consistent enough to allow prediction of the MHC composition of a fast-twitch fibre based on its  $\text{Ca}^{2+}/\text{Sr}^{2+}$ -activation characteristics. Significant differences were found between pure IIA fibres from SOL and EDL muscles with respect to  $\text{pCa}_{10}$ ,  $\text{pCa}_{50}$ ,  $\text{pCa}_{10}\text{-pSr}_{10}$  and  $\text{pCa}_{50}\text{-pSr}_{50}$ , which made it difficult to accurately predict the absolute values of  $\text{Ca}^{2+}/\text{Sr}^{2+}$ -activation parameters of a fast fibre from its pattern of MHC expression.

From the group of 12 fibres that expressed both fast and slow MHC isoforms only 25% were classified as  $\text{COMP}_{\text{s-f}}$  (3 fibres) 58.3% were classified as  $S_{\text{fast}}$  (7 fibres),

and 16.7% were classified as  $S_{\text{slow}}$  (2 fibres). Conversely, 75% of the  $\text{COMP}_{\text{s-f}}$  fibres were hybrid with respect to fast and slow MHC isoform expression.

Thus, whilst recognising that there is not 100% correspondence between the MHC isoform expression and isometric  $\text{Ca}^{2+}/\text{Sr}^{2+}$ -activation characteristics, the overall results indicate that in the adult rat muscles there is more than 90% overlap between the two methods of classification of fast and slow fibres. This is also reflected by Fig. 4.6, where the fibre type classification based on the  $\text{pCa}_{50}\text{-pSr}_{50}$  value alone is closely correlated with the fraction of fast MHC isoforms expressed in the fibre.

The partial rather than full correlation between the two methods demonstrates that MHC expression and isometric  $\text{Ca}^{2+}/\text{Sr}^{2+}$ -activation characteristics are not casually related. The  $\text{Ca}^{2+}/\text{Sr}^{2+}$ -activation characteristics are likely to depend on the isoform of troponin C (Tn C) expressed in the particular fibre (Fink *et al.*, 1990). As already mentioned in the introduction (see section 1.3.2.2), in skeletal mammalian fibres, TnC exists in two isoforms (one slow and one fast) that are known to have distinct properties with respect to the relative affinity for  $\text{Ca}^{2+}$  and  $\text{Sr}^{2+}$  (Ebashi & Endo, 1968) and to the number of  $\text{Ca}^{2+}$  binding sites. The high level of correlation between the expression of fast and slow MHC isoforms and the isometric  $\text{Ca}^{2+}/\text{Sr}^{2+}$ -activation characteristics found in the present study indicates that the expression of fast and slow Tn C isoforms and fast and slow MHC isoforms are closely correlated. Unfortunately, the Tn C isoforms present in the fibres examined in this study could not be identified due to the inability of the SDS-PAGE system used to separate these proteins; this precluded an examination of the relationship between MHC isoform and Tn C isoform expression.

There is compelling evidence that TnC is not the only determinant of the isometric force-pCa/pSr relationship because it is known that alteration in the structure of other myofibrillar components, including MHC, MLC, protein C, troponin T, tropomyosin can alter the position and the steepness of the isometric force-pCa/pSr curves (Moss *et al.*, 1995; Wilson & Stephenson, 1990). This explains the considerable variability in the various isometric  $\text{Ca}^{2+}/\text{Sr}^{2+}$ -activation characteristics within certain fibres expressing the same MHC isoform or combination of isoforms.

## Chapter 5

# Fibre-Type Populations and Ca<sup>2+</sup>-Activation Properties of Single Fibres in Soleus Muscles from SHR and WKY Rats

### 5.1 Introduction

The most widely used animal model for exploring the pathophysiology of genetic hypertension in man is the spontaneously hypertensive rat (SHR), which was originally established by Okamoto & Aoki (1963) from a colony of normotensive Wistar rats (Wistar-Kyoto, WKY). According to Pickar *et al.* (1994), in SHR the development of hypertension occurs in three stages: the rising of blood pressure (4- to 8-wk), the arrival of blood pressure to peak value (14- to 18-wk) and stabilisation of blood pressure and the appearance of adaptive changes in various organs ( $\geq 24$ -wk).

While there is general agreement that skeletal muscles of hypertensive humans contain a higher percentage of fast twitch fibres than the normotensive controls (Frisk-Holmberg *et al.*, 1983; Juhlin-Dannfelt *et al.*, 1979), the fibre type composition of skeletal muscles from SHRs is the subject of an ongoing controversy. Thus, Gray and colleagues have reported that soleus muscles from 6-28 wk SHRs, contain more

slow-twitch (type I) and fewer fast-twitch (type II) fibres than the homologous muscles of age-matched WKY rats (Atrakchi *et al.*, 1994; Gray, 1988). In contrast, Benbachir-Lamrini *et al.* (1990, 1993) and Lewis *et al.* (1994) have reported that soleus muscles from SHRs aged 4- to 17-wk contain fewer type I fibres and more type II fibres than the soleus of age-matched WKY rats.

It is important to note that all three groups cited above determined the fibre type composition of soleus muscles from SHR and WKY rats using myosin ATPase- (Atrakchi *et al.*, 1994; Benbachir-Lamrini *et al.*, 1990; Benbachir-Lamrini *et al.*, 1993; Gray, 1988; Lewis *et al.*, 1994) and succinate dehydrogenase-based (Atrakchi *et al.*, 1994; Gray 1988) histochemistry. However, as previously stated, both enzyme-based histochemistry (Hämäläinen & Pette, 1995) and immunohistochemistry (Bottinelli *et al.*, 1991) are strategies of limited suitability for studying fibre type composition in transforming muscles, since they cannot convincingly identify fibres co-expressing two/three myosin heavy chain (MHC) isoforms (hybrid fibres) (see also section 1.5). More recently, analysis of muscle proteins from whole muscles and from single muscle fibre segments using SDS-polyacrylamide gel electrophoresis (SDS-PAGE) has become the preferred strategy in research concerned with the effect of various conditions on myosin isoform expression/fibre type composition in skeletal muscle. As stated in section 1.5, the major advantage of this latter strategy is that it can rapidly detect and quantitate MHC isoform expression in whole muscles as well as in hybrid fibres (Pette & Staron, 1990; Pette & Staron 1997). Furthermore, this strategy allows detection, at the whole muscle or single fibre level, of changes in MLC isoform

expression (Pette & Staron, 1990; Pette & Staron, 1997; Staron & Pette, 1987) which can also occur in transforming muscles.

In the present study, the microelectrophoretic methodology has been used to compare the MHC isoform, MLC2 isoform, and fibre type composition of soleus muscles from SHR and WKY rats, at the three stages of development of hypertension defined by Pickar *et al.* (1994). A secondary aim of the study has been to assess whether the reduced specific tetanic force and contractile kinetics parameters reported by Gray and colleagues (Atrakchi *et al.*, 1994; Carlsen & Gray, 1987; Gray *et al.*, 1994a; Gray *et al.*, 1994b) and Lewis *et al.*, (1994) for SHR soleus are due in part to functional alterations of the myofibrillar compartment. For this purpose, the muscle preparation used was the skinned fibre, which allows direct activation of the myofibrillar compartment in solutions of carefully controlled free calcium concentrations (Stephenson *et al.*, 1994; Stephenson & Williams, 1982; Stephenson & Williams, 1981).

## 5.2 Methods

*Animals.* The male normotensive WKY rats and SHRs used in this study were bred at the Baker Medical Research Institute (Melbourne, Victoria) from stock obtained in 1985 from one of the original breeders of SHR (Y. Yamori) at the Shimane Institute of Health Science. The rats were stored and killed as described in section 2.1.

Prior to and on the day of the experiment, systolic blood pressure was measured in conscious rats by tail-cuff plethysmography (IITC Life Science

Instruments), while the animals were in a restriction chamber at 27 °C (Dilley *et al.*, 1994; Korner & Bobik, 1995) (details of the apparatus used as shown in Fig. 5.1). The animals used for this study belonged to three age groups, representing the three stages in the development of hypertension (Pickar *et al.*, 1994): (i) the rising phase of blood pressure, before the onset of hypertension (4-wk), (ii) the arrival of blood pressure to its peak value at the onset of hypertension (16- to 18-wk), and (iii) the maintenance of blood pressure at elevated levels (24-wk). On the day of the experiment the soleus muscles were quickly dissected and stored as described in section 2.2. One muscle was used for single fibre analyses and the contralateral muscle was used for preparing whole muscle homogenate.

*Preparation of single muscle fibre segments.* All fibre segments examined in this study were isolated and measured as described in section 2.3.1 & 2.3.2 and were analysed for myofibrillar protein isoforms by SDS-PAGE as described later in the text. A large proportion of the fibres were chemically skinned (as described in section 2.3.3) to allow determination of  $\text{Ca}^{2+}$ -activation characteristics, prior to the electrophoretic work.

*Determination of  $\text{Ca}^{2+}$ -activation characteristics of chemically skinned, single muscle fibres.*

Details related to mounting of single fibre segments to the force measuring system, fibre skinning and sarcomere length measurements can be found in sections 2.4.3, 2.3.3 and 2.4.4. At slack length, the average sarcomere length of the preparation was

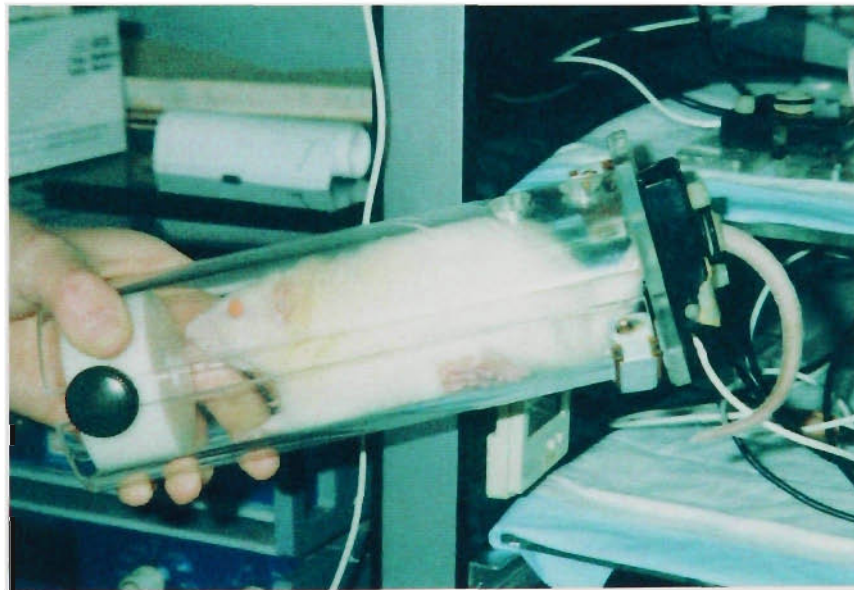


**Figure 5.1** Apparatus used to measure blood pressure of rats.

$2.65 \pm 0.02 \mu\text{m}$  (n=45) for fibres from the 16-wk- and 24-wk-old rats. This corresponds to the 'optimum' sarcomere length for maximum  $\text{Ca}^{2+}$  force development in *skinned* rat muscle fibres from adult rats (Stephenson & Williams, 1982). The 'slack' sarcomere length of fibres segments from the 4-wk-old rats was  $3.14 \pm 0.01 \mu\text{m}$  (n=12). Preliminary experiments showed that at this sarcomere length, the maximum  $\text{Ca}^{2+}$ -activated force developed in two fibre preparations from 4-wk old rats was greater than that produced when the fibres were allowed to shorten to a sarcomere length of  $2.7 \mu\text{m}$ . According to Heslinga *et al.* (1995), optimum sarcomere length can be estimated according to the equation

$$\text{optimum sarcomere length} = 2l_{\text{thin}} + l_{\text{bare}} + l_z$$

where  $l_{\text{thin}}$  is the thin filament length,  $l_{\text{bare}}$  is the bare zone length and  $l_z$  is the Z line width. If it is assumed that there are no age-related changes in the length of thin and thick filaments, the higher optimum sarcomere length displayed by fibre preparation in 4-wk old rats could be due to larger  $l_{\text{bare}}$  and/or  $l_z$ . Currently there are no data available on the  $l_{\text{bare}}$  and  $l_z$  in 4-wk old rats.

Details regarding preparation of  $\text{Ca}^{2+}$ -activating solutions, measurement of force responses and calculation of  $\text{Ca}^{2+}$ -activation parameters can be found in sections 2.4.5, 2.4.6.1 and 2.4.6.2. The pCa values are listed in Table 5.1. It is important to note that in this study, the second maximum  $\text{Ca}^{2+}$ -activated force response was on average 8.19 % ( $\pm 5.74$ ; mean  $\pm$  SD; range 0.4-21%) less than the first response.

**Table 5.1 pCa values of activating solutions.**

Solution number	pCa
1	>9
2	>8
3	6.68
4	6.51
5	6.21
6	6.02
7	5.81
8	5.55
9	5.34
10	5.15
11	4.96
12	4.27

*SDS-PAGE analysis of MHC and MLC isoforms.* MHC isoform analyses were performed on whole muscle homogenates and single muscle fibre segments, while MLC isoform analyses were performed on whole muscle homogenates only. Muscle homogenisation and protein determination were described in section 2.2. Details related to the set up of the gel apparatus and to basic electrophoretic procedures, such as gel preparation, sample preparation, gel staining and densitometry can be found in the appropriate sections within Chapter 2. The gel systems used for MHC isoform analysis is described in Appendix 2 (gelF 3.15A and gelF 3.17A). An internal standard was included in each gel (Fig. 5.2, lane 1) to ensure that the gel resolved all four MHC isoforms and enabled for correct identification of MHC bands in single muscle fibres. The gel system used for MLC2 isoform analysis is described in section 4.2.

Details regarding the estimation of MHC isoforms in whole muscle homogenate is described in section 2.5.5. The strategy described in section 2.5.5 was also used to estimate the relative proportion of MLC2 isoforms in a given muscle homogenate,

since  $\Delta OD_{1_{MLC2s-i}}$  was also found to be linearly related to the total protein concentration in the sample over the range of sample protein concentrations used (data not shown).

*Statistics.* Unless stated otherwise, all data are expressed as means  $\pm$  SE and statistical comparisons were performed on groups with at least 3 data points using a two-way analysis of variance followed by the Bonferroni test. Statistical significance was accepted at  $P < 0.05$ .

## 5.3 Results

### 5.3.1 Physical Characteristics

In Table 5.2 are shown the average systolic blood pressure (BP) readings for the WKY rats and SHRs examined in this study. The 4-wk-old SHRs had a mean BP value of 105.6mmHg, which was 25% higher than that of the age-matched WKY (84.8mmHg), but was 28% lower than the mean BP value for the 24-wk-old normotensive rats (146.0mm Hg). In contrast, the more mature SHRs (16 and 24 weeks old) had BP values which were 43-56% higher than the BP values for the age-matched WKY and markedly higher than the upper limit for normotensive animals. The highest average BP value for normotensive WKY rats was 146 mmHg for the 24-wk-old animals which is in full agreement with the highest average BP value of

150 mmHg reported for WKY rats aged 4-52 weeks (Benbachir-Lamrini *et al.*, 1990). Since the highest BP value recorded in WKY rats in this study was 165 mmHg, all rats which had a BP reading  $\leq$  165mmHg were regarded as normotensive.

The body weight (wt) of SHRs at 4 and 24 weeks of age was not significantly different from that of age matched WKY rats, while the 16-wk-old SHRs were slightly (8%), but significantly heavier ( $P<0.05$ ) than the age matched normotensive rats (Table 5.2). The mean soleus muscle wet wt/body wt values did not change with age in either of the two strains examined. The mean muscle wet wt/body wt values were, however, significantly higher in SHR than in WKY at all 3 ages examined.

**Table 5.2 Physical characteristics of SHR and WKY rats.**

	WKY			SHR		
	4-wk-old (7)	16-wk-old (8)	24-wk-old (7)	4-wk-old (7)	16-wk-old (6)	24-wk-old (7)
Systolic BP (mmHg)	84.8 $\pm$ 3.2	138.1 $\pm$ 4.8	146.0 $\pm$ 6.1	105.6 $\pm$ 3.7*	204.2 $\pm$ 4.6*	208.7 $\pm$ 4.5*
Body wt(g)	65 $\pm$ 3	331 $\pm$ 9	379 $\pm$ 9	68 $\pm$ 3	358 $\pm$ 5*	384 $\pm$ 8
soleus wet wt/body wt (mg/g)	0.44 $\pm$ 0.02	0.44 $\pm$ 0.01	0.42 $\pm$ 0.01	0.51 $\pm$ 0.02*	0.49 $\pm$ 0.01*	0.51 $\pm$ 0.01*

Values shown are means  $\pm$  SE. The number of animals is indicated in brackets.

\*Significantly different ( $P<0.05$ ) from age-matched WKY.

### 5.3.2 MHC isoform composition of whole muscles

Electrophoretic analyses of whole tissue homogenates prepared from WKY and SHR soleus muscles revealed three high molecular weight protein bands of decreasing electrophoretic mobility, corresponding to slow MHCI, fast MHCII<sub>d</sub> and fast MHCII<sub>a</sub> (Fig. 5.2). It is important to note for the same amount of protein applied, the SHR soleus sample displayed MHCI, MHCII<sub>a</sub> and MHCII<sub>d</sub> bands while the WKY soleus sample displayed only MHCI and MHCII<sub>a</sub>. The percentages of the MHC isoforms in muscle homogenates of 4-wk-, 16-wk-, and 24-wk-old SHRs and WKY rats are shown in Table 5.3.

**Table 5.3 MHC isoform composition of soleus muscles from SHR and WKY rats.**

MHC isoform	WKY			SHR		
	4-wk-old (7)	16-wk-old (8)	24-wk-old (7)	4-wk-old (7)	16-wk-old (6)	24-wk-old (7)
MHCI	70.7±3.2 <sup>#</sup>	90.8±3.1	89.1±0.8	56.5±2.5 <sup>#*</sup>	71.5±3.6*	74.6±1.3*
MHCII <sub>a</sub>	27.8±2.2 <sup>#</sup>	9.2±3.1	10.9±0.8	29.5±1.7	26.2±2.5*	22.7±1.9*
MHCII <sub>d</sub>	1.5±1.5	nd	nd	14.0±1.4 <sup>#*</sup>	2.4±2.4*	2.7±1.3*

The data are expressed as relative band density (% total MHC content). Values are means ± SE. The number of animals is indicated in brackets. <sup>#</sup>Significantly different ( $P < 0.05$ ) from 16-wk- and 24-wk-old animals of the same strain. \*Significantly different ( $P < 0.05$ ) from age-matched WKY. nd, not detectable.

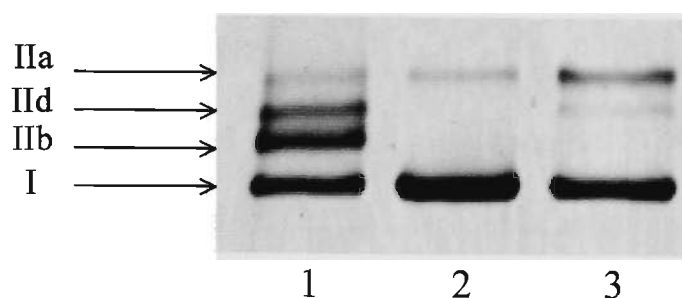


**Figure 5.2 Representative electrophoretic profile of MHC isoforms detected in soleus muscles from 24-wk-old WKY rats (lane 2) and SHRs (lane 3).** Whole tissue homogenates were prepared from WKY and SHR soleus muscles and the proteins were analysed by SDS-PAGE as described in Methods. Lane 1: laboratory MHC isoform marker containing the 4 MHC isoforms known to be expressed by adult rat hindlimb skeletal muscles: MHCI, MHCIIb, MHCIIId and MHCIIa. Amount of protein applied per electrophoretic well: 0.3  $\mu$ g.

At 4 weeks of age, the soleus muscle from SHR rats contained a lower proportion of MHCI (-14.2%) and a higher proportion of MHCII<sub>d</sub> (+12.5%) than the soleus muscle from the age-matched WKY rats. The proportion of MHCII<sub>a</sub> isoform was, however, similar in SHR and WKY rats.

An increase in age from 4- to 24-wk, was accompanied by clear changes in the relative proportion of MHC isoforms in the soleus muscles of both SHR and WKY rats. The direction of these changes was MHC isoform dependent, with the percentage of MHCI isoform increasing and the percentage of MHCII isoforms decreasing with age in both strains. For all MHC isoforms, the major age-related changes occurred during the rat development from 4- to 16-wks. Thus, the proportion of MHCI isoform increased between 4 and 16 weeks, by 20.1% in WKY and 15.0% in SHR, but it did not change significantly between 16- and 24-wks of age in either strain. The proportion of MHCII<sub>a</sub> decreased significantly (by 18.6%) in WKY between 4- and 16-wks, but did not change in SHR. Between 16- and 24-wks no significant change was detected in the proportion of MHCII<sub>a</sub> in either strain.

Finally, the proportion of MHCII<sub>d</sub> in WKY rats decreased from low (1.5% at 4-wks) to non-detectable levels at 16- and 24-wks, while in the SHR it decreased from 14.0% at 4-wks to ca 2.4% at 16-wks and this level remained unchanged in 24-wk-old rats. In summary, at all ages examined, the SOL muscle from SHR rats contained a statistically significant higher proportion of fast MHC isoforms (comprising both MHCII<sub>a</sub> and MHCII<sub>d</sub>) and a lower proportion of slow MHC isoform than SOL muscle from age-matched WKY rats.

### 5.3.3 MLC2 isoform composition of whole muscles

In agreement with the MHC isoform data, soleus muscles from SHR rats were found to contain a statistically significant lower proportion of MLC2s and a higher proportion of MLC2f than their WKY counterparts at all ages examined (see Fig. 5.3). In Fig. 5.3A are shown, side-by-side, two representative electrophoretograms of low molecular weight proteins produced by SDS-PAGE analyses of SHR and WKY soleus muscle homogenates from 24-wk-old rats, and the bar graph in Fig. 5.3B illustrates the differences between the calculated values for the ratio  $MLC2s/MLC2s_t$  (where  $MLC2s_t = MLC2s + MLC2f$ ) in soleus muscles of 4-wk-, 16-wk-, and 24-wk-old SHR and WKY rats.

### 5.3.4 Fibre type populations yielded by random dissection

Electrophoretic analyses of MHC isoform composition in muscle homogenates prepared from soleus muscles of SHR and WKY rats provide very useful information on strain-related differences in MHC expression at the whole muscle level, but give no indication on the types of fibres which make up the muscles compared. In order to obtain this information, microelectrophoretic analyses of MHC isoform expression were performed in segments of single fibres, randomly dissected from soleus muscles of SHR and WKY rats. These analyses showed that soleus muscles from 4-wk-,

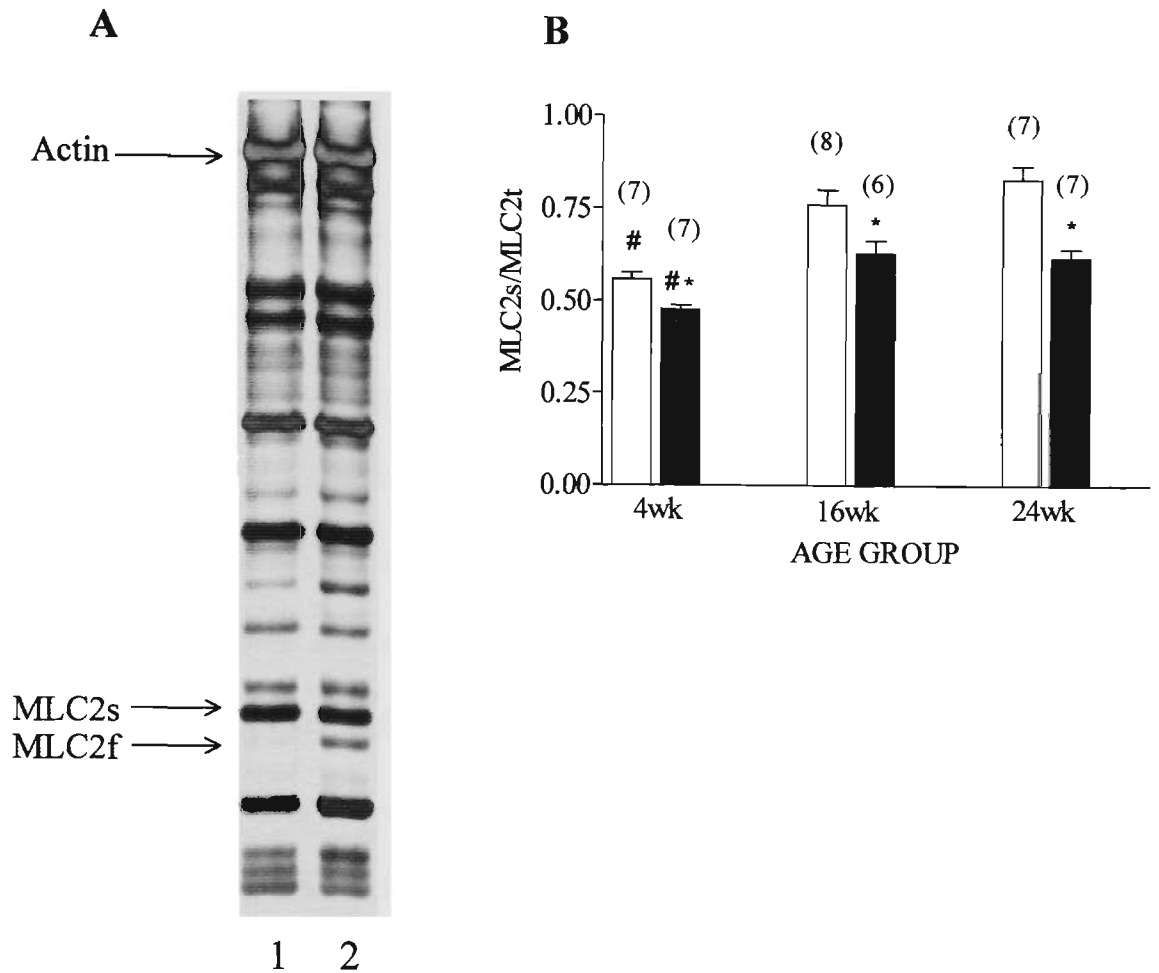


**Figure 5.3 A. Representative electrophoretogram of low molecular weight (<45 kDa) muscle proteins from 24-wk-old WKY (lane 1) and SHR (lane 2) soleus muscles.** Arrows indicate the bands corresponding to actin, slow MLC2 isoform (MLC2s) and fast MLC2 isoform (MLC2f).

**B. Bar chart for the ratio  $MLC2s/MLC2_t$  (where  $MLC2_t = MLC2s + MLC2f$ ) in soleus muscles of 4-wk-, 16-wk-, and 24-wk-old SHRs (filled bars) and WKY (open bars) rats.** #, Statistically significant difference between 4-wk-old and adult (16-wk and 24-wk) rats of the same strain. \*, Statistically significant difference between SHR soleus and age-matched WKY soleus. Amount of protein applied per electrophoretic well: 3  $\mu$ g.

16-wk-, and 24-wk-old WKY rats and age matched SHRs contain four fibre types: I (pure slow; containing MHCI), I+IIA (hybrid slow/fast, containing different proportions of MHCI *and* MHCIIa), IIA (pure fast, containing MHCIIa), and IIA+IID (hybrid fast/fast containing different proportions of MHCIIa *and* MHCIIId) (Fig. 5.4). In agreement with the MHC isoform composition data shown in Table 5.3, no fibres containing the MHCIIb isoform were detected in any of the muscles examined.

In Table 5.4 are shown, for each strain- and age- group examined, the proportions of each fibre type, expressed as percent of the number of fibres examined per rat ( $\%f_R$ ), the actual number of fibres, and percent of the total number of fibres examined per age group ( $\%f_T$ ). The data presented in the table were generated by analyses of 472 randomly dissected fibres (minimum 10 fibres/rat and 73 fibres/age group). It is important to note that a relatively large number of hybrid fibres were detected among the fibre segments dissected from the soleus muscle of SHRs of all ages and from soleus muscles of 4-wk-old WKY rats.

The proportions of type I and type I+IIA fibres isolated from the soleus muscles of 4 wk-old SHR were, on average, 1.4 and 1.9 times lower than those for 4-wk-old WKY rats. However, the proportion of type IIA fibres isolated from 4-wk-old SHR soleus muscle was 4.9 times greater than that for soleus muscle of age-matched WKY. Moreover, about 13% of the fibres dissected from the 4-wk SHR soleus muscles were type IIA+IID fibres, while no such fibres were found among the fibres dissected from the age matched WKY soleus.

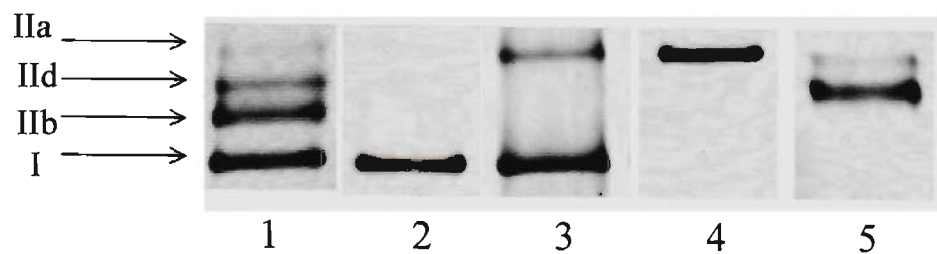


**Figure 5.4** Representative electrophoretograms of MHC isoform composition of the fibre types yielded, upon random dissection, by soleus muscles of SHR and WKY rats. Lane 1: laboratory marker containing the 4 MHC isoforms known to be expressed by adult rat hindlimb skeletal muscles: MHCI, MHCIIb, MHCIIc and MHCIIa. Lane 2: fast fibre (type I). Lane 3: hybrid slow/fast fibre (type I+IIA). Lane 4: fast fibre (type IIA). Lane 5: hybrid fast/fast fibre (type IIA+IIC). Sample size: 0.3 nl fibre per electrophoretic well. Details regarding the preparation of single fibres, their solubilisation in SDS-PAGE solubilising buffer and their microelectrophoretic analysis by SDS-PAGE are described in section 5.2.

**Table 5.4 Fibre type populations in soleus muscles from WKY and SHR.**

WKY									
Fibre type	4-wk-old (7; 73)			16-wk-old (8; 85)			24-wk-old (7; 79)		
	%f <sub>R</sub>	No of fibres	%f <sub>T</sub>	%f <sub>R</sub>	No of fibres	%f <sub>T</sub>	%f <sub>R</sub>	No of fibres	%f <sub>T</sub>
I (slow)	85.0±4.9	62	84.9	91.4±4.2	78	91.8	97.5±1.7 <sup>#</sup>	77	97.5 <sup>†</sup>
I+IIA(slow/fast)	11.1±4.0	8	11.0	2.8±1.8	2	2.4	0 <sup>#</sup>	0	0 <sup>†</sup>
IIA (fast)	3.9±1.9	3	4.1	4.8±2.8	4	4.7	2.5±1.7	2	2.5
IIA+IID(fast/fast)	0	0	0	1.0±1.0	1	1.1	0	0	0

SHR									
Fibre type	4-wk-old (7; 75)			16-wk-old (6; 73)			24-wk-old (7; 87)		
	%f <sub>R</sub>	No of fibres	%f <sub>T</sub>	%f <sub>R</sub>	No of fibres	%f <sub>T</sub>	%f <sub>R</sub>	No of fibres	%f <sub>T</sub>
I (slow)	60.0±8.4 <sup>*</sup>	46	61.4 <sup>†</sup>	75.3±6.8	56	76.4 <sup>†</sup>	74.1±2.8 <sup>*</sup>	65	74.7 <sup>†</sup>
I+IIA(slow/fast)	5.8±2.2	4	5.3	5.4±2.5	3	4.2	4.9±2.6 <sup>*</sup>	3	3.4 <sup>†</sup>
IIA (fast)	19.2±5.8 <sup>*</sup>	15	20.0 <sup>†</sup>	8.7±3.8	7	9.7	12.9±3.9 <sup>*</sup>	12	13.8 <sup>†</sup>
IIA+IID(fast/fast)	15.0±8.4 <sup>*</sup>	10	13.3 <sup>†</sup>	10.6±5.7	7	9.7 <sup>†</sup>	8.1±3.8 <sup>*</sup>	7	8.1 <sup>†</sup>

Data are expressed as percent of the number of fibres examined per rat (%f<sub>R</sub>), as actual number of fibres, and as percent of the total number of fibres examined per age group (%f<sub>T</sub>). About 10-12 single fibres were examined for each rat. The two numbers given in brackets for each group represent the number of rats and the total number of fibres analysed. Values are means ± SE. <sup>#,†</sup> Significantly different (P<0.05) from the 4-wk-old rats of the same strain (<sup>#</sup>, t-test; <sup>†</sup>, chi-square test for differences between proportions). <sup>\*</sup> <sup>†</sup> Significantly different (P<0.05) from age-matched WKY (<sup>\*</sup>, ANOVA with Bonferroni post-test; <sup>†</sup>, chi-square test for differences between proportions).

An increase in age was found to be accompanied, in the two strains, by an increase in the proportion of slow (type I) fibres and a general decrease in the proportion of fast (type IIA, I+IIA, and IIA+IID) fibres. It is important to note, however, that the proportion of IIA fibres found in the soleus muscle of 24-wk-old SHRs was significantly greater than that in the age-matched WKY rats. Moreover, the 24-wk SHR soleus produced a sizeable proportion of hybrid fibres (8.1% type IIA+IID and 4.9% I+IIA), while no fibres of these two types were detected among the fibres sampled from the soleus muscle of 24-wk-old WKY rats. As seen in Table 5.4, the most striking difference with respect to the proportion of fibre types produced by soleus muscles from SHRs and WKY rats relates to the significantly larger proportion of fast fibres (pure type IIA and hybrid fast/fast type IIA+IID) and hybrid fibres (types I+IIA and IIA+IID) detected among the fibres sampled from soleus muscles of SHR of all ages examined.

### 5.3.5 Correlation between MHC isoform composition, MLC2 composition and fibre type populations

As shown in Fig. 5.5A, the MHCI composition (%MHCI) of all muscles examined in this study was directly proportional to their relative content of MLC2s (MLC2s/MLC2<sub>t</sub>). Furthermore, for all muscles analysed, there was a tight correlation between the relative content of each MHC isoform detected (%MHC<sub>i</sub>) in the muscle

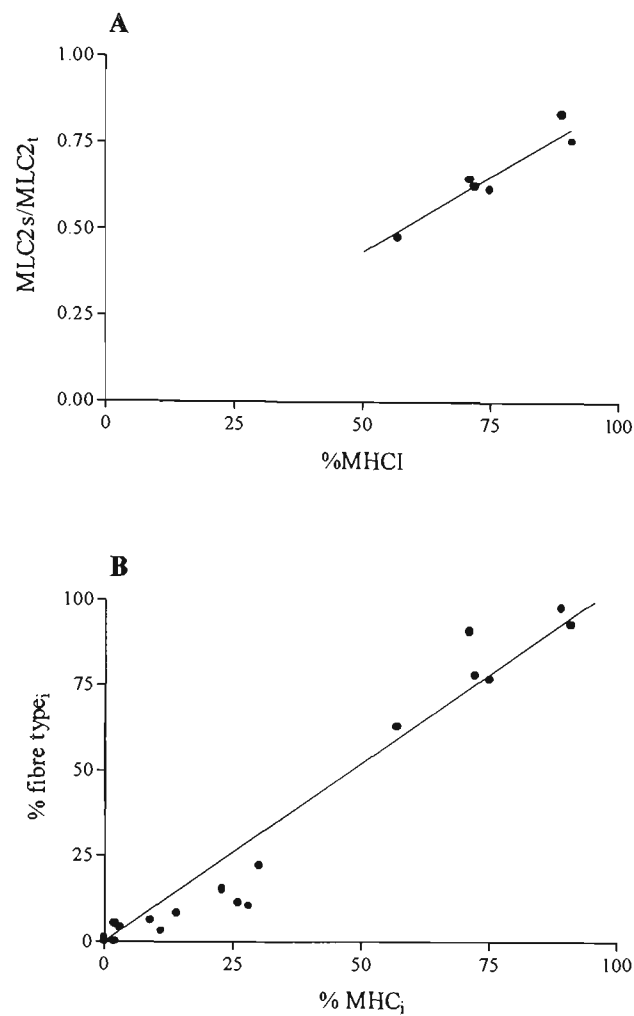


**Figure 5.5 A. The relationship between the proportion of MLC2s isoform (MLC2s/MLC2t) and MHCI isoform (% MHCI) in soleus muscles from SHR and WKY rats.** The data points, representing mean values for 6-8 rats, were obtained from Table 5.3 and Fig. 5.3B. **B. The correlation between the relative content of each MHC isoform detected (%MHC<sub>i</sub>) in the soleus muscle and the proportion of corresponding fibre type derived from the analysis of single fibre segments obtained by random microdissection of the contralateral soleus muscle.** When calculating the proportion of fibres corresponding to each MHC isoform (i.e. MHCI, MHCIIa and MHCIIId) represented in the muscles examined, the hybrid fibres which expressed two MHC isoforms (i.e. fibre types I+IIA and IIA+IID) were apportioned with equal weights to each of the two respective MHC<sub>i</sub> pools.

and the proportion of corresponding fibre type derived from the analysis of single fibre segments obtained by random microdissection of the contralateral soleus muscle (Fig. 5.5B). When calculating the proportion of fibres corresponding to each MHC isoform (i.e. MHCI, MHCIIa and MHCIIId) represented in the muscles examined, the hybrid fibres which expressed two MHC isoforms (i.e. fibre types I+IIA and IIA+IID) were apportioned with equal weights to each of the two respective MHC<sub>i</sub> pools. The good correlation found in this study between the MHC isoform composition of the *whole* soleus muscle and the proportion of fibre types produced by *single fibre* dissection indicates that, when the sample size is sufficiently large, the proportion of fibre types in the sample of dissected fibres is a reasonable approximation of the fibre type composition of the whole muscle.

### 5.3.6. Calcium activation characteristics of single fibres

Fibre diameter, maximum  $\text{Ca}^{2+}$ -activated force per cross sectional area ( $\text{CaF}_{\text{max}}/\text{CSA}$ ), sensitivity to  $\text{Ca}^{2+}$  of the isometric force response ( $\text{pCa}_{50}$ ) and the degree of cooperativity within the myofibrillar compartment with respect to calcium regulation of the contractile response ( $n_{\text{Ca}}$ ) were determined as described in the methods for individual fibre segments isolated from soleus muscles of 4-wk-, 16-wk- and 24-wk-old WKY and age-matched SHR, prior to electrophoretic analyses. The results are summarised in Tables 5.5-5.7.

As seen in Table 5.5, for each strain and each fibre type group that allowed a meaningful statistical analysis (at least 3 data points per sample), an increase in rat age was accompanied by a statistically significant increase in fibre diameter. Also, the diameter of type I and type IIA fibres from 16-wk-old SHRs appeared to be slightly, but significantly larger than that of age-matched controls. The lack of statistically significant differences between diameter values of other groups of fibres may be due to the low number of fibres in the respective groups.

The increase in age from 4- to 16-wk was accompanied by a statistically significant increase in the maximum  $\text{Ca}^{2+}$ -activated specific force ( $\text{CaF}_{\text{max}}/\text{CSA}$ ) developed by type I fibres from the soleus muscle of WKY (+35%) and SHR (+57%) (see Table 5.5). No further significant increase in average  $\text{CaF}_{\text{max}}/\text{CSA}$  was observed for either strain when the rat age increased from 16- to 24-wk. A similar trend was observed for all other fibre type groups. For each fibre type group,  $\text{CaF}_{\text{max}}/\text{CSA}$  developed by SHR soleus muscle fibres were not significantly different from those recorded for the age-matched WKY at all three ages examined. Assuming that the force per cross-bridge does not change this suggests that there were no differences in the number of cross-bridges per half sarcomere length per cross-sectional area.

Since SHR soleus contained a larger percentage of MHCIIa than MHCI and yielded a larger proportion of type IIA fibres than the WKY soleus (see Table 5.3 and 5.4), it was of interest to examine whether type IIA fibres developed a lower  $\text{CaF}_{\text{max}}/\text{CSA}$  than the type I fibres, which may explain in part the lower specific tetanic force reported in the literature (Atrakchi *et al.*, 1994; Carlsen & Gray, 1987; Gray *et al.*, 1994a; Gray *et al.*, 1994b; Lewis *et al.*, 1994) for SHR soleus.

**Table 5.5 Fibre diameter and maximum  $\text{Ca}^{2+}$ -activated force/cross-sectional area ( $\text{CaF}_{\text{max}}/\text{CSA}$ ;  $\text{kN}/\text{m}^2$ ) of electrophoretically typed, single soleus muscle fibres from WKY and age-matched SHR.**

	Fibre type I			Fibre type IIA			Fibre type I+IIA			Fibre type IIA+IID		
	Diameter ( $\mu\text{m}$ )	$\text{CaF}_{\text{max}}/\text{CSA}$ ( $\text{kN}/\text{m}^2$ )	Diameter ( $\mu\text{m}$ )	$\text{CaF}_{\text{max}}/\text{CSA}$ ( $\text{kN}/\text{m}^2$ )	Diameter ( $\mu\text{m}$ )	$\text{CaF}_{\text{max}}/\text{CSA}$ ( $\text{kN}/\text{m}^2$ )	Diameter ( $\mu\text{m}$ )	$\text{CaF}_{\text{max}}/\text{CSA}$ ( $\text{kN}/\text{m}^2$ )	Diameter ( $\mu\text{m}$ )	$\text{CaF}_{\text{max}}/\text{CSA}$ ( $\text{kN}/\text{m}^2$ )	Diameter ( $\mu\text{m}$ )	$\text{CaF}_{\text{max}}/\text{CSA}$ ( $\text{kN}/\text{m}^2$ )
<b>WKY</b>												
4-wk	42.1 $\pm$ 1.5 <sup>†#</sup> (62)	106.8 $\pm$ 10.5 <sup>†#</sup> (30)	36.3 $\pm$ 1.7 <sup>†</sup> (3)	62.9 $\pm$ 25.7 (3)	33.8 $\pm$ 2.8 (8)	154.3 $\pm$ 38.8 (4)	nd	nd	nd	nd	nd	nd
16-wk	60.2 $\pm$ 1.6 <sup>#</sup> (78)	144.4 $\pm$ 10.4 (48)	51.4 $\pm$ 7.9 (4)	275.8 285.7	39.3 62.4	107.8 362.0	68.9	106.8				
24-wk	68.5 $\pm$ 1.2 (77)	150.2 $\pm$ 16.1 (37)	70.0 71.9	108.6 111.1	nd	nd	nd	nd	nd	nd	nd	nd
<b>SHR</b>												
4-wk	39.1 $\pm$ 1.1 <sup>†#</sup> (46)	96.0 $\pm$ 11.3 <sup>†#</sup> (26)	36.7 $\pm$ 1.7 <sup>†#</sup> (15)	68.0 $\pm$ 17.1 <sup>#</sup> (10)	34.2 $\pm$ 1.7 <sup>†#</sup> (4)	38.5 79.7	38.3 $\pm$ 2.1 <sup>†#</sup> (10)	85.3 $\pm$ 21.0 (5)				
16-wk	66.6 $\pm$ 1.3* (56)	150.7 $\pm$ 11.6 (34)	67.9 $\pm$ 1.7* (7)	126.3 $\pm$ 15.1 (3)	63.5 $\pm$ 9.4 (3)	115.6 333.0	69.0 $\pm$ 2.6 (7)	97.7 $\pm$ 17.1 (7)				
24-wk	68.2 $\pm$ 1.3 (65)	161.2 $\pm$ 15.1 (32)	65.1 $\pm$ 2.3 (12)	134.9 $\pm$ 11.7 (9)	58.8 $\pm$ 4.1 (3)	128.1 294.4	71.7 $\pm$ 2.2 (7)	123.8 $\pm$ 19.4 (5)				

Values are means  $\pm$  SE for groups containing  $\geq 3$  fibres and individual values are given for groups containing  $< 3$  fibres. For groups containing  $\geq 3$  fibres, the number of fibres examined is indicated in brackets. <sup>†</sup> Significantly different ( $P < 0.05$ ) from 16-wk-old animals of the same strain. <sup>#</sup> Significantly different ( $P < 0.05$ ) from 24-wk-old animals of the same strain. \*Significantly different ( $P < 0.05$ ) from the age-matched WKY (double-sided t-test). nd, not detectable.

The comparison of the pooled data for type I and type IIA fibres from SHR and WKY soleus showed that type IIA fibres developed a statistically significantly lower  $\text{CaF}_{\text{max}}/\text{CSA}$  ( $P < 0.02$ ; Mann Whitney test) than type I fibres for 4-wk-old rats, but not for the other age groups.

Table 5.6 shows the summary of the  $\text{Ca}^{2+}$ -sensitivity data. Types IIA and IIA+IID fibres showed a significantly lower sensitivity to  $\text{Ca}^{2+}$  by a factor of 1.3 (lower  $\text{pCa}_{50}$  values by about 0.1 pCa units) than type I fibres. Interestingly, hybrid (I+IIA) fibres exhibited either  $\text{pCa}_{50}$  values characteristic of type I fibres (4-wk- and 16-wk-old WKYs) or of type IIA (4-wk-old SHR rats) fibres. The hybrid fast fibres (type IIA+IID) displayed  $\text{Ca}^{2+}$ -sensitivities similar to those of pure type IIA fibres. For all fibre type groups, no significant differences were observed between the average  $\text{pCa}_{50}$  values recorded for single fibres of the same type from soleus muscles of WKY rats and age-matched SHRs. Assuming that the length of the myosin and actin filaments does not change with age, the consistently higher  $\text{pCa}_{50}$  values by 0.1 log units noted for all fibre types from 4 wk-old animals of both strains may be related to differences in sarcomere length or interfilament distance (Stephenson & Williams, 1982).

**Table 5.6 Sensitivity to calcium of the myofibrillar compartment ( $pCa_{50}$ ) in chemically skinned, electrophoretically-typed, single soleus muscle fibres from WKY and age-matched SHR.**

Fibre type	WKY			SHR		
	4-wk-old	16-wk-old	24-wk-old	4-wk-old	16-wk-old	24-wk-old
I	6.18±0.02 <sup>#</sup> (27)	6.07±0.02 (43)	6.10±0.01 (32)	6.20±0.02 <sup>#</sup> (22)	6.10±0.02 (30)	6.09±0.01 (31)
IIA	6.04±0.02 (3)	5.95 6.02	5.96 6.04	6.07±0.02 <sup>#</sup> (10)	5.92 6.06	5.99±0.02 (8)
I+IIA	6.19±0.02 (3)	5.98 6.07		6.01 6.02	5.91 6.08	
IIA+IID		5.93		6.08±0.02 <sup>#</sup> (5)	5.95±0.02 (7)	5.95±0.04 (5)

Values are means ± SE for groups containing ≥3 fibres and individual values are given for groups containing <3 fibres. For groups containing ≥3 fibres, the number of fibres examined is indicated in brackets. <sup>#</sup>Significantly different ( $P<0.05$ ) from 16 wk- and 24 wk- old animals of the same strain.

As stated in section 2.4.6.2, the degree of cooperativity within the myofibrillar compartment with respect to contractile activation is indicated by the value of the Hill coefficient ( $n_{Ca}$ ). As shown in Table 5.7, type I fibres have a lower Hill coefficient than the fibres containing fast MHC isoforms (type IIA and IIA+IID). The hybrid type (I+IIA) fibres displayed Hill coefficients that were characteristic of either type I or type IIA fibres. No significant age-related differences were detected between the  $n_{Ca}$  values for soleus fibres from either strain or between the  $n_{Ca}$  values for soleus fibres from SHRs and WKY rats.

**Table 5.7. The degree of cooperativity within the myofibrillar system with respect to calcium regulation of the contractile response ( $n_{Ca}$ ) in chemically skinned, electrophoretically-typed, single soleus muscle fibres from WKY and age-matched SHR.**

Fibre type	WKY			SHR		
	4-wk-old	16-wk-old	24-wk-old	4-wk-old	16-wk-old	24-wk-old
I	3.79±0.30 (27)	3.18±0.15 (43)	3.36±0.14 (32)	3.15±0.24 (22)	3.59±0.18 (30)	3.73±0.21 (31)
IIA	5.33±1.39 (3)	5.83 6.20	5.14 6.17	4.88±0.40 (10)	4.62 4.77	5.06±0.54 (8)
I+IIA	4.06±0.88 (3)	3.96 5.51		2.88 3.86	3.55 5.58	
IIA+IID		5.04		6.45±0.61 (5)	5.24±0.48 (7)	5.64±0.31 (5)

Values are means ± SE for groups containing ≥3 fibres and individual values are given for groups containing <3 fibres. For groups containing ≥3 fibres, the number of fibres examined is indicated in brackets.

## 5.4 Discussion

This is the first study in which soleus muscles from SHRs and normotensive (WKY) rats, at three stages in the development of high blood pressure, were examined with respect to MHC isoform expression (%MHC<sub>i</sub>), MLC2 isoform expression (MLC2s/MLC2t) and fibre type populations (%f<sub>T</sub>), using electrophoretic analyses of muscle proteins from whole muscle homogenates and segments of randomly dissected single muscle fibres. For all muscles examined, the data produced by these three independent electrophoretic methods were closely correlated (Fig. 5.5). Ca<sup>2+</sup>-activation properties of the contractile apparatus in electrophoretically-typed fibres from SOL

muscles of the two strains were also determined using permeabilized single fibre preparations.

There was good agreement between the MHC composition of SOL muscle from WKY rats found in this study by SDS-PAGE and the MHC/fibre type composition of SOL muscle from normotensive rats of similar age, determined by others using histochemical techniques. For example, the MHC composition of SOL muscles from 24-wk-old WKY rats found in this study (MHCI: 89%; MHCIIa: 11%), (Table 5.3) is in close agreement with the fibre type composition reported by Armstrong & Phelps (1984) for 25- to 26-wk-old Sprague-Dawley rats (87% type I fibres, 13% type IIA fibres), by Kovanen (1989) for 25-wk-old Wistar rats (90% type I fibres, 10% type IIA fibres) and by Lewis *et al.*, (1994) for 12- to 17-wk-old WKY rats (93% type I fibres, 7% type IIA fibres).

A major conclusion from this study is that at all stages in the development of hypertension, soleus muscles of SHRs contain a statistically significantly higher proportion of MHCII and MLC2f isoforms than soleus muscles from age-matched WKY rats. This conclusion was further supported by the data obtained from the fibre type population study which showed that random sampling of single fibre segments from the SHR soleus produced a higher proportion of fibres expressing MHCII isoforms (type IIA; type I + IIA and type IIA+IID) than from soleus of age-matched WKY rats. As calculated from the data in Table 5.4, the average percentages of type I and type I+IIA fibres sampled from the soleus muscle of 4 wk-old SHRs were 1.4 times and 1.9 times lower than those from the age-matched WKY soleus.

A similar difference in the proportion of type I and type IIc/IntI (probably type I+IIA)

fibres was reported for soleus muscles from 4-wk-old SHR and WKY rats by Benbachir-Lamrini *et al.* (1990, 1993). By comparison, in the present study it was found that soleus muscles from 4-wk-old SHR produced about 8 times more fast fibres than the soleus from the age-matched WKY rats. A major contributor to this difference was the subpopulation of hybrid fast/fast (IIA+IID) fibres which amounted to 13.3% of the total number of fibres examined for this SHR age group, but was not detected in the fibre population dissected from WKY muscle. In the studies of Benbachir-Lamrini *et al.* (1990, 1993) the 4-wk SHR soleus contained only 1.7-2 times more type IIA fibres than the age matched WKY soleus and displayed no IIA+IID fibres. This difference between the results from this study and Benbachir-Lamrini's results are attributed to the higher sensitivity and resolving power of the microelectrophoretic method particularly with respect to hybrid fibres (Bottinelli *et al.*, 1991). An increase in age from 4 to 24 weeks, was accompanied by an increase in the proportion of type I fibres and a decrease in the proportion of type II fibres produced by soleus muscles from both rat strains. As a result of the decrease in fast fibres, the 24-wk-old WKY soleus yielded only 2.5% fast fibres (type IIA), while the 24-wk-old SHR soleus yielded about 21% fast fibres (comprising both IIA and IIA+IID fibre types) (Table 5.4). The higher proportion of fast fibres sampled from SHR soleus throughout maturation observed in this study is in agreement with the data obtained by Benbachir-Lamrini *et al.* for 8- to 10-wk-old (1993) and 12-wk-old (1990) animals and by Lewis *et al.* (1994) for 12- to 17-wk-old rats, but strongly disagrees with the data of Atrakchi *et al.* for 16- to 18-wk-old rats (1994) and Gray for 24- to 28-wk-old rats (1988).

The microelectrophoretic analyses of single muscle fibres in this study have provided valuable new information concerning the presence and the percentage of hybrid fibres (I+IIA and IIA+IID) in soleus muscles from SHR and WKY rats. As indicated by Hämäläinen & Pette (1995) and Bottinelli *et al.* (1991), identification of these fibres can be achieved by microelectrophoretic methodology but not by histochemical or immunohistochemical techniques (see section 1.5). In this study it was found that at 4 weeks of age, the WKY soleus yielded almost twice as many hybrid slow/fast (I+IIA) as the SHR soleus; however, this population of hybrid fibres decreased quite dramatically to non-detectable levels with rat maturation. In contrast, maturation in SHR was accompanied by only a slight decrease in the percentage of type I+IIA fibres sampled from soleus muscle. Furthermore, according to data from this study, soleus muscles from SHR of all ages produced a sizeable proportion of hybrid fast/fast fibres (IIA+IID), ranging from about 13% at 4-wk to about 8% at 24-wk, while only a very small proportion of such fibres (ca 1%) was yielded by soleus of 16-wk-old WKY rats. The presence of hybrid fibres is regarded by Pette & Staron (1997) as indicator of muscle transformation and their MHC composition as indicator of the direction of fibre-type transition. Seen in this context, the size of the hybrid fibre population and the combination of MHC isoforms detected in soleus muscles from SHR at the three ages examined, suggest that in SHR soleus, there is an active process of fibre type transition in the direction IID→IIA→I. This process takes place not only in the very young rats but also persists in mature animals. In contrast, the WKY soleus appears to undergo fibre transition (in the direction IIA→I) only in young rats (from 4 to 16 weeks of age). Thus, with respect to fibre transformation, the adult

SHR soleus resembles more the soleus from 4-wk-old WKY than that of the adult WKY, suggesting that many fibres of the adult SHR soleus muscle are still subjected to a process of transition.

The higher percentage of fast fibres and hybrid fibres in SHR than in WKY soleus muscle is in full agreement with previous reports that skeletal muscles of hypertensive humans contain a higher percentage of fast-twitch fibres than the normotensive controls (Frisk-Holmberg *et al.*, 1983; Juhlin-Dannfelt *et al.*, 1979). One can argue that this characteristic may not be related to high blood pressure, but to rat strain differences with respect to fibre type composition, since it occurred in 4-wk-old SHRs before the onset of hypertension. However, one cannot rule out a casual relationship between hypertension and MHC expression in the soleus muscle as it is clear from the present study that the blood pressure of the 4-wk-old SHR was significantly elevated compared with the age-matched controls (Table 5.2). To further explore the relationship between hypertension and the fibre type composition of SHR soleus muscles, one could extend this study to include several other normotensive and hypertensive rat strains.

In this study no statistically significant difference was found between single muscle fibres of the same type from SHR and WKY soleus muscles with respect to the maximum  $\text{Ca}^{2+}$ -activated isometric force response/cross sectional area and the sensitivity to  $\text{Ca}^{2+}$  of the contractile machinery. Furthermore, the degree of cooperativity of the contractile apparatus and  $\text{Ca}^{2+}$ -regulatory system with respect to  $\text{Ca}^{2+}$ -regulation of the contractile response, expressed by the Hill coefficient, was similar in single fibres of the same type from soleus muscles of SHRs and WKY rats.

Nevertheless, the pooled data for type I and type IIA fibres from SHR and WKY soleus showed that, in soleus muscles of 4-wk-old animals, there was a clear tendency for the type IIA fibres to develop lower  $\text{CaF}_{\text{max}}/\text{CSA}$  compared with the type I fibres ( $69.2 \pm 15.0 \text{ kN/m}^2$ ,  $n= 12$  vs.  $100.6 \pm 7.6 \text{ kN/m}^2$ ,  $n= 57$ ;  $P < 0.02$ , Mann Whitney). The higher percentage of type IIA fibres and the lower percentage of type I fibres in SHR soleus may explain in part previously reported observations with intact soleus muscles from young SHR rats (less than 10-wk-old), which developed 15% lower tetanic forces compared with their counterparts from WKY rats (Atrakchi *et al.*, 1994; Benbachir-Lamrini *et al.*, 1990). The difference in the maximal  $\text{Ca}^{2+}$ -activated specific force between type I and type IIA fibres was not statistically significant for the older rats of either strain.

In summary, the present study demonstrates that whilst for a given fibre type, there are no significant differences between SHR and WKY soleus muscles with respect to any of the  $\text{Ca}^{2+}$ -activation properties examined, the soleus muscles from SHRs and WKY rats are at different states of transformation as reflected by major differences in MHC composition and fibre type populations.

## Chapter 6

# A Study of Caffeine Threshold for Contraction in Electrophoretically-Typed Single Muscle Fibres from SHR and WKY Rats

### 6.1 Introduction

As already mentioned in section 5.1, several laboratories have reported that SOL muscles from SHRs display reduced specific tetanic force and lower kinetic parameters than control muscles from normotensive rats (Carlsen & Gray, 1987; Gray *et al.*, 1994a; Gray *et al.*, 1994b; Atrakchi *et al.*, 1994; Lewis *et al.*, 1994). However, the cellular mechanisms underlying these functional characteristics are still unclear.

In the study described in Chapter 5 it was shown that for a given electrophoretically-defined fibre type, there are no significant differences between SHR and WKY SOL muscle fibres with respect to maximum  $\text{Ca}^{2+}$ -activated specific tension, sensitivity to  $\text{Ca}^{2+}$  of the myofibrillar compartment and degree of cooperativity within the myofibrillar system with respect to  $\text{Ca}^{2+}$ -regulation of the contractile response. This

finding suggests that functional differences between SOL muscles from SHR and WKY rats cannot be attributed to alterations in the contractile and/or regulatory systems.

In an earlier study, Carlsen & Gray (1987) suggested the possibility that the ability of SOL muscles from hypertensive rats to release and sequester  $\text{Ca}^{2+}$  may be impaired; however, the possibility that SOL muscles from SHR and WKY rats may differ with respect to SR properties has not been explored so far. Therefore, the main aim of the work presented in this chapter was to determine and compare SR properties in mechanically skinned single fibres dissected from soleus muscles of SHR at the onset of hypertension (for details regarding the three stages in the development of hypertension see section 5.1) and of age matched WKY rats.

The experimental strategy chosen to achieve this aim involved the use of caffeine, the value of which as a chemical tool for probing SR function in normal and impaired skeletal muscles has been discussed in detail in a recent review by Herrmann-Frank *et al.* (1999) (see also section 1.3.1.1).

## 6.2 Materials and methods

*Animals.* The animals used for this study were male normotensive WKY rats and SHRs (aged 14-16 weeks) supplied by the Baker Medical Research Institute (Melbourne, Victoria, Australia). The rats were handled as in section 5.2 and muscles (SOL and EDL) were dissected and stored as described in section 2.2.

*Skinned fibre preparation.* Single fibres were isolated, measured and mechanically skinned, under oil, as described in sections 2.3.1, 2.3.2 and 2.3.3, respectively.

*Solutions and force measurements.* The solutions used for this series of experiments were as follows:

- (i) a weakly  $\text{Ca}^{2+}$ -buffered solution (solution *E*) in which the fibre was equilibrated prior to each exposure to caffeine,
- (ii) solution *E* containing caffeine in the concentration range 0.3-7.5mM (solution *Th-caff<sub>x</sub>*, where *x* represents the caffeine concentration),
- (iii) a high caffeine (30mM), low  $\text{Mg}^{2+}$  (0.02mM), SR- $\text{Ca}^{2+}$  release solution (solution *R*),
- (iv) SR- $\text{Ca}^{2+}$  loading solution (solution *L*)
- (v) solution *W-caff/Ca*, in which a fibre was washed after being exposed to solutions *R* or *L*
- (vi) a strongly  $\text{Ca}^{2+}$  buffered solution in which the fibre was relaxed (solution *rlx*) and
- (vii) a maximally  $\text{Ca}^{2+}$ -activating solution (solution *maxCa*).

The compositions of these solutions, which were prepared as described in section 2.4.5.1, are shown in Table 6.1.

**Table 6.1. Compositions of solutions used to determine caffeine threshold for contraction.**

Solutions	Mg <sub>total</sub> (mM)	Mg <sup>2+</sup> (mM)	EGTA <sub>total</sub> (mM)	HDTA <sub>total</sub> (mM)	Caffeine (mM)	pCa
<i>E</i>	7.2	0.6	0.2	49.8	-	7.1
<i>Th-caff<sub>x</sub></i> *	7.2	0.6	0.2	49.8	0.3-7.5	7.1
<i>R</i>	0.9	0.02	0.5	49.5	30	8.2
<i>W-caff/Ca</i>	7.2	0.6	0.5	49.5	-	8.2
<i>L</i>	8.8	1	50	-	-	6.2
<i>rlx</i>	10.3	1	50	-	-	>9
<i>maxCa</i>	8.1	1	50	-	-	4.3

All solutions contained (mM): Na<sup>+</sup>, 36; K<sup>+</sup>, 126; HEPES, 90; ATP<sub>total</sub>, 8; creatine phosphate, 10; NaN<sub>3</sub>, 1. The pH of all solutions was 7.10±0.01 (at 22°C) and the ionic strength was 234±2 mM. The osmolality of all solutions (not including caffeine) was 295±2 mosmol/kg.

\* The subscript (x) in Th-caff<sub>x</sub> stands for the concentration of caffeine in solution.

Caffeine-induced force responses (expressed as percent of the maximum Ca<sup>2+</sup>-activated force) were estimated from the height of the response peak (for caffeine concentrations ≤ 7.5 mM), or the area under the peak (for force responses developed in solution R) divided by the maximum Ca<sup>2+</sup>-activated force response (developed by the fibre preparation in solution *maxCa*).

*SDS-PAGE analysis of MHC isoforms in single muscle fibre segments.* After determination of caffeine thresholds for contraction, the MHC isoform composition of single fibre

segments was determined using the gel system, gel F3.17B (Appendix 2) and the procedures described in section 2.5.

*Statistical analyses.* Unless stated otherwise, all data are expressed as means  $\pm$  SE.

Statistical comparisons were performed on groups with at least three data points using either a two-way analysis of variance followed by the Bonferroni test or a *t*-test.

Statistical significance was accepted at  $P < 0.05$ .

## 6.3 Results

### 6.3.1 Types of fibres examined and strategy used for determining caffeine threshold for contraction

In this study, 'caffeine threshold' for contraction (*caff-th*) is defined as the concentration of caffeine that produces in a skinned fibre preparation a mechanical response corresponding to 10% of the maximum  $\text{Ca}^{2+}$ -activated force. Three parameters related to caffeine threshold were determined for each fibre: (i) the caffeine threshold at endogenous SR- $\text{Ca}^{2+}$  load (*caff-th<sub>E</sub>*), when the fibre segment was maintained at pCa 7.1 throughout the experiment, (ii) the caffeine threshold at maximal load (*caff-th<sub>M</sub>*), when the fibre segment was exposed to pCa 6.2 where, under the conditions described, the SR- $\text{Ca}^{2+}$  load is near maximal and the contraction-induced damage to the fibre is minimised (Fryer & Stephenson, 1996), and (iii) the ratio

$caff-th_M/caff-th_E (R_{caff-th})$ . As will be argued later in this section and in the Discussion (section 6.4),  $R_{caff-th}$  provides information on the slow/fast characteristics of the SR compartment.

Caffeine thresholds for contraction were determined in three fibre populations: 24 SOL fibres from WKY rats (controls), 32 SOL fibres from SHR (experimental) and 12 EDL fibres from WKY rats (reference type II fibres). The proportions of different fibre types detected in these fibre populations are given in Table 6.2.

**Table 6.2 Fibre types of randomly dissected single fibres in SOL and EDL muscles from SHR and WKY.** Values are expressed as percentage of the total number of fibres dissected (shown in brackets).

Fibre type	<b>SHR-SOL</b> (n=32)	<b>WKY-SOL</b> (n=24)	<b>WKY-EDL</b> (n=12)
I (slow)	59.4%	87.5%	
IIA (fast)	21.9%	4.2%	
IID (fast)	6.3%		8.3%
<b>I+IIA</b> (slow/fast)		8.3%	
<b>I+IIA</b> (slow/fast)	9.4%		
IIA+IID (fast/fast)	3.0%		8.3%
<b>IID+IIB</b> (fast/fast)			50.0%
<b>IID+IIB</b> (fast/fast)			33.4%

Note: Bolding was used to indicate the predominant MHC isoform in given hybrid fibre.

As shown in Fig. 6.1A, the strategy used to determine  $caff-th_E$  involved incubating a fibre segment, freshly dissected and mechanically skinned, in solution  $E$ , for 2 min, and then exposing it, for 30 sec on each occasion, to a succession of

*Th-caff<sub>x</sub>* solutions containing an increasing concentration of caffeine. Each fibre preparation was exposed to caffeine until it developed a force equivalent to at least 16 times the minimum measurable response (where the minimum measurable response was equal to 2.5 μN). All fibres were exposed to at least three *Th-caff<sub>x</sub>* solutions (covering the concentration range 0.3-0.9 mM). To minimise the depletion of SR-Ca<sup>2+</sup> store, the fibre was incubated for 30 sec in solution *E*, between exposures to caffeine. To determine the value of '*caff-th<sub>M</sub>*' (Fig. 6.1B), the SR, emptied in solution *R*, was loaded to almost maximal capacity, by incubating the fibre for 2 min in solution *L*, and then the fibre was exposed in a sequential manner to increasing [caffeine], as described for *caff-th<sub>E</sub>*.

To correct for the potential effects of caffeine on the myofibrillar compartment, at the end of the experiment described above, each fibre was treated with 2% Triton (which renders the SR non-functional), and then was exposed to another set of *Th-caff<sub>x</sub>* solutions identical to the set used for determining the caffeine threshold for contraction. Although the force responses elicited by caffeine in the Triton treated fibre preparation were very small (see Fig. 6.1C), they were nevertheless subtracted from the corresponding responses recorded when the SR was intact. The results expressed as a fraction of the maximum Ca-activated force were plotted as shown in Fig. 6.1D, the data points were best fitted with the Graph Pad prism software to a polynomial third order curve described by the equation  $y = ax^3 + bx^2 + cx + d$  (where  $y = \% \text{ max. force}$ ,  $x = [\text{caffeine}]$  and  $d = 0$ ). The value of caffeine threshold for contraction (i.e. the [caffeine] that produced 10% max. force) was generated by the software package.

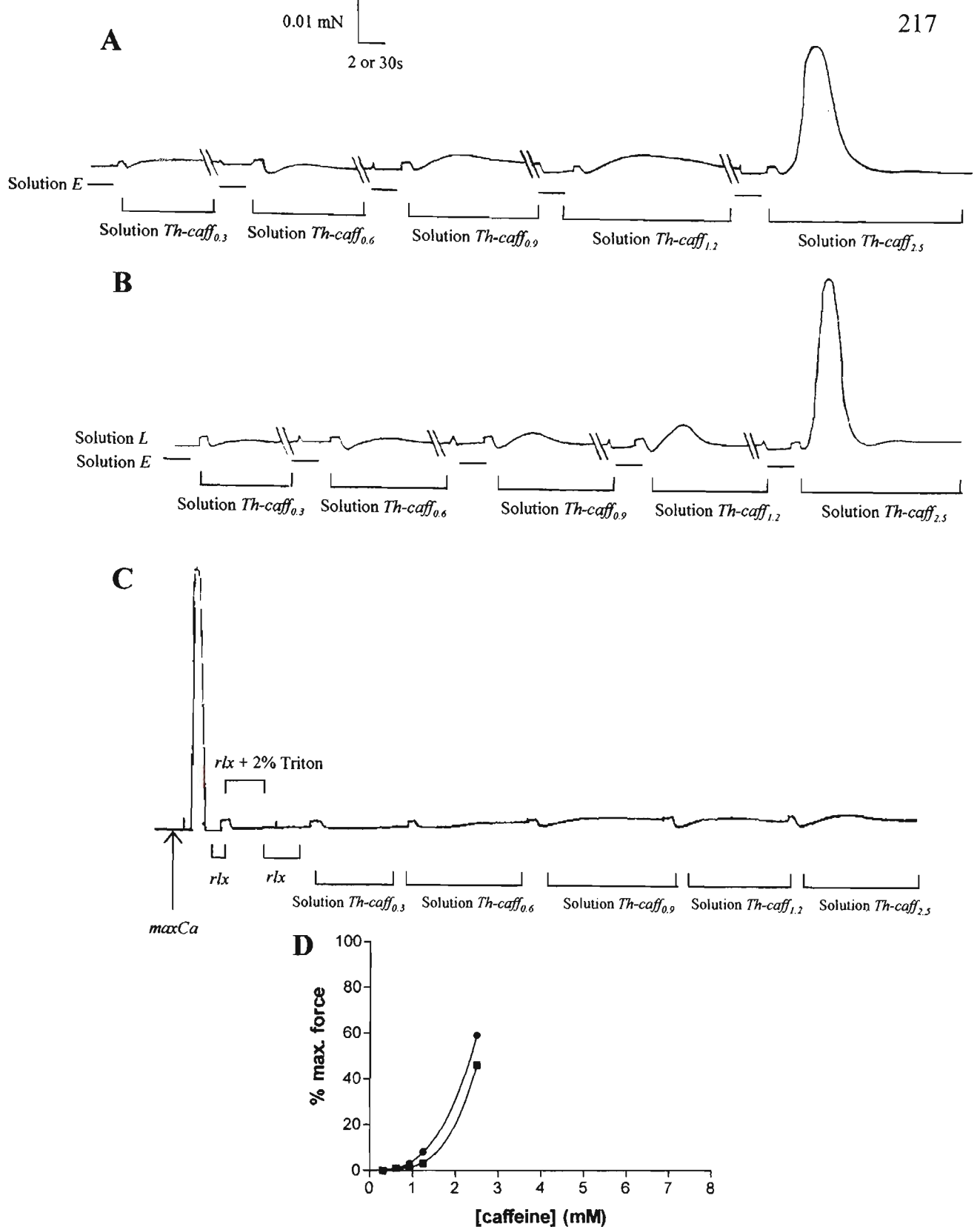


**Figure 6.1 Representative chart recordings of force responses and the data plot used when determining  $\text{caff-th}_E$  and  $\text{caff-th}_M$  of a single muscle fibre.**

A. Representative chart recording of force responses produced by a fibre subjected to increasing [caffeine] at endogenous SR- $\text{Ca}^{2+}$  load. B. Representative chart recording of force responses produced by a fibre subjected to increasing [caffeine] at maximal SR- $\text{Ca}^{2+}$  load. C. Representative chart recording of force responses produced by a Triton-treated fibre when exposed to increasing [caffeine]. D. Data points were fitted to a polynomial third-order curve to determine  $\text{caff-th}_E$  (■; 1.66 mM) and  $\text{caff-th}_M$  (●; 1.36 mM). Data were produced with a type I WKY fibre. Time scale: 2 s during incubation in caffeine solutions and 30s elsewhere.

### 6.3.2 Low caffeine induced force responses are related to SR $\text{Ca}^{2+}$ release

As seen in Fig. 6.1, low concentrations of caffeine produced very low force responses. To ensure that these responses were related to SR- $\text{Ca}^{2+}$  release, the mechanically skinned muscle fibre preparation was (i) incubated in solution *R* to deplete the SR, (ii) washed for 30 sec in solution *W-Caff/Ca*, (iii) loaded for 2 min in solution *L*, (iv) washed for 15 sec in solution *W-Caff/Ca*, (v) exposed to solution *Th-caff*<sub>0.3</sub> and (vi) exposed again to solution *R* to release the SR- $\text{Ca}^{2+}$  remaining after the caffeine exposure. Steps (ii)-(vi) were then repeated for different low caffeine containing *Th-caff*<sub>*x*</sub> solutions. If low force responses were due to caffeine induced SR- $\text{Ca}^{2+}$  release, this strategy was expected to show a caffeine concentration related-decrease in the SR- $\text{Ca}^{2+}$  content after each exposure of the fibre to low [caffeine] solutions.

In Fig. 6.2 are shown results obtained with the fibre used in the experiments described in Fig. 6.1, before it was treated with Triton. One can see that the area under the force responses, which is directly related to the SR- $\text{Ca}^{2+}$  content, decreased by about 19% after the fibre exposure to solution *Th-caff*<sub>0.9</sub>, suggesting that the value of *caff-th*<sub>*M*</sub> would be in the vicinity of 0.9 mM. Note that in this fibre, *caff-th*<sub>*M*</sub> was estimated to be 1.36 mM (see legend for Fig. 6.1D).

The results obtained with 19 SHR type I fibres are summarised in Fig. 6.3. In order to compare results obtained with all fibres, the data were normalised by dividing the areas under the force responses developed by each preparation in solution *R* after exposure to *Th-caff*<sub>*x*</sub> solutions containing 0.6-2.5 mM caffeine by the force response

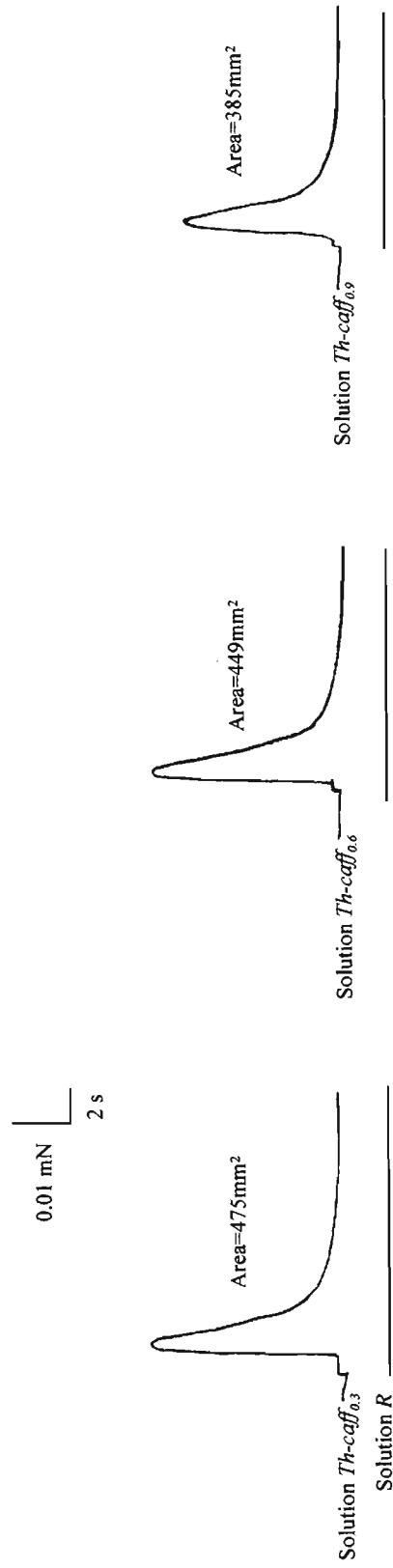


**Figure 6.2** Representative chart recordings of force responses produced by a fibre segment incubated in Solution  $R$  after having been exposed to Solution  $Th\text{-caff}_x$ . Note: the area under the peak, indicative of the  $SR\text{-Ca}^{2+}$  content, decreases as the  $[caffeine]$  in Solution  $Th\text{-caff}_x$  increases.

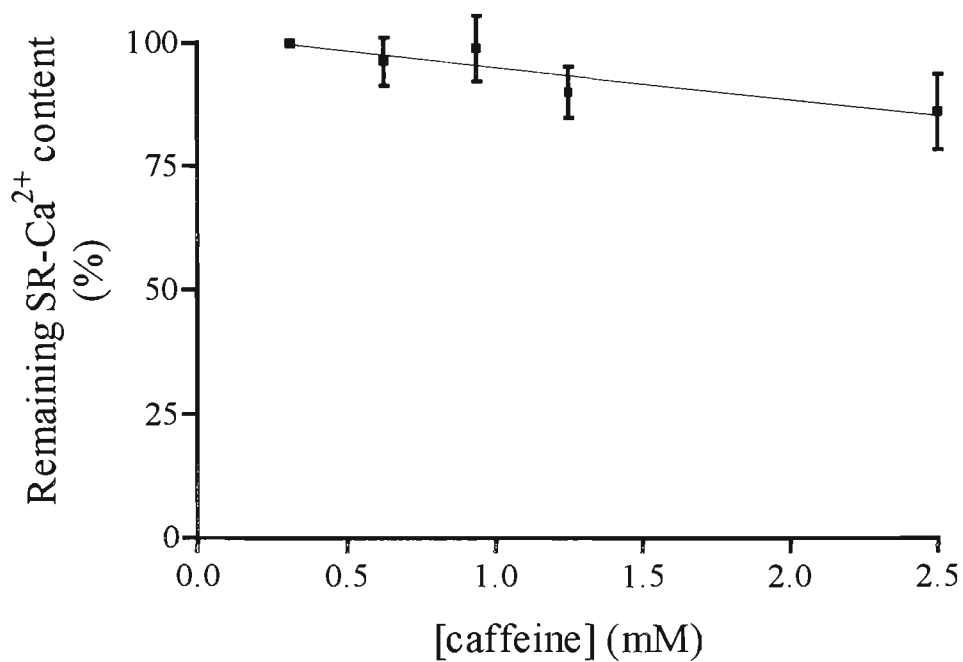


**Figure 6.3** Graph showing the gradual decrease in SR-Ca<sup>2+</sup> content after exposure of skinned fibre preparation to solutions containing the caffeine concentrations indicated on x-axis. Data shown here obtained from 19 SHR type I fibres.

developed by the preparation in solution *R* after exposure to solution *Th-caff*<sub>0.3</sub>. As shown in Fig. 6.3, the data were fitted by a straight line with a slope that was significantly different from 0 ( $P < 0.05$ ), which clearly demonstrates that under the conditions used in this study, low concentrations of caffeine released small but significant amounts of calcium from the SR compartment in mechanically skinned fibre preparations.

### 6.3.3 Strain-related and fibre type-related differences in caffeine threshold for contraction at endogenous SR-Ca<sup>2+</sup> load

The *caff-th*<sub>E</sub> values (means  $\pm$  SE; range; coefficient of variation) obtained for SHR-SOL, WKY-SOL and WKY-EDL muscle fibres are presented in Table 6.3; the values are organised according to MHC-based fibre type. As stated in section 6.2, statistical analyses were performed only on groups containing at least three fibres.

As shown by the data in Table 6.3, at endogenous SR-Ca<sup>2+</sup> load, the average *caff-th*<sub>E</sub> values for type I fibres in SHR-SOL and type I fibres in WKY-SOL did not differ significantly. Also, no significant differences were observed with respect to this parameter between type I fibres and type II fibres in SHR-SOL, where type II fibres included type IIA and type I+IIA fibres (fibres in which MHC isoform IIa was predominant].

**Table 6.3 Caffeine threshold at endogenous SR-Ca<sup>2+</sup> load [*caff-th<sub>E</sub>* (mM)] in SOL and EDL fibres from SHR and WKY rats.**

Fibre type	SHR-SOL			WKY-SOL			WKY-EDL		
	mean ± SEM	range	CV	mean ± SEM	range	CV	mean ± SEM	range	CV
I (slow)	1.44±0.07 (19)	0.91-2.05	21.8%	1.53±0.06 (21)	0.98-2.04	18.7%			
IIA (fast)	1.64±0.26 (7)	0.90-2.99	41.4%	1.50					
IID (fast)	1.14; 1.38						1.48		
I+IIA (slow/fast)				0.89; 1.08					
I+IIA (slow/fast)	1.84±0.19 (3)	1.47-2.11	18.0%						
IIA+IID (fast/fast)	1.77						2.96		
IID+IIB (fast/fast)							2.38±0.65 (6)†	0.86-4.71	66.5%
IID+IIB (fast/fast)							1.29±0.28 (4)	0.80-1.89	42.8%

Values are means ± SE for groups containing ≥3 fibres and individual values are given for groups containing <3 fibres. For groups containing ≥3 fibres, the number of fibres examined is indicated in parentheses. † Significantly different (*P*<0.05) from WKY-SOL type I (*t*-test).

The correlation between MHC-based fibre type and caffeine threshold at endogenous SR-Ca<sup>2+</sup> load was further examined using the fibre populations dissected from SOL and EDL muscles of WKY rats. Under the experimental conditions used in this study, the *caff-th<sub>E</sub>* value obtained for the SOL type I fibres ( $1.53 \pm 0.06$ ;  $n = 21$ ; range: 0.98 – 2.04; CV = 18.7%) was about 23% lower than that for the EDL type II fibres ( $1.99 \pm 0.36$ ;  $n = 12$ ; range: 0.8-4.71; CV = 64%), but this difference was not statistically significant. However, when comparing *caff-th<sub>E</sub>* values for type I fibres in SOL and fast-twitch subtypes in EDL muscles, it was found that type I fibres displayed *caff-th<sub>E</sub>* values that were significantly lower (-36%) than those of type **IID+IIB** fibres (in which MHC isoform IId was predominant). No statistically significant differences were found between type I and type **IID+IIB** fibres (in which MHC isoform IIb was predominant), or between the fast-twitch fibre subtypes **IID+IIB** and **IID+IIB**.

#### 6.3.4 Strain-related and fibre type-related differences in caffeine threshold for contraction at maximal SR-Ca<sup>2+</sup> load

As seen in Table 6.4, at maximal SR-Ca<sup>2+</sup> load, the caffeine thresholds for contraction recorded for type I fibres from SHR-SOL were significantly lower (-17%) than those displayed by type I fibres from WKY-SOL. At this SR-Ca<sup>2+</sup> load, as at endogenous SR-Ca<sup>2+</sup> load, SHR-SOL fibre types I, IIA and I+**IIA** displayed no significant differences with respect to *caff-th<sub>M</sub>* values.

**Table 6.4 Caffeine threshold at maximal SR-Ca<sup>2+</sup> load [*caff-th<sub>M</sub>* (mM)] in SOL and EDL fibres from SHR and WKY rats.**

Fibre type	SHR-SOL			WKY-SOL			WKY-EDL		
	mean ± SEM	range	CV	mean ± SEM	range	CV	mean ± SEM	range	CV
I (slow)	1.18±0.09 (19)*	0.65-2.03	33.3%	1.42±0.06 (21)‡	0.78-1.91	20.6%			
IIA (fast)	1.09±0.10 (7)	0.77-1.43	23.2%	1.41					
IID (fast)	1.00; 0.48						0.82		
I+IIA (slow/fast)				2.06; 0.71					
I+IIA (slow/fast)	1.54±0.28 (3)	0.99-1.87	31.1%						
IIA+IID (fast/fast)	0.89						1.54		
IID+IIB (fast/fast)							1.18±0.29 (6) ‡	0.15-2.05	60.8%
IID+IIB (fast/fast)							0.47±0.14 (4)	0.07-0.69	61.2%

Values are means ± SE for groups containing ≥3 fibres and individual values are given for groups containing <3 fibres. For groups containing ≥3 fibres, the number of fibres examined is indicated in parentheses. \* Significantly different ( $P < 0.05$ ) from WKY-SOL type I (*t*-test). ‡ Significantly different ( $P < 0.05$ ) from WKY-EDL type IID+IIB (ANOVA with Bonferroni post-test).

At maximal SR- $\text{Ca}^{2+}$  load, type I fibres from SOL-WKY displayed an average  $\text{caff-th}_M$  value ( $1.18 \pm 0.09$ ;  $n = 19$ ; range: 0.65-2.03; CV = 33.3%) which was about 20% higher than the corresponding value for type II EDL-WKY fibres ( $0.94 \pm 0.18$ ;  $n = 12$ ; range: 0.07-2.05; CV = 67%). Further comparison of  $\text{caff-th}_M$  values for fibres of type I (from SOL) and fast-twitch subtypes (from EDL) in WKY rats revealed that **IID+IIB** fibres displayed significantly lower  $\text{caff-th}_M$  values than type **IID+IIB** fibres and both type **IID+IIB** and type **IID+IIB** fibres displayed significantly lower  $\text{caff-th}_M$  values than type I fibres (SOL).

### 6.3.5 Strain-related and fibre type-related differences in the relative caffeine thresholds for maximal and endogenous SR- $\text{Ca}^{2+}$ loads

$R_{\text{caff-th}}$  was calculated for all fibres examined in this study and the values are presented in Table 6.5. An examination of the data reveals a large (49%), statistically significant difference between the average values of  $R_{\text{caff-th}}$  for type I ( $0.93 \pm 0.03$ ;  $n = 21$ ; range: 0.60-1.16; CV = 15.6%) and type II fibres ( $0.47 \pm 0.07$ ;  $n = 12$ ; range: 0.08-1.00 ; CV = 53.5%) in WKY muscles. This difference is further highlighted when the data are represented as frequency distribution plots (see Fig. 6.4). If one assumes that the SR in type I fibres from SOL-WKY has slow characteristics ( $\text{SR}^{\text{slow}}$ ) and in type II fibres from EDL-WKY has fast characteristics ( $\text{SR}^{\text{fast}}$ ), one can conclude from these results that the  $R_{\text{caff-th}}$  value is a good indicator of slow/fast characteristics of the SR in a given skeletal muscle fibre.

The median  $R_{caff-th}$  values for the slow-twitch and fast-twitch fibre populations presented in Fig. 6.4 were 1.00 and 0.46, respectively, and 0.73 was the midpoint between the two values. Based on the data obtained here it was decided to use this value of  $R_{caff-th}$  as a means (' $R-0.73$  criterion') for distinguishing between skeletal fibres containing a SR with slow characteristics ( $R_{caff-th} > 0.73$ ) and fibres containing a SR with fast characteristics ( $R_{caff-th} < 0.73$ ).

**Table 6.5 Relative caffeine threshold at maximal and endogenous SR-Ca<sup>2+</sup> loads ( $R_{caff-th} = caff-th_M/caff-th_E$ ).**

Fibre type	$R_{caff-th}$		
	SHR-SOL	WKY-SOL	WKY-EDL
I (slow)	0.82±0.05 (19)	0.93±0.03 (21)	-
IIA (fast)	0.71±0.06 (7)	0.94	
IID (fast)	0.88; 0.34		0.56
I+IIA (slow/fast)		2.31; 0.66	
I+IIA (slow/fast)	0.82±0.08 (3)		
IIA+IID (fast/fast)	0.50		0.52
IID+IIB (fast/fast)			0.53±0.13 (6)*
IID+IIB (fast/fast)			0.35±0.10 (4)*

Values are means ± SE for groups containing ≥3 fibres and individual values are given for groups containing <3 fibres. For groups containing ≥3 fibres, the number of fibres examined is indicated in parentheses. \* Significantly different ( $P < 0.001$ ) from WKY-SOL type I (ANOVA with Bonferroni post-test).

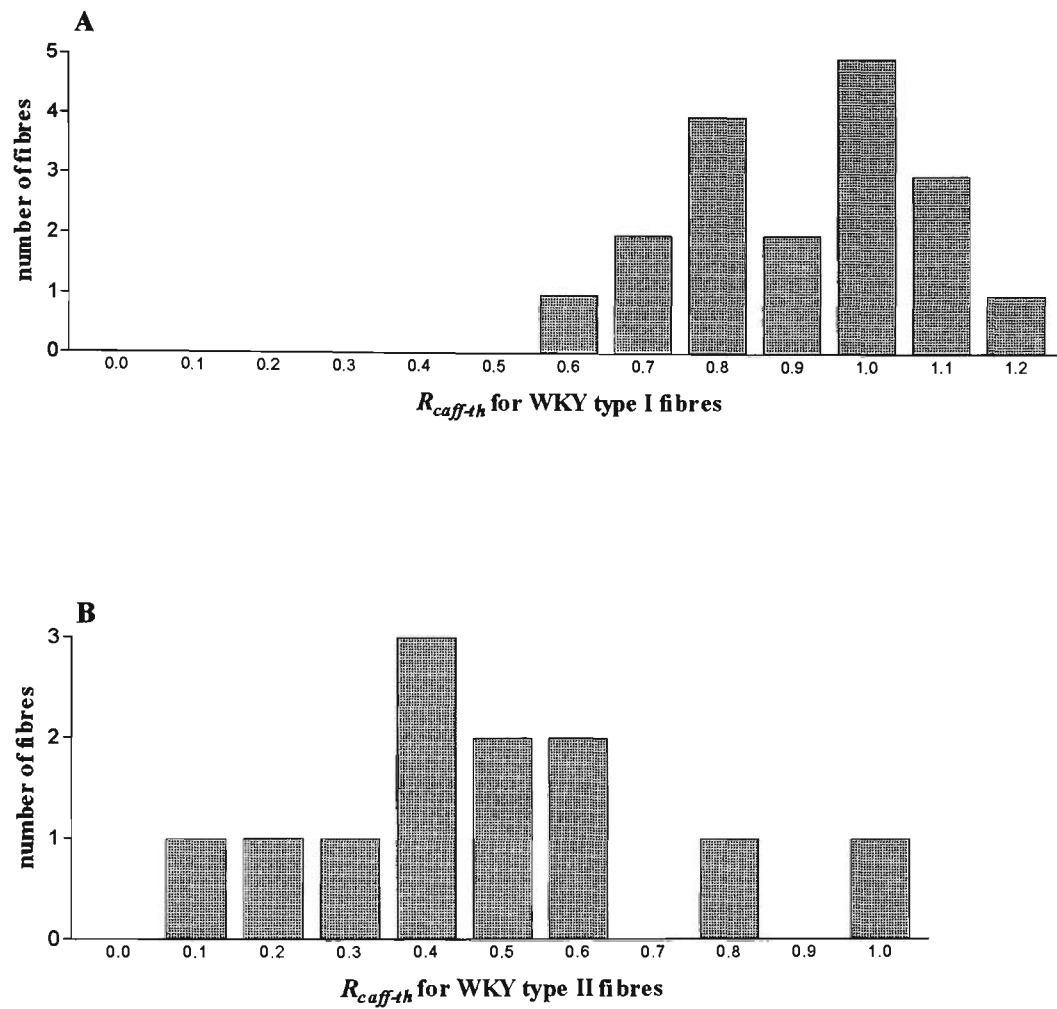


**Figure 6.4** The frequency distribution of  $R_{caff-th}$  values for WKY type I fibres from the SOL muscle (panel A) and WKY type II fibres from the EDL muscle (panel B).

The  $R-0.73$  criterion was subsequently used to examine and compare the populations of type I SOL fibres, dissected from SHR and WKY rats, with respect to the relative proportions of fibres with slow-twitch and fast-twitch SR characteristics. As seen in Fig. 6.5, the proportion of SR<sup>fast</sup> detected among the type I fibres from SHR-SOL was 5.3 times higher than that in the population of type I fibres from WKY-SOL.

The low number of fibres (<3) contained in most of the type II groups obtained from each type of muscle used in this study (SHR-SOL, WKY-SOL or WKY-EDL) precluded analyses SR characteristics in groups of fast twitch (type II) fibres from a given muscle type or from different muscles of a given strain. The only possible comparison was that between the type IIA fibre group (10 fibres) from SHR-SOL and the type II hybrid fibre population (comprising two type IIA + IID and ten type IID + IIB fibres) from WKY-EDL. This comparison revealed that the two fibre groups contained markedly different proportions of fibres with slow and fast SR characteristics (SHR-SOL : 40%-SR<sup>slow</sup> and 60%-SR<sup>fast</sup> ; WKY-EDL: 17%-SR<sup>slow</sup> and 83%-SR<sup>fast</sup>).

## 6.4 Discussion

At a given Ca<sup>2+</sup>-buffering capacity of the bathing solution, the caffeine threshold for contraction in a skinned muscle preparation is negatively correlated with both the sensitivity of the SR to caffeine and the sensitivity of the contractile apparatus

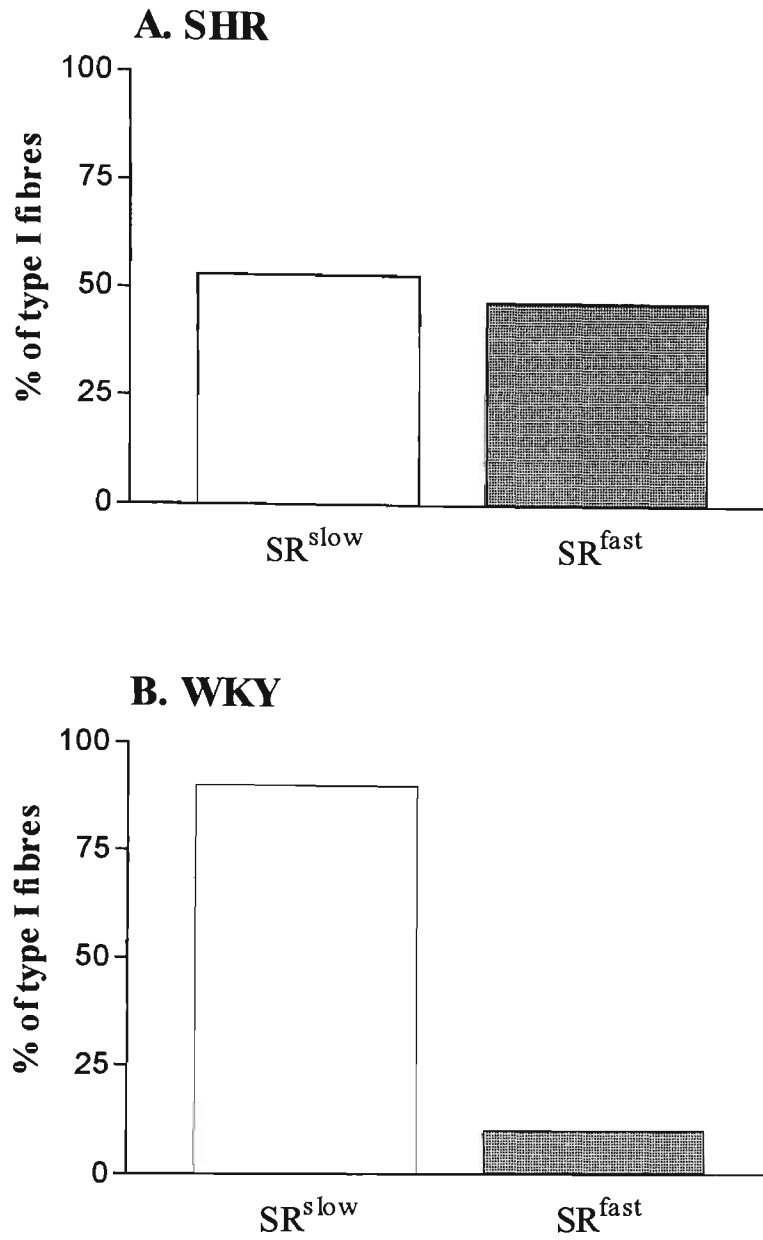


**Figure 6.5** The percentage of type I soleus fibres from SHR (panel A) and WKY (panel B) rats that displayed  $SR^{slow}$  or  $SR^{fast}$  properties.

to  $\text{Ca}^{2+}$ . In turn, the sensitivity (and therefore the caffeine threshold for contraction) of the SR to caffeine depends on the intrinsic properties of the SR- $\text{Ca}^{2+}$  release channels, the functional state of the channels as determined by various modulators (listed in section 1.3.1.1), the density of SR- $\text{Ca}^{2+}$  release channels, the SR volume and the total releasable SR- $\text{Ca}^{2+}$  content (see Stephenson *et al.*, 1998).

As reported in the Chapter 5 of this thesis, there are no obvious differences between SHR and WKY muscle fibres of the same electrophoretically defined fibre type with respect to the sensitivity of the contractile apparatus to the activator  $\text{Ca}^{2+}$ . Therefore, any differences found between the caffeine thresholds for contraction in such fibres will reflect differences with respect to the aforementioned SR-related properties.

In the present study, the caffeine threshold for contraction was measured, for each fibre, at endogenous SR- $\text{Ca}^{2+}$  loading (in a pCa 7.1 solution) and after the SR was loaded at pCa 6.2 (equivalent to maximal SR- $\text{Ca}^{2+}$  load). At pCa 6.2, the SR- $\text{Ca}^{2+}$  content has been shown to be substantially higher than the endogenous level in typically fast-twitch (type II) fibres but not in typically slow-twitch (type I) fibres (Fryer & Stephenson, 1996). Thus, based on the negative correlation between caffeine threshold for contraction and SR- $\text{Ca}^{2+}$  content, one would expect that if a fibre contained a significant fraction of SR with fast-twitch characteristics, its caffeine threshold for contraction would be considerably lower when the SR was loaded at pCa 6.2 than at endogenous SR- $\text{Ca}^{2+}$  level. Conversely, if a fibre contained a significant fraction of SR with slow-twitch characteristics one would expect that the caffeine threshold for contraction would be almost the same at endogenous and maximal

SR-Ca<sup>2+</sup> loads. Consistent with this view, the relative caffeine threshold for maximal and endogenous SR-Ca<sup>2+</sup> loads ( $R_{caff.th}$ ; Table 6.5) was close to 0.5 in all fast-twitch fibres (type II) from the WKY-EDL muscle whilst it approached unity in all slow-twitch fibres (type I) from the WKY-SOL muscles.

When the SR Ca<sup>2+</sup> content was maintained close to the endogenous level, there were no obvious differences with respect to caffeine thresholds for contraction between the type I fibres from the SHR and WKY soleus muscles of the rat. However, when the SR was loaded at pCa 6.2, the caffeine threshold for contraction decreased more in type I fibres from SHR than from the WKY rat. In view of the comments made above, this result could be directly explained if the SR in some of the type I SHR-SOL fibres had acquired fast-twitch SR characteristics. Further analysis of the type I fibre populations from SHR and WKY soleus muscles using the  $R-0.73$  criterion (which under the experimental conditions of this study was deemed to distinguish between slow and fast SR properties) confirmed that almost half of the type I fibres from SHR soleus displayed fast-twitch SR characteristics. This observation suggests that the faster contractile kinetics reported for the soleus muscle in SHRs than in the WKY rats are due to its high proportion of type I fibres containing SR with fast-twitch characteristics.

Another interesting finding of this study is that normal rat fast-twitch fibres are not homogeneous with respect to SR-properties, as evidenced by the significantly different caffeine thresholds at maximal load between type IID+IIB and type IID and IIB fibres in WKY-EDL (Table 6.4). Such differences could be explained by different functional states of the SR Ca<sup>2+</sup>-release channels, which in turn could be attributed to

varying degrees of channel phosphorylation (see Stephenson *et al.*, 1995).

It is noteworthy that, at endogenous SR-Ca<sup>2+</sup> load, the largest population of rat fast-twitch fibres (type **IID+IIB**) dissected from the WKY-EDL muscles, exhibited a significantly greater caffeine threshold for contraction than the type I fibres from the soleus muscle. This is in agreement with results obtained in several previous studies using intact (Fryer & Neering, 1989; Pagala & Taylor, 1998) or skinned rat muscle fibres (Danieli-Betto *et al.*, 1995), which showed that fibres from the EDL muscle display a significantly higher threshold for contraction than those from the SOL muscle. These inter-fibre type differences cannot be related only to differences between the SR properties of the two types of fibres because, type I and type II fibres differ significantly with respect to the Ca<sup>2+</sup>-sensitivity of the contractile apparatus and to the intracellular content of parvalbumin (a myoplasmic calcium binding protein and a potential contributor to differences in the sensitivity to caffeine in intact fibre studies).

The average values for *caff-th<sub>E</sub>* determined in the present study for SOL and EDL fibres were lower than those reported for rat fibres by Danieli-Betto *et al.* (1995). This could be due to differences in the ionic composition of solutions used and to differences in the skinning protocol (mechanical *versus* chemical) and to differences in the protocol employed to determine caffeine thresholds for contraction.

As already mentioned, almost half (9/19) of pure type I SHR-SOL fibres displayed fast-twitch SR characteristics. Furthermore, several (3/7) of pure type IIA SHR-SOL fibres displayed slow-twitch SR characteristics. Taken together these findings suggest that in rat skeletal muscles there is no tight relationship between MHC isoform expression and SR properties. A lack of correlation between the expression of

thick filament protein isoforms and various SR properties was also noted by several laboratories which monitored cellular events associated with low-frequency stimulation-induced muscle transformation (for review see Pette & Staron, 1990).

In conclusion, results presented in this section of the thesis demonstrate that SR in SOL fibres from SHR and WKY rats display significant functional differences which may explain the previously reported differences between the contraction kinetics of the SOL muscles from these two rat strains.

## Concluding remarks

Please note: The research question (rq) or methodological question (mq) addressed by each contribution listed in this section is identified in a bracket at the end of the contribution.

By using a combination of biochemical and physiological methods and perspectives, this study has contributed a large amount of novel information to the following areas of striated muscle research: (i) SDS-PAGE analysis of MHC isoforms in whole muscle homogenate and single muscle fibre preparations (Chapter 3), (ii) the correlation between MHC isoform expression and contractile activation characteristics of single, skinned fibres from SOL, EDL and DPH muscles of adult rat (Chapter 4), (iii) the correlation between caffeine thresholds for contraction and MHC isoform expression in single, skinned fibres from SOL and EDL muscles of adult rat (Chapter 6), (iv) the extent of overlap between the biochemical fibre typing technique based on MHC isoform composition and the physiological fibre typing technique based on contractile activation characteristics (Chapter 4), (v) cellular mechanisms underlying functional differences between SOL muscles from spontaneously hypertensive and normotensive rats (Chapters 5 and 6) and (vi) the heterogeneity and plasticity of rat skeletal and respiratory muscles (Chapters 4, 5 and 6). Notable contributions made by this study include:

- *A tabulated survey of 72 studies involving electrophoretic analyses of MHC expression was generated. The table, which contains also details of the methodological protocols used in these studies, has been formatted to allow rapid identification of the electrophoretic parameters most frequently modified and the range of values employed by various researchers concerned with the separation of MHC isoforms by SDS-PAGE. As it is, this table can, therefore, serve as a practical guide for trouble shooting in studies requiring electrophoretic separation of MHC isoforms on SDS-PA gels (see mq-1).*
- *Several lines of evidence were generated showing that the reproducibility of the SDS-PA gel systems currently used to separate MHC isoforms is related to the pair of MHC isoforms to be separated, being high for MHC I-MHC IIb, average for MHC IIb-MHC IIc and very low for MHC IIa-MHC IIc. The low reproducibility of MHC separation by SDS-PAGE, an issue not explicitly addressed so far in any of the relevant research articles or reviews surveyed as part of this study, has been attributed - at least in part - to the close correlation found to exist between the identity of the MHC isoforms under consideration and the direction and magnitude of the effects of different electrophoretic parameters on the separation of MHC isoforms (see mq-2 and mq-3).*
- *Convincing evidence was produced that non-transforming muscles obtained from functionally normal, adult animals, not previously subjected to intense or reduced mechanical activity, contain a large proportion of hybrid fibres. This finding lends further support to the previously stated possibility that some hybrid fibre types may be stable rather than transitory cellular species (see rq-1).*

- *Evidence was produced - for the first time - that adult rat DPH contains a small proportion of fibres expressing an 'atypical' combination of MHC isoforms (see rq-2).*
- *Evidence was produced that, in order to obtain structural and functional information on fast type fibres (pure or hybrid), both MHC isoform composition-based and  $Ca^{2+}/Sr^{2+}$ -activation characteristics-based fibre typing methods have to be used. This is because for such fibres MHC isoform expression and  $Ca^{2+}/Sr^{2+}$ -activation characteristics are not tightly correlated (see rq-3 and rq-4).*
- *Evidence was produced that in SOL and DPH muscles of the rat the expression of MHC and MLC isoforms are not tightly correlated (see rq-5).*
- *A comparative study was carried out on the MHC composition and the functional status of the contractile apparatus on SOL muscles from spontaneously hypertensive rats and their normotensive controls at three different stages of hypertension. The novel data produced by this study lends very strong support to the case for a shift in MHC expression, from slow to fast (rather than fast to slow) in SOL muscles from SHR rats. The evidence generated in this study brings the controversy regarding the fibre type composition of SHR and WKY rats practical to a close (rq-7 and rq-8).*
- *A study was carried out on the contractile activation characteristics of single SOL muscle fibres from SHR and age-matched WKY rats, at three different stages of hypertension. The data showed, for the first time, that functional differences between SOL muscles from age-matched SHR and WKY rats cannot be attributed*

to statistically significant differences between  $\text{Ca}^{2+}$ -activation characteristics of single fibres, when the fibres compared are of the same type (rq-9).

- *Using a population of type I (slow-twitch) SOL fibres and type II (fast-twitch) EDL fibres from adult rat, a protocol based on the SR sensitivity to caffeine was designed for identification of slow-twitch/fast-twitch SR characteristics in electrophoretically-defined fibres. The protocol involves (i) the use of the ratio of two caffeine thresholds for contraction, measured at two SR- $\text{Ca}^{2+}$  loads (endogenous and maximal), in a mechanically skinned muscle fibre preparations, as a criterion for distinguishing slow-twitch/fast-twitch SR characteristics, and (ii) the use of SDS-PAGE to analyse MHC isoform composition (rq-6).*
- *Evidence was produced that in rat adult muscles there is no tight correlation between MHC isoform composition and slow/fast SR characteristics. A direct implication of this finding is that knowledge of the MHC isoform composition of a given rat skeletal muscle fibre cannot be used to predict its characteristics with respect to SR function (see rq-6).*
- *Evidence was produced that the population of type I fibres dissected from SHR-SOL contain a higher proportion of fibres with fast SR characteristics than the population of fibres from WKY-SOL. This finding suggests a SR-related cellular mechanism for the lower kinetic parameters displayed by SHR-SOL muscles (see rq-9).*

## Bibliography

Adams, G.R., B.M. Hather, K.M. Baldwin, and G.A. Dudley. Skeletal muscle myosin heavy chain composition and resistance training. *J. Appl. Physiol.* 74(2): 911-915, 1993.

Adnet P.J., N.L. Bromberg, G. Haudecoeur, I. Krivosic, M.M. Adamantidis, H. Reyford, N. Bello, and R.M. Krivosic Horber. Fiber-type caffeine sensitivities in skinned muscle fibers from humans susceptible to malignant hyperthermia. *Anesthesiology.* 78(1): 168-77, 1993.

Aidley, D.J. *The physiology of excitable cells.* Cambridge University Press. 4<sup>th</sup> ed., 1998.

Allen, R.C., C.A. Saravis, and H.R. Maurer. *Gel electrophoresis and isoelectric focusing of proteins: Selected techniques.* Walter de Gruyter and Co., Berlin, 1984.

Alroy, J., and E.H. Kolodny. Lysosomal metabolism and its relevance to skeletal muscle. In: *Myology*, 2<sup>nd</sup> edn. (eds. Engel, A.G., and C. Franzini-Armstrong). McGraw-Hill Inc., New York, 1994.

Andersen, J.L., H. Klitgaard, and B. Saltin. Myosin heavy chain isoforms in single fibres from m. vastus lateralis of sprinters: influence of training. *Acta Physiol. Scand.* 151(2): 135-142, 1994.

Armstrong, R. B., and R. O. Phelps. Muscle fiber type composition of the rat hindlimb. *Am. J. Anat.* 171: 259-272, 1984.

Ashley, C.C., and D.G. Moisescu. Effect of changing the composition of the bathing solutions upon the isometric tension-pCa relationship in bundles of crustacean myofibrils. *J Physiol. (Lond.)* 270(3): 627-52, 1977.

Atrakchi, A., S.D. Gray, and R.C. Carlsen. Development of soleus muscles in SHR: relationship of muscle deficits to rise in blood pressure. *Am. J. Physiol.* 267: C827-C835, 1994.

Babu, A., S.P. Scordilis, E.H. Sonnenblick, and J. Gulati. The control of myocardial contraction with skeletal muscle troponin C. *J. Biol. Chem.* 262(12): 5815-5822, 1987.

Bagshaw, C.R. *Muscle contraction*. 1<sup>st</sup> edn. New York, Chapman and Hall, 1982.

Bamman, M.M., M.S. Clarke, D.L. Feeback, R.J. Talmadge, B.R. Stevens, S.A. Lieberman, and M.C. Greenisen. Impact of resistance exercise during bed rest on skeletal muscle sarcopenia and myosin isoform distribution. *J. Appl. Physiol.* 84(1): 157-163, 1998.

Bär, A., and D. Pette. Three fast myosin heavy chain in adult rat skeletal muscle. *FEBS Lett.* 235: 153-155, 1988.

Barnard, R.J., V.R. Edgerton, T. Furukawa, and J.B. Peter. Histochemical, biochemical and contractile properties of red, white and intermediate fibers. *Am. J. Physiol.* 220: 410-414, 1971.

Bassett, David R. Jr. Skeletal muscle characteristics: relationships to cardiovascular risk factors. *Med. Sci. Sports Exerc.* 26: 957-966, 1994.

Benbachir-Lamrini, L., H. Koubi, B. Sempore, M. H. Mayet, J. Frutoso, J. M. Cottet-Emard, and R. J. Favier. Soleus muscle alterations in spontaneously hypertensive rats are not dependent on activation of  $\beta_2$ -adrenergic receptors. *J. Auto. Nerv. Sys.* 44: 161-170, 1993.

Benbachir-Lamrini, L., B. Sempore, M. H. Mayet, and R. J. Favier. Evidence of a slow-to-fast fibre type transition in skeletal muscle from spontaneously hypertensive rats. *Am. J. Physiol.* 258: R352-R357, 1990.

Biral, D., R. Betto, D. Danieli-Betto, and G. Salviati. Myosin heavy chain composition of single fibres from normal human muscle. *Biochem. J.* 250(1): 307-308, 1988.

Bischoff, R. The satellite cell and muscle regeneration. In: *Myology*, 2<sup>nd</sup> edn. (eds. Engel, A.G., and C. Franzini-Armstrong). McGraw-Hill Inc., New York, 1994.

Blough, E.R., E.R. Rennie, F. Zhang, and P.J. Reiser. Enhanced electrophoretic separation and resolution of myosin heavy chains in mammalian and avian skeletal muscles. *Anal. Biochem.* 233: 31-35, 1996.

Bottinelli, R., R. Betto, S. Schiaffino, and C. Reggiani. Maximum shortening velocity and coexistence of myosin heavy chain isoforms in single skinned fast fibres of rat skeletal muscle. *J. Musc. Res. Cell Motil.* 15: 413-419, 1994.

Bottinelli, R., M.A. Pellegrino, M. Canepari, R. Rossi, and C. Reggiani. Specific contributions of various muscle fibre types to human muscle performance: an in vitro study. *J. Electromyogr. Kinesiol.* 9(2): 87-95, 1999.

Bottinelli, R., S. Schiaffino, and C. Reggiani. Force-velocity relations and myosin heavy chain isoform compositions of skinned fibres from rat skeletal muscle. *J. Physiol.* 437: 655-672, 1991.

Bradford, M.M. A rapid and sensitive method for the quantitation of microgram quantities of protein utilizing the principle of protein-dye binding. *Anal. Biochem.* 72: 248-254, 1976.

Brenner, B. Muscle mechanics II: skinned muscle fibres. In *Current methods in muscle physiology: advantages, problems and limitations*. (ed. Sugi, H.) New York, Oxford University Press, 1998.

Brooke, M.H., and K.K. Kaiser. Three 'myosin adenosine triphosphatase' systems: the nature of their pH lability and sulfhydryl dependence. *J. Histochem. Cytochem.* 18: 670-672, 1970.

Caiozzo, V.J., M.J. Baker, and K.M. Baldwin. Novel transitions in MHC isoforms: separate and combined effects of thyroid hormone and mechanical unloading. *J. Appl. Physiol.* 85(6): 2237-2248, 1998.

Caiozzo, V.J., M.J. Baker, S.A. McCue, and M. Baldwin. Single-fibre and whole muscle analyses of MHC isoform plasticity: interaction between T<sub>3</sub> and unloading. *Am. J. Physiol.* 273 (*Cell Physiol.* 42): C944-C952, 1997.

Canepari, M., V. Cappelli, M.A. Pellegrino, M.C. Zanardi, and C. Reggiani. Thyroid hormone regulation of MHC isoform composition and myofibrillar ATPase activity in rat skeletal muscles. *Arch. Physiol Biochem.* 106(4): 308-315, 1998.

Carlsen, R. C., and S. D. Gray. Decline of isometric force and fatigue resistance in skeletal muscles from spontaneously hypertensive rats. *Exp. Neurol.* 95: 249-264, 1987.

- Carraro, U., and A. Catani. A sensitive SDS-PAGE method separating myosin heavy chain isoforms of rat skeletal muscles reveals the heterogeneous nature of the embryonic myosin. *Biochem. Biophys. Res. Commun.* 116: 793-802, 1983.
- Chiasson, R.B. *Laboratory anatomy of the white rat*. 5<sup>th</sup> edn. Brown, Iowa, 1988.
- Close, R. Properties of motor units in fast and slow skeletal muscles of the rat. *J. Physiol.* 193: 45-55, 1967.
- Cordonnier, C., L. Stevens, F. Picquet, and Y. Mounier. Structure-function relationship of soleus muscle fibres from the rhesus monkey. *Pflugers Arch.* 430(1): 19-25, 1995.
- Craig, R. The structure of the contractile filaments. In: *Myology*, 2<sup>nd</sup> edn. (eds. Engel, A.G., and C. Franzini-Armstrong). McGraw-Hill Inc., New York, 1994.
- d'Albis, A., and G. Butler-Browne. The hormonal control of myosin isoform expression in skeletal muscle of mammals: a review. *Basic Appl. Myo.* 3(1): 7-16, 1993.
- d'Albis, A., C. Pantaloni, and J. Bechet. Myosin isoenzymes in adult rat skeletal muscles. *Biochimie.* 64: 399-404, 1982.
- Damiani, E., and A. Margreth. Characterization study of the ryanodine receptor and of calsequestrin isoforms of mammalian skeletal muscles in relation to fibre types. *J. Muscle Res. Cell Motil.* 15: 86-101, 1994.
- Danieli-Betto D., R. Betto, A. Megighian, M. Midrio, G. Salvati, and L. Larsson. Effects of age on sarcoplasmic reticulum properties and histochemical composition of fast- and slow-twitch rat muscles. *Acta Physiol. Scand.* 154(1): 59-64, 1995.

Danieli-Betto, D., R. Betto, and M. Midrio. Calcium sensitivity and myofibrillar protein isoforms of rat skinned skeletal muscle fibres. *Pflugers Arch.* 417(3): 303-308, 1990.

Danieli-Betto, D., E. Zerbato, and R. Betto. Type 1, 2A and 2B myosin heavy chain electrophoretic analysis of rat muscle fibers. *Biochem. Biophys. Res. Commun.* 138: 981-987, 1986.

Daugaard, J.R., J.L. Laustsen, B.S. Hansen, and E.A. Richter. Growth hormone induces muscle fibre type transformation in growth hormone-deficient rats. *Acta Physiol. Scand.* 164(2): 119-126, 1998.

Degens, H., F. Yu, X. Li, and L. Larsson. Effects of age and gender on shortening velocity and myosin isoforms in single rat muscle fibres. *Acta Physiol. Scand.* 163(1): 33-40, 1998.

Delbono, O., and G. Meissner. Sarcoplasmic reticulum  $Ca^{2+}$  release in rat slow- and fast-twitch muscles. *J. Membr. Biol.* 151: 123-130, 1996.

Demirel, H.A., S.K. Powers, H. Naito, M. Hughes, and J.S. Coombes. Exercise-induced alterations in skeletal muscle myosin heavy chain phenotype: dose-response relationship. *J. Appl. Physiol.* 86(3): 1002-1008, 1999.

Diffie, G.M., V.J. Caiozzo, S.A. McCue, R.E. Herrick, K.M. Baldwin. Activity-induced regulation of myosin isoform distribution: comparison of two contractile activity programs. *J. Appl. Physiol.* 74(5): 2509-2516, 1993.

- Diffie, G.M. F. Haddad, R.E. Herrick, and K.M. Baldwin. Control of myosin heavy chain expression: interaction of hypothyroidism and hindlimb suspension. *Am. J. Physiol.* 261(6): C1099-C1106, 1991.
- Dilley, R. J., P. Kanellakis, C.J. Oddie, and A. Bobik. Vascular hypertrophy in renal hypertensive spontaneously hypertensive rats. *Hypertension.* 24: 8-15, 1994.
- Dubowitz, V. and A.G.E. Pearse. Reciprocal relationship of phosphorylase and oxidative enzymes in skeletal muscle. *Nature.* 185: 701, 1960.
- Ebashi, S., and M. Endo. Calcium ion and muscle contraction. *Prog. Biophys. Mol. Biol.* 18: 123-183, 1968.
- Eddinger, T.J. Myosin heavy chain isoforms and dynamic contractile properties: skeletal versus smooth muscle. *Comp. Biochem. Physiol. Part B.* 119: 425-434, 1998.
- Eddinger, T.J., and R.L. Moss. Mechanical properties of skinned single fibres of identified types from rat diaphragm. *Am. J. Physiol.* 253(2): C210-C218, 1987.
- Edman, K.A., C. Reggiani, S. Schiaffino, and G. te Kronnie. Maximum velocity of shortening related to myosin isoform composition in frog skeletal muscle fibres. *J. Physiol. (Lond.)* 395: 679-694, 1988.
- Engel, W.K. The essentiality of histo- and cytochemical studies of skeletal muscle in the investigation of neuromuscular disease. *Neurol.* 12: 778-784, 1962.
- Fahim, M.A., J.A. Holley, and N. Robbins. Topographic comparison of neuromuscular junctions in mouse slow and fast twitch muscles. *Neuroscience.* 13: 227-235, 1984.

- Falempin, M., and S. Fodili In-Albon. Influence of brief daily tendon vibration on rat soleus in non-weight-bearing situation. *J. Appl. Physiol.* 87(1): 3-9, 1999.
- Fauteck, S.P., and S.K. Kandarian. Sensitive detection of myosin heavy chain composition in skeletal muscle under different loading conditions. *Am. J. Physiol.* 268: C419-C424, 1995.
- Fink, R.H., D.G. Stephenson, and D.A. Williams. Calcium and strontium activation of single skinned muscle fibres of normal and dystrophic mice. *J. Physiol. (Lond.)* 373: 513-25, 1986.
- Fink, R.H., D.G. Stephenson, and D.A. Williams. Physiological properties of skinned fibres from normal and dystrophic (Duchenne) human muscle activated by  $\text{Ca}^{2+}$  and  $\text{Sr}^{2+}$ . *J. Physiol. (Lond.)* 420: 337-353, 1990.
- Fitts, R.H., D.L. Costill, and P.R. Gardetto. Effect of swim exercise training on human muscle fiber function. *J. Appl. Physiol.* 66(1): 465-475, 1989.
- Franzini-Armstrong, C., and D.A. Fischman. Morphogenesis of skeletal muscle fibres. In: *Myology*, 2<sup>nd</sup> edn. (eds. Engel, A.G., and C. Franzini-Armstrong). McGraw-Hill Inc., New York, 1994.
- Frisk-Holmberg, M., B. Essén, M. Fredrikson, G. Ström, and L. Wibell. Muscle fibre composition in relation to blood pressure response to isometric exercise in normotensive and hypertensive subjects. *Acta Med. Scand.* 213: 21-26, 1983.
- Fritz, J.D., D.R. Swartz, and M.L. Greaser. Factors affecting polyacrylamide gel electrophoresis and electroblotting of high-molecular-weight myofibrillar proteins. *Anal. Biochem.* 180: 205-210, 1989.

- Fryer, M.W., and I.R. Neering. Actions of caffeine on fast- and slow-twitch muscles of the rat. *J. Physiol.* 416: 435-454, 1989.
- Fryer, M.W., and D.G. Stephenson. Total and sarcoplasmic reticulum  $\text{Ca}^{2+}$  contents of skinned fibres from rat skeletal muscle. *J. Physiol. (Lond.)* 493(2): 357-370, 1996.
- Galler, S.  $\text{Ca}^{2+}$ -,  $\text{Sr}^{2+}$ -force relationships and kinetic properties of fast-twitch rat leg muscle fibre subtypes. *Acta Physiol. Scand.* 167: 131-141, 1999.
- Galler, S., K. Hilber, B. Gohlsch, and D. Pette. Two functionally distinct myosin heavy chain isoforms in slow skeletal muscle fibres. *FEBS Lett.* 410: 150-152, 1997a.
- Galler, S., K. Hilber, and D. Pette. Stretch activation and myosin heavy chain isoforms of rat, rabbit and human skeletal muscle fibres. *J. Muscle Res. Cell Motil.* 18: 441-448, 1997b.
- Galler, S., T.L. Schmitt, K. Hilber, and D. Pette. Stretch activation and isoforms of myosin heavy chain and troponin-T of rat skeletal muscle fibres. *J. Muscle Res. Cell Motil.* 18(5): 555-561, 1997c.
- Galler, S., T.L. Schmitt, and D. Pette. Stretch activation, unloaded shortening velocity, and myosin heavy chain isoforms of rat skeletal muscle fibres. *J. Physiol. (Lond.)* 478: 513-521, 1994.
- Gerday, C., and J.M. Gillis. The possible role of parvalbumins in the control of contraction. *J. Physiol. (Lond.)* 258(2): 96P-97P, 1976.
- Gillespie, P.G., T. Hasson, J.A. Garcia, and D.P. Corey. Multiple myosin isozymes and hair-cell function. *Cold Spring Harb. Symp. Quant. Biol.* 61: 309-318, 1996.

- Gray, S. D. Histochemical analysis of capillary and fiber-type distributions in skeletal muscles of spontaneously hypertensive rats. *Microvas. Res.* 36: 228-238, 1988.
- Gray, S. D., R. C. Carlsen, and R. Atherley. Effect of chronic blood pressure reduction on soleus muscle contractile properties in spontaneously hypertensive rats. *Am. J. Physiol.* 267: R740-R746, 1994a.
- Gray, S. D., R. C. Carlsen, and J. Deng. Soleus muscle contractile properties in hypertensive rats. *Am. J. Physiol.* 267: R735-R739, 1994b.
- Grossman, E.J., R.R. Roy, R.J. Talmadge, H. Zhong, and V.R. Edgerton. Effects of inactivity on myosin heavy chain composition and size of rat soleus fibres. *Muscle Nerve.* 21: 375-389, 1998.
- Haddad, F., C. Arnold, M. Zeng, and K. Baldwin. Interaction of thyroid state and denervation on skeletal myosin heavy chain expression. *Muscle Nerve.* 20: 1487-1496, 1997.
- Hämäläinen, N., and D. Pette. The histochemical profiles of fast fiber types IIB, IID, and IIA in skeletal muscles of mouse, rat, and rabbit. *J. Histochem. Cytochem.* 41(5): 733-743, 1993.
- Hämäläinen, N., and D. Pette. Patterns of myosin isoforms in mammalian skeletal muscle fibres. *Microsc. Res. Tech.* 30: 381-389, 1995.
- Hämäläinen, N., and D. Pette. Slow-to-fast transitions in myosin expression of rat soleus muscle by phasic high-frequency stimulation. *FEBS Lett.* 399: 220-222, 1996.

- Harridge, S.D.R., R. Bottinelli, M. Canepari, M.A. Pellegrino, C. Reggiani, M. Esbjornsson, and B. Saltin. Whole-muscle and single-fibre contractile properties and myosin heavy chain isoforms in humans. *Pflugers Arch.* 432(5): 913-929, 1996.
- Heene, R. *Experimental Myopathies and Muscular Dystrophy*. Berlin, Springer-Verlag. 1975.
- Hernández, N., S.H. Torres, H.J. Finol, A. Sosa, and M. Cierco. Capillary and muscle fibre type changes in DOCA-salt hypertensive rats. *Anat. Rec.* 246(2): 208-216, 1996.
- Herrmann-Frank, A., H. Lüttgau, and D.G. Stephenson. Caffeine and excitation-contraction coupling in skeletal muscle: a stimulating story. *J. Muscle Res. Cell Motil.* 20(2): 223-237, 1999.
- Heslinga, J.W., G. te Kronnie, and P.A. Huijting. Growth and immobilization effects on sarcomeres: a comparison between gastrocnemius and soleus muscles of the adult rat. *Eur. J. Appl. Physiol.* 70: 49-57, 1995.
- Hilber, K., and S. Galler. Mechanical properties and myosin heavy chain isoform composition of skinned skeletal muscle fibres from a human biopsy sample. *Pflugers Arch.* 434(5): 551-558, 1997.
- Hoh, J.F.Y. Neural regulation of mammalian fast and slow muscle myosins: an electrophoretic analysis. *Biochem.* 14(4): 742-747, 1975.
- Horowicz, P. Excitation-contraction coupling in skeletal muscle. In: *Myology*, 2<sup>nd</sup> edn. (eds. Engel, A.G., and C. Franzini-Armstrong). McGraw-Hill Inc., New York, 1994.

- Hughes, S.M., M. Cho, I. Karsch-Mizrachi, M. Travis, L. Silberstein, L.A. Leinwand, and H.M. Blau. Three slow myosin heavy chains sequentially expressed in developing mammalian skeletal muscle. *Dev. Biol.* 158(1): 183-199, 1993.
- Isaacson, A., M.J. Hinkes, and S.R. Taylor. Contracture and twitch potentiation of fast and slow muscles of the rat at 20 and 37 C. *Am. J. Physiol.* 218(1): 33-41, 1970.
- Jaschinski, F., M. Schuler, H. Peuker, and D. Pette, D. Changes in myosin heavy chain mRNA and protein isoforms of rat muscle during forced contractile activity. *Am. J. Physiol.* 274: C365-C370, 1998.
- Juhlin-Dannfelt, A., M. Frisk-Holmberg, J. Karlsson, and P. Tesch. Central and peripheral circulation in relation to muscle-fibre composition in normo- and hypertensive man. *Clin. Sci.* 56: 335-340, 1979.
- Kirschbaum, B.J., H.B. Kucher, A. Termin, A.M. Kelly, and D. Pette. antagonistic effects of chronic low frequency stimulation and thyroid hormone on myosin expression in rat fast-twitch muscle. *J. Biol. Chem.* 265(23): 13974-13980, 1990.
- Klitgaard, H., O. Bergman, R. Betto, G. Salviati, S. Schiaffino, T. Clausen, and B. Saltin. Co-existence of myosin heavy chain I and IIa isoforms in human skeletal muscle fibres with endurance training. *Pflugers Arch.* 416(4): 470-472, 1990a.
- Klitgaard H., M. Zhou, S. Schiaffino, R. Betto, G. Salviati, and B. Saltin. Ageing alters the myosin heavy chain composition of single fibres from human skeletal muscle. *Acta Physiol. Scand.* 140(1): 55-62, 1990b.
- Korner, P. I., and A. Bobik. Cardiovascular development after enalapril in spontaneously hypertensive and wistar-kyoto rats. *Hypertension.* 25: 610-619, 1995.

- Kovanen, V. Effects of aging and physical training on rat skeletal muscle. An experimental study on the properties of collagen, laminin, and fibre types in muscles serving different functions. *Acta Physiol. Scand. Suppl.* 577: 1-56, 1989.
- Laemmli, U.K. Cleavage of structural proteins during the assembly of bacteriophage T<sub>4</sub>. *Nature Lond.* 227: 680-685, 1970.
- LaFramboise, W.A., M.J. Daood, R.D. Guthrie, P. Moretti, S. Schiaffino, and M. Ontell. Electrophoretic separation and immunological identification of type 2X myosin heavy chain in rat skeletal muscle. *Biochim. Biophys. Acta* 1035: 109-112, 1990.
- Lamb, G.D. Excitation-contraction coupling in skeletal muscle; comparisons with cardiac muscle. *Proc. Aust. Physiol. Pharmacol. Soc.* 30(1): 1-16, 1999.
- Lamb, G.D., and D.G. Stephenson. Effect of Mg<sup>2+</sup> on the control of Ca<sup>2+</sup> release in skeletal muscle fibres of the toad. *J. Physiol. (Lond)* 434: 507-528, 1991.
- Larsson, L., U. Müller, X. Li, and S. Schiaffino. Thyroid hormone regulation of myosin heavy chain isoform composition in young and old rats, with special reference to IIX myosin. *Acta Physiol. Scand.* 153: 109-116, 1995.
- Lee, Y.S., K. Ondrias, A.J. Duhl, B.E. Ehrlich, and D.H. Kim. Comparison of calcium release from sarcoplasmic reticulum of slow and fast twitch muscles. *J. Membr. Biol.* 122: 155-163, 1991.
- Lewis, D. M., A. J. Levi, P. Brooksby, and J. V. Jones. A faster twitch contraction of soleus in the spontaneously hypertensive rat is partly due to changed fibre type composition. *Exp. Physiol.* 79: 377-386, 1994.

Li, X., and L. Larsson. Maximum shortening velocity and myosin isoforms in single muscle fibres from young and old rats. *Am. J. Physiol.* 270: C352-C360, 1996.

Loughlin, M. *Muscle Biopsy: A laboratory investigation*. 1<sup>st</sup> edn. Butterworth-Heinemann Ltd., Oxford, 1993.

Loukianov, E., Y. Ji, D.L. Baker, T. Reed, J. Babu, T. Loukianova, A. Greene, G. Shull, and M. Periasamy. Sarco(endo)plasmic reticulum  $\text{Ca}^{2+}$  ATPase isoforms and their role in muscle physiology and pathology. *Ann. N.Y. Acad. Sci.* 853: 251-259, 1998.

Lynch, G.S., N.D. Duncan, S.P. Campbell, and D.A. Williams. Endurance training effects on the contractile activation characteristics of single muscle fibres from the rat diaphragm. *Clin. Exp. Pharmacol. Physiol.* 22: 430-437, 1995a.

Lynch, G.S., D.G. Stephenson, and D.A. Williams. Analysis of  $\text{Ca}^{2+}$  and  $\text{Sr}^{2+}$  activation characteristics in skinned muscle fibre preparations with different proportions of myofibrillar isoforms. *J. Muscle Res. Cell Motil.* 16(1): 65-78, 1995b.

Martonosi, A.N. Regulation of calcium by the sarcoplasmic reticulum. In: *Myology*, 2<sup>nd</sup> edn. (eds. Engel, A.G., and C. Franzini-Armstrong). McGraw-Hill Inc., New York, 1994.

Martrette, J.M., N. Hartmann, A. Westphal, and M. Divry. Effect of controllable stress on myosin heavy chain expression and muscle-specific protection by clomipramine. *J. Muscle Res. Cell Motil.* 19(7): 803-810, 1998.

Meissner, G. Ryanodine receptor/ $\text{Ca}^{2+}$  release channels and their regulation by endogenous effectors. *Annu. Rev. Physiol.* 56: 485-508, 1994.

- Metzger, J.M. Effects of troponin C isoforms on pH sensitivity of contraction in mammalian fast and slow skeletal muscle fibres. *J. Physiol.* 492(1): 163-172, 1996.
- Milton, R.L., and M.A. Behforouz. Na channel density in extrajunctional sarcolemma of fast and slow twitch mouse skeletal muscle fibres-functional implications and plasticity after fast motoneuron transplantation on to a slow muscle. *J. Muscle Res. Cell Motil.* 16: 430-439, 1995.
- Mitsumoto H., G.E. DeBoer, G. Bunge, J.T. Andrish, J.E. Tetzlaff, and R.P. Cruse. Fiber-type specific caffeine sensitivities in normal human skinned muscle fibers. *Anesthesiology.* 72(1): 50-4, 1990.
- Moiescu, D.G., and R. Thieleczek. Calcium and strontium concentration changes within skinned muscle preparations following a change in the external bathing solution. *J Physiol. (Lond.)* 275: 241-262, 1978.
- Moiescu, D.G., and R. Thieleczek. Sarcomere length effects on the  $Sr^{2+}$ - and  $Ca^{2+}$ -activation curves in skinned frog muscle fibres. *Biochim. Biophys. Acta* 546(1): 64-76, 1979.
- Moss, R.L., G.M. Diffie, and M.L. Greaser. Contractile properties of skeletal muscle fibres in relation to myofibrillar protein isoforms. *Rev. Physiol. Biochem. Pharmacol.* 126: 1-63, 1995.
- Mozdziak, P.E., M.L. Greaser, and E. Schultz. Myogenin, MyoD, and myosin heavy chain isoform expression following hindlimb suspension. *Aviat. Space Environ. Med.* 70(5): 511-516, 1999.

Murayama, T., N. Kurebayashi, and Y. Ogawa. Effects of caffeine and  $Mg^{2+}$  on the  $Ca^{2+}$  activation and inactivation sites of frog ryanodine receptor. *Biophys. J.* 74: A163, 1998.

Natori, R. The property and contraction process of isolated myofibrils. *Jikeikai. Med. J.* 1: 119-126, 1954.

Ogata, T., and M. Mori. Histochemical study of oxidative enzymes in vertebrate muscles. *J. Histochem. Cytochem.* 12: 171-182, 1964.

Oishi, Y. A. Ishihara, H. Yamamoto, and E. Miyamoto. Hindlimb suspension induces the expression of multiple myosin heavy chain isoforms in single fibres of the rat soleus muscle. *Acta Physiol. Scand.* 162(2): 127-134, 1998.

Okamoto, K., and K. Aoki. Development of a strain of spontaneously hypertensive rats. *Jpn. Circ. J.* 27: 282-293, 1963.

Ontko, J.A. Lipid metabolism in muscle. In: *Myology*, 2<sup>nd</sup> edn. (eds. Engel, A.G., and C. Franzini-Armstrong). McGraw-Hill Inc., New York, 1994.

Pagala, M.K.D., and S.R. Taylor. Imaging caffeine-induced  $Ca^{2+}$  transients in individual fast-twitch and slow-twitch rat skeletal muscle fibers. *Am. J. Physiol.* 274: C623-C632, 1998.

Pearson, A.M., and R.B. Young. *Muscle and Meat Biochemistry*. 1<sup>st</sup> edn. London, Academic Press Limited, 1989.

Peter, J.B., R.J. Barnard, V.R. Edgerton, C.A. Gilliespie, and K.E. Stempel. Metabolic profiles of three fiber types of skeletal muscle in guinea pigs and rabbits. *Biochem.* 11(14): 2627-2633, 1972.

Pette D., H. Peuker, and R.S. Staron. The impact of biochemical methods for single muscle fibre analysis. *Acta Physiol. Scand.* 166(4): 261-277, 1999.

Pette, D., and R.S. Staron. Cellular and molecular diversities of mammalian skeletal muscle fibres. *Rev. Physiol. Biochem. Pharmacol.* 116: 1-76, 1990.

Pette, D., and R.S. Staron. Mammalian skeletal muscle fibre type transitions. *Int. Rev. Cytol.* 170: 143-223, 1997.

Pickar, J. G., R. C. Carlsen, A. Atrakchi, and S. D. Gray. Increased Na<sup>+</sup>-K<sup>+</sup> pump number and decreased pump activity in soleus muscles in SHR. *Am. J. Physiol.* 267: C836-C844, 1994.

Picquet, F., L. Stevens, G. Butler-Browne, and Y. Mounier. Contractile properties and myosin heavy chain composition of newborn rat soleus muscles at different stages of postnatal development. *J. Musc. Res. Cell Motil.* 18: 71-79, 1997.

Powers, S.K., H.A. Demirel, J.S. Coombes, L. Fletcher, C. Calliaud, I. Vrabas, and D. Prezant. Myosin phenotype and bioenergetic characteristics of rat respiratory muscles. *Med. Sci. Sports Exerc.* 29(12), 1573-1579, 1997.

Prezant, D.J., M.L. Karwa, B. Richner, D. Maggiore, E.I. Gentry, and J. Cahill. Gender-specific effects of dexamethasone treatment on rat diaphragm structure and function. *J. Appl. Physiol.* 82(1): 125-133, 1997.

Ranvier, L. De quelques faits relatifs a l'histologie et a la physiologie des muscles stries. *Arch. Physiol. Norm. Pathol.* 1: 5, 1874.

- Rees, B.B., and D. G. Stephenson. Thermal dependence of maximum  $\text{Ca}^{2+}$  activated force in skinned muscle fibres of the toad *Bufo marinus* acclimated at different temperatures. *J. Exp. Biol.* 129: 309-327, 1987.
- Reiser, P.J., C.E. Kasper, M.L. Greaser, and R.L. Moss. Functional significance of myosin transitions in single fibers of developing soleus muscle. *Am. J. Physiol.* 254: C605-C613, 1988.
- Reiser, P.J., C.E. Kasper, and R.L. Moss. Myosin subunits and contractile properties of single fibers from hypokinetic rat muscles. *J. Appl. Physiol.* 63(6): 2293-2300, 1987.
- Reiser, P.J., and W.O. Kline. Electrophoretic separation and quantitation of cardiac myosin heavy chain isoforms in eight mammalian species. *Am. J. Physiol.* 274: H1048-H1053, 1998.
- Reiser, P.J., R.L. Moss, G.G. Giulian, and M.L. Greaser. Shortening velocity in single fibers from adult rabbit soleus muscles is correlated with myosin heavy chain composition. *J. Biol. Chem.* 260 (16): 9077-9080, 1985.
- Rivero, J.L., A.L. Serrano, E. Barrey, J.P. Valette, and M. Jouglin. Analysis of myosin heavy chains at the protein level in horse skeletal muscle. *J. Muscle Res. Cell Motil.* 20(2): 211-221, 1999.
- Rivero, J.L., R.J. Talmadge, and V.R. Edgerton. Fibre size and metabolic properties of myosin heavy chain-based fibre types in rat skeletal muscle. *J. Muscle Res. Cell Motil.* 19(7): 733-742, 1998.

- Rousseau, E., J. LaDine, Q. Liu, and G. Meissner. Activation of the  $\text{Ca}^{2+}$  release channel of skeletal muscle sarcoplasmic reticulum by caffeine and related compounds. *Arch. Biochem. Biophys.* 267: 75-86, 1988.
- Roy, R.R., R.J. Talmadge, K. Fox, M. Lee, A. Ishihara, and V.R. Edgerton. Modulation of MHC isoforms in functionally overloaded and exercised rat plantaris fibers. *J. Appl. Physiol.* 83(1): 280-290, 1997.
- Rüegg, J.C. *Calcium in Muscle Contraction*. 2<sup>nd</sup> edn. Berlin, Springer-Verlag, 1992.
- Rutshmann, M. B. Dahlmann, and H. Reinauer. Loss of fast-twitch isomyosins in skeletal muscles of the diabetic rat. *Biochem. J.* 221: 645-650, 1984.
- Saitoh, A., T. Okumoto, H. Nakano, M. Wada, and S. Katsuta. Age effect on expression of myosin heavy and light chain isoforms in suspended rat soleus muscle. *J. Appl. Physiol.* 86(5): 1483-1489, 1999.
- Salviati G., R. Betto, S. Ceoldo, V. Tegazzin, and A. Della Puppa. Caffeine sensitivity of sarcoplasmic reticulum of fast and slow fibers from normal and malignant hyperthermia human muscle. *Muscle Nerve.* 12(5): 365-370, 1989.
- Sant'Ana Pereira, J.A.A., S. Ennion, A.J. Sargeant, A.F.M. Moorman, and G. Goldspink. Comparison of the molecular, antigenic and ATPase determinants of fast myosin heavy chains in rat and human: a single-fibre study. *Pflügers Arch.* 435: 151-163, 1997.
- Sant'Ana Pereira, J.A.A., A. Wessels, L. Nijtmans, A.F.M. Moorman, and A.J. Sargeant. New method for the accurate characterization of single human skeletal muscle fibres demonstrates a relation between mATPase and MyHC expression in pure and hybrid fibre types. *J. Muscle Res. Cell Motil.* 16: 21-34, 1995.

Sarközi, S., P. Pouliquin, and A. Herrmann-Frank. Regulation of the mutant ryanodine receptor from malignant hyperthermia-susceptible muscle by calcium and 4-chloro-m-cresol. *Pflügers Arch.* 435: R177, 1998.

Schiaffino, S., L. Gorza, S. Sartore, L. Saggin, S. Ausoni, M. Vianello, K. Gundersen, and T. Lomo. Three myosin heavy chain isoforms in type 2 skeletal muscle fibres. *J. Musc. Res. Cell Motil.* 10: 197-205, 1989.

Schiaffino, S., and C. Reggiani. Molecular diversity of myofibrillar proteins: gene regulation and functional significance. *Physiol. Rev.* 76(2): 371-423, 1996.

Schiaffino, S., and G. Salviati. Molecular diversity of myofibrillar proteins: Isoforms analysis at the protein and mRNA level. In *Methods in Cell Biology*. (eds. C.P. Emerson and H. L. Sweeney) San Diego, Academic Press, 1998.

Sellers, J.R. Review. Myosins : a diverse superfamily. *Biochim. Biophys. Acta.* 1496: 3-22, 2000.

Shah A.J., M.K. Pagala, V. Subramani, S.A. Venkatachari, V. Sahgal. Effect of fiber types, fascicle size and halothane on caffeine contractures in rat muscles. *J. Neurol. Sci.* 88: 247-260, 1988.

Sieck, G.C., R.H. van Balkom, Y.S. Prakash, W.Z. Zhan, and P.N. Dekhuijzen. Corticosteroid effects on diaphragm neuromuscular junctions. *J. Appl. Physiol.* 86(1): 114-122, 1999.

Smith, D., H. Green, J. Thomson, and M. Sharratt. Capillary and size interrelationships in developing rat diaphragm, EDL, and soleus muscle fibre types. *Am. J. Physiol.* 256(1): C50-C58, 1989.

Snoj-Cvetko, E., V. Smerdu, J. Sketelj, I. Dolenc, A d'Albis, C. Janmot, and I. Erzen. Adaptive range of myosin heavy chain expression in regenerating soleus is broader than in mature muscle. *J. Musc. Res. Cell Motil.* 17, 401-409, 1996.

Sorrentino, V. and C. Reggiani. Expression of the ryanodine receptor type 3 in skeletal muscle: a new partner in excitation-contraction coupling?. *Trends Cardiovasc. Med.* 9: 54-61, 1999.

Staron, R.S., and D. Pette. Correlation between myofibrillar ATPase activity and myosin heavy chain composition in rabbit muscle fibers. *Histochem.* 86(1): 19-23, 1986.

Staron, R. S., and D. Pette. The multiplicity of combinations of myosin light chains and heavy chains in histochemically typed single fibres. Rabbit soleus muscle. *Biochem. J.* 243: 687-693, 1987.

Staron, R.S., and D. Pette. The continuum of pure and hybrid myosin heavy chain-based fibre types in rat skeletal muscle. *Histochem.* 100: 149-153, 1993.

Stephenson, D.G., G.D. Lamb, and G.M.M. Stephenson. Events of the excitation-contraction-relaxation (E-C-R) cycle in fast- and slow-twitch mammalian muscle fibres relevant to muscle fatigue. *Acta Physiol. Scand.* 162: 229-245, 1998.

Stephenson, D.G., G.D. Lamb, G.M.M. Stephenson, and M.W. Fryer. Mechanisms of excitation contraction coupling relevant to skeletal muscle fatigue In: *Fatigue: Neural and Muscular Mechanisms.* (eds. Gandevia, S.C.; R.M. Enoka, A.J. McComas, D.G. Stuart, and C.K. Thomas) New York, Plenum Press, 1995.

Stephenson, D.G., A.W. Stewart, and G.J. Wilson. Dissociation of force from myofibrillar MgATPase and stiffness at short sarcomere length in rat and toad skeletal muscle. *J. Physiol. (Lond.)* 410: 357-366, 1989.

Stephenson, D.G., and D.A. Williams. Calcium activated force responses in fast- and slow-twitch skinned muscle fibres of the rat at different temperatures. *J. Physiol.* 317: 281-302, 1981.

Stephenson, D.G., and D.A. Williams. Effects of sarcomere length on the force-pCa relation in fast- and slow-twitch skinned muscle fibres from the rat. *J. Physiol.* 333: 637-653, 1982.

Stephenson, G.M.M., A. O'Callaghan, and D.G. Stephenson. Single-fibre study of contractile and biochemical properties of skeletal muscles in streptozotocin-induced diabetic rats. *Diabetes.* 43: 622-628, 1994.

Stienen, G.J., J.L. Kiers, R. Bottinelli, and C. Reggiani. Myofibrillar ATPase activity in skinned human skeletal muscle fibres: fibre type and temperature dependence. *J. Physiol. (Lond.)* 493: 299-307, 1996.

Sugiura, T., H. Matoba, Y. Miyata, Y. Kawai, and N. Murakami. Myosin heavy chain isoform transition in ageing fast and slow muscles of the rat. *Acta Physiol. Scand.* 144: 419-423, 1992.

Sugiura, T., H. Miyata, Y. Kawai, H. Matoba, and N. Murakami. Changes in myosin heavy chain isoform expression of overloaded rat skeletal muscles. *Int. J. Biochem.* 25(11): 1609-1613, 1993.

Sugiura, T., and N. Murakami. Separation of myosin heavy chain isoforms in rat skeletal muscles by gradient sodium dodecyl sulfate-polyacrylamide gel electrophoresis. *Biomed. Res.* 11(2): 87-91, 1990.

Sullivan, V.K., S.K. Powers, D.S. Criswell, N. Tumer, J.S. Larochelle, and D. Lowenthal. Myosin heavy chain composition in young and old rat skeletal muscle: effects of endurance exercise. *J. Appl. Physiol.* 78(6): 2115-2120, 1995.

Syrový, I. Isoforms of contractile proteins. *Prog. Biophys. Molec. Biol.* 49: 1-27, 1987.

Syrový, I., and Z. Hodný. Review. Staining and quantification of proteins separated by polyacrylamide gel electrophoresis. *J. Chromat.* 569: 175-196, 1991.

Takagi, A., and M. Endo. Guinea pig soleus and extensor digitorum longus: A study on single-skinned fibers. *Exp. Neurol.* 55: 95-101, 1977.

Talmadge, R.J., and R.R. Roy. Electrophoretic separation of rat skeletal muscle myosin heavy-chain isoforms. *J. Appl. Physiol.* 75: 2337-2340, 1993.

Talmadge, R.J., R.R. Roy, and V.R. Edgerton. Distribution of myosin heavy chain isoforms in non-weight-bearing rat soleus muscle fibres. *J. Appl. Physiol.* 81(6): 2540-2546, 1996.

Talmadge, R.J., R.R. Roy, and V.R. Edgerton. Persistence of hybrid fibers in rat soleus after spinal cord transection. *Anat. Rec.* 255: 188-201, 1999.

- Taylor, A.D., B. Humphries, P. Smith, and R. Bronks. Electrophoretic separation of myosin heavy chain isoforms in the human M. vastus lateralis: references to reproducibility and relationships with force, electromechanical delay, fibre conduction velocity, endurance and electromyography. *Arch. Physiol. Biochem.* 105(1): 10-18, 1997.
- Termin, A., R.S. Staron, and D. Pette. Changes in myosin heavy chain isoforms during chronic low-frequency stimulation of rat fast hindlimb muscles. A single-fiber study. *Eur. J. Biochem.* 186(3): 749-754, 1989a.
- Termin, A., R.S. Staron, and D. Pette. Myosin heavy chain isoforms in histochemically defined fibre types of rat muscle. *Histochem.* 92: 453-457, 1989b.
- Thompson, L.V., and M. Brown. Age-related changes in contractile properties of single skeletal fibers from the soleus muscle. *J. Appl. Physiol.* 86(3): 881-886, 1999.
- Tortora, G.J., and S.R. Grabowski. *Principles of Anatomy and Physiology*. 8th edn. U.S.A. HarperCollins College Publishers, 1996.
- van Balkom, R.H., P.N. Dekhuijzen, H.T. Folgering, J.H. Veerkamp, J.A. Fransen, and C.L. van Herwaarden. Effects of long-term low-dose methylprednisolone on rat diaphragm function and structure. *Muscle Nerve.* 20(8): 983-990, 1997.
- Vescovo, G. F. Serafini, L. Facchin, P. Tenderini, U. Carraro, L. Dalla Libera, C. Catani, and G.B. Ambrosio. Specific changes in skeletal muscle myosin heavy chain composition in cardiac failure: differences compared with disuse atrophy as assessed on microbiopsies by high resolution electrophoresis. *Heart* 76(4): 337-343, 1996.

- Wada, M., N. Hämäläinen, and D. Pette. Isomyosin patterns of single type IIB, IID and IIA fibres from rabbit skeletal muscle. *J. Muscle Res. Cell Motil.* 16(3): 237-242, 1995.
- Wada, M. T. Okumoto, K. Toro, K. Masuda, T. Fukubayashi, K. Kikuchi, S. Niihata, and S. Katsuta. Expression of hybrid isomyosins in human skeletal muscle. *Am. J. Physiol.* 271: C1250-C1255, 1996.
- Wada, M., and D. Pette. Relationships between alkali light-chain complement and myosin heavy-chain isoforms in single fast-twitch fibers of rat and rabbit. *Eur. J. Biochem.* 214(1): 157-161, 1993.
- West, J.M., and D.G. Stephenson.  $\text{Ca}^{2+}$  and  $\text{Sr}^{2+}$  activation properties of skinned muscle fibres with different regulatory systems from crustacea and rat. *J. Physiol. (Lond.)* 462: 579-596, 1993.
- Widrick, J.J., J.G. Romatowski, M. Karhanek, and R.H. Fitts. Contractile properties of rat, rhesus monkey, and human type I muscle fibers. *Am J. Physiol.* 272(1): R34-R42, 1997.
- Williams, D.A., S.I. Head, G.S. Lynch, and D.G. Stephenson. Contractile properties of skinned muscle fibres from young and adult normal and dystrophic (*mdx*) mice. *J. Physiol.* 460: 51-67, 1993.
- Wilson, G.J., and D.G. Stephenson. Calcium and strontium activation characteristics of skeletal muscle fibres from the small marsupial *Sminthopsis macroura*. *J. Muscle Res. Cell Motil.* 11(1): 12-24, 1990.
- Winegrad, S. Studies of cardiac muscle with high permeability to calcium produced by treatment with ethylenediaminetetraacetic acid. *J. Gen. Physiol.* 58: 71-93, 1971.

Wood, D.S., J. Zollman, and J.P. Reuben. Human skeletal muscle: Properties of the 'chemically skinned' fiber. *Science* 187: 1075-1076, 1975.

Yu, F., H. Degens, X. Li, and L. Larsson. Gender- and age-related differences in the regulatory influence of thyroid hormone on the contractility and myosin composition of single rat soleus muscle fibres. *Pflugers. Arch.* 437: 21-30, 1998.

Zhou, M.Y., H. Klitgaard, B. Saltin, R.R. Roy, V.R. Edgerton, and P.D. Gollnick. Myosin heavy chain isoforms of human muscle after short-term spaceflight. *J. Appl. Physiol.* 78(5): 1740-1744, 1995.

## Appendix 1

**Table A1 Composition of separating gels in the Laemmli (L) and in the Talmadge & Roy (T-R) gel systems.**

Component	L	T-R
	(Laemmli, 1970)	(Talmadge & Roy, 1993)
Acrylamide (% w/v)	8 or 10	7.84
Bis (% w/v)	0.267 or 0.213	0.157
%C value	2.6	2.0
Tris (pH 8.8) (mM)	375	200
Glycerol (% v/v)	-	30
Glycine (mM)	-	100
SDS (% w/v)	0.1	0.4
AP (% w/v)	0.025	0.10
TEMED (% v/v)	0.025	0.05

**Table A2 Composition of the stacking gels in four gel systems.** Note: 'L' is a modified version of the original stacker used by Laemmli (1970). 'M' is a modified version of the Modzdiak *et al.* (1999) stacker. The modification in the Modzdiak stacker was the substitution of methylenebisacrylamide (Bis) for N,N' diallyltartardiamide as the cross-linker.

Component	L	'L'	'L' <sup>G+</sup>	T-R	'M'
	(Laemmli, 1970)	(modified Laemmli, 1970)	('L' + 40% glycerol)	(Talmadge & Roy, 1993)	(Modzdiak <i>et al.</i> , 1999)
Acrylamide (% w/v)	3.00	4.00	4.00	3.92	2.56
Bis (% w/v)	0.08	0.107	0.107	0.08	0.45
%C value	2.6	2.6	2.6	2.0	15
Tris (pH 6.7) (mM)	125	125	125	70	100
Glycerol (% v/v)	-	-	40	30	10
EDTA (mM)	-	-	-	4	-
SDS (% w/v)	0.1	0.1	0.1	0.4	0.1
AP (% w/v)	0.025	0.1	0.1	0.1	0.05
TEMED (% v/v)	0.025	0.05	0.05	0.05	0.5

**Table A3. Composition of running buffers in three gel systems.** Laemmli (L), Danieli-Betto (D-B) and Talmadge & Roy (T-R).

Component	<b>L</b>	<b>D-B</b>	<b>T-R</b>	
	(Laemmli, 1970)	(Danieli-Betto <i>et al.</i> , 1986)	(Talmadge and Roy, 1993)	
			Upper	Lower
Tris (mM)	25	32.5	100	50
Glycine (mM)	192	288	150	75
SDS (% w/v)	0.1	0.1	0.1	0.05

## Appendix 2

Gel systems used to generate data shown in Figures in Chapter 3. Gel systems used in Fig 3.1. will be referred to as gel F3.1A,B and gel F3.1C,D. Note: Composition of stackers and running buffers (RB) are shown in Appendix 1, Tables A2 and A3.

gel reference	Separating gel										Stacker				Running Conditions			
	[A] (%, w/v)	[B] (%, w/v)	C (%)	[Tris] (mM)	[glycerol] (%, v/v)	[glycine] (mM)	[SDS] (%, w/v)	[AP] (%, w/v)	[TEMED] (%, v/v)	[RB]	E (V/cm)	Time (hours)	Temp (°C)					
gel F3.1A,B	6-10	0.15	1.5-2.5	375	40	50	0.1	0.075	0.05	L <sup>G<sup>H</sup></sup>	L	9.1	24	16-21				
gel F3.1C,D	7.3&10	0.13&0.17	1.7	375	40	50	0.1	0.075	0.05	L <sup>G<sup>H</sup></sup>	L	9.1	24	16-21				
gel F3.2	7.3	0.11-0.19	1.5-2.5	375	40	50	0.1	0.075	0.05	L <sup>G<sup>H</sup></sup>	L	9.1	24	16-21				
gel F3.3	6.7	0.15	2.2	375-700	40	0	0.1	0.075	0.03	L <sup>G<sup>H</sup></sup>	D-B	11.4	26	16-21				
gel F3.4	6.7	0.15	2.2	375	40	0-100	0.1	0.075	0.05	L <sup>G<sup>H</sup></sup>	L	9.1	24	16-21				
gel F3.5	9.0	0.16	1.7	375	37	50	0.1	0.05	0.05	L' & L <sup>G<sup>H</sup></sup>	L	11.4	30	12-14				
gel F3.6A,C,E	8.5	0.14	1.6	375	40	0	0.1	0.075	0.03	L <sup>G<sup>H</sup></sup>	D-B	11.4&13.6	26	16-21				
gel F3.6B,D	7.5	0.17	2.3	375	37	50	0.1	0.075	0.05	L <sup>G<sup>H</sup></sup>	L	11.4&17.0	30	2-4				
gel F3.7	7.5	0.17	2.3	375	37	50	0.1	0.075	0.05	L <sup>G<sup>H</sup></sup>	L	11.4	24&34	16-21				
gel F3.8	10.0	0.17	1.7	375	37	50	0.1	0.075	0.05	L'	L	11.4	30	2-4/12-14/16-21				
gel F3.9	10.0	0.17	1.7	375	37	50	0.1	0.075	0.05	L <sup>G<sup>H</sup></sup>	L	11.4	30	2-4 & 10-12				
gel F3.10A,D,G	8.0	0.16	2.0	200	30&40	100	0.4	0.1	0.05	T-R	T-R	9.7	24	16-21				
gel F3.10B,E,H	8.0	0.16	2.0	200	40&42.5	100	0.4	0.1	0.05	T-R	T-R	14.8	24	16-21				
gel F3.10C,F,I	8.0	0.16	2.0	200	40&45	100	0.4	0.1	0.05	T-R	T-R	13.6	24	16-21				
gel F3.11	8.0	0.16	2.0	200	40	100	0.4	0.1	0.05	T-R & L <sup>G<sup>H</sup></sup>	T-R	13.6	24	16-21				
gel F3.12	8.0	0.16	2.0	200	40	100	0.4	0.1	0.05	T-R	T-R & D-B	9.7	24	16-21				

Appendix 2 continued

gel reference	Separating gel										Stacker				Running Conditions		
	[A] (%, w/v)	[B] (%, w/v)	C (%)	[Tris] (mM)	[glycerol] (%, v/v)	[glycine] (mM)	[SDS] (%, w/v)	[AP] (%, w/v)	[TEMED] (%, v/v)	RB	E (V/cm)	Time (hours)	Temp (°C)				
gel F3.13	8.0	0.16	2.0	200	40	100	0.4	0.1	0.05	T-R	9.7	24	16-21				
gel F3.14	8.0	0.16	2.0	200	30	100	0.4	0.03	0.1	M'	10.2	24	5				
gel F3.15A	8.0	0.16	2.0	200	30	100	0.4	0.03	0.1	M'	10.2	24	5				
gel F3.15B,C	8.0	0.16	2.0	200	42.5	100	0.4	0.1	0.05	T-R	14.8	24	16-21				
gel F3.16A	7.9	0.10	1.2	425	40	-	0.3	0.05	0.075	L <sup>G+</sup>	13.6	24	16-21				
gel F3.16B	10.0	0.17	1.7	375	37	50	0.1	0.075	0.05	L'	11.4	30	13				
gel F3.16C	8.0	0.16	2.0	200	30	100	0.4	0.03	0.1	M'	10.2	24	5				
gel F3.17A	6.7	0.15	2.2	375	40	-	0.1	0.075	0.03	L <sup>G+</sup>	11.4	24	16-21				
gel F3.17B	8.0	0.16	2.0	200	38	100	0.4	0.1	0.05	T-R	14.8	24	16-21				
gel F3.17C	8.0	0.16	2.0	200	30	100	0.4	0.03	0.1	M'	10.2	24	5				

## Appendix 3

Gel systems used to generate data shown in Tables in Chapter 3. Gel systems used in Table 3.1. will be referred to as gel T3.1-1 etc. Note: Composition of stackers and running buffers (RB) are shown in Appendix 1, Tables A2 and A3.

	Separating gel							Stacker					Running Conditions		
	[A] (%, w/v)	[B] (%, w/v)	C (%)	[Tris] (mM)	[glycerol] (%, v/v)	[glycine] (mM)	[SDS] (%, w/v)	[AP] (%, w/v)	[TEMED] (%, v/v)	RB	E (V/cm)	Time (hours)	Temp (°C)		
gel T3.1-1	7.5	0.17	2.3	375	35&37	50	0.1	0.075	0.05	T <sup>G+</sup>	L	11.4	24	16-21	
gel T3.1-2	7.5	0.17	2.3	375	35&37	50	0.1	0.075	0.05	T <sup>G+</sup>	L	11.4	34	16-21	
gel T3.1-3	7.3	0.13	1.7	375	37&40	50	0.1	0.075	0.05	T <sup>G+</sup>	L	11.4	30	16-21	
gel T3.1-4	10.0	0.17	1.7	375	37&40	50	0.1	0.075	0.05	T <sup>G+</sup>	L	11.4	30	16-21	
gel T3.1-5	7.3	0.13	1.7	375	37&40	50	0.1	0.075	0.05	T <sup>G+</sup>	L	11.4	30	2-4	
gel T3.1-6	10.0	0.17	1.7	375	37&40	50	0.1	0.075	0.05	T <sup>G+</sup>	L	11.4	30	2-4	
gel T3.1-7	7.5	0.17	2.3	375	40&42.5	50	0.1	0.075	0.05	T <sup>G+</sup>	L	11.4	24	16-21	
gel T3.1-8	7.5	0.17	2.3	375	40&42.5	50	0.1	0.075	0.05	T <sup>G+</sup>	L	11.4	30	2-4	
gel T3.2-1	6.7	0.15	2.2	375	40	-	0.1	0.075	0.03	T <sup>G+</sup>	D-B	11.4	24	16-21	
gel T3.2-2	8.0	0.16	2.0	200	38	100	0.4	0.1	0.05	T-R	T-R	14.8	24	16-21	
gel T3.2-3	8.0	0.16	2.0	200	30	100	0.4	0.03	0.1	M'	T-R	10.2	24	5	

## Appendix 4

Gel systems used to generate data used in the text in Chapter 3. Gel system in used in the text will be referred to as gel txt-1 etc.  
 Note: Composition of stackers and running buffers (RB) are in shown Appendix 1, Tables A2 and A3.

	Separating gel							Stacker				Running Conditions		
	[A] (%, w/v)	[B] (%, w/v)	C (%)	[Tris] (mM)	[glycerol] (%, v/v)	[glycine] (mM)	[SDS] (%, w/v)	[AP] (%, w/v)	[TEMED] (%, v/v)	RB	E (V/cm)	Time (hours)	Temp (°C)	
gel txt-1	6.7	0.15	2.2	375	40	0	0.1	0.075	0.05	L <sup>G<sub>H</sub></sup>	L & D-B	9.1	24	16-21
gel txt-2	7.5	0.17	2.3	375	37	50	0.1	0.075	0.05	L <sup>G<sub>H</sub></sup>	L	11.4	34	2-4
gel txt-3	7.5	0.17	2.2	375	37	50	0.1	0.075	0.05	L <sup>G<sub>H</sub></sup>	L	11.4	40	2-4
gel txt-4	7.5	0.17	2.2	375	37	50	0.1	0.075	0.05	L <sup>G<sub>H</sub></sup>	L	11.4	30	2-4
gel txt-5	9.0	0.16	1.7	375	37	50	0.1	0.075	0.05	L <sup>G<sub>H</sub></sup>	L	11.4	30	12-14
gel txt-6	9.0	0.16	1.7	375	37	50	0.1	0.05	0.05	L <sup>L</sup>	L	11.4	30	2-4
gel txt-7	9.0	0.17	1.9	375	37	50	0.1	0.05	0.05	L <sup>G<sub>H</sub></sup>	L	11.4	30	2-4
gel txt-8	10.0	0.17	1.7	375	37	50	0.1	0.075	0.05	L <sup>G<sub>H</sub></sup>	L	11.4	30	2-4
gel txt-9	10.0	0.17	1.7	375	37	50	0.1	0.05	0.05	L <sup>L</sup>	L	11.4	30	2-4
gel txt-10	10.0	0.17	1.7	375	37	50	0.1	0.075	0.05	L <sup>G<sub>H</sub></sup>	L	13.6	30	2-4
gel txt-11	10.0	0.17	1.7	375	37	50	0.1	0.075	0.05	L <sup>G<sub>H</sub></sup>	L	11.4	30	12-14

## Appendix 5.1

Types of modifications of the original Laemmli (1970) SDS-PAGE protocol detected in a group of randomly selected studies that have used this gel system for separating MHC isoforms. Letters refer to the following: A, [acrylamide] (% w/v); C, %C value; T<sub>r</sub>, [Tris] (mM); G<sub>r</sub>, [glycerol] (% v/v); G<sub>c</sub>, [glycine] (mM); E<sub>D</sub>, [EDTA] (mM); S, [SDS] (% w/v); A<sub>p</sub>, [ammonium persulfate] (% w/v); T<sub>M</sub>, [TEMED] (% v/v); V, voltage (V) or I, current (mA) (Note: the available data did not allow for the estimation of the electric field); Time, running time [hours; overnight (o/n)]; Temp, running temperature (°C). Symbols are defined in the footnote of the table. A hyphen is used instead of a value for unmodified parameter of for parameters for which the value was not specified.

Reference	Separating gel						Stacking gel						Running buffer				Running conditions						
	A	C	T <sub>r</sub>	G <sub>r</sub>	G <sub>c</sub>	S	A <sub>p</sub>	T <sub>M</sub>	A	C	T <sub>r</sub>	G <sub>r</sub>	E <sub>D</sub>	S	A <sub>p</sub>	T <sub>M</sub>	T <sub>r</sub>	G <sub>c</sub>	S	V or I	Time	Temp	
Carraro & Catani, 1983.	5&7.5	-	-	25	-	-	-	-	4	-	-	25	-	-	-	-	-	-	-	-	-	-	-
Reiser <i>et al.</i> , 1985.	10	-	-	10	-	-	-	-	3.5	-	-	10	-	-	-	-	-	-	-	-	-	-	-
Danieli-Betto <i>et al.</i> , 1986.	6	-	-	40	-	-	-	-	4	-	-	40	-	-	-	-	32.5	288	-	50V	o/n	-	-
Reiser <i>et al.</i> , 1987.	10	-	-	10	-	-	-	-	3.5	-	-	10	-	-	-	-	-	-	-	-	-	-	-
Bär & Pette, 1988.	5-8§	-	-	25	-	-	-	-	3.5	-	-	25	-	-	-	-	-	-	-	-	-	24	-
Reiser <i>et al.</i> , 1988.	15	-	-	10	-	-	-	-	3.5	-	-	10	-	-	-	-	-	-	-	-	-	-	-
Biral <i>et al.</i> , 1988.	6	-	-	33	-	-	-	-	4	-	-	33	-	-	-	-	32.5	288	-	50V	o/n	-	-
Termin <i>et al.</i> , 1989a.	5-8§	-	-	25	-	-	-	-	4	-	-	25	-	-	-	-	-	-	-	22mA	20	12	-
Termin <i>et al.</i> , 1989b.	5-8§	-	-	25	-	-	-	-	3.5	-	-	25	-	-	-	-	-	-	-	120V	24	-	-
Fits <i>et al.</i> , 1989.	10	-	-	10	-	-	-	-	3.5	-	-	10	-	-	-	-	-	-	-	-	-	-	-
Schiaffino <i>et al.</i> , 1989.	6	-	-	37.5	-	-	-	-	-	-	-	-	-	-	-	-	-	-	-	-	-	-	-
Kirschbaum <i>et al.</i> , 1990.	5-8§	-	-	25	-	-	-	-	-	-	-	25	-	-	-	-	-	-	-	-	-	-	-
Danieli-Betto <i>et al.</i> , 1990.	6	-	-	40	-	-	-	-	4	-	-	40	-	-	-	-	32.5	288	-	50V	o/n	-	-
Sugiura & Murakami, 1990.	5-8§	-	-	30-40	-	-	-	-	3.5	-	-	35	-	-	-	-	-	-	-	*	*	8	-
Klitgaard <i>et al.</i> , 1990a.	6	-	-	37.5	-	-	-	-	4	-	-	37.5	-	-	-	-	32.5	288	-	50V	o/n	-	-

## Appendix 5.1 continued.

Reference	Separating gel						Stacking gel						Running buffer			Running conditions							
	A	C	T <sub>r</sub>	G <sub>r</sub>	G <sub>c</sub>	S	A <sub>p</sub>	T <sub>M</sub>	A	C	T <sub>r</sub>	G <sub>r</sub>	E <sub>D</sub>	S	A <sub>p</sub>	T <sub>M</sub>	T <sub>r</sub>	G <sub>c</sub>	S	V or I	Time	Temp	
Klitgaard <i>et al.</i> , 1990a.	6	-	-	37.5	-	-	-	-	4	-	-	37.5	-	-	-	-	32.5	288	-	50V	o/n	-	
Klitgaard <i>et al.</i> , 1990b.	6	-	-	37.5	-	-	-	-	4	-	-	37.5	-	-	-	-	-	-	-	-	-	-	
LaFramboise <i>et al.</i> , 1990.	4.8-5.8	2.7&5	-	25-33	-	-	0.03	0.1&0.17	2.9-3.9	2.7&5	-	-	-	-	-	-	-	-	-	#	#	-	
Diffie <i>et al.</i> , 1991.	7	-	-	40	-	-	-	-	4	-	-	40	-	-	-	-	32.5	288	-	120V	4-4.5	-	
Hämäläinen & Pette, 1993.	6-11§	-	-	20-25	-	-	-	-	3.5	-	-	25	-	-	-	-	-	-	-	-	-	48	
Staron & Pette, 1993.	7-10§	-	-	25	-	-	-	-	3	-	-	25	-	-	-	-	-	-	-	120V	o/n	-	
Sugiura <i>et al.</i> , 1993.	5-8§	-	-	30-40	-	-	-	-	3.5	-	-	35	-	-	-	-	-	-	-	*	*	8	
Wada & Pette, 1993.	7-10§	-	-	25-35	-	-	-	-	3.5	-	-	25	-	-	-	-	-	-	-	120V	24	-	
Adams <i>et al.</i> , 1993.	7	-	-	40	-	-	-	-	4	-	-	40	-	-	-	-	32.5	288	-	120V	7	-	
Diffie <i>et al.</i> , 1993.	7	-	-	40	-	-	-	-	4	-	-	40	-	-	-	-	32.5	288	-	120V	4-4.5	-	
Hughes <i>et al.</i> , 1993.	5.5	-	-	35	-	-	0.03	0.1&0.17	-	-	-	-	-	-	-	-	-	-	-	†	22-24	15	
Galler <i>et al.</i> , 1994.	5-8§	-	-	25	-	-	-	-	3.5	-	-	25	-	-	-	-	-	-	-	120V	28	-	
Andersen <i>et al.</i> , 1994.	6	-	-	37.5	-	-	-	-	-	-	-	37.5	-	-	-	-	-	-	-	†	†	-	
Bottinelli <i>et al.</i> , 1994.	6	-	-	40	-	-	-	-	4	-	-	40	-	-	-	-	32.5	288	-	50V	o/n	-	
Zhou <i>et al.</i> , 1995.	6	-	-	37.5	-	-	0.03	0.1	-	-	-	-	-	-	0.1	0.15	-	-	-	†	†	-	
Sant'ana Pereira <i>et al.</i> , 1995.	6	3	-	37.5	-	-	-	-	4	3	-	37.5	-	-	-	-	32.5	288	-	20mA	18	18	
Hämäläinen & Pette, 1995.	6-11§	-	-	20-25	-	-	-	-	3.5	-	-	25	-	-	-	-	-	-	-	-	-	48	8
Larsson <i>et al.</i> , 1995.	5.8	-	-	30	-	-	0.029	0.07	3.9	-	-	30	-	-	0.4	0.1	-	-	-	120V	22-24	10	
Fauteck & Kandarian, 1995.	6.8	2.7	-	30	-	-	0.03	0.1	3.4	2.7	-	-	-	-	0.045	0.15	25	250	-	360V†	24	-	

## Appendix 5.1 continued.

Reference	Separating gel						Stacking gel						Running buffer						Running conditions				
	A	C	T	G <sub>r</sub>	G <sub>c</sub>	S	A <sub>p</sub>	T <sub>M</sub>	A	C	T	G <sub>r</sub>	E <sub>D</sub>	S	A <sub>p</sub>	T <sub>M</sub>	T	G <sub>c</sub>	S	E	Time	Temp	
Harridge <i>et al.</i> , 1996.	6	-	-	40	-	-	-	-	4	-	-	40	-	-	-	-	32.5	288	-	50V	o/n	-	-
Stienen <i>et al.</i> , 1996.	6	-	1500	35	-	0.4	-	-	4	-	500	35	-	0.4	-	-	32.5	288	-	100V	24	20	20
Vescovo <i>et al.</i> , 1996.	6.8	2.7	-	37.5	-	-	-	-	3.9	2.7	12.5	37.5	-	-	-	-	50	384	0.2	4mA	24	-	-
Galler <i>et al.</i> , 1997b.	5-8§	-	-	25	-	-	-	-	3.5	-	-	25	-	-	-	-	-	-	-	-	120V	28	-
Galler <i>et al.</i> , 1997c.	5-8§	-	-	25	-	-	-	-	3.5	-	-	25	-	-	-	-	-	-	-	-	120V	28	-
Widrick <i>et al.</i> , 1997.	5&10	-	-	10	-	-	-	-	3&3.5	-	-	10	-	-	-	-	-	-	-	-	-	-	-
Hilber & Galler, 1997.	5-8§	-	-	25	-	-	-	-	3.5	-	-	25	-	-	-	-	-	-	-	-	120V	24	-
Picquet <i>et al.</i> , 1997.	6	-	-	-	-	-	-	-	4	-	-	-	-	-	-	-	-	-	-	-	-	-	-
Jaschinski <i>et al.</i> , 1998.	5-8§	-	-	25	-	-	-	-	4	-	-	25	-	-	-	-	-	-	-	-	22mA	20	12
Canepari <i>et al.</i> , 1998.	6	-	-	40	-	-	-	-	4	-	-	40	-	-	-	-	32.5	288	-	100V	20	-	-
Daugaard <i>et al.</i> , 1998.	6	-	-	37.5	-	-	-	-	4	-	-	40	-	-	-	-	32.5	288	-	50V	24	-	-
Oishi <i>et al.</i> , 1998.	5-8§	-	-	30-40	-	-	-	-	3.5	-	-	35	-	-	-	-	-	-	-	-	11mA	24	4
Falempin & Fodili In-Albon, 1999.	5&7.5	-	-	25	-	-	-	-	4	-	-	25	-	-	-	-	-	-	-	-	-	-	-

§ Gradient separating gel. \* 50V/plate through the stacking gel and then 150V/plate for 18hrs. # 100V through the stacking gel then 200V for 7hrs or 50V for 22-24hrs or 120V for 22-24hrs. † 80V through the stacking gel then 160V. ‡ 70V o/n then 200V for 3-4hrs. ¥ Intermittent voltage.

## Appendix 5.2

Types of modifications of the Talmadge & Roy (1993) SDS-PAGE protocol detected in a group of randomly selected studies that have used this gel system for separating MHC isoforms. Letters refer to the following: A, [acrylamide] (% w/v); C, % C value; T<sub>r</sub>, [Tris] (mM); G<sub>r</sub>, [glycerol] (% w/v); G<sub>c</sub>, [glycine] (mM); E<sub>D</sub>, [EDTA] (mM); S, [SDS] (% w/v); A<sub>p</sub>, [ammonium persulfate] (% w/v); T<sub>M</sub>, [TEMED] (% w/v); V, voltage (V) or I, current (mA) (Note: the available data did not allow for the estimation of the electric field); Time, running time [hours; overnight (o/n)]; Temp, running temperature (°C). Symbols are defined in the footnote of the table. A hyphen is used instead of a value for unmodified parameter of for parameters for which the value was not specified.

Reference	Separating gel						Stacking gel						Running buffer			Running conditions							
	A	C	T <sub>r</sub>	G <sub>r</sub>	G <sub>c</sub>	S	A <sub>p</sub>	T <sub>M</sub>	A	C	T <sub>r</sub>	G <sub>r</sub>	E <sub>D</sub>	S	A <sub>p</sub>	T <sub>M</sub>	T <sub>r</sub>	G <sub>c</sub>	S	V or I	Time	Temp	
Lynch <i>et al.</i> , 1995a.	9.6	4	375	35	-	-	1.25	0.3	3.94	4	500	-	-	-	1.25	0.3	-	-	-	90V	-	-	4
Sullivan <i>et al.</i> , 1995.	-	-	-	40	-	-	-	-	-	-	-	-	-	-	-	-	-	-	-	-	-	-	8-10
Snoj-Cvetko <i>et al.</i> , 1996.	-	-	-	-	-	-	-	-	-	-	-	-	-	-	-	-	-	-	-	-	-	28	†
Taylor <i>et al.</i> , 1997.	5.88	-	-	-	-	-	-	0.1	-	-	-	-	-	-	-	0.2	250	192	0.1	†	†	†	†
Roy <i>et al.</i> , 1997.	-	-	-	-	-	-	-	-	-	-	-	-	-	-	-	-	-	-	-	-	-	-	-
Caiozzo <i>et al.</i> , 1997.	8	1.3	-	-	-	-	-	-	-	-	-	-	-	-	-	-	100	150	0.1	275V	-	-	4
Sant'Ana Pereira <i>et al.</i> , 1997.	8	-	-	-	-	-	-	-	4	-	-	-	-	-	-	-	-	-	-	-	-	-	-
Haddad <i>et al.</i> , 1997.	-	-	-	-	-	-	-	-	-	-	-	-	-	-	-	-	-	-	-	275V	22	-	8
Powers <i>et al.</i> , 1997.	-	-	-	-	-	-	-	-	-	-	-	-	-	-	-	-	-	-	-	-	-	20	8
Prezant <i>et al.</i> , 1997.	-	-	-	-	-	-	-	-	-	-	-	-	-	-	-	-	-	-	-	-	-	25.5	4

## Appendix 5.2 continued.

Reference	Separating gel							Stacking gel							Running buffer			Running conditions					
	A	C	T	G <sub>r</sub>	G <sub>c</sub>	S	A <sub>p</sub>	T <sub>M</sub>	A	C	T	G <sub>r</sub>	E <sub>D</sub>	S	A <sub>p</sub>	T <sub>M</sub>	T	G <sub>c</sub>	S	V or I	Time	Temp	
Reiser & Kline, 1998.	-	-	-	5-45	-	-	-	-	-	-	-	5	-	-	-	-	#	-	-	-	275V	-	8
Grossman <i>et al.</i> , 1998.	-	-	-	-	-	-	-	-	-	-	-	-	-	-	-	-	-	-	-	-	-	-	-
Banman <i>et al.</i> , 1998.	-	-	-	-	-	-	-	-	-	-	-	-	-	-	-	-	\$	\$	\$	150V	20	‡	6
Martrette <i>et al.</i> , 1998.	-	-	-	-	-	-	-	-	-	-	-	-	-	-	-	-	-	-	-	-	-	28	6
Demirel <i>et al.</i> , 1999.	-	-	-	-	-	-	-	-	-	-	-	-	-	-	-	-	-	-	-	-	-	20	8
Rivero <i>et al.</i> , 1999.	-	-	-	-	-	-	-	-	-	-	-	-	-	-	-	-	-	-	-	-	130V	-	-
Mozdziak <i>et al.</i> , 1999.	-	-	-	-	-	-	0.03	0.1	2.56	1.5	100	10	0	0.1	0.05	0.5	*	-	-	-	-	-	4

† gel run in the cold room (no more data available on the temperature). ‡ 70V for 0.5hrs then 150V for 3hrs. § Gels run in the refrigerator (no more data available on the temperature). \*Upper running buffer contained 7.5 mM β-mercaptoethanol. # Upper running buffer contained 10 mM β-mercaptoethanol. ‡ Gels run in an ice bath (no more data available on the temperature). \$ Upper running buffer contains 300 mM Tris, 450 mM Glycine and 0.3% SDS. Lower running buffer contains 50 mM Tris, 75mM Glycine and 0.05%SDS.

## Appendix 5.3

A group of randomly selected studies that have separated MHC isoforms but gave no reference for the protocol used, and only provided the information presented in this table. Letters refer to the following: A, [acrylamide] (% w/v); C, % C value; T<sub>r</sub>, [Tris] (mM); G<sub>r</sub>, [glycerol] (% v/v); G<sub>c</sub>, [glycine] (mM); E<sub>D</sub>, [EDTA] (mM); S, [SDS] (% w/v); A<sub>P</sub>, [ammonium persulfate] (% w/v); T<sub>M</sub>, [TEMED] (% v/v); V, voltage (V) or I, current (mA) (Note: the available data did not allow for the estimation of the electric field); Time, running time [hours; overnight (o/n)]; Temp, running temperature (°C). Symbols are defined in the footnote of the table. A hyphen is used instead of a value for parameters which were not specified.

Reference	Separating gel						Stacking gel						Running buffer			Running conditions							
	A	C	T <sub>r</sub>	G <sub>f</sub>	G <sub>c</sub>	S	A <sub>P</sub>	T <sub>M</sub>	A	C	T <sub>r</sub>	G <sub>f</sub>	E <sub>D</sub>	S	A <sub>P</sub>	T <sub>M</sub>	T <sub>r</sub>	G <sub>c</sub>	S	V or I	Time	Temp	
Wada <i>et al.</i> , 1995.	7.5	1	375	30	-	0.1	0.02	0.1	4	1	125	-	-	0.1	0.1	0.1	-	-	-	-	180V	18	†
Wada <i>et al.</i> , 1996.	6.8	2.6	200	30	100	0.4	0.05	0.1	3.5	2.6	70	-	4	0.4	0.1	0.1	-	-	-	-	150V	40	†
Blough <i>et al.</i> , 1996.	9	0.5	750	12	-	0.1	0.1	0.08	2.9	5	125	-	-	0.1	0.03	0.12	25*	192	0.1	-	-	-	18
Li & Larsson, 1996.	6	-	-	30	-	-	0.029	0.07	4	-	-	30	-	-	0.04	0.1	-	-	-	-	120V	22-24	10
Hämäläinen & Pette, 1996.	7	0.85	720	29	-	0.1	-	-	4	4.3	160	-	-	0.1	-	-	-	-	-	-	120V	24	§
Degens <i>et al.</i> , 1998.	6	-	-	30	-	-	-	-	4	-	-	30	-	-	-	-	-	-	-	-	120V	22-24	15
Yu <i>et al.</i> , 1998.	6&7	-	-	30	-	-	0.03	0.07	4	-	-	30	-	-	0.04	0.1	-	-	-	-	120V	24	15
Saitoh <i>et al.</i> , 1999.	7.5	-	-	-	-	-	-	-	3.5	-	-	-	-	-	-	-	-	-	-	-	200V	36	4

\* Upper running buffer was identical but also contained 25 mM β-mercaptoethanol. † Gels run at room temperature (no more data available on the temperature). ‡ Gels run in cold room (no more data available on the temperature). § Gels cooled with tap water (no more data available on the temperature).



